DETERMINATION OF CHARACTERISTICS OF ADSORBENT FOR ADSORPTION HEAT PUMPS

A Thesis Submitted to
the Graduate School of Engineering and Sciences of
İzmir Institute of Technology
in Partial Fulfillment of the Requirements for the Degree of

MASTER OF SCIENCE

in Energy Engineering

by
Şefika Çağla SAYILGAN

November 2013
İZMİR

We approve the thesis of **Şefika Çağla SAYILGAN**

Examining Committee Members:

Prof. Dr. Semra ÜLKÜ
Department of Chemical Engineering, Izmir Institute of Technology

Prof. Dr. Fehime ÖZKAN
Department of Chemical Engineering, Izmir Institute of Technology

Assist. Prof. Dr. Hasan DEMİR
Department of Chemical Engineering, Osmaniye Korkut Ata University

20 December 2013

Prof. Dr. Semra ÜLKÜ
Supervisor, Department of
Chemical Engineering
Izmir Institute of Technology

Assoc. Prof. Dr. Moghtada MOBEDİ
Co-Supervisor, Department of
Mechanical Engineering
Izmir Institute of Technology

Prof. Dr. Gülden GÖKÇEN AKKURT
Head of the Department of Energy
Engineering

Prof. Dr. R. Tuğrul SENGER
Dean of the Graduate School of
Engineering and Sciences

ACKNOWLEDGEMENTS

I would like to thank to my advisors, Prof. Dr. Semra ÜLKÜ and Assoc. Prof. Dr. Moghtada MOBEDİ for their supervision, guidance and support during my MSc studies. I am also thankful to Prof. Dr. Fehime Özkan and Assist. Prof. Dr. Hasan Demir for their valuable recommendations and contributions.

I would like to express my gratitude to Zeynep Elvan Yıldırım, Dr. Gamze Gediz İliş, Assist. Prof. Dr. Güler Narin, Dr. Filiz Yaşar Mahlıçlı, Seda Güneş, Dr. Senem Yetgin, Melda Büyüköz, Damla Taykoz, Ekrem Özer and Research Specialist Dr. Burcu Alp for their helps and supports.

I wish to express my love and gratitude to my beloved family; my brother Utkan GÜNDOĞAN, my mother Tayibe GÜNDOĞAN, my dad Ethem GÜNDOĞAN, my nephew Yağız GÜNDOĞAN and my sister in-law Dilek GÜNDOĞAN for their understanding and endless love, through the duration of my life.

This thesis is dedicated to my lovely husband Fırat SAYILGAN who encouraged me to start MSc, waited with me till morning during the experiments and has supported me for all times.

ABSTRACT

DETERMINATION OF CHARACTERISTICS OF ADSORBENT FOR ADSORPTION HEAT PUMPS

Adsorption heat pumps, which are environmentally friendly and operating with thermal sources, have gained attention in recent years. Although they have higher primary energy efficiency than traditional heat pumps, adsorption heat pumps require improvements due to the low COP and SCP/SHP values. The selection of appropriate working pair, the determination of adsorption equilibrium and kinetics of the pair is quite important in the design of adsorption heat pumps.

In this study, the working pairs used in adsorption heat pumps were discussed, and the models used in adsorption equilibria and kinetics were explained. In the experimental part, the effect of the adsorption and desorption temperatures on adsorption capacity and mass diffusivity were investigated. Type RD silica gel-water and zeolite 13X-water were selected as working pairs in the adsorption experiments. Accordingly, two volumetric systems were constructed; adsorption experiments were conducted and pressure changes were recorded against time.

The experimental studies showed that the adsorption capacity was decreased with increasing adsorption temperature and with decreasing desorption temperature, and zeolite 13X-water pair had higher adsorption capacity than type silica gel-water pair under the same conditions. Type II and Type I isotherms were observed for type RD silica gel-water pair and zeolite 13X-water pair, respectively.

The effective diffusivity of zeolite 13X-water pair was found in the range of $2x10^{-8}$-$9x10^{-9}$ m^2/s for the short time period and in the range of $7x10^{-10}$-10^{-8} m^2/s for the long time period. In addition, it was seen that the effective diffusivity was effected from the initial adsorptive concentration and the effective diffusivity was decreased with increasing adsorbate concentration. This may be related to the effects of the heat transfer resistance, surface resistance or hydration and migration of the cations in the structure of the zeolite 13X.

ÖZET

ADSORPSİYONLU ISI POMPALARI İÇİN ADSORBENT ÖZELLİKLERİNİN BELİRLENMESİ

Çevre dostu olan ve termal kaynaklar ile çalıştırılan adsorpsiyonlu ısı pompaları son yıllarda önem kazanmıştır. Birincil enerji verimlilikleri geleneksel ısı pompalarına göre daha yüksek olmasına rağmen, düşük COP ve SCP/SHP değerlerinden dolayı adsorpsiyonlu ısı pompalarının geliştirmeleri gerekmektedir. Adsorpsiyonlu ısı pompası tasarımında uygun çalışma çiftinin seçilmesi, çalışma çiftinin denge ve kinetik özelliklerinin belirlenmesi oldukça önemlidir.

Bu çalışmada, adsorpsiyonlu ısı pompalarında kullanılan çalışma çiftleri tartışılmış, ve adsorpsiyon dengesi ve adsorpsiyon kinetiğinde kullanılan modeller açıklanmıştır. Deneysel çalışmalarda, adsorpsiyon ve desorpsiyon sıcaklıklarının adsorpsiyon kapasitesi ve kütle yayılımı üzerine etkileri incelenmiştir. Adsorpsiyon deneyleri için çalışma çiftleri olarak tip RD silika jel-su ve zeolit 13X-su seçilmiştir. Bunun için iki adet volumetrik sistem kurulmuş; adsorpsiyon deneyleri yapılmış ve basınç değişimleri zamana göre kaydedilmiştir.

Deneysel çalışmalar göstermiştir ki adsorpsiyon kapasitesi adsorpsiyon sıcaklığı arttıkça ve desorpsiyon sıcaklığı azaldıkça artmaktadır, ve aynı şartlar altında zeolit 13X-su çiftinin adsorpsiyon kapasitesi tip RD silika jel-su çiftinden daha yüksektir. Tip II ve tip I izotermleri sırasıyla tip RD silika jel-su çifti ve zeolit 13X-su çifti için gözlenmiştir.

Zeolit-su çiftinin efektif difüzivitesi adsorpsiyonun başlangıç bölgesinde $2x10^{-8}$-$9x10^{-9}$ m^2/s aralığında ve son bölgesinde ise $7x10^{-10}$-10^{-8} m^2/s aralığında bulunmuştur. Ayrıca, efektif difüzivitenin başlangıç adsorptive konsantrasyonundan etkilendiği ve adsorpsiyon konsantrasyonu arttıkça azaldığı görülmüştür. Bu durum ısı transfer direncinin, yüzey direncinin ya da zeolit 13X'in yapısında bulunan katyonların hidrasyonunun ve migrasyonunun etkisine bağlı olabilir.

TABLE OF CONTENTS

LIST OF FIGURES

Figure **Page**

LIST OF TABLES

Tables **Page**

NOMENCLATURE

b	Langmuir Constant
c	adsorptive concentration in fluid phase, kg kg^{-1}
COP	coefficient of performance
D	diffusivity, m^2 s^{-1}
D_c	intracrystalline diffusivity, m^2 s^{-1}
D_p	pore diffusivity, m^2 s^{-1}
D_{eff}	intracrystalline diffusivity, m^2 s^{-1}
D_{kn}	knudsen diffusivity, m^2 s^{-1}
D_m	molecular diffusivity, m^2 s^{-1}
D_s	surface diffusivity, m^2 s^{-1}
D_0	reference diffusivity, m^2 s^{-1}
E	activation energy, J mol^{-1}
E_m	energy density, kJ kg^{-1}
G	Gibbs free energy, kJ kg^{-1}
H	enthalpy, kJ kg^{-1}
h_{fg}	heat of vaporization, kJ/kg^{-1}
K	Henry's law constant
m	mass of dry adsorbent, kg
P	pressure, Pa
P^{sat}	saturation pressure, Pa
q	adsorbed amount, kg kg^{-1}
q_m	monolayer capacity, kg kg^{-1}
q_∞	amount of adsorbed at equilibrium, kg kg^{-1}
$\bar{q}$	average adsorbate concentration, kg kg^{-1}
q_{st}	isosteric heat of adsorption, kJ kg^{-1}
Q_{ev}	heat of evaporation, kJ kg^{-1}
Q_{ab}	heat of isosteric heating process, kJ kg^{-1}
Q_{bc}	heat of isobaric desorption process, kJ kg^{-1}
Q_{cd}	heat of isosteric cooling process, kJ kg^{-1}
Q_{da}	heat of isobaric adsorption process, kJ kg^{-1}
r	pore radius, m

R	particle radius, m
S	entropy, kJ K^{-1}
SCP	specific cooling power, W kg^{-1}
SHP	specific heating power, W kg^{-1}
T	temperature, °C or K
T^{sat}	saturation temperature, K
x	mass fraction of adsorbed adsorbate per dry adsorbent, kg kg^{-1}

Greek letters

$\Delta_a h$	differential heat of adsorption, J mol^{-1}
$\Delta_a H$	integral heat of adsorption, J kg^{-1}
ΔH	heat of adsorption, kJ kg^{-1}
ε_p	porosity
λ	fraction of the adsorbate added in the step
τ_{cycle}	period of cycle
ρ	density, kg m^{-3}
τ	dimensionless time variable

Subscripts

ads	adsorption
cond	condensation
eff	effective
ev	evaporator or evaporation
eq	equilibrium
i	initial
reg	regeneration
sat	saturation
∞	infinite

CHAPTER-1

INTRODUCTION

The increase in the share of energy consumption for cooling and heating applications in both industry and daily life has drawn attention to energy storage, recovery and efficiency. In recent years, the researchers have focused on the use of adsorption technologies in energy recovery and storage systems, especially due to the role of traditional heating and cooling systems in the depletion of ozone layer and in the increase of global warming (Tchernev 1978; Ülkü 1986).

The adsorption-desorption cycle was first used by Close and Dunkle (1977) in order to obtain warm and relatively dry air by using silica gel. By using adsorption-desorption cycle, open and closed systems can be constructed. While the main task in an open cycle systems is dehumidification of air, the extraction of heat from low temperature source to high temperature source is the aim of the closed cycle systems. According to the third energy source, closed cycle systems can be classified as mechanical heat pumps and thermal driven heat pumps. Although the mechanical heat pumps have high coefficient of performance (COP) value, thermal driven heat pumps gained attention due to the environmental issues in recent years.

Thermal driven heat pumps can utilize the waste and solar heat as a third energy source. Thus, they are environmentally friendly systems. Adsorption heat pumps, absorption heat pumps and chemical heat pumps are the kinds of the thermal driven heat pumps. Although adsorption heat pumps are still under investigation, they have some advantages compared of absorption and mechanical heat pumps. Besides having higher primary energy efficiency, they do not contain any hazardous materials and they can operate without noise and vibration.

An adsorption heat pump consists of four components: an evaporator, a condenser, an adsorbent bed and an expansion valve. The adsorbent bed is filled with adsorbent and the working fluid is circulated between adsorber, evaporator and condenser. In adsorption heat pump cycle, which consist of four thermodynamic steps; isosteric heating, isobaric heating (desorption), isosteric cooling and isobaric cooling (adsorption), the adsorption and desorption processes enable the working fluid to

circulate in the cycle without requirement of mechanical energy. Thus, selection of appropriate working pair is quite important for adsorption heat pump systems.

The selection of working pair usually depends on the adsorption isotherm. Although the identification of adsorbent (high affinity, high capacity and selectivity to adsorbate) is usually the only technical consideration, the temperature dependence of the adsorption equilibrium gains attention in the applications of thermal driven processes such as energy storage, refrigeration and heat pumps. The efficiency of the adsorption heat pump mainly depends on the parameters of coefficient of performance (COP), specific cooling/heating power (SCP/SHP) and the energy storage density of the pair, which depend on the operating conditions of the adsorption and desorption processes, and net amount adsorbate of cycled in the system.

There are several adsorbate-adsorbent pairs used in energy recovery systems. Activated carbon-methanol, silica gel-water and zeolite-water are the common working pairs preferred in adsorption systems. While zeolite-water pair is generally selected for heating purposes due to high adsorption capacity, heat of adsorption and energy density, silica gel-water pair is generally preferred for cooling applications and activated carbon-methanol is preferred for applications where temperature is below 0°C (Ülkü 1986).

The long time period of adsorption and desorption processes reduces the specific cooling/heating power of the adsorption heat pump system. The cycle time of adsorption process can be reduced by the enhancement of the heat and mass transfer rate of the pair which depend on the particle size, diffusivity of adsorptive in adsorbent, thermal conductivity of the adsorbent and operating conditions of the process. The mass transfer of fluid through adsorbent occurs in five steps; transport of fluid from bulk fluid to the exterior film surrounding the adsorbent particle, diffusion of the fluid through the surrounding the particle, diffusion of fluid in the pores of the adsorbent particle, diffusion of the fluid along the adsorbent surface and adsorption of solute on the adsorbent surface with surface reaction due to physical or chemical interaction (Cansever-Erdoğan 2011). In a biporous adsorbent, one or more of these steps controls the adsorption rate of the system.

The aim of this study is to investigate the effect of temperature on the adsorption capacity and rate of mass diffusivity. Due to the lack of the enough studies for adsorbate-adsorbent pairs, especially zeolite-water pair, type RD silica gel-water and zeolite 13X-water were selected as working pairs. The experiments were performed at different adsorption temperatures by using both pairs and at different desorption

temperatures by using zeolite 13X-water pair. The detailed information is given in Chapter 5.

The working principles of energy recovery and storage systems are explained in Chapter 2. Also, the adsorption phenomena and the common working pairs used in energy recovery systems are given in this chapter by summarizing the previous studies performed by researchers.

The adsorption equilibrium is represented in Chapter 3. Equilibrium models derived by researchers are summarized. In addition, the heat of adsorption and the experimental methods used in determination of adsorption equilibrium are discussed in this chapter.

In Chapter 4, the detailed information about adsorption kinetics and the adsorption kinetics models are given. The performed studies for reaction based models and diffusion based models are also tabulated in this chapter.

The characterization of the adsorbent and the experimental set up are discussed in the Chapter 5, which is titled as Materials and Methods. Two different experimental setups and the procedures are explained in details.

In Chapter 6, the results are given and discussed. This chapter consists of three parts; the characterization of adsorbents, the effect of adsorption temperature on adsorption equilibrium and the effect of desorption temperature on adsorption equilibrium and kinetics.

The conclusion is given in Chapter 7. The summary of the performed studies and suggestions about these studies are given in this chapter.

CHAPTER 2

ADSORPTION IN ENERGY STORAGE and RECOVERY SYSTEMS

In this chapter, energy recovery and storage systems will be explained. Also, the detailed information about the adsorption phenomena and the common adsorbate-adsorbent pairs used in energy recovery systems are mentioned.

2.1. Energy Recovery and Storage Systems

In recent years, due to the effect of chlorofluorocarbons and similar chemicals on depletion of ozone layer and global warming, studies on adsorption technologies in energy systems, i.e. recovery, storage and conversion of thermal energy, has gained attention. Thermal energy sources such as solar energy, waste energy and peak electricity can be recovered as sensible heat or latent heat during the desorption step and this energy can be used in adsorption step. By using the adsorption-desorption cycle, open or closed cycle systems can be constructed.

2.1.1. Open Cycle Systems

In open cycle systems, adsorbent bed is the key component. The main task of the bed is to dehumidify the air that is passing through it. While the humid air is passing through the bed , its temperature is rising due to the heat of adsorption (Ülkü and Mobedi 1989). The outcoming air can be used for drying and space heating purposes. Continuity of the process can be achieved by the use of two or more beds of adsorbent: while one adsorbs moisture, the other is regenerated by any thermal energy source such as geothermal energy, peak electricity, waste heat or hot combustion gases (Ülkü 1986; Ülkü and Mobedi 1989; Ülkü and Çakıcıoğlu 1991).

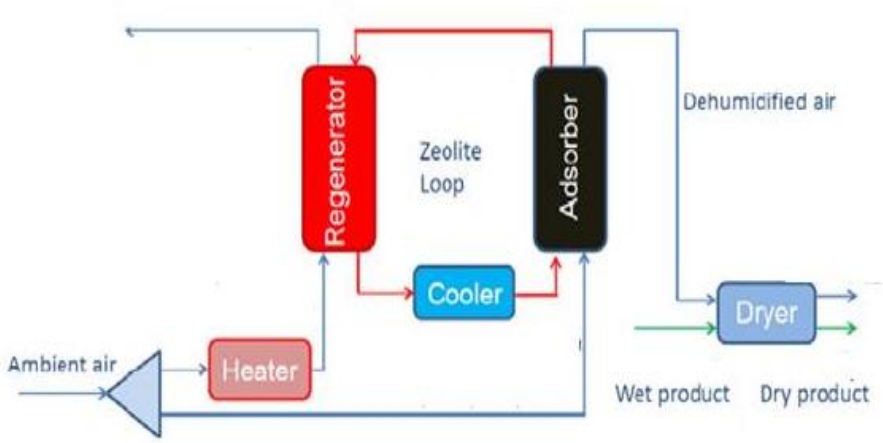

Figure 2.1. Air drying and heating system
(Source: Atuonwu et al. 2011)

2.1.2. Closed Cycle Systems

Main application areas for closed cycle systems are heat pumps and heat transformers. Devices which extract heat from low temperature source to high temperature source are known as heat pumps. Transfer of heat is made by using a third energy source (Figure 2.2).

According to the third energy source, heat pumps can be classified as mechanical heat pumps and thermal driven heat pumps. Adsorption heat pumps, absorption heat pumps and chemical heat pumps are defined as thermal driven heat pumps.

An adsorption heat pump, which can use solar energy and waste energy as third energy source, is environmentally friendly equipment. It works without vibration and operation cost is lower than mechanical systems.

A basic adsorption heat pump consists of four main components: adsorbent bed, evaporator, condenser and an expansion valve. The operation of adsorption heat pump can be outlined by isoster diagrams (Figure 2.3).

a-b: Isosteric heating of the adsorbent bed from T_a to T_b

b-c: Isobaric heating and desorption. Bed temperature is rising from T_b to T_c and desorbed vapor is condensed in condenser at T_{cond}.

c-d: Isosteric cooling of the adsorbent bed from T_c to T_d

d-a: Isobaric cooling and adsorption. Temperature of bed is decreasing from T_d to T_a and vapor coming from evaporator at T_{ev} is adsorbed.

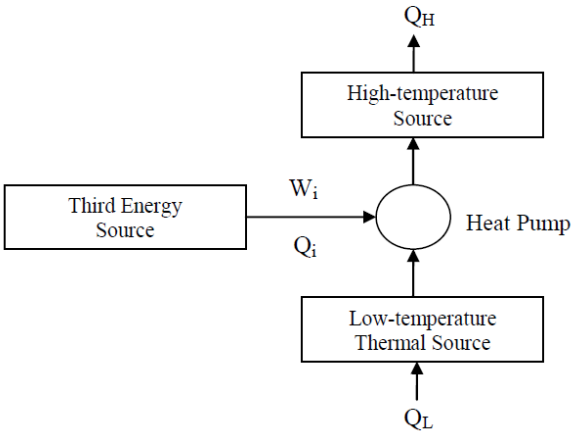

Figure 2.2. Working Principle of Heat Pump
(Source: Yıldırım 2011)

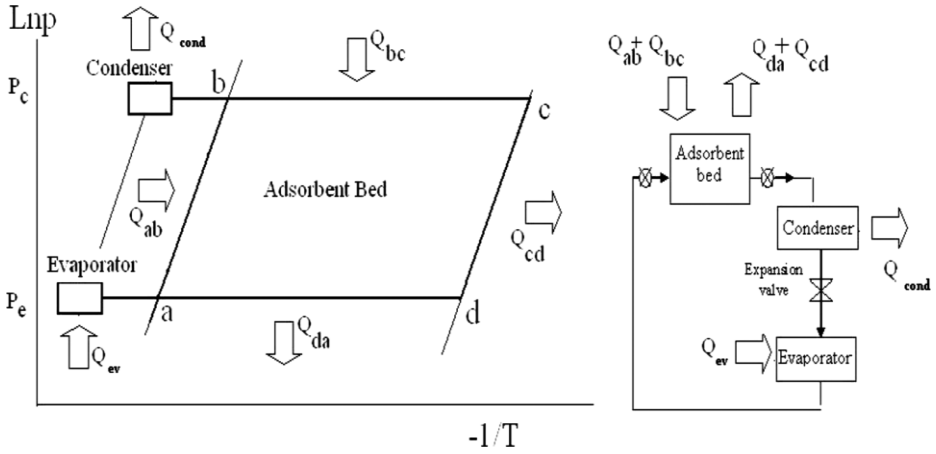

Figure 2.3. Components of Adsorption Heat Pump and Isoster Diagram

The criteria which determine the performance of an adsorption heat pump are the coefficient of performance (COP) and specific cooling and heating powers (SCP/SHP). The basic definition of the COP is the ratio of the amount of useful output to the amount of energy input. In another words, it is the ratio of heat taken from the low temperature heat source (or high temperature source) to the heat transferred from a third energy source. For an adsorption heat pump, the cooling and heating COP can be given as;

$$COP_{cooling}=\frac{Q_{ev}}{Q_{ab}+Q_{bc}} \tag{2.1}$$

$$COP_{heating}=\frac{Q_{c}+Q_{cd}+Q_{da}}{Q_{ab}+Q_{bc}} \tag{2.2}$$

Another important parameter for adsorption heat pump systems is SCP/SHP which can be defined as the cooling/heating power per unit mass of adsorbent and cycle time of adsorption operation. In adsorption heat pump system, it is important to increase the specific cooling power value. Large heat transfer coefficient and short cycle time are the parameters that affect the specific cooling power.

$$SCP=\frac{Q_{e}}{m\tau_{cycle}} \tag{2.3}$$

$$SHP=\frac{Q_{c}+Q_{cd}+Q_{da}}{m\tau_{cycle}} \tag{2.4}$$

Adsorption heat pumps are discontinuous systems. This problem can be solved by the design of multi-bed adsorption heat pump. Another problem in adsorption heat pumps is the requirement of high vacuum which leads to the leakage problem. Differently from the mechanical heat pumps, adsorption heat pumps can also be operated by solar energy, peak electricity, waste heat and geothermal energy in addition to electrical energy. Thus, although COP and SCP adsorption heat pumps are low, the primary energy efficiency is comparable with mechanical heat pump. While the primary energy efficiency of traditional heat pump is %90-100, it is %130-180 for thermal driven heat pumps (Ülkü et al. 1987).

Adsorbent bed is the most important component of the system. One of the main drawbacks of the adsorption heat pump is the low thermal conductivity of the adsorbent. Due to low thermal conductivity of adsorbent, heat transfer rate is low. Therefore, adsorption and desorption cycle periods become longer. Beside thermal conductivity, the characteristics of adsorbate-adsorbent pair, such as density, adsorption equilibria, diffusivity and heat of adsorption, are the other factors that affect the adsorbent bed design.

Energy density is one the most important parameters in choosing the working pair for adsorption heat pump. It is a function of regeneration temperature and heat of adsorption and can be found by the equation (Ülkü and Mobedi 1989);

$$E_m = \int_1^2 (q_{st})dx + \int_1^2 (C_a + x_2 C_w)dT \qquad (2.5)$$

Where 1 and 2 represents the initial and final conditions during the desorption process, C_a and C_w are the specific heat of adsorbent and adsorbate, respectively. The effect of regeneration temperature on energy density is illustrated in Figure 2.4.

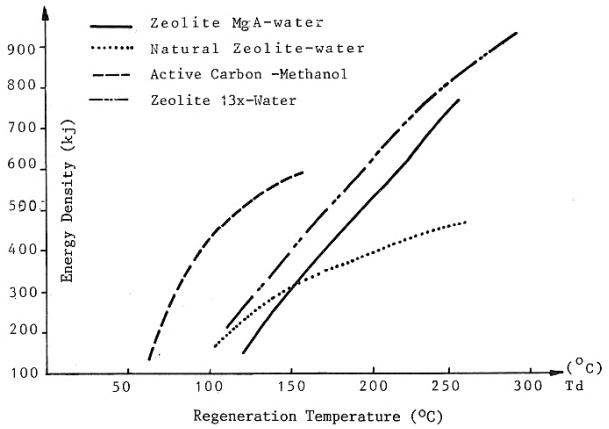

Figure 2.4. Effect of regeneration temperature on energy density
(Source: Ülkü and Mobedi 1989)

2.2. Adsorption

The *adsorption* term first appeared in 1881 to predicate the condensation of gases on free surfaces contrary to gaseous absorption where the molecules of gas penetrate into the mass of the absorbing solid (Gregg and Sing 1982). Adsorption is a surface phenomena which occurs at the solid-fluid interface due to the molecular or atomic interactions. The solid particle, which adsorbs the fluid, is called *adsorbent*. The adsorbed phase, which may be liquid or gas, is called as *adsorbate* and adsorbable substance in the fluid phase is called as *adsorptive*. The adsorbed layer can be removed by increasing the temperature or the decreasing pressure. This process is known as *desorption* (Figure 2.5).

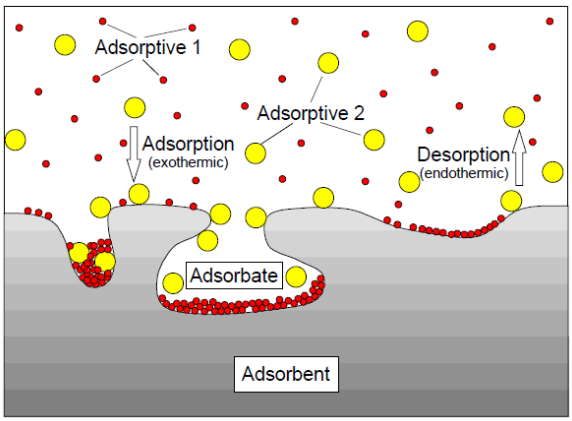

Figure 2.5. Schematic view of adsorption phenomena

Adsorption may occur in two different ways according to the interactions of the adsorbent and adsorbate which are named as physical adsorption (physisorption or Van der Waals) and chemical adsorption (chemisorption). The adsorption processes with nonspecific interactions are generally referred as physisorption. In chemisorption processes, electrons are shared or transferred between two phases. Since chemical bonds occur between the adsorbate and the surface of the adsorbent, new chemical compound is formed. As a result of this, interactions are very strong at the chemisorption processes with respect to the physisorption processes. Also, only monolayer is observed in chemisorption and it is slower than the physisorption process.

Dispersion and short range repulsive forces, H-bonds and covalent bonds can be involved in adsorption processes. In addition, if the solid or the gas is polar in nature, there will be also electrostatic (coulombic) forces comprising dipole-dipole, dipole-induced dipole interactions (Appendix A).

Due to the specific interactions between adsorbate and adsorbent, the heat of adsorption of chemisorption is higher than physisorption and is observed in the short range. However, there are different heat of adsorption ranges for physical and chemical adsorption processes (Table 2.1).

Table 2.1. Heat of Adsorption Ranges for Physisorption and Chemisorption Processes

Researcher & Year	**Physisorption (kJ/mol)**	**Chemisorption (kJ/mol)**
Thomas (1998)	10-40	-
Keller (2005)	10-50	70-200
Inglezakis and Poulopoulos (2006)	5-40	40-800

Adsorption of vapor on a solid surface is a spontaneous process, so the overall free energy change for the process is negative. On the other hand, during the adsorption process, the adsorbing molecules lose a degree of freedom and their entropy decreases. From the thermodynamic relationship given in Equation 2.6 it is obvious that for ΔG to be negative, ΔH should be negative. So, adsorption process generally becomes exothermic.

$$\Delta G=\Delta H-T\Delta S \tag{2.6}$$

However, endothermic behavior can also be observed in some cases. For instance, due to the lateral protein-protein interactions and conformational changes in the adsorbed protein, adsorption becomes endothermic (Katiyar et al. 2010).

2.3. Adsorbate-Adsorbent Pairs Used in Energy Recovery Systems

Characteristics of the adsorbate-adsorbent pairs and selection of the appropriate working pair are the most important task of the adsorption heat pump systems since the available adsorbents are not developed for the purpose of the energy recovery. Availability, low cost, non-toxicity, corrosiveness and minimum loss in performance with repeated cycle are the general constraints for the selection of working pair. Besides, the properties that influence the energy density and the performance are;

- Affinity of the pair for each other
- Adsorption capacity
- Shape of isotherm
- Heat of adsorption
- Thermal conductivity
- Diffusivity of adsorbate through the adsorbent
- Specific heat of the pair
- Rate of adsorption and desorption under specified conditions and possibility of regeneration with available source
- Hysteresis upon thermal cycling
- Cyclic repeatability

- Volume change between loaded states

Water is the most suitable adsorbate for most of the applications due to its features such as nontoxicity and high latent heat of evaporation. Methanol can be used instead of water especially for applications where temperature is lower than 0°C.

2.3.1. Water as Adsorbate

Water is perhaps the most important chemical substance in human life. The molecular structure and the interactions of water molecules with solid surfaces is a trend topic in research areas such as meteorology, electrochemistry, solar energy conversion and physical chemistry.

Water molecules have some special properties. The water molecule is non-linear and the oxygen atom has a higher electronegativity than hydrogen atoms, so while the oxygen atom carries negative charge, the hydrogen atoms are positively charged. Consequently, water is a polar molecule with an electrical dipole moment (Figure 2.6).

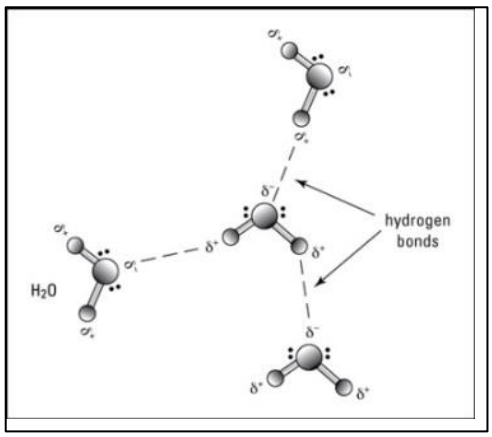

Figure 2.6. Hydrogen bonding in water

In addition to the molecular structure of water, it is used in adsorption processes according to the properties such as non-toxicity, availability, low cost, non-flammability and affinity for the adsorbents.

2.3.2. Adsorbents

In energy systems, some thermophysical properties are required for a good choice of adsorbent.

- Good compatibility with adsorbate
- High surface area
- High adsorption capacity
- Quick response of adsorption capacity to temperature change
- High thermal conductivity
- High mass diffusivity
- Thermal stability

Adsorbents can be classified according to their pore sizes, nature of surfaces and nature of structures. Different pore size classifications were made by researchers as given in Table 2.2.

Table 2.2. Pore Size Classifications
(Source: Zdravkov et al. 2007)

Classification	**Specific pore sizes, d(nm)**					
	Macro	**Meso**	**Micro**	**Super**	**Ultra**	**Sub**
IUPAC	>50	2:50	<2, 2-0.4	0.7:2	<0.7	<0.4
Dubinin	>200-400	200-400>d>3-3.2	<1.2-1.4	3-3.2>d>1.2-1.4	-	-
Cheremkoj	>2000	-	2000>d>200	-	<2:4	<200
Kodikara	10^4-10^5	-	10^3-3*10^4	25-10^3	<3-4	-

The surface structures are also important in classification of adsorbents. According to the affinity of solid to water, adsorbents can be separated as hydrophilic and hydrophobic. Most zeolites have great affinity to water. Low silica zeolites (Zeolite A and X) and the intermediate Si/Al zeolites (chabazite, erionite, clinoptilolite, mordenite and zeolite Y, etc.) are known as hydrophilic and high silica zeolites (beta, ZSM-5 and silicalite, etc.) are called hydrophobic (Flanigen 2001). On the other hand,

activated carbon is considered to be hydrophobic although small amount of water can be adsorbed on oxygen containing sites of activated carbon.

2.3.3. Working Pairs Used in Energy Systems

Although sensible heat is one of the simplest ways for energy storage, there are limitations due to the requirement of large volumes of storage material. Use of heat of adsorption as a latent heat method has gained attention in recent years. However, the selection of appropriate working pair is still one of the main problems for the design of energy system. Several studies were performed in order to determine the proper working pair. The common adsorbate-adsorbent pairs used in energy recovery systems are active carbon-methanol, zeolite-water and silica gel-water.

2.3.3.1. Activated Carbon-Methanol

Actived carbons are carbonaceous solids with a specific surface structure. The surface of the activated carbon is generally nonpolar. However the surface oxide groups in the structure of the actived carbon makes the surface slightly polar. Therefore, although actived carbon has a hydrophobic surface, water can be adsorbed in oxygen containing sites.

Actived carbon has a high surface area and micropore volume. Also, the bimodal (sometimes trimodal) pore size distribution enables adsorbate molecules to access interior of the solid easily (Do 1998) (Figure 2.7). The property of large pore volume enables actived carbon to adsorb nonpolar or weakly polar molecules more easily than other adsorbents. For example, equal weight of actived carbon can adsorb methane twice that zeolite 5A can adsorbed under the same conditions (Yang 2003). Since only non-specific, van der Waals forces are available as the main force for adsorption, the heat of adsorption of activated carbon is usually lower than the other sorbents.

Activated carbons are available in different forms such as powders, microporous, granulated, molecular sieves and carbon fibers. Wang et al. (1997) compared the methanol adsorption of carbon fibre types (ACF_0, ACF_1, ACF_2, ACF_3)

with activated carbon (AC) which were degassed at 120°C under vacuum. They concluded that ACF adsorbed methanol much faster than that of AC based on the isobaric measurement of adsorption capacity: while AC–methanol pairs took three to four days, ACF–methanol took only 12–20 h for the adsorption process at 50°C. The disadvantage of the carbon fibre is the low thermal conductivity which is as low as 0.0893 W/mK (Hamamoto et al. 2006) and is nearly insulating materials. Although carbon fibres have low thermal conductivity than silica gel, the study of San and Lin (2008) indicated that the activated carbon/methanol pair yielded a higher vapor pressure than the silica gel/water pair did and a larger overall heat transfer coefficient was obtained. The pair was also preferred for its high cyclic adsorption capacity.

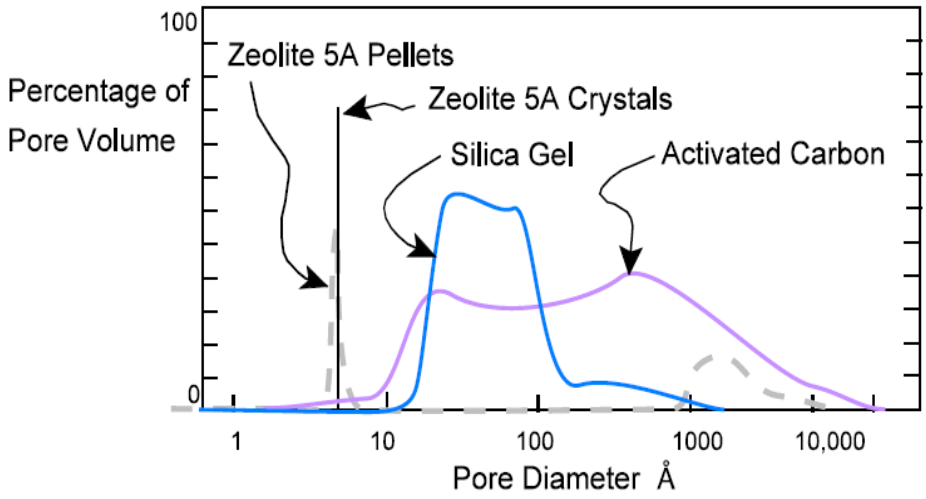

Figure 2.7. Pore Size Distribution of Common Adsorbents
(Source: Knaebel 2003)

According to Hu (1998), decomposition of the methanol into other compounds starts to occur at 120°C although the rate of the decomposition may be very low. Therefore, temperatures above 120°C should be avoided. Since methanol can evaporate at a temperature below 0°C, activated carbon-methanol is generally preferred in ice-making and refrigeration systems. Some of the performed studies in energy recovery and storage systems by using activated carbon-methanol pair are presented in Table 2.3.

Table 2.3. Performed Studies in Energy Systems with Activated Carbon-Methanol Pair

Year	Researcher	Purpose	Temperature (°C)	Max. Adsorption Capacity (kg/kg)	Maximum COP
1998	Wang et al.	Ice Making	-15-100	1.17 (kg/kg day)	0.15-0.23
2000	Leite et al.	Ice Making	-	0.322	0.13
2006	Hamamoto et al.	Cooling	15-150	0.25-0.35	-
2008	San and Lin	Cooling	30-90	0.259	≈ 0.4

2.3.3.2. Silica Gel-Water

Silica gel ($SiO_2.xH_2O$) is an amorphous synthetic silica compound which is hydrated form of silicon dioxide. Since the hydroxyl in the structure of the silica gel can form hydrogen bonds with the polar oxides, it is defined as the adsorption center of silica gel. There is about 5% mass water which cannot be removed and connected to the single hydroxyl group on the surface of silica atoms. If silica gel is heated up to 150°C, it loses this water and adsorption capacity decreases (Srivastava and Eames 1998). Thus, desorption temperature should not be higher than 150°C and should be applied to available low temperature energy sources such as waste heat, solar energy and geothermal energy for adsorption heat pumps.

The most commonly used silica gel types are Type A, Type 3A, Type B and Type RD. High thermal conductivity and surface area give advantage to type RD silica gel in the adsorption processes rather than type A.

Ng et al. (2001) compared the adsorption of water between three types of silica gel. In their study, the silica gels were regenerated at 90°C and 140°C. Although all types of silica gel types have a similar behavior at temperature 90°C, it is observed that the response time for regeneration of Type 3A silica gel is smaller than Type A and Type RD silica gel at 140°C due probably to its higher porous volume. They also determined the equilibrium characteristics of Type 3A and Type RD silica gel with water in temperature ranges of 30-65°C and pressure ranges of 500-6500 Pa and decided that the isotherm was well defined by Henry's relationship. A similar study was

conducted by Chua et al. (2002) and Wang et al. (2004) with Type A and Type RD silica gels at temperature ranges 25-65°C and pressure ranges 500-7000 Pa. In contrast to Ng et al. (2001), Chua et al. (2002) and Wang et al. (2004) observed that the isotherms of selected silica gels-water pairs were defined by Toth's relationship. On the other hand, Aristov et al. (2006) discussed the equilibrium and kinetic behavior of Type RD silica gel-water pair at 29-64°C and 650-6400 Pa with thermogravimetric method. They reported that the equilibrium relationship is described by Dubinin Polanyi potential instead of Toth's and Henry's relationship.

The water adsorption on silica gel was investigated by Demir et al. (2011) by using Tian-Calvet microcalorimetry. The silica gel was regenerated at 120°C and 10^{-5} mbar for 24 h. While the adsorption capacity was higher than %10 (kg_w/kg_s) at the temperature range of 30-40°C, the capacity decreased to %2 (kg_w/kg_s) for the temperatures higher than 75°C (Figure 2.8). Also, the average isosteric heat of adsorption was determined as 2644 kJ/kg for this pair. The effective diffusivity was obtained by using the analytical solution of one-dimensional unsteady isothermal diffusion mass transfer for a spherical particle. While the effective diffusivity for the short time period was in the range of $3.92x10^{-13}$-$2.28x10^{-10}$ m^2/s, in the long term period the range was $1.26x10^{-10}$-$7.03x10^{-11}$ m^2/s.

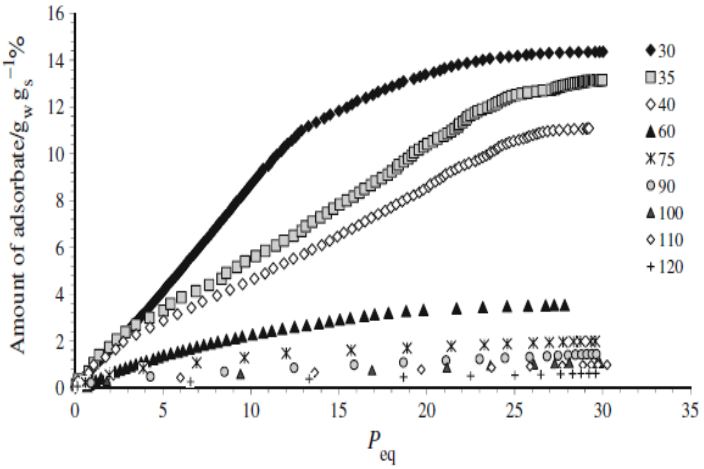

Figure 2.8. Isotherms of water vapor on silica gel
(Source: Demir et al. 2011)

Silica gel-water pair has been used in energy recovery and storage systems since 1970s. However, it does not work at evaporating temperature below 0°C. Some of the performed studies of silica gel-water pair are given in Table 2.4.

Table 2.4. Performed Studies in Energy Systems with Silica gel-Water Pair

Year	Researcher	Purpose	Temperature (°C)	Max. Adsorption Capacity (kg/kg)	Heat of Adsorption (kJ/kg)	Maximum COP
1979	Shigeishi et al.	Drying	30-150	0.37	2560	-
1984	Sakoda and Suzuki	Cooling	20-120	0.25	2800	-
1993	Ülkü	Cooling Heating	-	0.15	-	0.631 1.573
2001	Tahat	Cooling Heating	20-70	0.25	2712	-
2002	Aristov et al.	Air conditioning	20-150	0.55	2440	0.79
2003	Dawoud and Aristov	-	50	0.20	-	-
2004	Akahira et al.	Cooling	50-80	0.28	2800	0.36-0.46
2004	Chua et al.	Chilling	30-90	0.14	2693	0.38
2007	Freni et al.	Chilling	35-100	0.3	-	0.15-0.30
2008	San and Lin	Cooling	30-90	0.116	-	≈ 0.4
2011	Demir et al.	-	30-40	0.1-0.15	2644	-

2.3.3.3. Zeolite-Water

Structure of Zeolite

Zeolites are porous crystalline aluminosilicates. The framework of the zeolite is structurally based on an infinitely extending three dimensional network of AlO_4 and SiO_4 tetrahedra linked to each other by sharing all oxygens. The zeolite structure is represented as;

$$M_{x/n}\left[(AlO_2)_x(SiO_2)_y\right].wH_2O \qquad (2.7)$$

Where M is the cation of valence n, w is the number of water molecules, the ratio y/x has the value of 1-5 due to the structure and the sum of x and y defines the total number of tetrahedra in the unit cell.

Due to the lack of the electrical charge in the region of the AlO_4 tetrahedra, additional positive charges are required to balance the electrical charge and to obtain a stable crystal structure. Replaceable and easily removable cations such as Na, K, Ca and Mg are used as additional positive charges in zeolites. The location, size and number of cations in the zeolite structure are the factors that affect the adsorption properties since they are the adsorption sites of the zeolites.

The porous solid materials that act as sieves on a molecular scale are named as molecular sieves. Molecular sieve zeolites have uniform pore sizes in the range of 3Å-10Å determined by the unit structure of the crystal. The molecules with larger diameter than these pores will be completely excluded. The dehydrated crystalline zeolites have high internal surface area available for adsorption and they show high molecular sieve effect (Breck 1974).

There exist more than 50 natural zeolites and about 150 types of synthetic zeolites which are named by one letter or a group of letters such as 4A, 13X and 5A. Some physical properties of commercial zeolites are given in Table 2.5 (Sircar and Myers 2003).

Table 2.5. Physical properties of Commercial Zeolites
(Source: Sircar and Myers 2003)

Zeolite	**Crystal Framework Si/Al ratio**	**Crystal Structure symmetry**	**Crystal density (g/m^3)**	**Common ion-exchanged forms**	**Pellet density (g/m^3)**	**Bulk density (g/m^3)**	**Nominal pore opening (Å)**
A	0.7-1.2	Cubic	1.52	Na, K, Ag, Mg, Ca	1.20	0.72	3,4,5
X	1.0-1.5	Cubic	1.47	Na, Li, Ca, Ba	1.05	0.68	7.5 (NaX) 10.0 (CaX)
Chabazite	1.6-3.0	Trigonal	1.67	Na, Ca	1.16	0.73	4.9
Clinoptilolite	4.2-5.2	Monoclinic	1.85	K, Ca	-	-	3.5
Silicalite	Very high	Orthorhombic	1.79	none	-	-	3

The micropore structure of zeolite is determined by crystal lattice, so it is precisely uniform and this property separates zeolites from other microporous adsorbents. The adsorption ability of zeolites is related to the proportion between Si and Al, and the adsorption ability increases when this proportion decreases. When the Si/Al ratio increases, the thermal stability also increases. Less energy is required to break the Al-O bonds instead of Si-O bonds. Although most of the zeolites are hydrophilic, aluminum-deficient zeolites with low hydroxyl content becomes hydrophobic (Halasz et al. 2002).

Regeneration of zeolites is generally accomplished at temperatures above 350°C. The regeneration conditions for common zeolites are given in Table 2.6 (Breck 1974). However, the regeneration of zeolites requires attention due to the poor hydrothermal stability of aluminum-rich zeolites at high temperatures. Also, during dehydration process, the cation sites in channels and in the framework cavities changed (Tsitsishvili et al. 1992). So, the temperature of the zeolite should be raised slowly, 2-3°C/min (Yucel and Ruthven 1980), maintaining vacuum during degasing.

Table 2.6. Summary of Zeolite Dehydration
(Source: Breck 1974)

Zeolite	TGA	Structure	Remarks
Erionite	Cont., 14.8%	Stable 750°C	Stable to H2O at 375°C
Faujasite	Cont., 26.2%	Stable to 475°C	-
X	Cont., 26.2%	No change 700°C	Stability varies with cation
Y	Cont., 26%	No change 760°C	Stability varies with cation
Chabazite	Cont., 23%	No change 700°C	Stability varies with cation
Clinoptilolite	Cont., 14%	No change 750°C	-

Adsorption of Water on Zeolite

Zeolites can be used for different purposes. They can be used as adsorbent, ion-exchanger or catalyst in applications such as energy storage and recovery systems, air drying, hydrogenation and dehydrogenation and removal of NH_4 from waste water.

The cationic sites of the zeolites determine the adsorption properties of zeolites and these sites have strong affinity for water. The adsorption of water on zeolites is caused by the specific interactions between water molecules and exchangeable cations

which have the hydrophilic properties. Barrer (1966) observed that the non-specific interactions have a very small effect on water adsorption on zeolite and yields low heat of adsorption value.

The effect of the cations on adsorption capacity and heat of adsorption of zeolite X-water pair were determined by Dzhigit et al. (1971). The increase in cation dimensions and the decrease in number of large cavities per g zeolite led to decrease in both adsorption capacity and heat of adsorption.

In water adsorption on zeolites, a rectangular isotherm is generally observed. According to Carrott et al. (1990) while the amount of adsorption at low relative pressures depends on the specific interactions between adsorbate and adsorbent, the micropore size and shape affect the adsorption at higher relative pressures.

Several studies in applications of energy recovery and storage systems with zeolite have been reported. For instance, Ülkü et al. (1985) determined the performance of natural zeolites for energy storage and air drying systems. They found that if a waste heat at 200°C was obtained, 0.12 kg H_2O/kgdryzeolite was adsorbed. By this way, energy stored in the temperature range of 20-200°C will be 600 kJ/kgdryzeolite. When the temperature range is changed to 20-110°C, the energy stored will be reduced to 310 kJ/kgdryzeolite.

Ülkü and Mobedi (1989) studied adsorption in energy storage systems for different adsorbate-adsorbent pairs. They concluded that for high temperature long term operations zeolite MgA-water is most suitable pair due to its high adsorption capacity and energy density. The study of Cacciola and Restuccia (1995) supported that result. They compared zeolite 4A-water, zeolite 13X-water and activated carbon-methanol pairs for heating and cooling applications and decided that zeolite-water pair is more applicable for heating purposes. Many other researchers used zeolite-water pair in their studies for energy recovery and storage systems. Some of these studies are summarized in Table 2.7.

Ryu et al. (2001) discussed the adsorption equilibrium and kinetics of water on zeolite 13X by using gravimetric method. They made desorption of zeolite 13X for 7 hours in a furnace at 340°C and performed adsorption experiments in the temperature range of 25-45°C and pressure range of 660-9300 Pa. Although type I isotherm is generally observed for zeolite 13X-water pair, they obtained Type II isotherm for this pair which may result from the inefficient regeneration of zeolite 13X.

Kim et al. (2003) also performed a volumetric study for adsorption of water on zeolite 13X which was regenerated at 150°C in a drying vacuum oven. It was seen that while type II isotherm was observed at 20°C, Type I isotherm was obtained at higher temperatures (Figure 2.9).

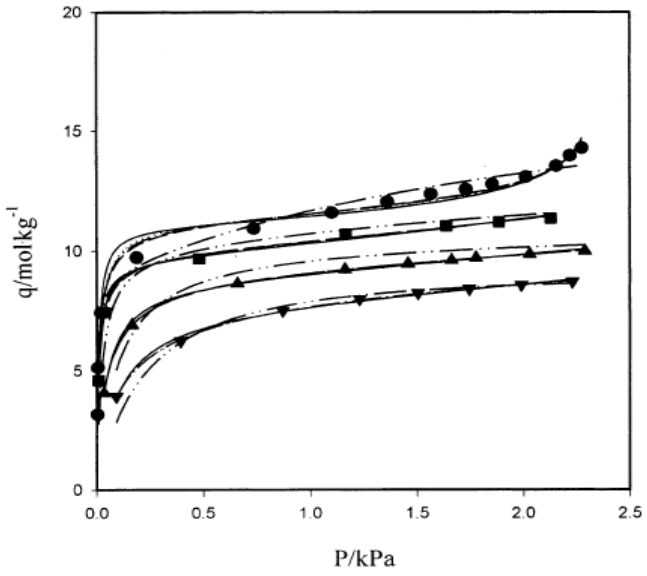

Figure 2.9. Experimental and correlated isotherms for water vapor adsorption onto zeolite 13X at various temperatures: ●293.2K; ■, 313.2 K; ▲, 333.1 K; ▼, 353.1 K (Source: Kim et al. 2003)

The regeneration of adsorbents requires attention in most studies. The effect of desorption temperature on adsorbed amount of water on clinoptilolite was studied by Ozkan (1991) and Cakicioglu-Ozkan and Ulku (2005). The sample was regenerated at temperatures of 160, 250, 400 and 600°C for 16 h under vacuum higher than 10^{-3} Pa. It was found that when the temperature was raised up to 400°C, the amount of adsorbate also increased due to an effective regeneration. However, if the regeneration temperature was increased to 600°C, the degradation in the framework structure of zeolite occurs and the adsorption amount decreased (Figure 2.10). According to the adsorption equilibria and kinetics of water-clinoptilolite pair, Ozkan (1991) also concluded that this pair could be used in air drying and energy storage systems.

The effect of regeneration temperature on coefficient of performance of adsorption heat pumps for different working pairs was studied by San and Lin (2008). For silica gel-water and activated carbon-methanol pairs the COP values decrease when the temperature is greater than 120°C. On the other hand, when the temperature of

zeolite 13X-water pair is raised from 120°C to 150°C, both the COP value and adsorption capacity increase.

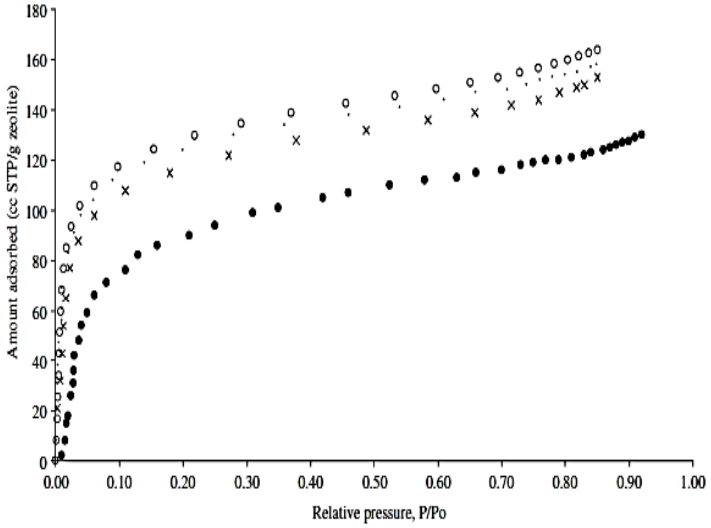

Figure 2.10. Water vapor adsorption isotherm of the CLI outgassed at 160°C (×), 250°C (•), 400°C (○) and 600°C (●) (Source: Ozkan 1991; Cakicioglu-Ozkan and Ulku 2005)

Table 2.7. Performed Studies in Energy Systems with Zeolite-Water Pair

Year	Researcher	Zeolite Type	Purpose	Temperature (°C)	Max. Adsorption Capacity (kg/kg)	Heat of Adsorption (kJ/kg)	Maximum COP
1978	Tchernev	Chabazite	Heating Cooling	25-120	0.26	-	0.70 0.42
1979	Shigeishi et al.	13X	Drying	30-350	0.3	4400	-
1979	Shigeishi et al.	4A	Drying	30-350	0.22	4400	-
1982	Gopal et al.	13X	-	25-250	0.33	2770-5000	-
1986	Ülkü	Natural zeolite	Cooling Heating	-	0.14	3000	1.33 0.34
1986	Ülkü	Clinoptilolite	Cooling Heating	20-240	0.12	3000	1.65
1986	Ülkü et al.	Natural zeolite	Cooling Heating	-	-	3540	0.09 0.37
1991	Ülkü and Çakıcıoğlu	Clinoptilolite	Drying	-	0.01-0.115	2500-10000	-
2005	Liu and Leong	13X	Cooling	25-200	-	3200	0.43
2006	Wang et al	13X	Air Conditioning	40-450	-	-	0.25
2008	San and Lin	13X	Cooling	30-120	0.236	-	0.2
2009	Bauer et al.	ALPO/Al	Refrigeration	27-120	0.07-0.15	2644	-

CHAPTER 3

ADSORPTION EQUILIBRIA

Adsorption equilibria can be defined as the amount of adsorbate taken up by the adsorbent at specified temperature and pressure. Surface characteristic and pore structure of the adsorbent, adsorbate characteristic and working temperature and pressure identify the adsorption equilibrium.

Adsorption equilibrium can be represented by equilibrium relationships and plots. If the adsorbed amount is plotted as a function of pressure at constant temperature, the plot is called as isotherm (Figure 3.1a). Isobar represents the plot of amount adsorbed as a function of temperature at constant pressure (Figure 3.1b). Finally, if the pressure is plotted as a function of temperature at constant amount of adsorbate, then the plot is called as isoster (Figure 3.1c). In all types of plots, the pressure represents the adsorptive concentration in equilibrium.

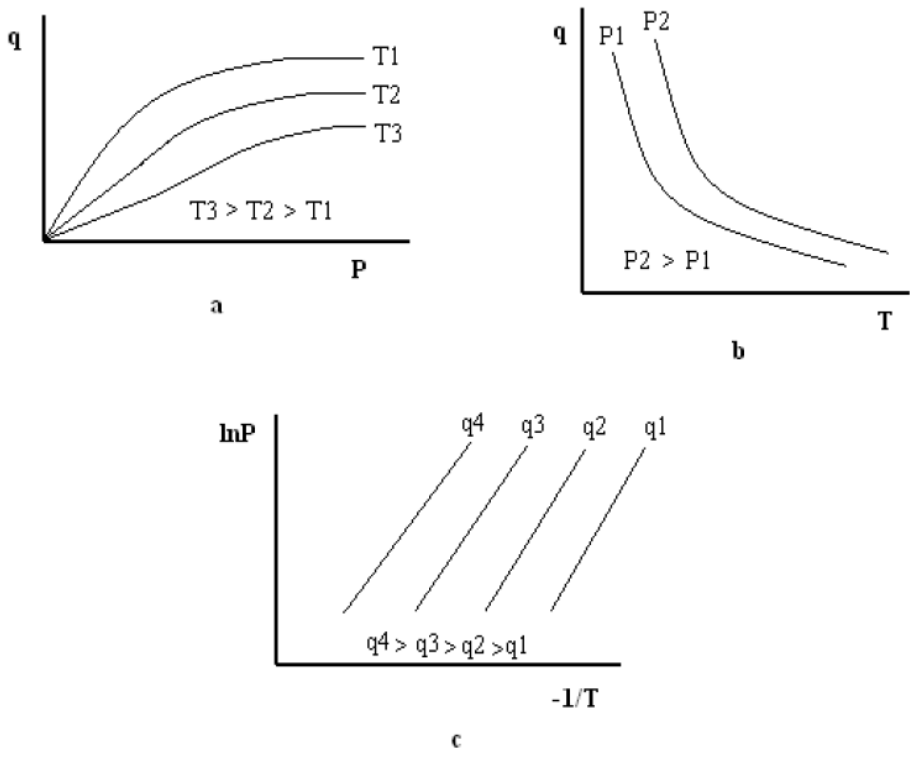

Figure 3.1. Adsorption Equilibrium plots a) isotherm, b) isobar, c) isoster

Due to the interactions between adsorbate and adsorbent, the isotherms of different working pairs are classified into six classes in the IUPAC classification (Gregg and Sing, 1982).

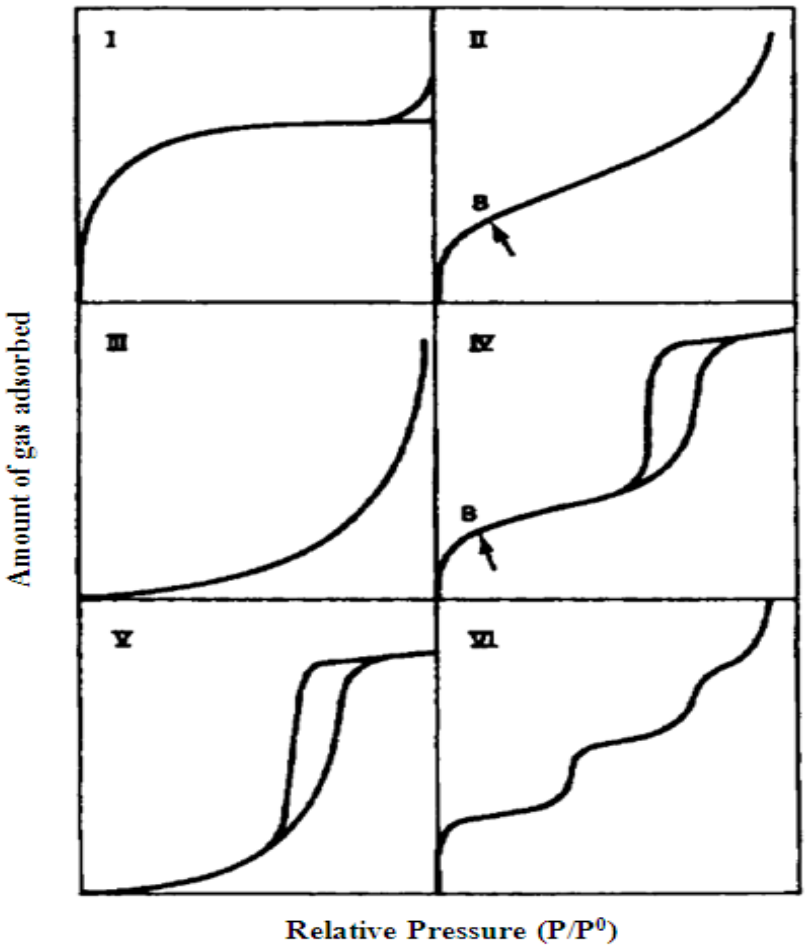

Figure 3.2. Types of adsorption isotherms

Type I isotherm is generally observed in adsorption on microporous adsorbents having relatively small external surface area. The flat in the isotherm means that the pores of the adsorbent are filled with adsorbate, and monolayer coverage is observed.

Type II isotherm refers to adsorption on non-porous or macroporous adsorbent. Point B in type II represents the end of the monolayer coverage and start of multilayer adsorption.

Type III isotherm is related to adsorption on macroporous or non-porous adsorbents. Since the interactions of molecules are larger than the interactions between the adsorbate and adsorbent, multilayer adsorption is observed.

Although there is a similarity between type II and type IV isotherms, hysteresis loop is observed in type IV isotherm because of the capillary condensation in mesopores.

Type V isotherm is also observed in mesoporous adsorbents. Type IV and Type V isotherms are characteristics of multilayer adsorption and as in the case of type III isotherm; type V isotherm is related to weak interactions between adsorbate and adsorbent.

Type VI isotherm is related to the stepwise multilayer adsorption in non-porous adsorbents. The height of the steps represents the capacity of monolayer adsorption.

3.1. Adsorption Equilibrium Models

There are several models defining adsorption equilibrium for which coefficients are calculated by experimental studies. Henry's, Freundlich, Langmuir, Toth's and Dubinin-Astakhov, Dubinin-Radushkevich relationships are some of these models.

3.1.1 Henry's Relationship

Henry's equation is the most common equation and form basis for many equilibrium equations. All the adsorbate molecules are isolated from their neighbors at low concentration or low pressure of adsorbate. In both cases, Henry's relationship which is a function of temperature and pressure represents the adsorption equilibrium. Henry's equation which has been used widely in literature (Yucel and Ruthven 1980; Ruthven 1984; Suzuki 1990; Valsaraj and Thibodeaux 1999; Ng et al. 2001). It is defined by:

$$q=KP \tag{3.1}$$

Where q denotes adsorption adsorbed amount K is adsorption equilibrium constant and derived from Van't Hoff equation.

$$K=K_0 e^{\Delta H/RT} \tag{3.2}$$

3.1.2. Langmuir Relationship

This is a theoretical equation which is derived by the assumption that the surface is homogeneous. In other words the heat of adsorption is independent of surface coverage (Ruthven 1984; Do 1998). The adsorbate molecules are adsorbed on specific sites of the adsorbate and only monolayer coverage is observed.

According to Langmuir's relationship, for an ideal surface, the adsorption rate will equal to the desorption rate. The Langmuir relationship is based on this equality. Langmuir equation is defined by the equation 3.3. Several researchers such as Hall et al. (1966), Parfitt (1978), Gregg and Sing (1982), Ruthven (1984), Do et al. (1992), Kim et al. (2003), Hamamoto et al. (2006), Cansever-Erdoğan and Ülkü (2011) have used this equation in order to define adsorption equilibrium in their studies.

$$q=q_m \frac{bP}{1+bP} \tag{3.3}$$

Where P is pressure and q_m is the monolayer coverage. Parameter b is the Langmuir (affinity) constant and it represents the strength of the interaction since it directly depends on the heat of adsorption or activation energy for desorption (Do 1998).

3.1.3. Freundlich Relationship

Freundlich equation is an empirical equation to describe the adsorption equilibrium. Freundlich relationship has been used in several studies performed by Sakoda and Suzuki (1986), Gray and Do (1992), Cho and Kim (1992), Afonso and Silveria (2005), Liu and Leong (2006), Gerente et al. (2007) and Leppäjärvi et al. (2012). It is represented by the equation given below:

$$q=q_\infty * \left(\frac{P}{P^{sat}}\right)^{1/n} \tag{3.4}$$

Where q_∞ is the limiting amount adsorbed, n is a constant, q is the equilibrium adsorbed amount, P is the pressure and P^{sat} is the saturation pressure at a specific temperature. The parameter n is usually greater than unity, and the larger this parameter is, the more deviation from linearity is observed in the isotherm.

3.1.4. Toth's Relationship

Toth's Equation is one of the frequently used empirical formula which can be valid at low and high pressure ranges. It originates from Henry's equation. This equation describes many systems well with sub-monolayer coverage, and it has the following form used by several researchers such as Do (1998), Chua et al. (2002), Kim et al. (2003), Wang et al. (2009), Leppäjärvi et al. (2012):

$$q=\frac{K_0 \exp(\Delta H_{ads}/RT)P}{\left\{1+\left[K_0/q_m \exp(\Delta H_{ads}/RT)P\right]^n\right\}^{1/n}} \tag{3.5}$$

Where q is the adsorbed quantity of adsorbate by the adsorbent under equilibrium conditions, q_m denotes the monolayer capacity, P is the equilibrium pressure of the adsorbate in the gas phase, T is the equilibrium temperature of the gas-phase adsorbate, R is the universal gas constant, ΔH_{ads} is the isosteric enthalpies of adsorption, K_0 is the pre-exponential constant and n is a parameter which is usually less than unity and defines the heterogeneity of the system. If parameter n diverges from 1, the system will be more heterogeneous (Do 1998).

3.1.5. Dubinin-Radushkevich Relationship

Dubinin-Radushkevich equation is a semi-empirical equation where adsorption process follows a pore-filling mechanism. The chemical potential is a function of adsorbed amount in the case of pore filling mechanism, while it is independent from adsorbed amount in the case of surface layering. Dubinin-Radushkevich equation is represented by;

$$q=q_0 \exp\left[-\gamma\left(T\ln\frac{P_{sat}}{P}\right)^2\right] \tag{3.6}$$

Where γ is the constant for specific pair, q_0 is the saturated adsorption capacity, T is the temperature, P_{sat} is the saturation pressure and P is the pressure.

Dubinin-Radushkevich relationship is generally used in the description of sub-critical vapor adsorption on microporous solids such as activated carbon and zeolite. Gregg and Sing (1982), Ülkü and Mobedi (1989), Lavanchy et al. (1996), Jaroniec (1997), Teng et al. (1996), Sumathy et al. (2003), Saha et al. (2007) have explained the equilibrium relationship of adsorbate-adsorbent pair by using D-R relationship in their studies.

3.1.6. Dubinin-Astakhov Relationship

When the degree of the heterogeneity increases due to a wider pore size distribution, Dubinin-Radushkevich does not describe the equilibrium data well. Therefore, Dubinin and Astakhov (1971) proposed the Dubinin-Radushkevich equation to allow for the surface heterogeneity. Dubinin-Astakhov relationship is represented as:

$$q=q_0 \exp\left[-D\left(T\ln\frac{P_{sat}}{P}\right)^n\right] \tag{3.7}$$

Where q_0 is the saturated adsorption capacity and P_{sat} is the saturation pressure. D and n are the constants of the equation which depend on the working pairs.

A modified form of Dubinin Astakhov relationship which was used by authors such as TamainotTelto and Critoph (1997), Critoph (2000), Chahbani et al. (2004), Wang et al. (2009) can be given as:

$$q=q_0 \exp\left(-K\left(\frac{T_z}{T^{sat}}-1\right)^n\right) \tag{3.8}$$

Where q_0 is the saturated adsorption capacity and T^{sat} is the saturation temperature. K and n are the constants of the equation which depend on the working pairs.

3.1.7. Three-term Langmuir Relationship

When the simple Langmuir relationship is inadequate in description of adsorption equilibrium, it is convenient to use two or three terms of Langmuir relationship with the assumption that there are two or three sites for adsorption with energy of adsorption constant at each site (Parfitt 1978). So, especially in systems that zeolite is used as adsorbent, three-term Langmuir relationship can be used in the definition of adsorption equilibria. The equation of the three term Langmuir relationship can be given as:

$$q=\frac{q_{s1}b_1P}{1+b_1P}+\frac{q_{s2}b_2P}{1+b_2P}+\frac{q_{s3}b_3P}{1+b_3P} \tag{3.9}$$

where $q_{s,i}$ and b_i (i=1,2,3) are functions of temperature and defined as;

$$q_{s,1}=\sum_{i=0}^{3}\frac{a_i}{T^i} \tag{3.10}$$

$$q_{s,2}=\sum_{i=0}^{3}\frac{c_i}{T^i} \tag{3.11}$$

$$q_{s,3}=0.276-q_{s,1}-q_{s,2} \tag{3.12}$$

$$b_i=b_{0,i}\exp\left(\frac{E_i}{T}\right) \tag{3.13}$$

3.1.8. Experimental Correlations

Experimental correlation which is convenient for energy storage applications can be used to evaluate adsorption equilibrium. The equilibrium condition for working pair can be determined by the following equation:

$$\ln P = a(q) + \frac{b(q)}{T} \tag{3.14}$$

$$a(q) = a_0 + a_1 q + a_2 q^2 + a_3 q^3 \tag{3.15}$$

$$b(q) = b_0 + b_1 q + b_2 q^2 + b_3 q^3 \tag{3.16}$$

Where P is the pressure (mbar), T is the temperature (K), a and b are the parameters depending on q which is the percentage content of the adsorbate.

Ülkü et al. (1986), Mobedi (1987), Douss and Meunier (1988), Cacciola and Restuccia (1995) and San (2006) have used experimental correlations in order to define adsorption equilibria of working pairs used in energy recovery systems.

3.2. Heat of Adsorption

The thermodynamic relationship that indicates the exothermic behavior of an adsorption process was given in Equation 2.6. The heat evolved from the system is known as the heat of adsorption. When heat is released, a portion of heat energy is absorbed by the solid while the remaining is dispersed to surrounding. The absorbed portion of energy increases the adsorbent temperature and slows down the adsorption rate of the process (Do 1998). The information about the interactions between the fluid and the solid phases can be obtained from the heat of adsorption value. High value of heat of adsorption points to the strength of the interactions between the adsorbate and adsorbent. Also, the temperature profile for the regeneration of adsorbent can be determined by using the magnitude heat of adsorption. For a specific pair, heat of adsorption depends on temperature, pressure and surface coverage.

Heat of adsorption can be described by three equations: differential heat of adsorption, integral heat of adsorption and isosteric heat of adsorption

3.2.1. Differential Heat of Adsorption

In an adiabatic process which means there is no heat transfer with the surrounding, the heat evolved during the adsorption is known as the differential heat of adsorption. It can be also defined as the internal energy change of a complete adsorption process, produced by a small amount of adsorbate at constant temperature, volume and surface area.

$$\Delta_a h = -\left(\frac{\partial Q}{\partial n_a}\right)_T + V\left(\frac{\partial P}{\partial n_a}\right)_T \tag{3.17}$$

Where $\Delta_a h$ is the differential heat of adsorption in the adsorbed phase, Q is the heat transferred, n_a is the amount of adsorbate, V is the volume of the system and P is the pressure (Gregg and Sing 1982). The differential heat of adsorption can be directly measured by the calorimetric method.

3.2.2. Integral Heat of Adsorption

Integral heat of adsorption is the total heat released from initial state to final state of adsorbate loading at constant temperature. The integral heat of adsorption is obtained by integrating the differential heat of adsorption against the amount of adsorbate. It is formulized as the following equation:

$$\Delta_a H = \int_0^{n_a} \Delta_a h dn_a \tag{3.18}$$

Where $\Delta_a H$ is the integral enthalpy of adsorbed phase.

3.2.3. Isosteric Heat of Adsorption

Under equilibrium conditions, the Gibbs free energy of adsorbate and adsorptive is equal. Isosteric heat of adsorption can be calculated by using the adsorption isotherms and Clausius-Clapeyron relation by neglecting the difference of the heat capacity of adsorbate in two phases.

$$\frac{d\ln P}{d(-1/T)} = -\frac{\Delta H}{R} = \frac{q_{st}}{R} \tag{3.19}$$

Where P is the pressure, T is the temperature, $-\Delta H$ is the heat released during the adsorption and is called as isosteric heat of adsorption, q_{st}, and R is gas constant.

According to the ideal Langmuir relationship, the heat of adsorption is independent of adsorbate amount when the adsorption sites are energetically homogenous and when there is no interaction between adsorbates. However, it is not logical to ignore the surface heterogeneity and the interactions between adsorbates in real systems. In many systems, the heat of adsorption decreases with the increasing surface coverage. Due to the application area, the desired value of heat of adsorption changes. For instance, while high heat of adsorption is desired for heating applications, low value of heat of adsorption is generally preferred for cooling purposes.

3.3. Experimental Techniques to Determine Adsorption Isotherm and Differential Heat of Adsorption

In the selection of the appropriate working pair for an energy recovery system, the adsorption equilibrium should be well defined. From the adsorption equilibrium data, the maximum adsorption capacity and heat of adsorption can be derived. The adsorption isotherm can be determined by using different experimental techniques as a function of pressure at constant temperature. Thus, the amount of adsorption of working pairs at various temperatures and pressures should be measured. Volumetric, gravimetric and calorimetric methods are three common techniques to obtain adsorption isotherm and heat of adsorption.

3.3.1. Volumetric Method

The volumetric method which is also known as manometry is the most common technique in measuring adsorbed amount. In this method, the pressure changes before and after adsorption in a closed system are measured. In calculation of adsorbate amount on adsorbent, the equation of ideal gas relationship is generally used.

Basic set up of the volumetric system is shown in Figure 3.3. A volumetric system mainly consists of an adsorption vessel, a gas storage vessel and a vacuum pump in order to study at low pressure.

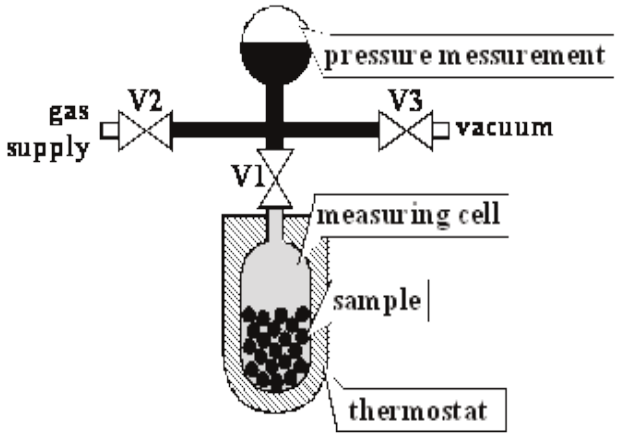

Figure 3.3. Basic set up for volumetric system

Kim et al. (2003) studied the adsorption equilibrium of alumina, zeolite 13X and zeolite x/activated carbon composite and water pairs with volumetric system. They determined the physical properties of the adsorbents by micromeritics (ASAP 2010), using nitrogen as adsorbate at 77 K. Ng et al. (2001), Chua et al. (2002) and Wang et al. (2004) also used ASAP 2010 device to characterize the silica gel and measured adsorbed amount of water vapor on silica gel by a volumetric system. Özkan (1991) used a volumetric measurement device, Coulter Omnisorp 100 CX, in order to determine the adsorption properties of clinoptilolite-water pair. Furthermore, Ülkü et al. (1998) obtained the adsorption and desorption isotherms of water vapor for wool and Balköse et al. (1998) carried out a study water vapor adsorption on humidity-indicating silica gel by Coulter Omnisorp 100 CX.

3.3.2. Gravimetric Method

Gravimetric technique in adsorption processes is used to characterize porous media, to determine adsorption equilibria and to investigate adsorption kinetics. In gravimetric system, the amount of the adsorbed is directly determined by measuring the weight change of adsorbent as a function of time by using a microbalance system. The pressure of the adsorbate is kept constant in the gravimetric method. It is possible to observe the approach to equilibrium during the adsorption process at the displayer in the gravimetric method, which is the main advantage compared to volumetric method. The setup of gravimetric analyzer is given in Figure 3.4.

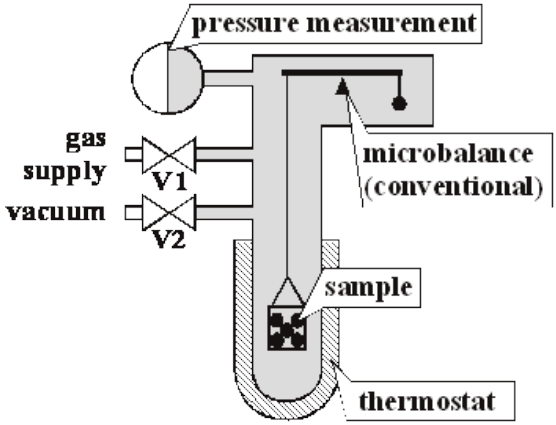

Figure 3.4. Schematic view of gravimetric analyzer

Several studies have been reported on estimation of adsorption equilibrium and kinetics gravimetrically by using thermo-gravimetric analyzer (TGA), magnetic suspension balance. For instance, in addition to volumetric method Ülkü et al. (1998) obtained the adsorption and desorption isotherms of water vapor for wool by gravimetric method employing a Cahn 2000 electronic microbalance. Ryu et al. (2001) determined the adsorption isotherm of zeolite 13X-water pair and observed that the isotherm was well fitted with the Freundlich-Langmuir model. Aristov et al. (2006) studied kinetics of Fuji RD silica gel-water pair by using CAHN 2000 thermobalance in the temperature range of 29-64°C and pressure range of 6.5-34 mbar. Cakıcıoglu-Ozkan and Ulku (2008) performed a study to measure the kinetics of water adsorption on clinoptilolite. Another study was conducted by Cortes et al. (2010). They studied water adsorption on zeolite 13X and compared thermo-gravimetry by mass spectroscopy.

3.3.3. Calorimetric Method

Calorimetric method is based on the measuring heat which might be generated (exothermic process), consumed (endothermic process) or simply dissipated by a sample. There are several calorimetric techniques mentioned in literature. The main four categories which are used in physisorption systems are adiabatic calorimeters, diathermal conduction calorimeters, diathermal compensation calorimeters and isoperibol calorimeters (Rouquerol et al. 1999).

In adiabatic calorimeters, in order to prevent any exchange of thermal energy between sample and surrounding, the sample temperature is followed by surrounding temperature. In diathermal-conduction calorimeters, by using either a heat flowmeter or a phase change detection system, sample temperature follows surroundings temperature by simple conduction. Due to the complexity of the systems and uncertainty, the diathermal compensation calorimeters and the isoperibol calorimeters are not used today.

In all calorimetric techniques, Tian-Calvet calorimetric system which is a type of diathermal-conduction calorimeters is the most suited system for studying the relatively slow thermal process associated with gas adsorption in isothermal microcalorimetry. Tian-Calvet microcalorimetry consists of three main components which are sample bed, heat sink and thermopile (Figure 3.5). The sample cell is placed into the sample bed. Thermopile which is made from thermocouples and connected in series covers the sample bed. The functions of the thermopile are to release heat from sample cell to heat sink block during adsorption and to generate signal. The signal is received as mW versus time by software. The differential heat of adsorption is obtained by integrating the curve (Demir, 2008).

Dunne et al. (1996) measured isosteric heat of adsorption and adsorption isotherms for a series of gases increasing size and magnitude of quadrupole moment (Ar, O_2, N_2, CH_4, C_2H_6, SF_6, CO_2) on adsorbents of varying pore structure and ion type (NaX, H-ZSM-5, Na-ZSM-5) by Tian-Calvet calorimetry. Also, Spiewak and Dumesic (1997) measured differential heat of adsorption on reactive catalysis surfaces.

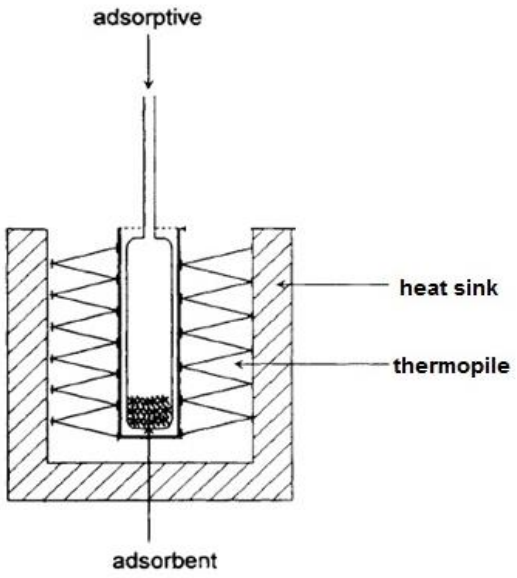

Figure 3.5. Schematic View of Tian-Calvet Calorimetry

A study was performed by Ertan (2004) in order to determine N_2, CO_2 and Ar adsorption on zeolite 5A and 13X at 25°C. Ülkü et al. (2006) investigated the adsorption of water vapor on zeolitic tuff and zeolite 4A to evaluate the availability of substitution of zeolitic tuff with zeolite 4A in air drying and heat pumps. Demir et al. (2011) studied the adsorption of silica gel-water pair by and also determined the differential heat of adsorption of this pair.

CHAPTER 4

ADSORPTION KINETICS

4.1. Mass Transfer in and Through an Adsorbent Particle

To design an adsorption heat pump, the kinetic performance of the working pair should be known in addition to the adsorption equilibria. The understanding of the adsorption dynamics and determination of the adsorption rate of the system is important in the estimation of the response time for the process.

Adsorption dynamics can be explained by the movement of the working fluid in and through the adsorbent particle and occurs in five steps as shown in Figure 4.1. In the first step, the fluid is transferred from bulk solution to the external surface of the particle (1-2) which has porous structures and the adsorbate molecules diffuse through the pores of the adsorbent (2-3). If the adsorbent has a microporous structure, the adsorbate also diffuses into the micropores (3-4). As mentioned before, adsorption occurs due to the physical or chemical interactions between the fluid and the solid states (4-5). In the last step, diffusion of the adsorbed molecules in the sorbed state occurs (5-6).

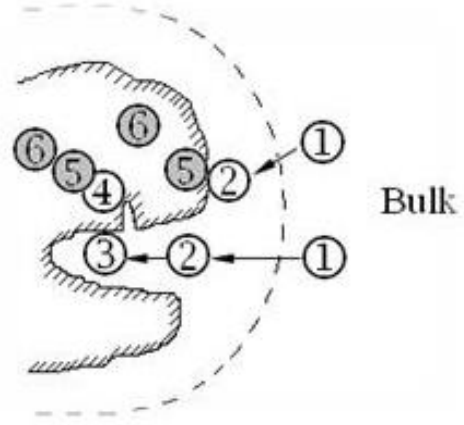

Figure 4.1. Adsorption steps

For a biporous adsorbent, although the resistances related to all these steps (diffusional resistance in bulk fluid, diffusional resistance in laminar fluid film, skin resistance at the surface of the particle, diffusional resistance in the meso and

macropores, a possible barrier to mass transfer at the external surface of the microparticle, and diffusional resistance in the micropores within the microparticles) are quite effective, one of these steps may control the transport process.

When the diffusional resistance in the macropores controls the adsorption rate, the rate depends on the particle size of the adsorbent and there is a concentration gradient through the macropores. On the other hand, in the case of diffusional resistance in micropore control, the adsorption rate depends on the crystal size instead of particle size of the adsorbent. Also, the concentration through the particle is uniform.

4.1.1. Diffusion in Micropores

Since the adsorbate molecules and the micropores are nearly equal in size, the interactions between the fluid and the pore wall in microporous adsorbents are became dominated. In such systems, the adsorbate molecules cannot escape from the pores and the diffusion occurs with a random jump of the adsorbate molecules from one site to next site. It is difficult to distinguish the fluid phase and solid phase in micropores because of the strong interactions and these phases are considered as a single phase. So, the diffusion can be defined as the "intracrystalline diffusion" or "micropore diffusion".

As mentioned above, diffusion through micropores is independent from the particle size. For a spherical and microporous particle, the mass transfer equation can be written by Fick's second law:

$$\frac{\partial q}{\partial t} = \frac{1}{r^2}\frac{\partial}{\partial r}\left(r^2 D_c \frac{\partial q}{\partial r}\right) \tag{4.1}$$

Where r is the pore radius, D_c is the intracrystalline diffusivity and q(r,t) is the adsorbed phase concentration.

Based on the Fick's law, simplified models were derived to calculate the micropore diffusion from the uptake curves (Boyd et al. 1947; Carman and Haul 1954; Crank 1975; Karger and Ruthven 1992). These models which are used for isothermal systems are summarized in Table 4.1.

4.1.2. Diffusion in Macropores

During the adsorption on a porous particle, the adsorptive molecules diffuse through the pores of the adsorbent. The transfer of the molecules through these pores is controlled by three different mechanisms due to the relationship between the mean free path of molecules and pore diameter. These mechanisms are; Knudsen diffusion, molecular diffusion and surface diffusion.

When the mean free path is larger than the pore diameter, the collisions between molecules and solid surface occur. This type of diffusion is called as Knudsen diffusion (Figure 4.2a.). Knudsen diffusivity changes only with temperature, and it is independent from pressure since the mechanism does not depend on intermolecular collisions as shown in Equation 4.2;

$$D_{kn}=97r\sqrt{\frac{T}{M}} \tag{4.2}$$

Where r is the radius of the pore, T is temperature and M is the molecular weight of the adsorptive.

If the pore diameter is larger than the mean free path of the molecule, the collisions occur between molecules instead of collisions between molecules and solid surface (Figure 4.2b.). This type of diffusion is known as molecular diffusion. The equation of molecular diffusion can be written as;

$$D_m=\frac{1}{3}\sqrt{\frac{8kT}{\pi M}}\frac{kT}{\sqrt{2}\pi\sigma^2 P} \tag{4.3}$$

Where k is Boltzmann constant, σ is the collision diameter, P is pressure, T is temperature and M is the molecular weight of the adsorptive.

The diffusion in the pores and the diffusion in the fluid phase can be explained by Knudsen or molecular diffusion mechanisms. However, the diffusion through the physically adsorbed phase cannot be explained by these mechanisms. Although the mobility of the adsorbed phase is less than the gas phase mobility, there is an additional

flux in the cases of the high concentration of the adsorbed phase and the appreciable thickness of the adsorbed layer. Therefore, the diffusivity, which is known as surface diffusion, is given by the sum of the pore and surface contributions (Figure 4.2c.). The effective diffusivity for a single particle can be defined as;

$$D_{eff}=D_{kn}+\left(\frac{1-\varepsilon_p}{\varepsilon_p}\right)KD_s \tag{4.4}$$

Where D_s is the surface diffusivity and D_p is the contributions of Knudsen and molecular diffusion.

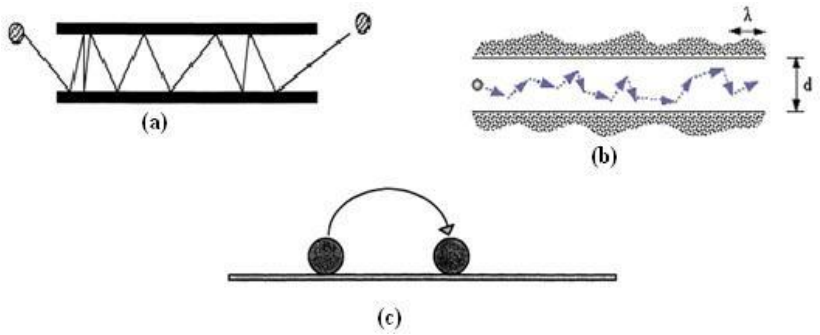

Figure 4.2. Macropore diffusion mechanisms a) Knudsen diffusion b) Molecular diffusion c) Surface diffusion

In contrast to the micropore diffusion, the macropore diffusion depends on the particle size of the adsorbent. The most significant property of the macropore diffusion is the dependence of the uptake rate to the micropore capacity since the accumulation of the adsorbate occurs in the micropores (Karger and Ruthven 1992). For a spherical particle the mass transfer equation for macropore can be written as;

$$\left(1-\epsilon_p\right)\frac{\partial q}{\partial t}+\epsilon_p\frac{\partial c}{\partial t}=\epsilon_p D_p\left(\frac{\partial^2 c}{\partial R^2}+\frac{2}{R}\frac{\partial c}{\partial R}\right) \tag{4.5}$$

Where D_p is the pore diffusivity, ϵ_p is the porosity of the adsorbent particle, R is the particle radius. It is assumed that the pore diffusivity is independent from concentration which is generally valid for Knudsen diffusion mechanism.

4.2. Adsorption Kinetics Models

The determination of the kinetics of the adsorption is important in evaluation of the performance of an adsorption system. Several simplified models have been derived to illustrate the adsorption kinetics (Boyd et al. 1947; Ho and McKay 1998; Qui et al. 2009). The adsorption kinetics data can be defined by reaction based and diffusion based models which are different in nature. While diffusion in fluid film, pores and sorbed state are considered individually in diffusion based models, the physical and chemical interactions at the solid surface are considered at reaction based models.

4.2.1. Reaction Based Models

4.2.1.1. Pseudo First Order Rate Equation

The pseudo first order rate equation is derived by Lagergren in 1898 to describe the process of liquid-solid phase adsorption of oxalic acid and malonic acid on charcoal (Ho et al. 2000). The equation, which is given as in Equation 4.6, is believed to be the earliest rate equation based on the adsorption capacity.

$$\frac{dq_t}{dt} = k_1 (q_e - q_t) \tag{4.6}$$

Where q_e and q_t are the sorption capacities at equilibrium and at time t, respectively, and k_1 is the rate constant of the pseudo first order sorption. In adsorption kinetic analysis, Equation 4.6 is transformed into its linear form;

$$\log (q_e - q_t) = \log (q_e) - \frac{k_1}{2.303} t \tag{4.7}$$

The main disadvantages of the pseudo first order equation are that the linear equation (Equation 4.7) does not give theoretical q_e values that agree with experimental q_e values, and the plots are only linear approximately in the first 30 min.

4.2.1.2. Pseudo Second Order Rate Equation

The pseudo second order rate equation is used to describe the rate of sorption of a second order mechanism, and is given as (Ho and McKay 1998):

$$\frac{dq_t}{dt}=k_2\left(q_e-q_t\right)^2 \tag{4.8}$$

Where q_e and q_t are the sorption capacities at equilibrium and at time t, respectively, and k_2 is the rate constant of the pseudo second order sorption In developing mathematical model to describe the sorption process, it is assumed that the sorption follows the Langmuir relationship.

When Equation 4.8 is integrated at boundary conditions t=0 to t=t and q_t=0 to q_t=q_t, the linearized form can be obtained as:

$$\frac{t}{q_t}=\frac{1}{k_2 q_e^2}+\frac{1}{q_e}t \tag{4.9}$$

4.2.1.3. Elovich Model Equation

The adsorption rate may decrease by time due to an increase in the surface coverage of the reactions involving chemisorption of gases on solid surfaces without desorption of adsorbents. Elovich model equation was derived by Elovich and Zhabrova in 1939 in order to investigate the H_2 and C_2H_4 adsorption on nickel. It is used to describe such chemisorption systems and can be expressed as (Taylor and Thon 1951; Juang and Chen 1997):

$$\frac{dq}{dt}=\alpha\ \exp(-\alpha q) \tag{4.10}$$

Where q is the amount of solute adsorbed at time t, and α and α are constants during any experiment. In linearized form (Equation 4.11) to simplify the Elovich equation it is assumed that aαt >> 1 at boundary conditions q=0 at t=0 and q=q at t=t;

$$q=\alpha \ln(\alpha\alpha) +[\alpha\ln(t)] \quad (4.11)$$

4.2.1.4. Ritchie Equation

Ritchie (1977) enhanced a model for gas-solid adsorption processes which is alternative to Elovich's equation. Ritchie (1977) assumed that the rate of adsorption depends solely on the fraction of sites which are unoccupied at time t**,** then

$$\frac{d\theta}{dt}=\alpha(1-\theta)^n \quad (4.12)$$

Where θ is the fraction of surface sites which are occupied by adsorbed gas, n is the number of surface sites occupied by each molecule of adsorbed gas and α is the rate constant.

It is assumed that no site is occupied at t=0. When q is the amount of adsorption at time t:

$$\frac{q_\infty^{n-1}}{(q_\infty-q)^{n-1}}=(n-1)\alpha t+1 \quad (4.13)$$

Where q_∞ is the amount adsorbed after infinite time. If the reaction is second order (n=2), Equation 4.13 becomes:

$$\frac{q_\infty}{(q_\infty-q)}=\alpha t+1 \quad (4.14)$$

The linearized form of Equation 4.14 is:

$$\frac{1}{q}=\frac{1}{\alpha q_\infty t}+\frac{1}{q_\infty} \quad (4.15)$$

4.2.2. Diffusion Based Models

Since the adsorption rate at the surface is generally rapid, the overall rate of adsorption is generally controlled by heat and mass transfer resistances instead of intrinsic sorption kinetic. The diffusion of an adsorbate molecule consists of two main steps: the diffusion outside the particle and diffusion inside the particle. The diffusion outside the particle occurs in the fluid film and according to the pore structure of the adsorbent, the intraparticle diffusion occurs inside the particle. One or sometimes more than one mechanism becomes dominated in controlling adsorption rate.

4.2.2.1. Fluid Film (External) and Surface (Skin) Diffusion Models

When there is more than one component in the fluid, external resistance related to molecular diffusion through the laminar fluid film surrounding the particle occurs. The film resistance depends on the hydrodynamic conditions around the adsorbent particles in the bed, the properties of the fluid, the particle size and particle surface roughness.

The external resistance through the laminar fluid film can be correlated by the following the equation (Karger and Ruthven 1992):

$$\frac{d\bar{q}}{dt} = k_f a(C - C^*) \tag{4.17}$$

Where k_f is the film mass transfer coefficient, ɑ is specific external area, C is the adsorptive concentration in bulk phase and C^* is the adsorptive concentration at equilibrium with adsorbent phase concentration at the particle surface. When the equilibrium relationship is linear (q*=KC), Equation 4.17 becomes:

$$\frac{d\bar{q}}{dt} = \frac{3k_f}{KR_p}(q^* - \bar{q}) \tag{4.18}$$

Where q* is the final equilibrium adsorbed phase concentration. For a step change in concentration at time zero, the boundary conditions are;

$$t<0, \qquad C=q=0 \tag{4.18a}$$

$$t>0, \qquad C=C_{\infty}=q_{\infty}/K \tag{4.18b}$$

The integrated form of Equation 4.18 can be given as

$$\frac{\bar{q}}{q_{\infty}}=1\text{-}\exp\left[-\frac{3k_f t}{KR_p}\right] \tag{4.19}$$

Equation 4.19 can also be written as Equation 4.20, which has the same form with pseudo-first order equation (Boyd et al. 1947);

$$\log\,(1\text{-}F)=-\frac{R}{2.303}t \tag{4.20}$$

Where R is defined as $3D^{l}/r_0\Delta r_0\kappa$ and F is fractional attainment of equilibrium and can be given as;

$$F=\frac{q}{q_{\infty}} \tag{4.21}$$

In order to distinguish the fluid film diffusion and pseudo first order rate equation, log(1-F) versus t graph should be plotted. If pseudo first order rate equation is rate controlling, the slope is independent from particle size, film thickness or equilibrium coefficient.

Except nonporous adsorbents, it is a good approximation to neglect the fluid film resistance since diffusion through the particle is generally slower. On the other hand, due to the constriction of the pore mouth, blockage of the large pores near the surface of the particle or from the deposition of the extraneous materials at the crystal surface, the surface (skin) resistance may be observed (Ruthven et al. 2010). Mathematically, the surface resistance has a very similar solution with fluid film diffusion equation (Equation 4.19).

$$\frac{d\bar{q}}{dt}=\frac{3k_s}{R_p}\left(q^*-\bar{q}\right) \tag{4.22}$$

$$\frac{\bar{q}}{q_\infty}=1-\exp\left[-\frac{3k_s t}{R_p}\right] \tag{4.23}$$

Where $k_s=D_s/\delta$ is the ratio of the effective diffusivity and the thickness of the solid surface film (Karger and Ruthven 1992).

4.2.2.2. Intraparticle Diffusion Model

Since adsorbents have a porous structure in general, it is not a realistic approach to neglect the intraparticular diffusion. The pore structure and the interactions between the adsorbate and the solid surface affect the intraparticle diffusion rate, so it becomes system dependent. It is important to select the appropriate intraparticular diffusion model since the models have different assumptions and boundary conditions.

Boyd et al. (1947) derived particle diffusion model to define the diffusion in and through the adsorbent particle. In this model, it is assumed that the initial concentration of adsorbate and diffusivity is constant. The equilibrium relationship is considered to be linear where $C^s=\kappa C^l$. Boyd et al. (1947) gives the diffusion equation for $u=C^s r$ as:

$$\frac{\partial u}{\partial t}=D^i\left(\frac{\partial^2 u}{\partial r^2}\right) \tag{4.24}$$

Where r is the radius of the spherical surface of concentration C^s in the solid and D^i is the internal diffusion coefficient. Equation 4.24 is solved with the initial boundary conditions:

$$u=0 \quad \text{at } r=0 \quad \text{for} \quad t\geq 0 \tag{4.24a}$$

$$u=r\kappa C^l \quad \text{at } r=r_0 \quad \text{for} \quad t\geq 0 \tag{4.24b}$$

$$u=rC_0^s \quad \text{at} \quad t=0 \quad \text{for} \quad 0<r<r_0 \tag{4.24c}$$

With the assumption of a constant initial concentration in the solid, Boyd and et al. (1947) derived the fractional attainment to equilibrium in and through particle:

$$F=1-\frac{6}{\pi^2}\sum_{n=1}^{\infty}\frac{1}{n^2}\exp\left(-\frac{D^i\pi^2n^2t}{r_0^2}\right) \tag{4.25}$$

For small times, Equation 4.25 becomes:

$$F=q/q_\infty=\frac{6}{r_0}\sqrt{\frac{Dt}{\pi}} \tag{4.26}$$

Crank (1975) summarized diffusion models for different particle shapes. Although most of the researchers represent the Equation 4.25 as Crank's model (Equation 4.27), the first derivation of the fractional attainment of equilibrium was made by Barrer (1941) and Boyd et al. (1947) as mentioned above.

$$\frac{m_t}{m_\infty}=\frac{\bar{q}-q_0}{q_\infty-q_0}=1-\frac{6}{\pi^2}\sum_{n=1}^{\infty}\frac{1}{n^2}\exp\left(-\frac{n^2\pi^2D_ct}{{r_c}^2}\right) \tag{4.27}$$

Ruthven (1984) categorizes diffusion in and through adsorbent as micropore diffusion control and macropore diffusion control (Table 4.1). In gas adsorption processes, the equilibrium constant is generally large and effective diffusivity is too small compared with pore diffusivity. Therefore, Karger and Ruthven (1992) suggest that the controlling resistance cannot be presumed from the magnitude of the effective diffusivity. In addition, the value of equilibrium constant of Henry's relationship, K, will decrease with concentration for a system that has type I isotherm. Therefore, an increasing trend of effective diffusivity with concentration, which is also observed in micropore diffusion control, occurs.

Weber and Morris also have derived an intraparticular diffusion model (Malash and El-Khaiary 2010) and claim that if the rate controlling mechanism is intraparticular diffusion, a plot of adsorbate amount against square root of time should yield a straight line passing through the origin (Table 4.1). The model of Weber and Morris is the most widely used diffusion model for intraparticular diffusion especially for biosorption systems (Gerente et al. 2007).

Linear Driving Force (LDF) Model

Linear driving force model, which was derived for adsorption chromatography by Glueckauf et al. (1955), is one of the most important and the earliest intraparticular mass transfer rate equation. While derivation of the equation Glueckauf et al. (1955) assume that the mean internal concentration rate is directly proportional to the difference between the surface concentration and the mean internal concentration. Also, the temperature of the particle is considered to be uniform. Linear driving force model can be given as (Glueckauf 1955):

$$\frac{d\bar{q}}{dt} = \frac{15D}{r^2}(q-\bar{q}) \tag{4.28}$$

Actually, in the first derivation of the linear driving force model, the dimensionless LDF coefficient is set equal to the 14, however Glueckauf (1955) indicates that the value of 15 should be applied when dimensionless time (Dt/r^2) is bigger than 0.1.

The LDF model can be applied to the studies of fixed bed adsorber dynamics and various adsorption processes such as breakthrough behavior, simulated moving bed systems, and pressure swing adsorption (Li and Yang 1999).

In 1953, Vermeulen proposed a quadratic approximation for a step-function change in concentration as following (Glueckauf 1955):

$$\frac{\partial\bar{q}}{\partial t} = \frac{\pi^2 D}{r^2}\frac{q^2-\bar{q}^2}{2\bar{q}} \tag{4.29}$$

This equation is superior to the LDF model when the adsorption isotherm is very steep, in other words when the Langmuir constant approaches an irreversible isotherm (Ryu et al. 2001).

An alternative solution to LDF model is obtained by Liaw et al. (1979) by the consideration of the parabolic concentration profile. The solution of the model gives exactly the same equation with Glueckauf solution (Table 4.1).

Due to the limitation in the dimensionless time of the LDF model, researchers made alternative derivations to the LDF model. For instance, for the rapid adsorption-

desorption cycles such as those encountered in pressure swing adsorption (PSA), application of the LDF model becomes dubious (Suzuki 1990). Nakao and Suzuki (1983) compared the LDF model with the numerical solution of the diffusion equation and proposed a graphical correlation from which the LDF coefficient can be determined as a function of the dimensionless cycle time (Chihara and Suzuki 1983). Do et al. (1986) indicate that the parabolic concentration profile also give large errors for short cycle times and derived a fourth degree approximation (Serbezov and Sotirchos 2001).

Shrinking Core Model

The diffusion models, which are derived from the Fick's law and based on the assumption of the linear equilibrium isotherm and constant diffusivity, are not valid for a large concentration change. When the isotherm is favorable type I isotherm (Langmuir isotherm), it can be approximated as rectangular (irreversible) isotherm which has an analytical solution for the uptake curve (Karger and Ruthven 1992).

$$c=0, \quad q^*=0, \qquad c>0, \quad q^*=q_s \tag{4.30}$$

In shrinking core model, all adsorption occurs at the adsorption front (shock front) where $R=R_f$ and intracrystalline diffusion is assumed to be sufficiently rapid to maintain sorbate concentration uniform through microparticle (Figure 4.3).

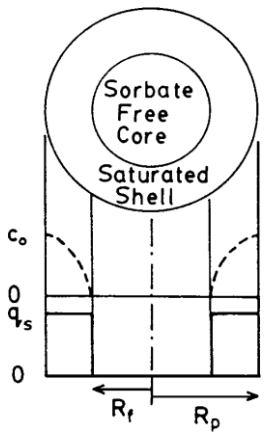

Figure 4.3. Schematic diagram showing the form of the concentration profiles within the fluid phase (c) and adsorbed phase (q) for irreversible adsorption in a spherical particle

In the model, it is assumed that the flow of sorbate through pores is constant in the region of Rp > R > Rf and the uptake curve for sphere is given by;

$$6\tau=1+2\left(1-\frac{m_t}{m_\infty}\right)-3\left(1-\frac{m_t}{m_\infty}\right)^{2/3} \tag{4.31}$$

The expression of τ represents the time required for the (shock) front to penetrate to the center of the sphere. These expressions are only valid for the constant pressure systems due to the constant boundary conditions (Karger and Ruthven 1992).

$$\tau=\frac{\epsilon_p D_p}{R_p^2}\frac{c_0}{q_s}t \tag{4.32}$$

4.2.3. Calculation of Diffusion Coefficient

The determination of the diffusion coefficient for an adsorption system is difficult, especially due to the change in the boundary conditions and assumptions. There are several theoretical models derived to calculate the diffusivity. The diffusivity constant is calculated by matching experimental curve with a theoretical model curve for the relevant boundary conditions and assumptions. The most popular equations which are based on Fick's second law and used for adsorption processes are shown in Table 4.1. The general assumptions used in derivation of these models are;

- The shape of the particle is spherical
- The initial concentration of adsorbate in the solution is constant
- The initial concentration in the solid is zero
- The system is isothermal

Table 4.1. Models for Diffusion Calculation

INTRAPARTICLE DIFFUSION FOR AN INFINITE SYSTEM VOLUME (CONSTANT BOUNDARY CONDITIONS)				
ASSUMPTIONS	• General assumptions are involved • Adsorption equilibrium relationship is linear • Mass transfer equation is based on the Fick's law • Diffusivity is constant			
RESEARCHER & YEAR	**SPECIFICATIONS**	**EQUATION**	**BOUNDARY CONDITIONS**	**WORKING PAIRS**
Karger and Ruthven (1992)	*The diffusional resistance in micropores is rate controlling mechanism *Uptake rate is independent from particle size *The concentration at the surface of the solid is constant, q_∞	$\frac{m_t}{m_\infty}=\frac{\bar{q}-q_0}{q_\infty-q_0}=1-\frac{6}{\pi^2}\sum_{n=1}^{\infty}\frac{1}{n^2}\exp\left(-\frac{n^2\pi^2 D_c t}{r_c{}^2}\right)$ For small times; $\left(\frac{m_t}{m_\infty}<0.3\right)$ $\frac{m_t}{m_\infty}=6\left(\frac{D_c t}{r_c{}^2}\right)^{1/2}\left[\frac{1}{\sqrt{\pi}}+2\sum_{n=1}^{\infty}\text{i erfc}\left(\frac{nr_c}{\sqrt{D_c t}}\right)-3\frac{D_c t}{r_c{}^2}\right]$ For long times; $\left(\frac{m_t}{m_\infty}>0.7\right)$ $\frac{m_t}{m_\infty}=1-\frac{6}{\pi^2}\exp\left(-\frac{\pi^2 D_c t}{r_c{}^2}\right)$	$t<0$, $C=C_0$, $q=q_0$ (independent of r and t) $t\geq 0$, $C=C_\infty$, $q(r_c, t)=q_\infty$ $\left(\frac{\partial q}{\partial r}\right)_{r=0}=0$ for all t	*Silica gel-water *Zeolite-water

(cont. on next page)

Table 4.1 (cont.)

Karger and Ruthven (1992)	*Diffusional resistance in macropores is rate controlling mechanism *Uptake rate depends on the particle size *There is a concentration gradient through the macropores *Pore diffusivity is independent from concentration	$\frac{\partial c}{\partial t}=\frac{\epsilon_p D_p}{\epsilon_p+(1-\epsilon_p)K}\left(\frac{\partial^2 c}{\partial R^2}+\frac{2}{R}\frac{\partial c}{\partial R}\right)$ $K=K_0 e^{-\Delta H/RT}$ $D_{eff}=\frac{\epsilon_p D_p}{\epsilon_p+(1-\epsilon_p)K}$ $\frac{m_t}{m_\infty}=\frac{\bar{q}-q_0}{q_\infty-q_0}=1-\frac{6}{\pi^2}\sum_{n=1}^{\infty}\frac{1}{n^2}\exp\left(-\frac{n^2\pi^2 D_c t}{r_c^2}\right)$ For small times ; $\left(\frac{m_t}{m_\infty}<0.3\right)$ $\frac{m_t}{m_\infty}=6\left(\frac{D_{eff}t}{R^2}\right)^{1/2}\left[\frac{1}{\sqrt{\pi}}+2\sum_{n=1}^{\infty} i\,\mathrm{erfc}\left(\frac{nR}{\sqrt{D_{eff}t}}\right)-3\frac{D_{eff}t}{R^2}\right]$	$c(R,0)=c_0,\quad q(R,0)=q_0$ $c(R_p,t)=c_\infty\quad q(R_p,t)=q_\infty$ $\left(\frac{\partial c}{\partial t}\right)_{R=0}=\left(\frac{\partial q}{\partial t}\right)_{R=0}=0$	*Silica gel-water
ASSUMPTIONS	• General assumptions are involved • Adsorption equilibrium relationship is nonlinear, Langmuir system • Mass transfer equation is based on the Fick's law • Diffusion coefficient depends on the concentration			
Garg and Ruthven (1973)	*Diffusional resistance in macropores is controlling the uptake rate	$\frac{\partial \bar{q}}{\partial t}=\frac{\epsilon_p}{w(1-\epsilon_p)}\frac{D_p}{R^2}\frac{\partial}{\partial R}\left(R^2\frac{\partial \bar{c}}{\partial R}\right)$ $\frac{\partial \bar{c}}{\partial \bar{q}}=\frac{(1+b\bar{c})^2}{bq_s}=\frac{b}{q_s}\frac{1}{(1-\bar{q}/q_s)^2}$ $\frac{\partial \bar{q}}{\partial t}=\frac{\epsilon_p}{w(1-\epsilon_p)}\frac{D_p}{bq_s}\frac{1}{R^2}\frac{\partial}{\partial R}\left(\frac{R^2}{(1-\bar{q}/q_s)^2}\frac{\partial \bar{q}}{\partial R}\right)$ $D_e=\frac{\epsilon_p}{w(1-\epsilon_p)}\frac{D_p}{bq_s(1-\bar{q}/q_s)^2}$	t=0: $\bar{q}(R,0)=0$ $\bar{q}(R_p,t)=\frac{q_s bc}{1+bc}$ $\left.\frac{\partial \bar{q}}{\partial R}\right\|_{R=0}=0$	*Hydrocarbons-5A molecular sieve pellet (Ruthven & Derrah, 1972)

(cont. on next page)

Table 4.1 (cont.)

Ruthven (1984)	*Diffusional resistance in micropores is rate controlling mechanism	$D_c=D_0\left(1-\frac{q}{q_s}\right)^{-1}$ $\frac{\partial q}{\partial t}=\frac{D_0}{r^2}\frac{\partial}{\partial r}\left(\frac{r^2}{(1-q/q_s)}\frac{\partial q}{\partial r}\right)$ For small concentrations $\frac{m_t}{m_\infty}=\frac{\bar{q}-q_0}{q_\infty-q_0}=1-\frac{6}{\pi^2}\sum_{n=1}^{\infty}\frac{1}{n^2}\exp\left(-\frac{n^2\pi^2D_ct}{r_c{}^2}\right)$	$q(r,0)=q_0'$ $q(r_c,t)=q_0$ $\left(\frac{\partial q}{\partial r}\right)_{r=0}=0$	*zeolite 4A-ethane
Liaw et al. (1979)	*Concentration profile is a parabola	$\frac{\partial q}{\partial t}=\frac{1}{r^2}\frac{\partial}{\partial r}\left(r^2D_c\frac{\partial q}{\partial r}\right)$ $q(t,r)=A(t)+B(t)r^n$ $A(t)=q(t,R_p)-\frac{(2n+1)}{(2n-2)}\left[\left(q_t(t,R_p)-\bar{q}_t\right)\right]$ $B(t)=\frac{5}{nR_p{}^n}\left[\left(q_t(t,R_p)-\bar{q}_t\right)\right]$ $\left[\frac{\partial q_t}{\partial r}\right]_{r=R_p}=nB(t)R_p^{n-1}=\frac{5}{R_p}\left[\left(q_t(t,R_p)-\bar{q}_t\right)\right]$ $\frac{\partial \bar{q}_t}{\partial t}=\frac{15D}{R_p^2}\left(q_i^*-\bar{q}_t\right)$		*Silica Gel Type RD- Water *Hydrocarbons on activated carbon and silica gel

(cont. on next page)

Table 4.1 (cont.)

Malash and El-Khaiary (2010) (Weber-Morris model)	*The film diffusion model is not significant or significant for a short period	$q=k_i t^{0.5}$		p-chlorophenol-activated carbon
INTRAPARTICLE DIFFUSION FOR AN FINITE SYSTEM VOLUME				
ASSUMPTIONS	• General assumptions are involved • Adsorption equilibrium relationship is linear • Mass transfer equation is based on the Fick's law • Diffusivity is constant			
Carman and Haul (1954)	*The sorbate is pure gas or vapor, C is measured by the pressure	$\lambda=\frac{(P_\infty-P_1)}{(P_2-P_\infty)}$ $1-\frac{m_t}{m_\infty}=\frac{(P-P_\infty)}{(P_2-P_\infty)}$ $1-\frac{m_t}{m_\infty}=\sum_{n=1}^{\infty}\frac{6\lambda(1+\lambda)\exp\left(Dq_n^2 t/r^2\right)}{9(1+\lambda)+\lambda^2 q_n^2}$ For small times; $1-\frac{m_t}{m_\infty}=(1+\lambda)\left[\frac{\gamma_1}{\gamma_1+\gamma_2}\,e\,erfc\,\frac{3\gamma_1}{\lambda}\sqrt{\tau}+\frac{\gamma_2}{\gamma_1+\gamma_2}\,e\,erfc-\frac{3\gamma_2}{\lambda}\sqrt{\tau}\right]-\lambda$ Where $\tau=\frac{Dt}{a^2}$	Initial Condition $C=C_2$, $q=0$ at $0<r<a$ when $t=0$ Boundary Condition $\frac{\partial q}{\partial r}=0$ at r=a for all t $q=\alpha C$ at $r=0$ $t>0$ $\frac{V_g}{2A}\frac{dC}{dt}=D\frac{\partial q}{\partial r}$ at x=0, t>0	*butane-silica gel *zeolite molecular sieves-hydrocarbons (Karger&Ruthven, 1992)

(cont. on next page)

Table 4.1 (cont.)

Ma and Lee (1976)	*A homogeneous solid with both macropores and micropores *Adsorption equilibrium is reached at the boundary surface of the crystals	$-\frac{3(1-\varepsilon_p)}{r_c}D_c\left(\frac{\partial q}{\partial r}\right)_{r=r_c}+\frac{\varepsilon_p D_p}{R^2}\frac{\partial}{\partial R}\left(R^2\frac{\partial c}{\partial R}\right)=\varepsilon_p\frac{\partial c}{\partial t}$ $V\frac{\partial C}{\partial t}=-N\varepsilon_p D_p 4\pi R^2\frac{\partial c}{\partial R}$	$t=0 \quad c=c_0$ $t>0 \quad c=c(t)$ $\left(\frac{\partial c}{\partial R}\right)_{R=0}=\left(\frac{\partial q}{\partial r}\right)_{r=0,,R=R}$ $r=r_c \quad q=Kc$ For bulk solution; $t=0 \quad C=C_0$	n-butane, isobutene and 1-butane in Davison CaX(Na) sieve
EXTERNAL FLUID FILM OR SKIN RESISTANCE FOR AN INFINITE SYSTEM VOLUME				
Karger and Ruthven (1992)	*Laminar fluid-film diffusion is rate controlling mechanism *There is no concentration gradient through the particle *There is an equilibrium between the adsorbed phase and the fluid phase concentrations at the surface *The adsorption equilibrium relationship is linear	$\frac{d\bar{q}}{dt}=\frac{3k_f}{KR_p}(q^*-\bar{q})$ $\frac{\bar{q}}{q_\infty}=1-\exp\left[-\frac{3k_f t}{KR_p}\right]$	$t<0, \; C=q=0$ $t>0, \; C=C_\infty=q_\infty/K$	*b-promophenol-Active Carbon *phenol-activated carbon *alkali metal cations-resinous zeolite (Boyd, Adamson et al., 1947)

(cont. on next page)

Table 4.1 (cont.)

Karger and Ruthven (1992)	*Skin resistance at the solid surface is the rate controlling mechanism *The adsorption equilibrium is linear *The diffusivity is constant	$\frac{d\bar{q}}{dt}=\frac{3k_s}{R_p}(q^*-\bar{q})$ $\frac{\bar{q}}{q_\infty}=1-\exp\left[-\frac{3k_s t}{R_p}\right]$ Where $k_s=D_s/\delta$		*n-decane-NaMgA zeolites
DUAL RESISTANCES FOR AN INFINITE SYSTEM VOLUME				
Ruthven (1984)	*Diffusional resistance in both micropores and macropores controls the adsorption rate *A step change concentration at the external surface of the macroparticle	$\frac{m_t}{m_\infty}=1-\frac{18}{\beta+3\alpha}\sum_{m=1}^{\infty}\sum_{n=1}^{\infty}\left(\frac{n^2\pi^2}{p_{n,m}^4}\right)\frac{e^{-p_{n,m}^2 D_c t/r_c^2}}{\left\{\alpha+\frac{\beta}{2}\left[1+\frac{\cot p_{n,m}}{p_{n,m}}\left(p_{n,m}\cot p_{n,m}-1\right)\right]\right\}}$ Where $\alpha p_{n,m}^2-n^2\pi^2=\beta(p_{n,m}\cot p_{n,m}-1)$ $\alpha=\left(\frac{D_c}{r_c^2}\right)/\left(\frac{D_p}{R_p^2}\right)$ $\beta=3\alpha(1-\epsilon_p)q_0/\epsilon_p c_0$	Micropore; $\frac{\partial q}{\partial r}(0,t)=0$ $q(r_c,t)=Kc(R,t)$ Macropore; $\frac{\partial c}{\partial R}(0,t)=0$ $c(R_p,t)=c_0$ $q(r,0)=c(R,0)=0$	

(cont. on next page)

Table 4.1 (cont.)

Karger and Ruthven (1992)	*Both micropore and external fluid film resistances control the uptake rate *The equilibrium relationship is linear	$D\left.\frac{\partial q}{\partial r}\right\|_{r_c}=k_f(C_\infty-c_s)=\frac{k_f}{K}\left(q_\infty-q\|_{r_c}\right)$ $\frac{m_t}{m_\infty}=\frac{\bar{q}-q_0}{q_\infty-q_0}=1-\sum_{n=1}^{\infty}\frac{6L^2\exp\left(-\beta_n^2 D_c t/r_c^2\right)}{\beta_n^2\left[\beta_n^2+L(L-1)\right]}$ Where $L=k_f r_c/KD_c$ $\beta_n\cot\beta_n+L-1=0$	$t\geq 0$, $C=C_\infty$, $q(r_c, t)=q_\infty$	
Karger and Ruthven (1992)	*Both macropore and external fluid film resistances control the uptake rate *The equilibrium relationship is linear	$\epsilon_p D_p\left.\frac{\partial q}{\partial r}\right\|_{R_p}=k_f(C_\infty-c_s)$ $\frac{m_t}{m_\infty}=\frac{\bar{q}-q_0}{q_\infty-q_0}=1-\sum_{n=1}^{\infty}\frac{6L^2\exp\left(-\beta_n^2 D_p t/R_p^2\right)}{\beta_n^2\left[\beta_n^2+L(L-1)\right]}$ $L=k_f R_p/\epsilon_p D_p$		

4.3. Previous Studies for Adsorption Kinetic Models

The previous studies on adsorption kinetics date back to 1940s. Barrer (1941) summarized the diffusion in and through solids. Boyd et al. (1947) derived fractional attainment to equilibrium equation with the same assumptions of Barrer (1941). In Table 4.2, the performed studies for both reaction and diffusion based models are presented.

Table 4.2. Previous Studies for Adsorption Kinetics

Year	Researcher	Adsorption Kinetic	Process	Model
1947	Boyd et al.	Diffusion based	Adsorption of alkali metal cations by resinous zeolite	Fluid film diffusion (≤0.003 M) Particle diffusion (≥0.1M)
1953	Reichenberg	Diffusion based	sodium-hydrogen exchange **on** sulfonated cross-linked polystyrenes	Fluid Film diffusion (<0.05 N) Particle diffusion (>1 N)
1955	Glueckauf	Diffusion based	-	Linear diriving force model
1966	Hall et al.	Diffusion based	-	Pore and Solid diffusion model
1974	Letterman et al.	Diffusion based	Sorption of phenol from aqeous solution by activated carbon	Fluid film diffusion model
1977	Mathews and Weber	Diffusion based	Phenol, p-bromophenol, p-toluene sulfonate-activated carbon	Fluid film diffusion model (for initial period)
1977	Ritchie	Reaction based	*Hydrogen-graphon *H_2 on MoS_2 + Al_2O_3 catalyst *Water vapor-vycor fibre	Ritchie Equation
1979	Liaw et al.	Diffusion based	-	Linear Driving Force Model (parabolic concentration profile)
1984	Yoshida et al.	Diffusion based	R-Na^++$Zn^{2+}(NO_3^-)_2$ R-Na^++$Ce^{3+}(NO_3^-)_3$	Fluid film+solid diffusion model
1986	Sakoda and Suzuki	Diffusion based	Water vapor- Fuji Type A silica gel	Surface Diffusion (Linear Driving Force Model)
1992	Gray and Do	Diffusion based	n-butane-activated carbon	Pore diffusion model

(cont. on next page)

Table 4.2 (cont.)

1997	Malek and Farooq	Diffusion based	Hydrocarbons- silica gel and activated carbon	Particle diffusion (Linear driving force model)
1997	Juang and Chen	Reaction based	Sorption of metal ions (Fe(III), Co(II), Ni(II), Cu(II), and Zn(II)) from sulfate solution with resin	Elovich's equation
1998	Ho and McKay	Reaction based	Sorption of basic dyes from aqueous solution by sphagnum moss peat	Pseudo second order
1999	Li and Yang	Diffusion based	N_2-zeolite 4A	Parabolic concentration profile
1999	Valsaraj and Thibodeaux	Diffusion based	Sorption kinetics of hydrophobic organic compounds on suspended sediments in the water column	Linear driving force model
2000	Cheung et al.	Reaction based	removal of cadmium ions from water by sorption onto bone char	Elovich's equation
2000	Chahbani and Tonduer	Diffusion based	Pressure swing adsorption of binary mixture and activated carbon	Pore diffusion and corrected solid diffusion
2000	Ho and McKay	Reaction based	Divalent metal ions from aqeous solution by sphagnum moss peat	Pseudo second order
2000	Ruthven	Diffusion based	-	Shrinking core model
2001	Chen et al.	Diffusion based	Dyes-pith	Pore-surface diffusion model
2001	Ko et al.	Diffusion based	Copper and Cadmium ions onto bone char	Film-pore diffusion model

(cont. on next page)

Table 4.2 (cont.)

2001	Ryu et al.	Diffusion based	Water-zeolite 13X	Nakao and Suzuki model
2002	Ko et al.	Diffusion based	Acid dyes-activated carbon	Branched pore model
2003	Cheung et al.	Reaction based	Copper ions-chitosan	Comparison (Elovich's)
2003	Sun and Yang	Comparison	Sorption of basic dyes from aqeous solution by modified peat resin	Intraparticular diffusion
2003	Hui et al.	Diffusion based	Basid blue dye 69 and Acid blue dye 25 onto peat and wood	Pore-surface diffusion model
2004	Choy et al.	Diffusion based	Metal ions onto bone char	Fluid Film diffusion (250-500μm) Intraparticular diffusion (500-710μm)
2004	Chua et al.	Diffusion based	Silica gel-water	Linear driving force model
2004	Hamadi et al.	Reaction based	Paraquat dichloride from aqueous solution by activated carbon	Pseudo second order
2004	Aristov et al.	Diffusion based	Fuji type RD silica gel-water	Pore diffusion model
2007	Cheung et al.	Diffusion based	Acid dye- chitosan	Intraparticular diffusion
2007	Gerente et al.	Comparison	Remove of metals from waste water by chitosan	-
2007	Zhang and Qu	Diffusion based	Moisture transport on silica gel-calcium chloride comporsite adsorbent	Crank diffusion model
2009	Qui et al.	Comparison	-	-
2010	Fujiki et al.	Diffusion based	p-nitrophenol-granular activated carbon	Fluid film diffusion model + Intraparticular diffusion model
2010	Ruthven et al.	Diffusion based	Methanol-ferrierite	Surface (Skin) diffusion model

CHAPTER 5

MATERIALS AND METHODS

In a design of an adsorption heat pump, the selection of appropriate working pair is quite important. The adsorption equilibrium and kinetics of the pair should be well known. The detailed information about the adsorption equilibria and kinetics were given in chapter 3 and chapter 4.

In addition to the high adsorption capacity and high mass diffusivity of the pair, the temperature dependence of the pair should also be determined when dealing with energy storage systems since the energy density of the pair highly depends on the operating conditions of adsorption and desorption steps.

In order to understand the nature of the adsorbents, firstly, the textural characterization was performed. Then, two volumetric systems were constructed and adsorption experiments were conducted for different adsorption and desorption temperatures. The materials used and the experimental procedure are explained in details in this chapter.

5.1. Materials

In this study, zeolite 13X supplied from Sigma-Aldrich Co. (4-8 mesh) and Type RD silica gel supplied from Fuji Silysia Chemical Ltd. (8-14 mesh) were used as adsorbent, and water was used as adsorptive.

5.1.1. Characterization of Adsorbents

The textural properties (pore size distribution, specific surface area and pore volume) of both Type RD silica gel and zeolite 13X were analyzed by ASAP 2010M micromeritics. The analyses were conducted by N_2 at its normal boiling temperature of -196°C. The type RD silica gel was degassed at 100°C under vacuum pressure of $6*10^{-3}$ mbar and zeolite 13X was degassed at 300°C under vacuum pressure of $6*10^{-3}$ mbar.

Thermogravimetric analysis (TGA) of type RD silica gel and zeolite 13X were performed by thermal gravimetric analyzer (Shimadzu TGA-51). The analyses of the adsorbents were carried out at a heating rate of 2°C/min, under 40 mL/min N_2 flow. While the analyze of zeolite 13X was performed up to temperature of 800°C, the type RD silica gel analyze was performed up to temperature of 400°C.

The elemental composition of zeolite 13X was determined using energy dispersive x-ray spectroscopy (EDX) on the particle. The data was collected for the external surface and cross section of the particle. The energy of the beam was 8 kV.

5.2. Experimental

5.2.1. Volumetric Adsorption Systems

The setup constructed for type RD silica gel-water pair is shown in Figure 5.1. The main components are three vessels, pressure (vacuum) transducer, vacuum pump, three manual valves, data logger, and temperature controller.

Vessel 1 (500 mL) contained water in liquid phase and vessel 2 (500 mL) stored water vapor, which was vaporized in the vessel 1. Adsorbent particles were placed in Vessel 3 (50 mL). As seen in Figure 5.1, there were three manual valves to manipulate the flow of the water vapor between vessels.

The pressure of the system was measured by a MKS Series 902P vacuum transducer which was connected to the vapor vessel. The measuring pressure range and operating temperature range of the transducer was 0.1-1000 Torr (0.13- 133 kPa) with an accuracy of 1% of reading and 0-50°C, respectively.

Pressure transducer was connected to a digital scanning and controlling device (MKS Series PDR 900-1 controller) which had a display range of 10^{-10}-1500 Torr. It was connected to the computer having software of MKS Series in order to collect the data. The pressure was scanned at adjusted time intervals and logged to a Microsoft Excel worksheet.

The evacuation of the system and regeneration of adsorbent particles were performed by using a Varian – Turbo-V 70 SH100 vacuum pump with $50m^3/h$ pumping and 1425 rpm operating speeds. The operating range of the pump was $760\text{-}10^{-3}$ torr.

Adsorption is a temperature dependent process. Therefore, the temperature of the entire system should be homogeneous and must be kept constant. Cole Parmer flexible heating cords were used in order to provide constant temperature distribution. The heating cords were connected to PC441 type PID controller manufactured by ORDEL. The desired temperature and heating time were set to the controller. The K-type thermocouples were used to control the temperature of the system. Also, Cole-Parmer Digi-Sense scanning thermometer was used as data logger. The temperatures were recorded for every 5 minutes by using the K-type thermocouples located to different points of the system.

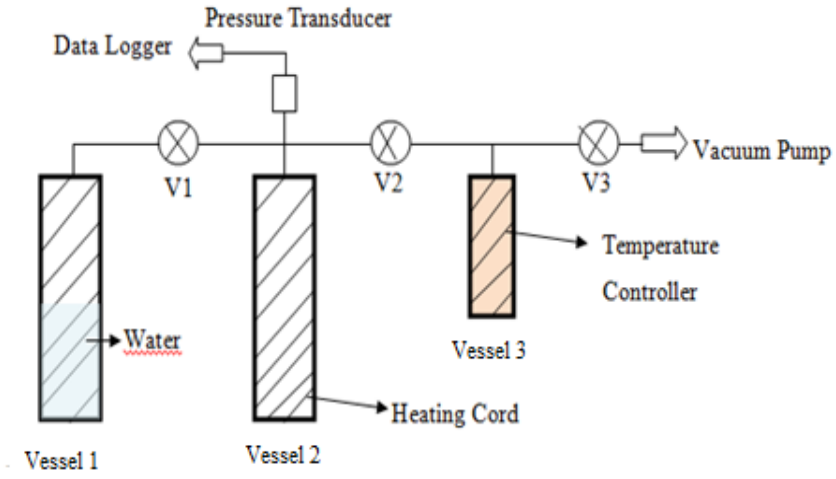

Figure 5.1. Schematic view of experimental setup for silica gel

The system constructed for zeolite 13X-water pair experiments was a bit different from the system of silica gel-water pair (Figure 5.2). Since zeolite 13X can adsorbed water vapor at very low concentration (pressure) and it requires higher desorption temperatures for complete regeneration, the system was improved. First, the design of the adsorbent bed (vessel 3) was changed. The heating of the adsorbent bed was made by screw clamp heater. In addition, four globe valves were used in this system.

The vacuum pump used in zeolite 13X-water pair system was the nXDS10i Scroll Pump manufactured by Edwards Ltd. The pumping speed was 11.4 m^3/h. The pump ultimate was $7*10^{-3}$ mbar, and the nominal rotational speed was 1800 rpm.

Both the silica gel-water pair and zeolite 13X-water pair systems were insulated by fiberglass materials in order to prevent the condensation and provide homogeneous temperature distribution along the system.

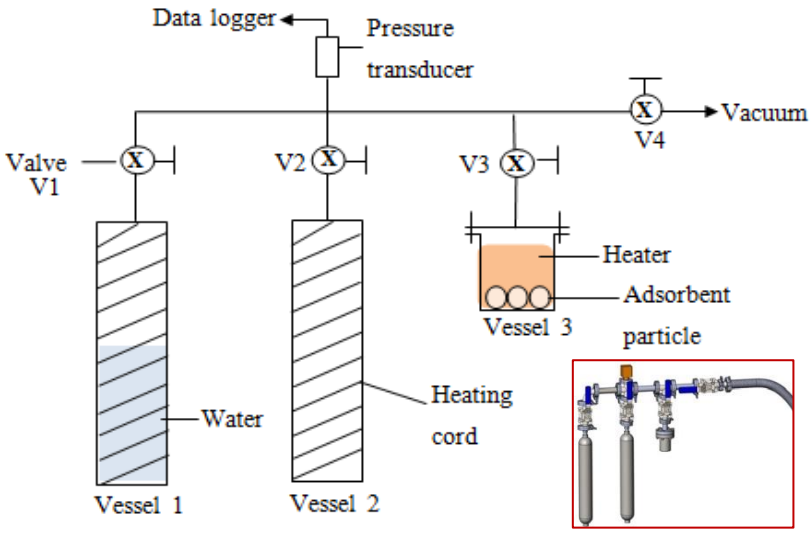

Figure 5.2. Schematic view of experimental setup for zeolite 13X-water pair

5.3. Experimental Procedure

The adsorption experiments were performed at pressure range of 0-6000 Pa. The air leakage into the system from the environment should be prevented. It is especially important for zeolite 13X experiments. The leakage tests of the setups for both Type RD silica gel-water and zeolite 13X-water pairs were performed as a first step of the experiments.

The condensation tests were performed as a second step of the experiments. Since the adsorbate concentration was calculated using the pressure change in the system, it should be ensured whether the condensation reduced the pressure or the adsorption occurred. The condensation test was done before the placement of the adsorbent particles into adsorbent vessel. Leakage and condensation test results are presented in Appendix D. Leakage rates for type RD silica gel-water and zeolite 13X-water pair systems were found as 0.35 Pa/min and 0.02 Pa/min, respectively.

After completion of condensation and leakage tests, the adsorption experiments were started. The Type RD silica gel-water pair experiments were performed to

determine the adsorption capacity and diffusivity at different adsorption temperatures of 45°C and 60 °C for constant regeneration temperature of 90°C (Table 5.1). The experimental steps for Type RD silica gel-water pair were:

1) All the three valves were closed
2) Temperature and pressure loggings were on,
3) Temperature controllers connected to vessel 2 and vessel 3 were set to 90 °C desorption temperature and run,
4) Vacuum pump was turned on,
5) V3 and V2 were opened,
6) Evacuation was continued for 30 hours at 90 °C,
7) After 30 hours the temperature controllers were set to the experiment temperature while evacuation continued,
8) When the temperature of the system reached to the experiment temperature, V2 and V3 were closed,
9) Vacuum pump was closed,
10) V1 was opened for approximately 5 minutes and then closed,
11) Pressure change in pipes and vapor vessel was observed for 5 minutes
12) If no pressure drop was observed, V2 was opened until equilibrium pressure was reached and then it was closed.

The adsorption capacity and effective diffusivity of zeolite 13X-water pair were determined for different adsorption and desorption temperatures (Table 5.1). Experimental steps for zeolite 13X-water pair were almost the same with Type RD silica gel-water pair:

1) All four valves were closed
2) Temperature and pressure loggings were on,
3) Temperature controllers connected to vessel 2 and vessel 3 were set to the desired desorption temperature and the temperature controller connected to the pipes was set to the 50°C.
4) Vacuum pump was turned on,
5) V2, V3 and V4 were opened,
6) Evacuation was continued for a week at selected regeneration temperature,

7) After a week, the temperature controllers were set to the desired adsorption temperature while evacuation continued,
8) When the temperature of the system reached to the adsorption temperature and come to equilibrium, V3 and V4 were closed,
9) Vacuum pump was closed,
10) V1 was opened to send some amount of vapor to the vessel 2 and closed,
11) Pressure change in pipes and vapor vessel was observed for 15 minutes
12) If no pressure drop was observed, V3 was opened until the equilibrium pressure was reached and then closed.

Table 5.1. Performed Experiments

Working Pair	**Desorption Temperature (°C)**	**Adsorption Temperature (°C)**	**Initial Adsorptive Pressure (Pa)**
Type RD silica gel-water	90	45	Increasing
		90	
Zeolite 13X-water	60	35	Increasing
	90	35	Increasing
			2000
			980
		45	Increasing
		60	
	120	35	Increasing
			2000
	150		Increasing
			2000
	200		Increasing

During desorption of the system, the evacuation of the liquid vessel was also provided. The evacuation procedure of the liquid vessel was;

1) V2 and V3 were closed,
2) V1 was opened for a while,

3) V1 was closed,

4) V2 and V3 were opened again. The effect of evacuation of liquid vessel is shown in Appendix E.

The steps 10 to 12, which were defined above, were repeated for both type RD silica gel-water and zeolite 13X-water pair until the maximum adsorption capacity was reached. The amount of adsorbate was calculated from the pressure changes between step 10 and step 12. The verification of the experiments for each temperature was made by repeating the experiment two times. The sample calculations are given in Appendix C.

CHAPTER 6

RESULTS AND DISCUSSION

The characterization of adsorbents performed by TGA, EDX and volumetric adsorption system are given in this chapter. The effect of adsorption and desorption temperatures on adsorption equilibrium and kinetics of type RD silica gel-water and zeolite 13X-water pairs are presented and discussed in this chapter.

6.1. Characterization of Adsorbents

The textural properties of type RD silica gel and zeolite 13X obtained by volumetric analyzer are presented in Table 6.1. Since N_2 cannot introduce into small pores of the zeolite 13X, the real values of pore size distribution are not obtained.

Table 6.1. Textural Properties of Adsorbents

Property	Type RD silica gel	Zeolite 13X
Single point surface area (m^2/g)	991.99	654.68
BET surface area (m^2/g)	1004.4	643.14
Langmuir surface area (m^2/g)	1428.4	942.30
Micropore area (m^2/g)	215.4	602.12
External surface area (m^2/g)	-	41.01
Single point total volume (cm^3/g)	0.58	0.29
Micropore volume (cm^3/g)	0.13	0.31
Average pore diameter (4V/A by BET) (Å)	22.9	17.75
Maximum pore volume (HK model) (cm^3/g)	0.42	0.33
Median pore diameter (Å)	7.22	6.05
Micropore surface area (D-A model)	1194.18	1335.13
Limiting micropore volume (D-A model) (cm^3/g)	0.60	0.35
Mean equivalent pore diameter (D-A) (Å)	20.13	10.41

The elemental composition of zeolite 13X was obtained from the EDX results (Table 6.2). The chemical analysis revealed the Si/Al ratio of 1.55 and 1.65 at cross

section and external surface, respectively. This ratio is given for zeolite X in the range of 1-1.5 in the literature (Breck 1974; Rouquerol et al. 1999).

Table 6.2. Elemental compositions of zeolite 13X

Element	Cross Section (wt%)	External Surface (wt%)
O	46.50	46.13
Na	11.36	12.38
Mg	1.64	1.94
Al	15.21	13.85
Si	23.57	22.84
P	0.55	0.75
S	-	0.50
K	-	0.30
Ca	0.40	0.44
Fe	0.77	0.88

The weight percent losses of the zeolite 13X and type RD silica gel were determined by thermogravimetric analysis (TGA). The TGA curve of zeolite 13X is shown in Figure 6.1. The water content in the structure of zeolite can be classified in three categories; external water, loosely bound water and tightly bound water. Therefore, the dehydration of the zeolite 13X takes place in three steps. Up to 65°C, the externally bound water which was ≈3% of the sample mass was removed. The loosely bound water (≈7%) was then removed until 130°C. After 130°C, slow desorption of tightly bound water (≈10%) took place and desorption of zeolite 13X was completed at 440°C. At 630°C, there was an interruption in the TGA curve which led to the deterioration in the framework of the zeolite 13X.

The TGA curve for type RD silica gel is presented at Figure 6.2. It was seen that the dehydration of type RD silica gel was occurred at 60°C. In the temperature interval of 25 to 140°C the water in macropores, mesopores and micropores of type RD silica gel was completely removed. After 140°C, the removal of hydroxyl groups from strained silanol groups [SiO_2.(OH)] started (Cabello et al., 2008; El-Naggar 2013).

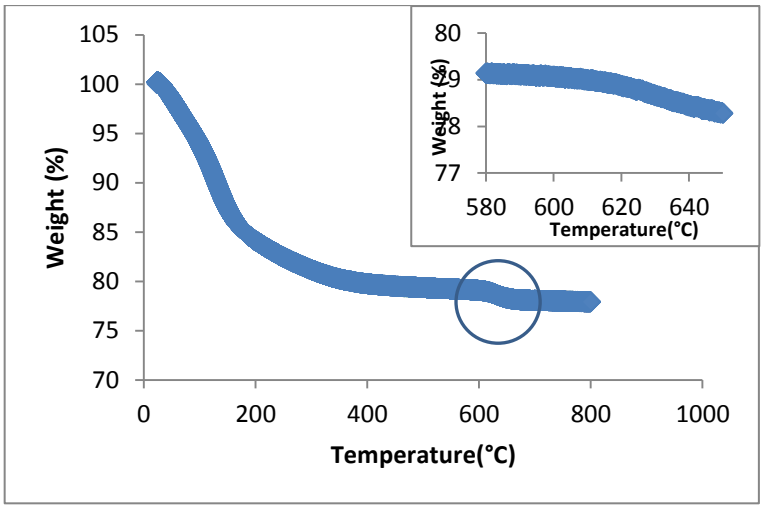

Figure 6.1. TGA curve of zeolite 13X

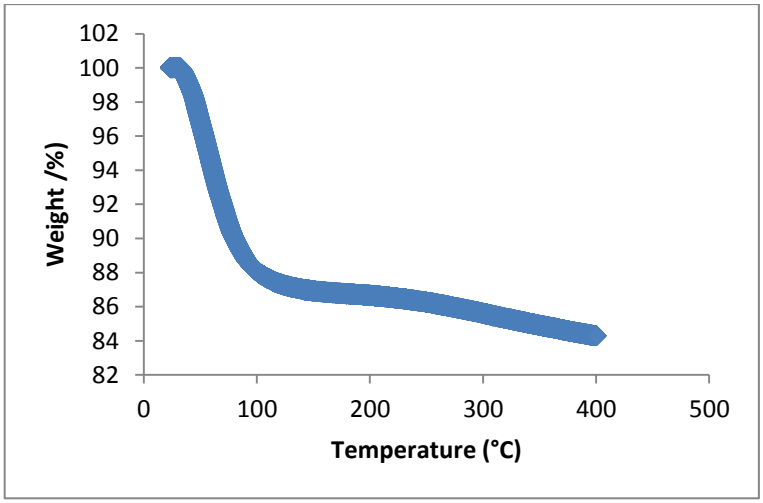

Figure 6.2. TGA curve of type RD silica gel

6.2. Adsorption Equilibria

6.2.1. Type RD Silica Gel-Water Pair

Adsorption of water vapor on type RD silica gel, which was dehydrated at temperature of 90°C, was performed at 45 and 60°C. Figure 6.3 is a representative diagram for the change of pressure and temperature with time at 60°C (See also Appendix E). As seen from Figure 6.3, nine pulses are done and for each pulse, the pressure drops to the equilibrium pressure which does not change with time until the

next pulse. Moreover, the adsorbent bed temperature is kept constant during the experiment (Figure 6.3).

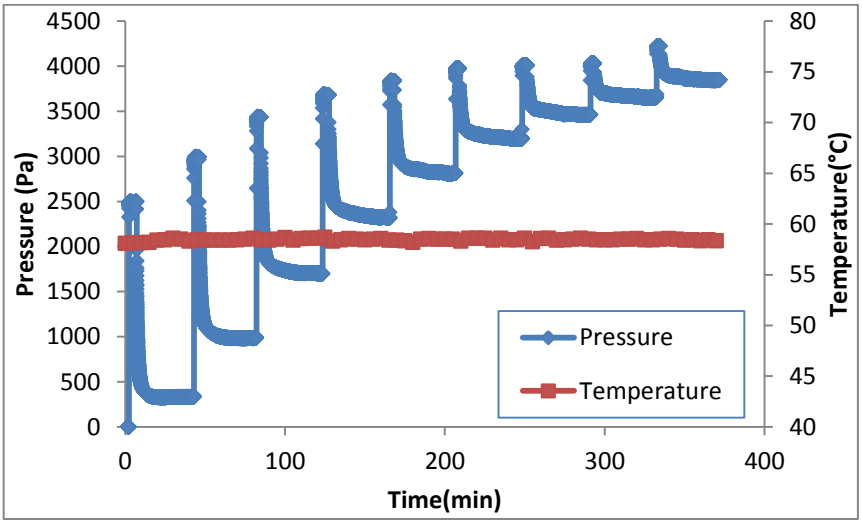

Figure 6.3. Pressure and temperature changes of adsorption of type RD silica gel-water pair at 60°C (T_{reg}=90°C)

The amount of adsorbate was calculated by using the ideal gas law (see also Appendix C) and adsorption isotherms were obtained at different temperatures. The effect of adsorption temperature on adsorption capacity can be seen in Figure 6.4 at temperatures of 35°C (Yıldırım 2011), 45°C and 60°C. It revealed that the adsorption capacity was decreased when the temperature was increased. At the pressure of 3000 Pa, the adsorption capacities at 35, 45 and 45°C were 28%, 17% and 9%, respectively.

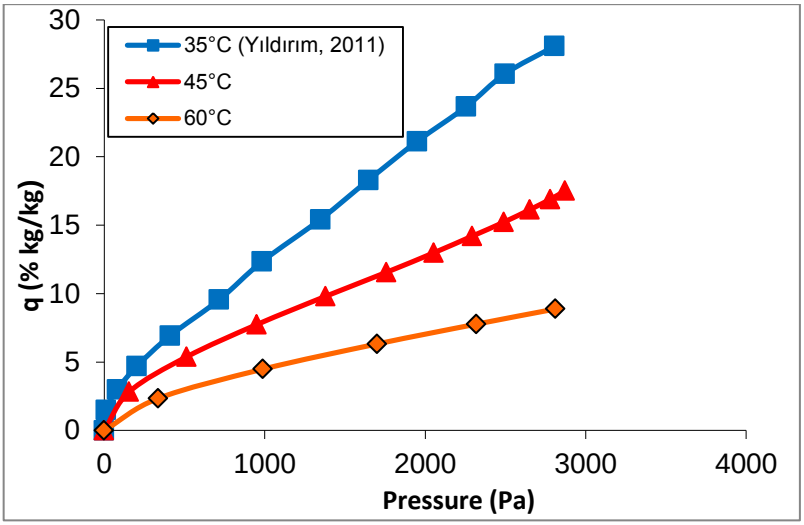

Figure 6.4. Adsorption isotherms of type RD silica-water pair at temperature of 35, 45 and 60°C

According to the IUPAC classification, type II isotherm which indicated the microporous structure of the adsorbent was observed for type RD silica gel-water pair.

According to Leppäjärvi et al. (2012), the temperature dependency of the adsorption equilibria can be represented by using saturation pressure especially for water adsorption on zeolites. Since the saturation capacity, q_m^{sat}, is independent from temperature and the dimensionless parameter n, which relates to the heterogeneity of the of the surface, is constant for the adsorbate-adsorbent pair at different temperatures (See Chapter 3), Leppäjärvi et al. (2012) indicated that the isotherms at different temperatures overlap when they are plotted as a function of relative pressure. In order to observe the applicability in type RD silica gel-water system, the amount of adsorbate vs. relative pressure plots is drawn for three temperatures (Figure 6.5). It was seen that the curves overlapped which meant that the amount of adsorbate was the same for different temperatures at the constant relative pressure. Thus, adsorption behavior of the working pair can be determined for different adsorption temperatures based on the adsorption data at only one temperature.

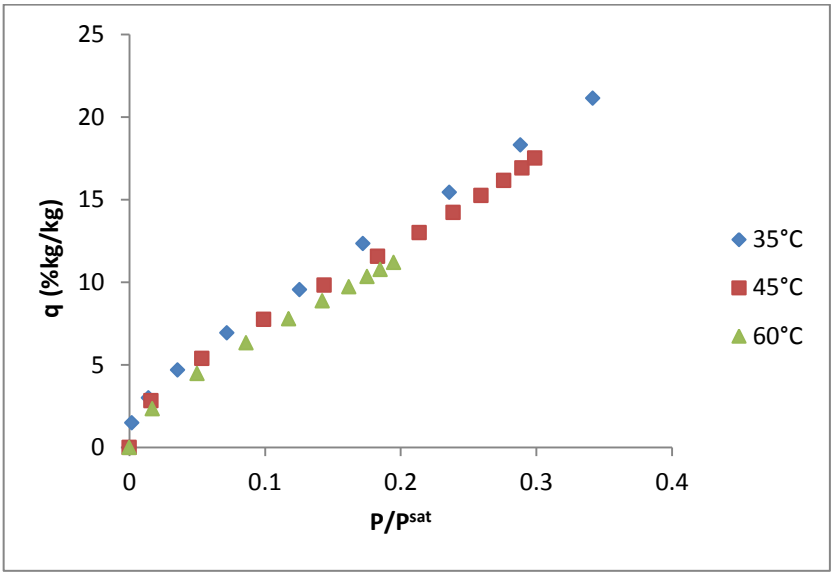

Figure 6.5. Adsorption isotherms of type RD silica gel-water pair as a function of P/P^{sat}

The isosteric heat of adsorption was also determined by using adsorption isotherms of type RD silica gel-water pair (Equation 3.19). The Clausius-Clapeyron diagram drawn for concentrations of 2, 4, 6, 8 and 10 (% kg/kg) was used to find the isosteric heat of adsorption value (Figure 6.6). The slope of LnP versus -1/T graph gave the q_{st}/R value (Equation 6.1). The change of isosteric heat of adsorption of type RD

silica gel-water pair by adsorbate loading is given in Figure 6.7. By means of the isosteric heat of adsorption value, the coefficient performance of an adsorption heat pump can be evaluated.

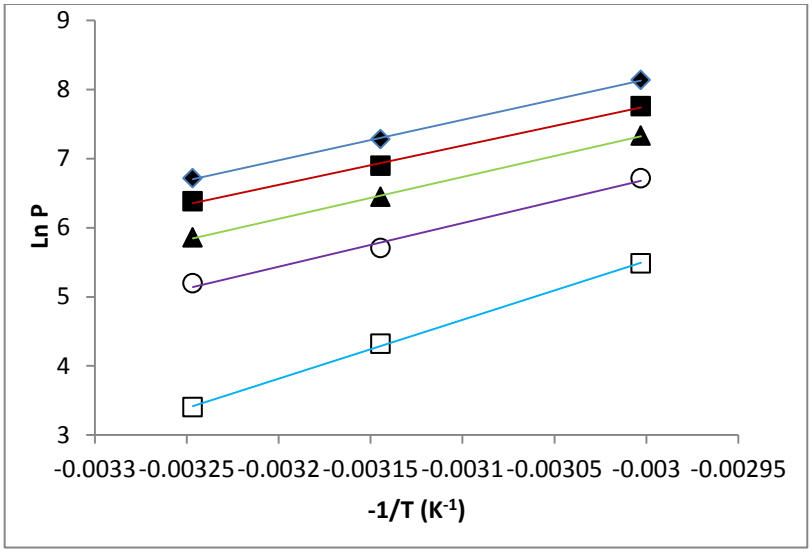

Figure 6.6. Clausius-Clapeyron diagram of type RD silica gel-water pair; ♦10%; ■8%; ▲6%; ○4%; □ 2%

$$\ln P = 8511.1\left(-\frac{1}{T}\right) + 31.052 \qquad \text{for q (\% kg/kg)} = 2 \qquad (6.1a)$$

$$\ln P = 6301.7\left(-\frac{1}{T}\right) + 25.604 \qquad \text{for q (\% kg/kg)} = 4 \qquad (6.1b)$$

$$\ln P = 6064.9\left(-\frac{1}{T}\right) + 25.538 \qquad \text{for q (\% kg/kg)} = 6 \qquad (6.1c)$$

$$\ln P = 5678.6\left(-\frac{1}{T}\right) + 24.794 \qquad \text{for q (\% kg/kg)} = 8 \qquad (6.1d)$$

$$\ln P = 5847.8\left(-\frac{1}{T}\right) + 25.69 \qquad \text{for q (\%k g/kg)} = 10 \qquad (6.1e)$$

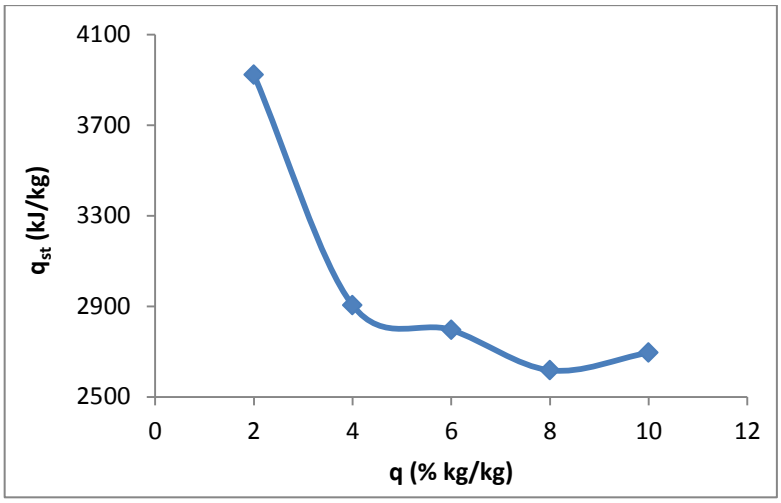

Figure 6.7. Change of isosteric heat of adsorption with adsorbate loading for type RD silica gel-water pair

6.2.2. Zeolite 13X-Water Pair

The results of the adsorption equilibria of zeolite 13X-water pair at different adsorption and desorption temperatures are illustrated in this part. The adsorption isotherm of zeolite 13X, which was regenerated at 90°C was obtained at 35, 45 and 60°C. The representative pressure and temperature change curve for 35°C are illustrated in Figure 6.8 (See also Appendix E). The water vapor adsorption of zeolite 13X at low adsorptive concentration can be understood clearly.

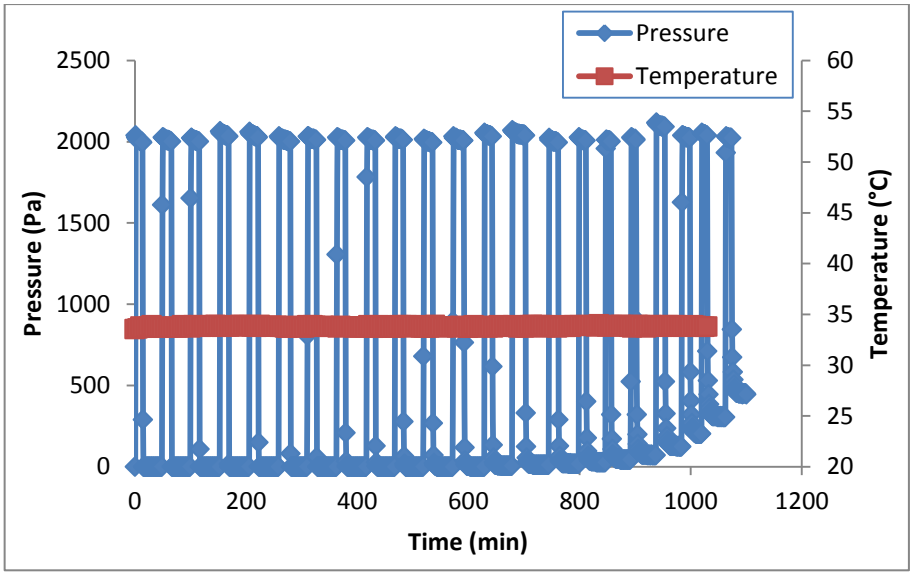

Figure 6.8. Pressure and temperature changes of zeolite 13X-water pair (T_{reg}=90°C)

Figure 6.9 presents the adsorption isotherms of zeolite 13X-water pair at 35, 45 and 60°C. The adsorption capacities of zeolite 13X-water pair were approximately 23%, 21% and 19% (kg/kg) for the adsorption temperatures of 35, 45 and 60°C at the pressure of 1500 Pa, relatively. It was observed that zeolite 13X adsorbed water vapor more than type RD silica gel at the same temperature and pressure.

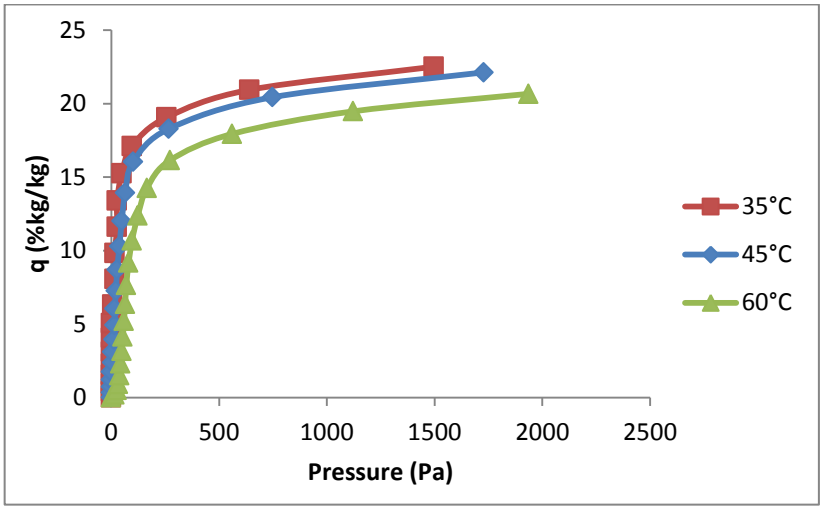

Figure 6.9. Adsorption isotherms at different adsorption temperatures (T_{reg}=90°C)

The adsorption equilibria is also presented by the plot of P/P^{sat} versus amount of water vapor adsorbed on zeolite 13X (Figure 6.10). By means of Figure 6.10, the adsorption isotherm of zeolite 13X-water pair at 25°C was produced (Figure 6.11). It was found that the adsorption capacity was 24% (kg/kg) at 1500 Pa.

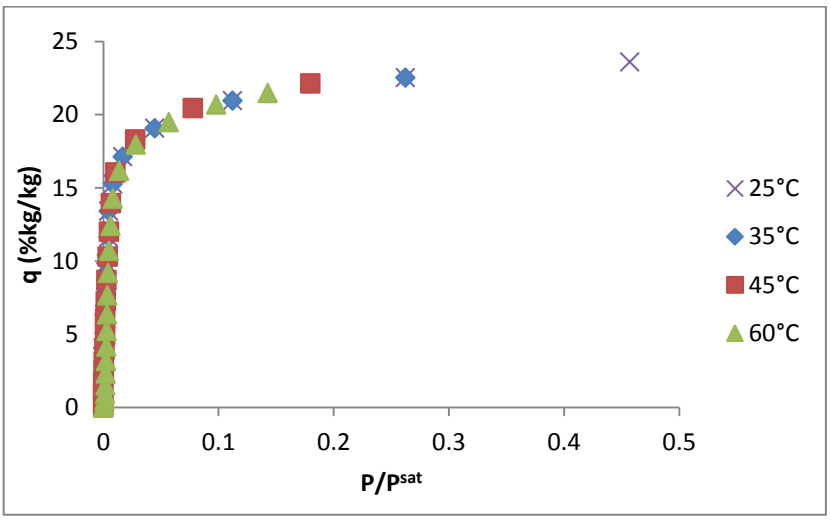

Figure 6.10. Adsorption isotherms of zeolite 13X-water pair as a function of P/P^{sat} (T_{reg}=90°C)

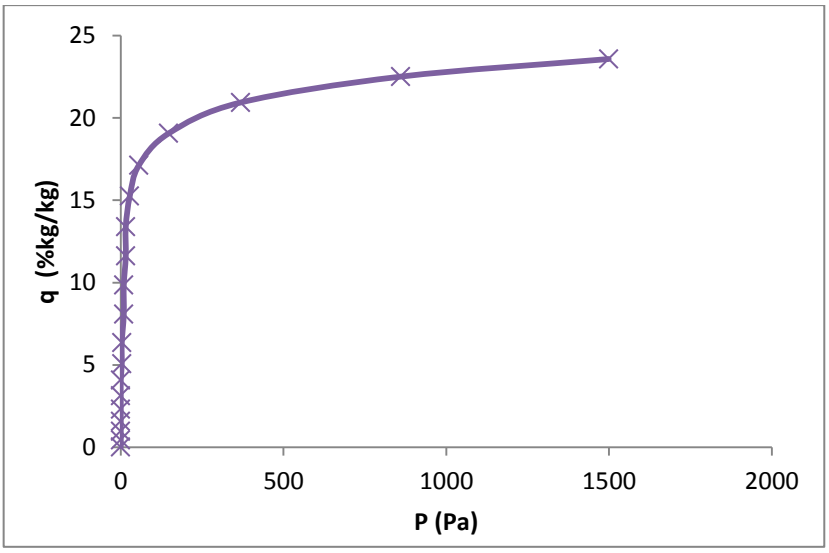

Figure 6.11. Adsorption isotherm of zeolite 13X-water pair at 25°C

The isosteric heat of adsorption of zeolite 13X-water pair which was regenerated at 90°C (Figure 6.12) was calculated by using Clausius-Clapeyron diagram for the adsorbate concentrations of 2, 5, 10, 14 and 19 (%kg/kg). The equations obtained from the diagram for each adsorbate concentration are presented at equation 6.2. The average isosteric heat of adsorption was found as 4087 kJ/kg which was compatible with the values given in literature (Ülkü and Mobedi 1989).

$$\ln P=-15191\left(-\frac{1}{T}\right)+49.379 \qquad \text{for q (\% kg/kg)=2} \qquad (6.2a)$$

$$\ln P=7901.3\left(-\frac{1}{T}\right)+27.62 \qquad \text{for q (\% kg/kg)=5} \qquad (6.2b)$$

$$\ln P=7312.2\left(-\frac{1}{T}\right)+26.547 \qquad \text{for q (\% kg/kg)=10} \qquad (6.2c)$$

$$\ln P=7525.1\left(-\frac{1}{T}\right)+27.739 \qquad \text{for q (\% kg/kg)=14} \qquad (6.2d)$$

$$\ln P=6319.9\left(-\frac{1}{T}\right)+25.843 \qquad \text{for q (\%k g/kg)=19} \qquad (6.2e)$$

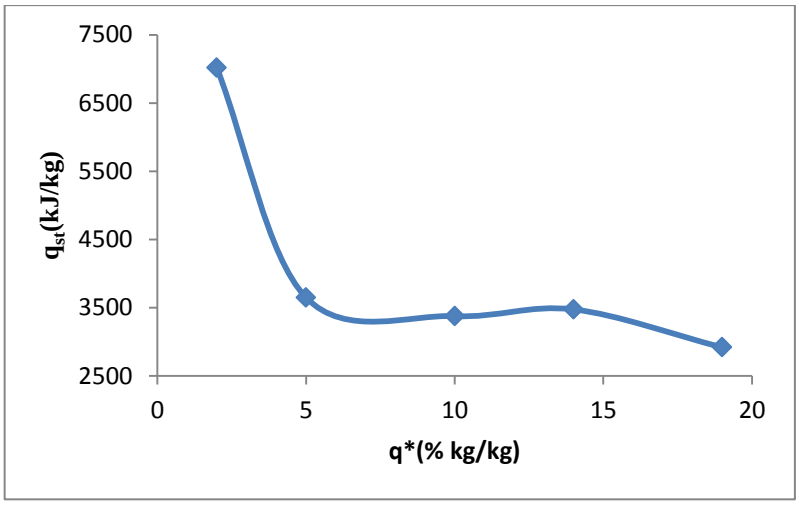

Figure 6.12. Isosteric heat of adsorption for zeolite 13X-water pair (T_{reg}=90°C)

For the effect of desorption temperature on adsorption equilibria, zeolite 13X was regenerated at different temperatures of 60, 90, 120, 150 and 200°C and adsorption was run at 35°C. According to the TGA results, the increase in adsorption capacity was expected up to the desorption temperature of 440°C. The experimental results for different regeneration temperatures are shown in Figure 6.13 for the pressure range of 0-1500 Pa at the adsorption temperature of 35°C. Although the adsorption capacity increased with the increase in desorption temperature, there was no significant change in adsorbate amount between temperatures of 150-200°C. Type I isotherm was observed for all desorption temperatures.

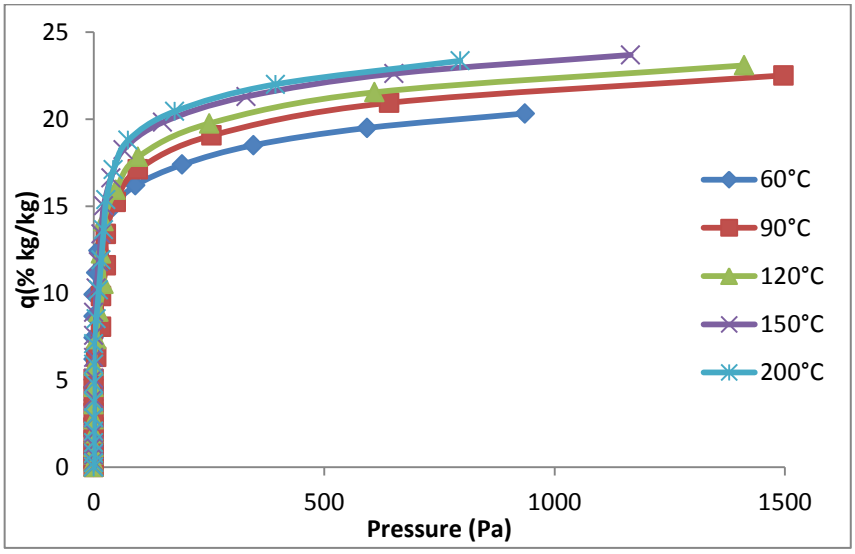

Figure 6.13. Adsorption isotherms of zeolite 13X-water pair at 35°C for different regeneration temperatures

The equilibrium data were analyzed by using the linear form of Langmuir relationship given in Equation 6.3. The equation parameters, q_m and b, were found by means of the plot of P/q versus P graph. The values of Langmuir relationship constants and the correlation coefficient (R^2) are illustrated in Table 6.3.

The Langmuir relationship constants were also calculated from the graph of P/P^{sat} (Figure 6.10). The monolayer capacity and parameter b, which was dimensionless was calculated as 0.24 (kg/kg) and 231, respectively.

Table 6.3. Parameters of Langmuir Relationship

Desorption Temperature (°C)	**Adsorption Temperature (°C)**	**q_m(kg/kg)**	**b (Pa^{-1})**	**R^2**
60	35	0.199	0.177	0.998
90	35	0.224	0.070	0.998
	45	0.223	0.029	0.997
	60	0.213	0.011	0.990
120	35	0.229	0.089	0.998
150		0.233	0.137	0.998
200		0.241	0.101	0.999

6.3. Adsorption Kinetics

The representative uptake curves of type RD silica gel-water and zeolite 13X-water pairs for successive runs with adsorptive concentration (pressure) change are illustrated in Figure 6.14 and Figure 6.15, respectively (See also Appendix F). The data of Figure 6.14 was collected at time intervals of 5 seconds and the data of Figure 6.15 was collected at time intervals of 60 seconds. The number given in parenthesis at the legends of the Figure 6.14 and Figure 6.15 indicates the pressure range of each pulse. It was observed that zeolite 13X-water pair was reached equilibrium faster than type RD silica gel-water pair under the same conditions. According to Ruthven (2012), the rapid initial uptake followed by a slow approach to equilibrium relates to the effect of heat transfer resistance. Furthermore, the shape of the curves changed which might be the reason of the effect of surface resistance control.

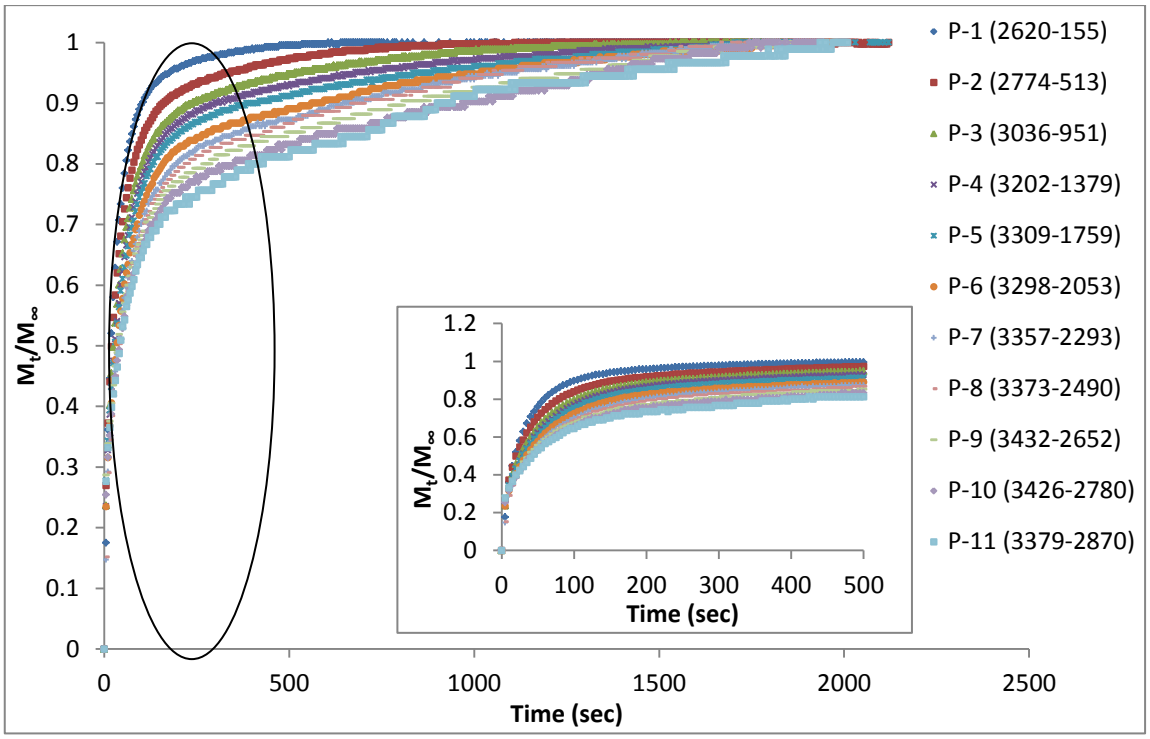

Figure 6.14. Uptake curves of type RD silica gel-water at 45°C (T_{reg}=90°C)

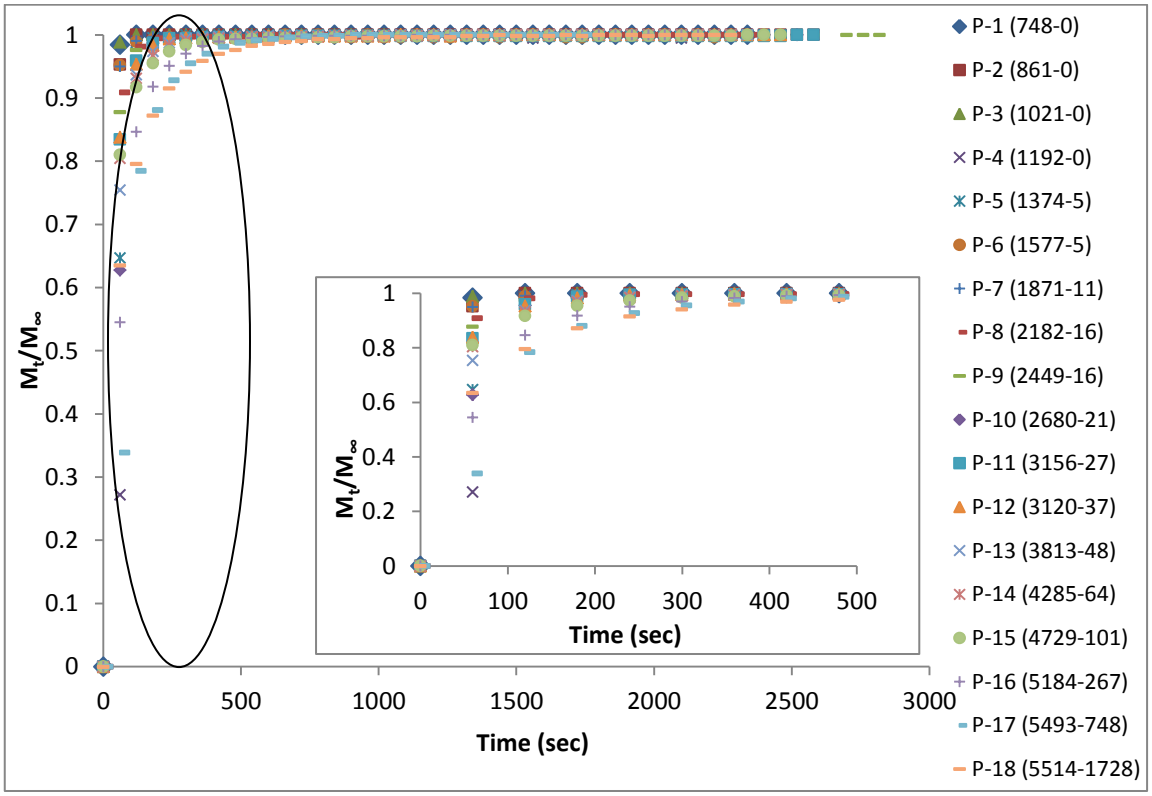

Figure 6.15. Uptake curves of zeolite 13X-water at 45°C (T_{reg}=90°C)

The representative uptake curves for successive runs with constant adsorptive concentration at logarithmic scale were also drawn in order to determine the controlling mechanism of the adsorption (Figure 6.16). It was observed that the controlling mechanism changed with successive runs. According to the Karger and Ruthven (1992), the possibility of redistribution of cations among energetically sites is higher for zeolite X than zeolite A. Therefore, the change in controlling mechanism might be explained by the hydration and migration of cations in the structure of zeolite 13X.

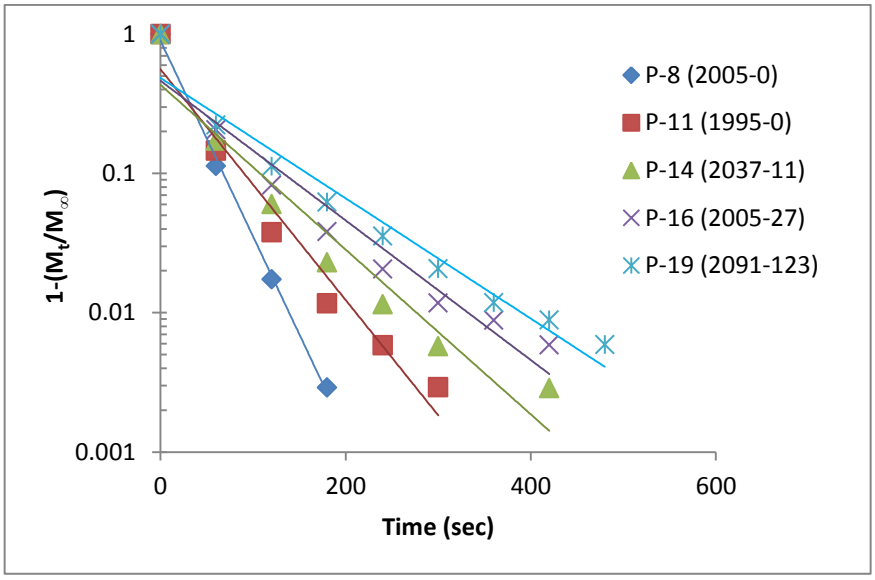

Figure 6.16. Uptake curve of zeolite13X-water pair at logarithmic scale for adsorption temperature of 35°C (T_{reg}=90°C)

The diffusivity of zeolite 13X-water pairs was calculated for both infinite system volume (constant boundary conditions) and finite system volume. Long term solution (M_t/M_∞>0.7) of Equation 4.27 (Table 4.1) was used to obtain diffusivity of water vapor for the assumption of infinite system volume. The plot of $\ln(1-M_t/M_\infty)$ versus time was plotted for each pulses. In a such plot, the slope gives $-\pi^2 D_{eff}/r^2$ and the intercept gives $\ln(-6/\pi^2)$ when the intraparticle diffusion is a rate controlling mechanism. On the other hand, if the plot passes through the origin, it shows the surface resistance (Karger and Ruthven 1992). The representative linear curve at the 16th pulse is presented at Figure 6.17 for zeolite 13X-water pair which was regenerated at 90°C (See also Appendix F). It was observed that the experimental data fitted the intraparticle diffusion better than surface resistance in the long time period. The effective diffusivities for short time period (M_t/M_∞<0.5) and long time period (M_t/M_∞>0.75) was also calculated. In order to

obtain short time period data, the pressure data was collected at time interval of 1 second. The effective diffusivity for the short time period was found from the slope of M_t/M_∞ versus $t^{0.5}$. Figure 6.18 is the representative fractional approach to equilibrium curve at 11th pulse of the adsorption of zeolite 13X-water pair, which was regenerated at 120°C. It was observed that the experimental data was represented better by the theoretical data calculated from Equation 4.27 by short time period effective diffusivity.

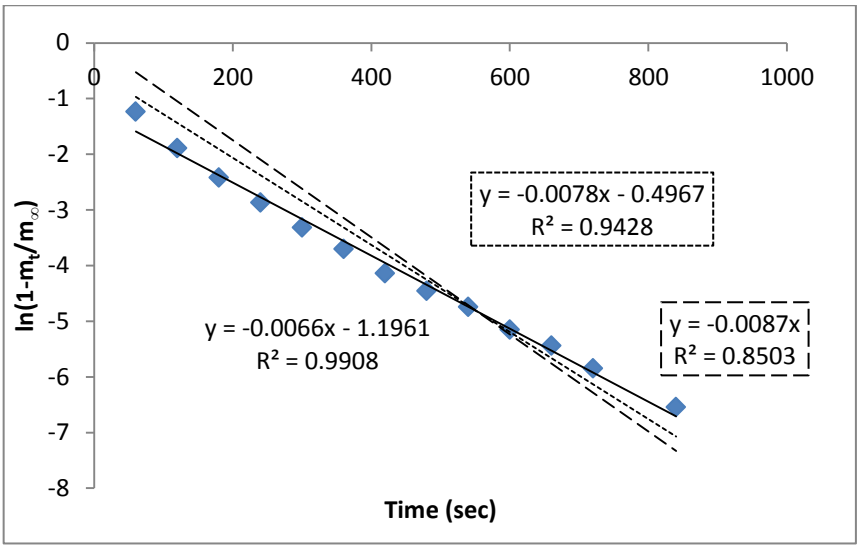

Figure 6.17. Linear curve of zeolite 13X-water pair at 35°C (T_{reg}=90°C) ─ experimental; …. Long term intraparticle diffusion; ---- surface resistance

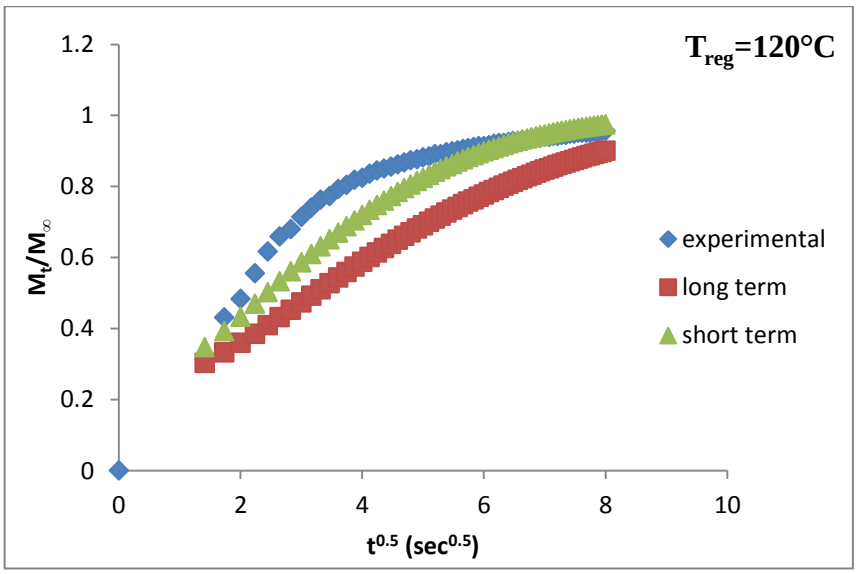

Figure 6.18. Experimental and theoretical amount of fractional approach to equilibrium of zeolite 13X-water pair at 35°C (11th pulse)

The diffusivity of water vapor for the assumption of finite system volume was calculated by the analytical solution given by Carman and Haul (1954) and is represented in Table 4.1. Although the experiments were performed in a finite volume system, the fraction of the adsorbate added in the step, λ, was generally closed to zero for the zeolite 13X-water pair especially at high desorption temperatures. Carman and Haul (1954) indicate that when λ is zero it corresponds to sorption from limited volume of fluid to a solid of infinite extent. The representative curves of infinite volume system and finite volume system are shown in Figure 6.19a and Figure 6.19b for desorption temperatures of 90°C and 120°C, respectively. The fraction of adsorbate added in the step was 0.095 in the pressure range of 4680-641 Pa for regeneration temperature of 90°C and the effective diffusivities for infinite and finite systems were 2.13×10^{-9} m^2/s and 9.56×10^{-10} m^2/s, respectively. For the desorption temperature of 120°C, the fraction of adsorbate added in the step was 0.037 in the pressure range of 4370-250 Pa and the diffusivities were 1.81×10^{-9} m^2/s for infinite system volume and 3.19×10^{-10} m^2/s for finite system volume.

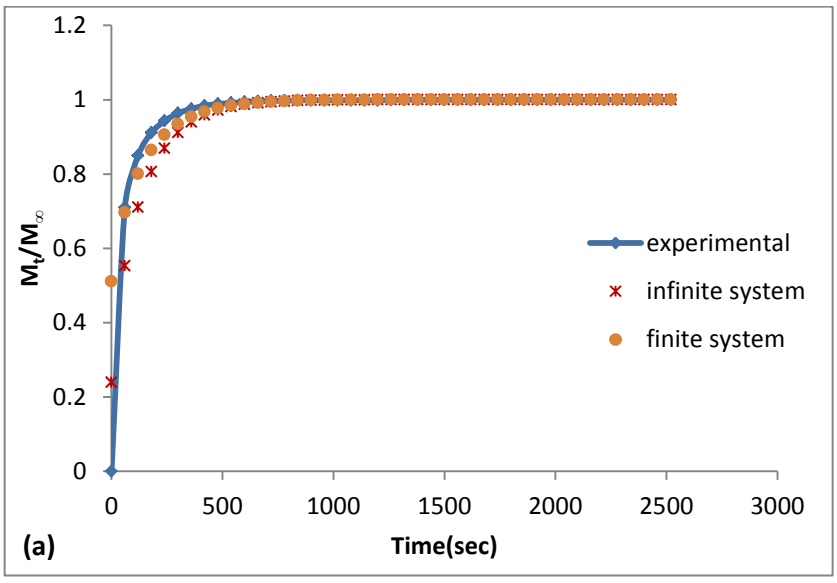

Figure 6.19. Experimental and theoretical uptake curves; a) T_{reg}=90°C; b) T_{reg}=120°C

(cont. on next page)

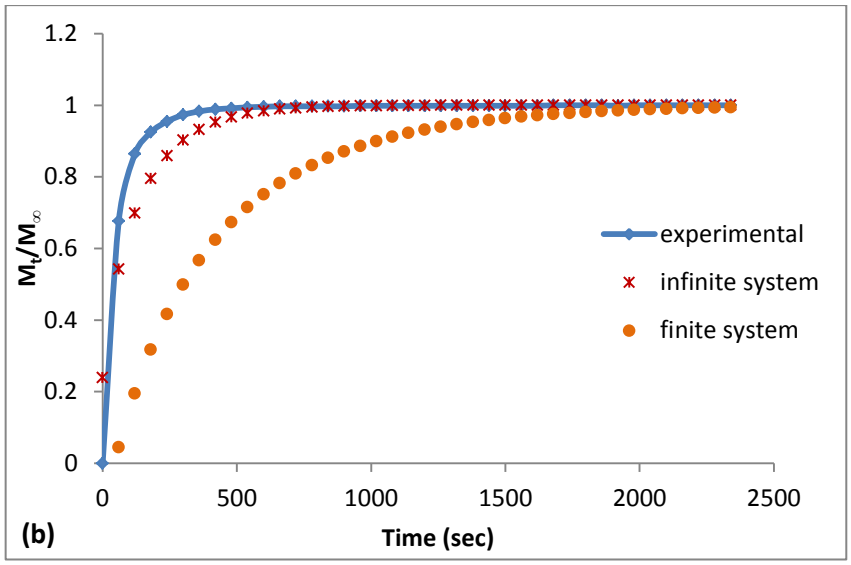

Figure 6.19 (cont.)

The concentration dependence of diffusivity was studied by several researchers (Özkan, 1991; Karger and Ruthven 1992; Beyhan, 2011; Ruthven, 2012). Özkan (1991) performed a study with clinoptilolite-water pair and found that the diffusivity decreased with the increasing adsorbate concentration at the linear part of the isotherm. Karger and Ruthven (1992) explained the unusual pattern of concentration dependence of diffusivity, which was resulted from the increasing significance of heat transfer resistance at higher concentration levels, of X and Y zeolites. Ruthven (2012) reevaluated his previous studies on the adsorption of propane and n-butane in zeolite 5A. He stated that the regeneration procedure greatly influenced the uptake rate and diffusion coefficient. Even, observed controlling resistance change from intraparticle diffusion control to surface resistance control.

The change of effective diffusivity with amount of adsorbate for different desorption temperatures and for increasing initial adsorptive concentration are presented in Figure 6.20 (See also Appendix F). The effective diffusivity of water vapor on zeolite 13X was in the range of $7x10^{-10}$-$1x10^{-8}$ m^2/s and decreased with increasing amount of water vapor adsorbed on zeolite 13X which may arise from heat transfer resistance and surface resistance effect or the interactions between cations and water vapor molecules. Furthermore, the diffusion was affected from the regeneration conditions such as regeneration temperature, vacuum conditions and the heating rate. Therefore, as indicated by Ruthven (2012), the discrepancies in the previous works

resulted from the regeneration conditions and the regeneration conditions should be analyzed carefully.

In addition to the regeneration conditions, the initial adsorptive concentration (pressure) is another factor that affects the effective diffusivity. The adsorption experiments at 35°C were performed at initial adsorptive pressure of ≈ 2000 Pa for regeneration temperatures of 90, 120 and 150°C and at initial adsorptive pressure of ≈ 980 Pa for regeneration temperatures of 90°C. It was observed that the maximum adsorption capacity was not affected from the initial pressure of pulses. However, the time required in order to reach maximum adsorption capacity and the effective diffusivity was depends on the initial adsorptive concentration. The representative curve of effect of initial adsorptive concentration on effective diffusivity for desorption temperature of 90°C was illustrated in Figure 6.21. The change of effective diffusivity with adsorbate concentration at constant initial adsorptive concentration for different regeneration temperatures are illustrated in Figure 6.22. The pressure data were collected at time interval of 60 seconds for the desorption temperature of 90°C and at time interval of 1 second for the desorption temperatures of 120 and 150°C. The sharp decrease in effective diffusivity was observed below adsorption capacity of 10% (kg/kg) for the regeneration temperature of 150°C.

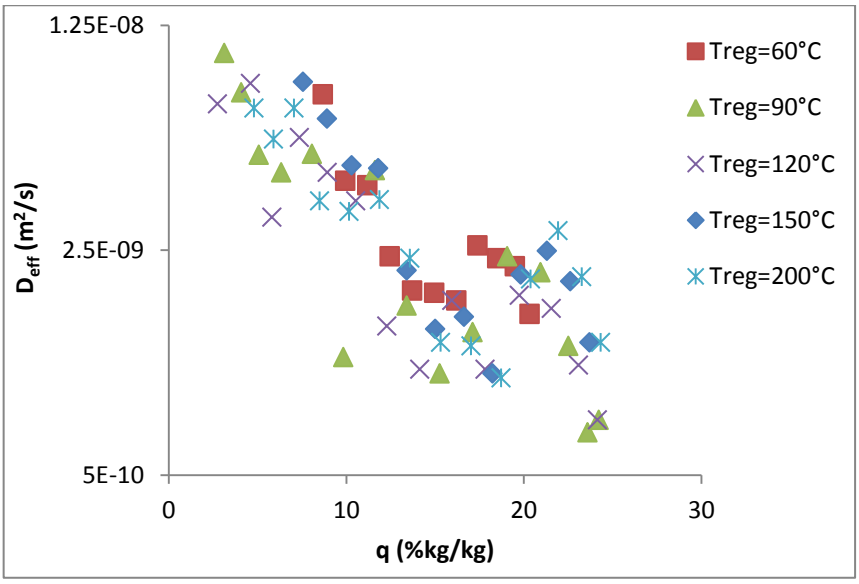

Figure 6.20. The change of effective diffusivity with amount of water vapor adsorbed on zeolite 13X at 35°C for different regeneration temperatures

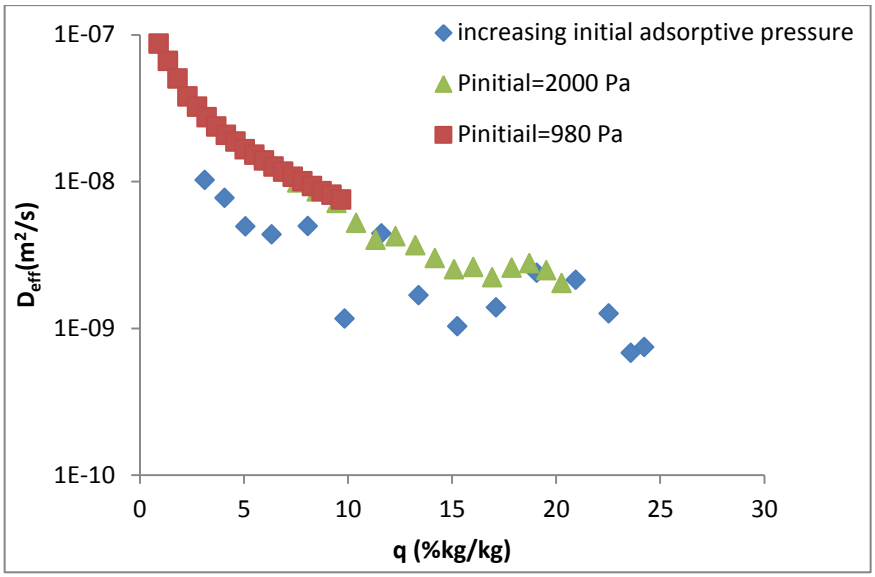

Figure 6.21. Effect of initial adsorptive concentration on the effective diffusivity (T_{reg}=90°C)

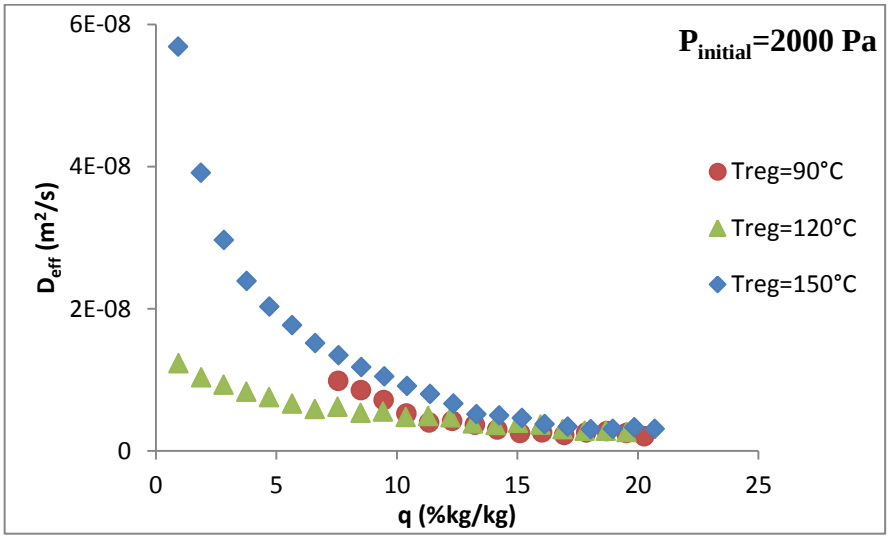

Figure 6.22. The change of effective diffusivity with amount of water vapor adsorbed on zeolite 13X at 35°C for different regeneration temperatures

The diffusivity of type RD silica gel-water pair and zeolite 13X-water pair was calculated by using the long term (M_t/M_∞>0.7) solution given by Karger and Ruthven (1992) in Table 4.1 for different adsorption temperatures of 35, 45 and 60°C. It was observed that the effective diffusivity decreased with increasing adsorbate concentration (Figure 6.23a and Figure 6.23b). For the long term effective diffusivity, it was found that the adsorption temperature didnot have a significant effect on diffusivity.

Additionally, the increasing adsorptive concentration have significant effect zeolite 13X-water pair rather than type RD silica gel-water pair.

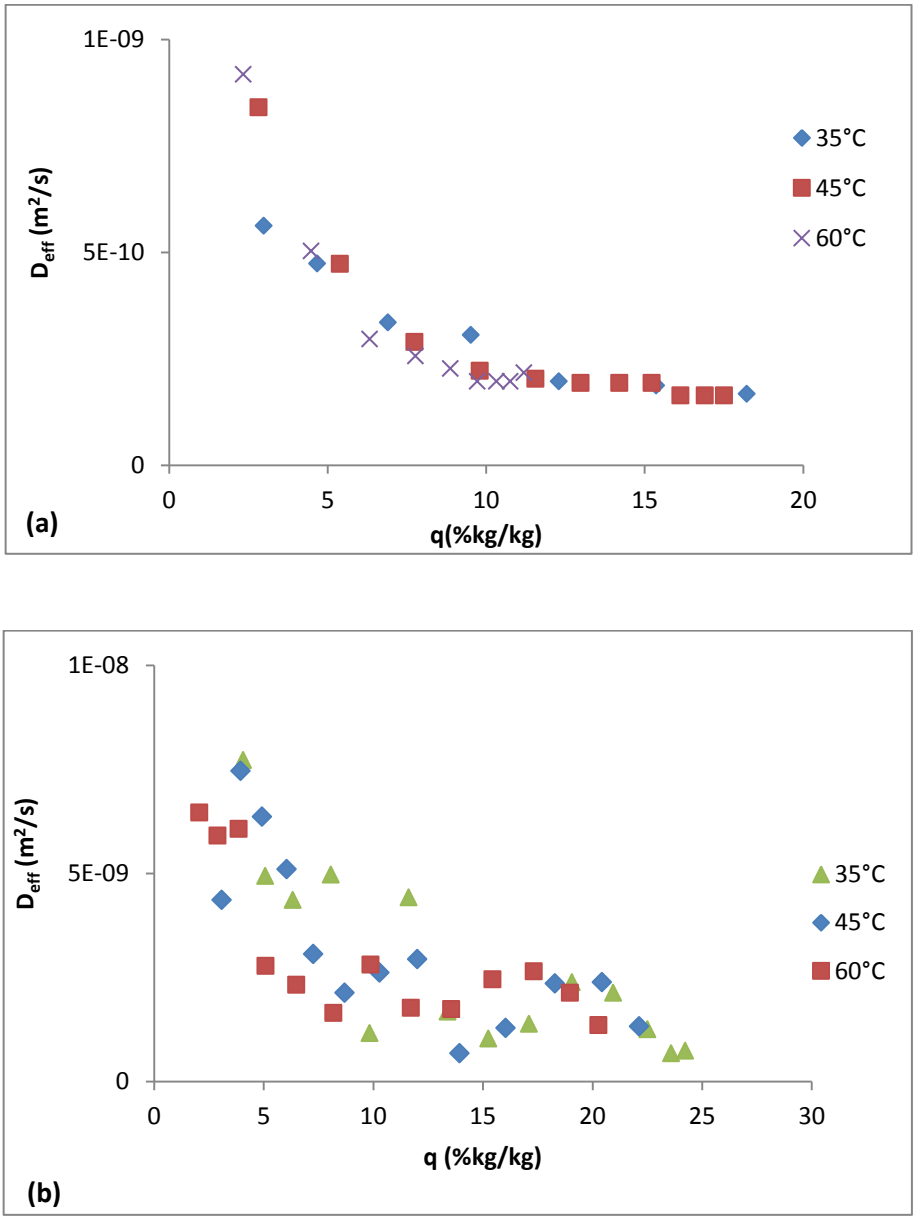

Figure 6.23. The change of effective diffusivity with adsorbate concentration a) Type RD silica gel-water pair; b) Zeolite 13X-water pair (T_{reg}=90°C)

CHAPTER 7

CONCLUSIONS

The adsorption technology for energy recovery systems has gained attention due to the demand for environmentally friendly systems. In this study, the working principle and of the adsorption heat pumps were explained in detail. The selection of the working pair for these systems has become crucial. However, it is still under investigation since the special pair hasnot been improved, yet. The common working pairs used in energy recovery and storage systems such as silica gel-water, active carbon-methanol and zeolite-water were discussed.

In selection of the pair, the structural and thermal properties of the adsorbent should be known. Thus, the textural properties such as surface area, pore volume and pore size distribution and thermal stability of adsorbents were investigated. In addition to the structural and physical properties of the adsorbent, the equilibrium conditions and adsorption kinetics should be well defined in order to determine the appropriate adsorbate-adsorbent pair. The eqilibrium relationships and the experimental methods in order to obtain the adsorption isotherm were explianed in details. Furthermore, the adsorption kinetic models for different boundary conditions and assumptions were summarized.

According to the performed investigations, the following remarks can be concluded;

- The attractiveness of adsorption heat pump is mainly based on the energy recover, storage and density of the pair which depends on the operating conditions of the adsorption and desorption steps such as minimum and maximum temperatures of the cycle, net amount of adsorbate cycled in the system. Thus, the characterization and behavior of adsorbents for the specific adsorptive should be investigated in order to determine the operation conditions of the adsorption heat pump.
- Since the adsorption is a temperature dependence process, the thermal stability of the adsorbent should also be well known,

- The adsorption capacity depends on both adsorption and desorption temperatures, and pressures. Thus, the assumptions and the operation conditions of the derived models for adsorption equilibria should be analyzed while comparing the suitable model for the working pair
- In addition to equilibrium conditions, the adsorption kinetics should be known to determine the response time of the adsorption-desorption cycle,

The experimental study was performed by volumetric setups in order to determine the adsorption capacity and kinetics of type RD silica gel-water and zeolite 13X-water pairs. The effective diffusivity of water vapor was also calculated for these pairs individually.

The adsorption experiments were run at 45 and 60°C for type RD silica gel-water pair which were regenerated at 90°C. The adsorption experiments for zeolite 13X-water pair were consisted of two parts. In the first part, the adsorption at different temperatures (35, 45 and 60°C) at constant regeneration temperature was performed. In the second part, the adsorption temperature was kept constant at 35°C and the experiments were done for different regeneration temperatures such as 60, 90, 120, 150 and 200°C.

The remarks for adsorption equilibria of type RD silica gel-water pair that could be concluded from the experimental studies are:

- According to the IUPAC classification, type RD silica gel-water pair showed type II isotherm,
- The maximum adsorption capacity of type RD silica gel-water pair for the adsorption temperatures of 35, 45 and 60°C were %28, %17 and %9, respectively,
- The temperature dependency of adsorption of the working pair can be described by using the saturation vapor pressure since the saturation capacity of the pair is independent from temperature,
- The average heat of adsorption of type RD silica gel-water pair was 2980 kJ/kg,

The remarks for adsorption equilibria of zeolite 13X-water pair that could be concluded from the experimental studies are:

- Zeolite 13X-water pair showed type I isotherm according to the IUPAC classification,
- The adsorption capacity of zeolite 13X-water pair which was regenerated at 90°C were %23, %21 and %19 for temperatures of 35, 45 and 60°C at 1500 Pa, respectively,
- The adsorption capacity of zeolite 13X-water pair was higher than type RD silica gel-water pair at the same temperature and pressure,
- The average heat of adsorption of zeolite 13X-water pair was found as 4087 kJ/kg,
- The adsorption capacity of zeolite 13X-water increased from %21 (kg/kg) to %24 (kg/kg) at 1000 Pa when the desorption temperature was increased from 90°C to 200°C.
- The theoretical calculated adsorption capacity from the experimental data using Langmuir relationship was 0.224, 0.223 and 0.213 (kg/kg) for the adsorption temperatures, 35,45 and 60°C, respectively,
- The theoretical calculated adsorption capacity from the experimental data using Langmuir relationship increased from 0.199 (kg/kg) to 0.241 (kg/kg) when the desorption was increased from 60°C to 200°C,
- The Langmuir constants, q_m and b, was found as 0.24 kg/kg and 231, respectively for the monolayer capacity.

The following remarks for adsorption kinetics were concluded from the experimental studies;

- Zeolite 13X adsorbed water vapor faster than type RD silica gel,
- The operation conditions such as regeneration time and initial adsorptive concentration affected the diffusivity of the pair,
- The effect of different mechanisms changed with succesive runs,
- In the long time period (M_t/M_∞>0.7), the diffusivity was not effected from the adsorption temperature for both working pairs,
- The effective diffusivity of water vapor on zeolite 13X was in the range of $7x10^{-10}$-$1x10^{-8}$ m^2/s at 35°C for increasing initial adsorptive concentration at different regeneration temperatures,

- The long time period effective diffusivity of zeolite 13X-water pair for constant initial adsorptive pressure of 2000 Pa was in the range of 10^{-9}-10^{-8} m^2/s for the regeneration temperatures of 90, 120 and 150°C,
- The short time period effective diffusivity ($M_t/M_\infty<0.5$) of zeolite 13X-water pair was almost constant ($2x10^{-8}$-$9x10^{-9}$ m^2/s) for the constant initial adsorptive pressure of 2000 Pa for the regeneration temperatures of 120 and 150°C,
- The long time period effective diffusivity of zeolite 13X, which was regenerated at 90°C, for constant initial adsorptive pressure of 980 Pa was in the range of $1x10^{-7}$-$7x10^{-9}$ m^2/s,
- The experimental data was better represented with the theoretical data calculated by short time period effective diffusivity,
- The decrease in effective diffusivity with adsorbate loading might be arised from heat transfer resistance and surface resistance effect or the migration and hydration of the cations,
- The previous studies on adsorption kinetics should be reevaluated by taking, initial water concentration, cation migration and hydration, and surface resistance into account.

REFERENCES

Afonso, M.R.A. and Jr V. Silveria. "Characterization of Equilibrium Conditions of Adsorbed Silica-Gel/Water Bed According to Dubinin-Astakhov and Freundlich." *Thermal Engineering* 4, (2005): 3-7.

Akahira, A., K. C. A. Alam, Y. Hamamoto, A. Akisawa and T. Kashiwagi. "Mass Recovery Four-Bed Adsorption Refrigeration Cycle with Energy Cascading." *Applied Thermal Engineering* 25, no. 11-12 (2005): 1764-1778.

Aristov, Y. I., G. Restuccia, G. Cacciola and V. N. Parmon. "A Family of New Working Materials for Solid Sorption Air Conditioning Systems." *Applied Thermal Engineering* 22, no. 2 (2002): 191-204.

Aristov, Y. I., M. M. Tokarev, A. Freni, I. S. Glaznev and G. Restuccia. "Kinetics of Water Adsorption on Silica Fuji Davison Rd." *Microporous and Mesoporous Materials* 96, no. 1-3 (2006): 65-71.

Arunan, E., G. R. Desiraju, R. A. Klein, J. Sadlej, S. Scheiner, I. Alkorta, D. C. Clary, R. H. Crabtree, J. J. Dannenberg, P. Hobza, H. G. Kjaergaard, A. C. Legon, B. Mennucci and D. J. Nesbitt. "Defining the Hydrogen Bond: An Account (Iupac Technical Report)." *Pure and Applied Chemistry* 83, no. 8 (2011): 1619-1636.

Atuonwu, J. C., G. van Straten, H. C. van Deventer and A. J. B. van Boxtel. "Optimizing Energy Efficiency in Low Temperature Drying by Zeolite Adsorption and Process Integration." *Pres 2011: 14th International Conference on Process Integration, Modelling and Optimisation for Energy Saving and Pollution Reduction, Pts 1 and 2* 25, (2011): 111-116.

Balkose, D., S. Ulutan, F. C. I. A. Ozkan, S. Celebi and S. Ulku. "Dynamics of Water Vapor Adsorption on Humidity-Indicating Silica Gel." *Applied Surface Science* 134, no. 1-4 (1998): 39-46.

Barrer, R. M. *Diffusion in and through Solids*, Edited by The Cambridge Series of Physical Chemistry, 1941.

Barrer, R. M. "Specifity in Physical Sorption." *Journal of Colloid and Interface Science* 21, (1966): 415-434.

Bauer, J., R. Herrmann, W. Mittelbach and W. Schwieger. "Zeolite/Aluminum Composite Adsorbents for Application in Adsorption Refrigeration." *International Journal of Energy Research* 33, no. 13 (2009): 1233-1249.

Boyd, G. E. , A. W. Adamson and L. S. Myers. "The Exchange Adsorption of Ions from Aqueous Solutions by Organic Zeolites. Ii. Kinetics." *Kinetics of Ion Exchanged Sorption Processes* 69, (1947): 2836-2848.

Breck, D. W. *Zeolite Molecular Sieves: Structure, Chemistry and Use*: John Wiley & Sons, 1974.

Buckingham, A. D., J. E. Del Bene and S. A. C. McDowell. "The Hydrogen Bond." *Chemical Physics Letters* 463, no. 1-3 (2008): 1-10.

Cabello, C. I., G. Bertolini, S. Amaya, R. Arizaga and M. Trivi. "Hydrophilic Character Study of Silica-Gel by a Laser Dynamic Speckle Method." *Rev. Cub. Física* 25, (2008): 67-69.

Cacciola, G. and G. Restuccia. "Reversible Adsorption Heat-Pump - a Thermodynamic Model." *International Journal of Refrigeration-Revue Internationale Du Froid* 18, no. 2 (1995): 100-106.

Cakicioglu-Ozkan, F. and S. Ulku. "The Effect of Hcl Treatment on Water Vapor Adsorption Characteristics of Clinoptilolite Rich Natural Zeolite." *Microporous and Mesoporous Materials* 77, no. 1 (2005): 47-53.

Cakicioglu-Ozkan, F. and S. Ulku. "Diffusion Mechanism of Water Vapour in a Zeolitic Tuff Rich in Clinoptilolite." *Journal of Thermal Analysis and Calorimetry* 94, no. 3 (2008): 699-702.

Cansever-Erdoğan, B. "Cr (Vi) Removal with Natural, Surfactant Modified and Bacteria Loaded Zeolites." Izmır Institute of Technology, 2011.

Cansever-Erdoğan, B. and S. Ülkü. "Ammonium Sorption by Gördes Clinoptilolite Rich Mineral Specimen." *Applied Clay Science* 54, (2011): 217-225.

Carman, P. C. and R. A. W. Haul. "Measurement of Diffusion Coefficients." *Proceedings of the Royal Society of London. Series A, Mathematical and PhysicalSciences* 222, (1954): 109-118.

Carrott, P. J. M., M. B. Kenny, R. A. Roberts, K. S. W. Sing and C. R. Theocharis. "The Adsorption of Water-Vapor by Microporous Solids." *Characterization of Porous Solids Ii* 62, (1991): 685-692.

Chahbani, M. H., J. Labidi and J. Paris. "Modeling of Adsorption Heat Pumps with Heat Regeneration." *Applied Thermal Engineering* 24, no. 2-3 (2004): 431-447.

Chahbani, M. H. and D. Tondeur. "Mass Transfer Kinetics in Pressure Swing Adsorption." *Separation and Purification Technology* 20, no. 2-3 (2000): 185-196.

Chen, B. N., C. W. Hui and G. McKay. "Pore-Surface Diffusion Modeling for Dyes from Effluent on Pith." *Langmuir* 17, no. 3 (2001): 740-748.

Chen, Z., W. Ma and M. Han. "Biosorption of Nickel and Copper onto Treated Alga (Undaria Pinnatifida): Application of Isotherm and Kinetic Models." *Journal of Hazardous Materials* 155, no. 1-2 (2008): 327-333.

Cheung, C. W., J. F. Porter and G. McKay. "Elovich Equation and Modified Second-Order Equation for Sorption of Cadmium Ions onto Bone Char." *Journal of Chemical Technology and Biotechnology* 75, (2000): 963-970.

Cheung, W. H., J. C. Y. Ng and G. Mckay. "Kinetic Analysis of the Sorption of Copper(Ii) Ions on Chitosan." *Journal of Chemical Technology and Biotechnology* 78, no. 5 (2003): 562-571.

Cheung, W. H., Y. S. Szeto and G. McKay. "Intraparticle Diffusion Processes During Acid Dye Adsorption onto Chitosan." *Bioresource Technology* 98, no. 15 (2007): 2897-2904.

Chihara, K. and M. Suzuki. "Air Drying by Pressure Swing Adsorption." *Journal of Chemical Engineering of Japan* 16, no. 4 (1983): 293-299.

Cho, S. H. and J. N. Kim. "Modeling of a Silica-Gel Water-Adsorption Cooling System." *Energy* 17, no. 9 (1992): 829-839.

Choy, K. K. H., D. C. K. Ko, C. W. Cheung, J. F. Porter and G. McKay. "Film and Intraparticle Mass Transfer During the Adsorption of Metal Ions onto Bone Char." *Journal of Colloid and Interface Science* 271, no. 2 (2004): 284-295.

Chua, H. T., K. C. Ng, A. Chakraborty, N. M. Oo and M. A. Othman. "Adsorption Characteristics of Silica Gel Plus Water Systems." *Journal of Chemical and Engineering Data* 47, no. 5 (2002): 1177-1181.

Close, D. J. and R. V. Dunkle. "Use of Adsorbent Beds for Energy Storage in Drying of Heating Systems." *Solar Energy* 19, (1977): 233-238.

Cortes, F. B., F. Chejne, F. Carrasco-Marin, C. Moreno-Castilla and A. F. Perez-Cadenas. "Water Adsorption on Zeolite 13x: Comparison of the Two Methods Based on Mass Spectrometry and Thermogravimetry." *Adsorption-Journal of the International Adsorption Society* 16, no. 3 (2010): 141-146.

Crank, J. *The Mathematics of Diffusion*. Second ed.: Oxford University Press, 1975.

Critoph, R. E., Z. Tamainot-Telto and G. N. L. Davies. "A Prototype of a Fast Cycle Adsorption Refrigerator Utilizing a Novel Carbon-Aluminium Laminate." *Proceedings of the Institution of Mechanical Engineers Part a-Journal of Power and Energy* 214, no. A5 (2000): 439-448.

Dawoud, B. and Y. Aristov. "Experimental Study on the Kinetics of Water Vapor Sorption on Selective Water Sorbents, Silica Gel and Alumina under Typical Operating Conditions of Sorption Heat Pumps." *International Journal of Heat and Mass Transfer* 46, no. 2 (2003): 273-281.

Demir, H. "An Experimental and Theoretical Study on the Improvement of Adsorption Heat Pump Performance." İzmir Institute of Technology, 2008.

Demir, H., M. Mobedi and S. Ulku. "Microcalorimetric Investigation of Water Vapor Adsorption on Silica Gel." *Journal of Thermal Analysis and Calorimetry* 105, no. 1 (2011): 375-382.

Do, D. D. *Adsorption Analysis: Equilibria and Kinetics*. Vol. 2 Series on Chemical Engineering Edited by Ralph T. Yang: Imperial College Press, 1998.

Do, D. D., R. G. Jordi and D. M. Ruthven. "Sorption Kinetics in Zeolite Crystals with Finite Intracrystal Mass Exchange - Isothermal Systems." *Journal of the Chemical Society-Faraday Transactions* 88, no. 1 (1992): 121-131.

Douss, N. and F. Meunier. "Effect of Operating Temperatures on the Coefficient of Performance of Active Carbon-Methanol Systems." *Heat Recovery Systems & Chp* 8, no. 5 (1988): 383-392.

Dubinin, M. M. and V. A. Astakhov. "Development of the Concepts of Volume Filling of Micropores in the Adsorption of Gases and Vapors by Microporous Adsorbents." *Bulletin of the Academy of Sciences of the USSR, Division of chemical science* 20, no. 1 (1971): 3-7.

Dunne, J. A., M. Rao, S. Sircar, R. J. Gorte and A. L. Myers. "Calorimetric Heats of Adsorption and Adsorption Isotherms .2. O-2, N-2, Ar, Co2, Ch4, C2h6, and Sf6 on Nax, H-Zsm-5, and Na-Zsm-5 Zeolites." *Langmuir* 12, no. 24 (1996): 5896-5904.

Dzhigit, O. M., A. V. Kiselev, K. N. Mikos, G. G. Muttik and Rahmabov.Ta. "Heats of Adsorption of Water Vapour on X-Zeolites Containing Li+, Na+, K+, Rb+ and Cs+ Cations." *Transactions of the Faraday Society* 67, no. 578 (1971): 458-&.

El-Naggar, A. Y. "Thermal Analysis of the Modified and Unmodified Silica Gels to Estimate Their Applicability as Stationary Phase in Gas Chromatography." *Journal of Emerging Trends in Engineering and Applied Sciences* 4, (2013): 144-148.

Ertan, A. "Co2, N2 and Ar Adsorption on Zeolites." Izmır Institute of Technology, 2004.

Flanigen, E. M. "Zeolites and Molecular Sieves: An Historical Perspective." *Studies in Surface Science and Catalysis* 137, (2001): 11-35.

Freni, A., F. Russo, S. Vasta, M. Tokarev, Y. I. Aristov and G. Restuccia. "An Advanced Solid Sorption Chiller Using Sws-1ll." *Applied Thermal Engineering* 27, no. 13 (2007): 2200-2204.

Fujiki, J., N. Sonetaka, K. P. Ko and E. Furuya. "Experimental Determination of Intraparticle Diffusivity and Fluid Film Mass Transfer Coefficient Using Batch Contactors." *Chemical Engineering Journal* 160, no. 2 (2010): 683-690.

Garg, D. R. and D. M. Ruthven. "Theoretical Prediction of Breakthrough Curves for Molecular-Sieve Adsorption Columns .1. Asymptotic Solutions." *Chemical Engineering Science* 28, no. 3 (1973): 791-798.

Gerente, C., V. K. C. Lee, P. Le Cloirec and G. McKay. "Application of Chitosan for the Removal of Metals from Wastewaters by Adsorption - Mechanisms and Models Review." *Critical Reviews in Environmental Science and Technology* 37, no. 1 (2007): 41-127.

Glueckauf, E. "Theory of Chromatography Part.10- Formula for Diffusion into Spheres and Their Application to Chromatography." *Trans. Faraday Soc.* 51, (1955): 1540-1551.

Gopal, R., B. R. Hollebone, C. H. Langford and R. A. Shigeishi. "The Rates of Solar-Energy Storage and Retrieval in a Zeolite-Water System." *Solar Energy* 28, no. 5 (1982): 421-424.

Gray, P. G. and D. D. Do. "A Graphical-Method for Determining Pore and Surface Diffusivities in Adsorption Systems." *Industrial & Engineering Chemistry Research* 31, no. 4 (1992): 1176-1182.

Gregg, S. J. and K. S. W. Sing. *Adsorption, Surface Area and Porosity* Second ed.: Academic Press, 1982.

Halasz, I., S. Kim and B. Marcus. "Hydrophilic and Hydrophobic Adsorption on Y Zeolites." *Molecular Physics* 100, no. 19 (2002): 3123-3132.

Hall, K. R. , L. C. Eagleton, A. Acrivos and T. Vermeulen. "Pore and Solid Diffusion Kinetics in Fixed Bed Adsorption under Constant Pattern Conditions." *Industrial & Engineering Chemistry Fundamentals* 5 no. no.2 (1966): 212-223.

Hamadi, N. K., S. Swaminathan and X. D. Chen. "Adsorption of Paraquat Dichloride from Aqueous Solution by Activated Carbon Derived from Used Tires." *Journal of Hazardous Materials* 112, no. 1-2 (2004): 133-141.

Hamamoto, Y., K. C. A. Alam, B. B. Saha, S. Koyama, A. Akisawa and T. Kashiwagi. "Study on Adsorption Refrigeration Cycle Utilizing Activated Carbon Fibers. Part 1. Adsorption Characteristics." *International Journal of Refrigeration-Revue Internationale Du Froid* 29, no. 2 (2006): 305-314.

Ho, Y. S. and G. Mckay. "The Kinetics of Sorption of Basic Dyes from Aqueous Solution by Sphagnum Moss Peat." *The Canadian Journal of Chemical Engineering* 76, no. 4 (1998): 822-827.

Ho, Y. S. and G. McKay. "A Comparison of Chemisorption Kinetic Models Applied to Pollutant Removal on Various Sorbents." *Process Safety and Environmental Protection* 76, no. B4 (1998): 332-340.

Ho, Y. S. and G. McKay. "The Kinetics of Sorption of Divalent Metal Ions onto Sphagnum Moss Peat." *Water Research* 34, no. 735-742 (2000).

Ho, Y. S., J. C. Y. Ng and G. McKay. "Kinetics of Pollutant Sorption by Biosorbents: Review." *Separation and Purification Reviews* 29:2, (2000): 189-232.

Hu, E. J. "A Study of Thermal Decomposition of Methanol in Solar Powered Adsorption Refrigeration Systems." *Solar Energy* 62, no. 5 (1998): 325-329.

Hui, C. W., B. N. Chen and G. McKay. "Pore-Surface Diffusion Model for Batch Adsorption Processes." *Langmuir* 19, no. 10 (2003): 4188-4196.

Inglezakis, V. J. and S. G. Poulopoulos. *Adsorption, Ion Exchange and Catalysis: Design of Operations and Environmental Applications* 2006.

Jaroniec, M. "Fifty Years of the Theory of the Volume Filling of Micropores." *Adsorption-Journal of the International Adsorption Society* 3, no. 3 (1997): 187-188.

Juang, R. S. and M. L. Chen. "Application of the Elovich Equation to the Kinetics of Metal Sorption with Solvent-Impregnated Resins." *Industrial & Engineering Chemistry Research* 36, no. 3 (1997): 813-820.

Karger, J. and D. M. Ruthven. *Diffusion in Zeolites and Other Microporous Solids*: John Wiley & Sons, 1992.

Katiyar, A., S. W. Thiel, V. V. Guliants and N. G. Pinto. "Investigation of the Mechanism of Protein Adsorption on Ordered Mesoporous Silica Using Flow Microcalorimetry." *Journal of Chromatography A* 1217, no. 10 (2010): 1583-1588.

Keller, J. U. *Gas Adsorption Equilibria Experimental Methods and Adsorptive Isotherms*: Springer, 2005.

Kim, J. H., C. H. Lee, W. S. Kim, J. S. Lee, J. T. Kim, J. K. Suh and J. M. Lee. "Adsorption Equilibria of Water Vapor on Alumina, Zeolite 13x, and a Zeolite X/Activated Carbon Composite." *Journal of Chemical and Engineering Data* 48, no. 1 (2003): 137-141.

Kiselev, A. V. "Non-Specific and Specific Interactions of Molecules of Different Electronic Structures with Solid Surfaces." *Faraday Soc.* 40, (1965): 205-218.

Knaebel, K.S. - Adsorption Research Inc, "Adsorbent Selection" (accessed 23.12.2013 2013).

Ko, D. C. K., J. F. Porter and G. McKay. "Film-Pore Diffusion Model for the Fixed-Bed Sorption of Copper and Cadmium Ions onto Bone Char." *Water Research* 35, no. 16 (2001): 3876-3886.

Ko, D. C. K., J. F. Porter and G. McKay. "A Branched Pore Model Analysis for the Adsorption of Acid Dyes on Activated Carbon." *Adsorption-Journal of the International Adsorption Society* 8, no. 3 (2002): 171-188.

Lavanchy, A., M. Stockli, C. Wirz and F. Stoeckli. "Binary Adsorption of Vapours in Active Carbons Described by the Dubinin Equation." *Adsorption Science & Technology* 13, no. 6 (1996): 537-545.

Leite, A. P. F. and M. Daguenet. "Performance of a New Solid Adsorption Ice Maker with Solar Energy Regeneration." *Energy Conversion and Management* 41, no. 15 (2000): 1625-1647.

Leppajarvi, T., I. Malinen, J. Kangas and J. Tanskanen. "Utilization of P-I(Sat) Temperature-Dependency in Modelling Adsorption on Zeolites." *Chemical Engineering Science* 69, no. 1 (2012): 503-513.

Letterman, R. D. , J. E. Quon and R. S. Gemmell. "Film Transport Coefficient in Agitated Suspensions of Activated Carbon." *Journal (Water Pollution Control Federation)* 46, no. no. 11 (1974): 2536-2546.

Li, Z. and R. T. Yang. "Concentration Profile for Linear Driving Force Model for Diffusion in a Particle." *Aiche Journal* 45, no. 1 (1999): 196-200.

Liaw, C. H., J. S. P. Wang, R. A. Greenkorn and K. C. Chao. "Kinetics of Fixed-Bed Adsorption: A New Solution." *Aiche Journal* 25, (1979): 376-381.

Liu, Y. and K. C. Leong. "The Effect of Operating Conditions on the Performance of Zeolite/Water Adsorption Cooling Systems." *Applied Thermal Engineering* 25, no. 10 (2005): 1403-1418.

Ma, Y. H. and T. Y. Lee. "Transient Diffusion in Solids with a Bipore Distribution." *Aiche Journal* 22, no. 1 (1976): 147-152.

Malash, G. F. and M. I. El-Khaiary. "Piecewise Linear Regression: A Statistical Method for the Analysis of Experimental Adsorption Data by the Intraparticle-Diffusion Models." *Chemical Engineering Journal* 163, no. 3 (2010): 256-263.

Malek, A. and S. Farooq. "Kinetics of Hydrocarbon Adsorption on Activated Carbon and Silica Gel." *Aiche Journal* 43, no. 3 (1997): 761-776.

Mathews, A. P. and W. J. Weber. "Effects of External Mass Transfer and Intraparticle Diffusion on Adsorption Rates in Slurry Reactors." *AIChE Symposium Series* 73, no. no.166 (1977): 91-98.

Mobedi, M. "Adsorpsiyonlu Isı Pompaları Üzerinde Teorik Ve Deneysel Bir Çalışma." Dokuz Eylül University, 1987.

Myers, D. *Surfaces, Interfaces and Colloids: Principles and Applications*. Second ed. Newyork: John Wiley & Sons, Inc, 1999.

Ng, K. C., H. T. Chua, C. Y. Chung, C. H. Loke, T. Kashiwagi, A. Akisawa and B. B. Saha. "Experimental Investigation of the Silica Gel-Water Adsorption Isotherm Characteristics." *Applied Thermal Engineering* 21, no. 16 (2001): 1631-1642.

Özkan, S.F. "Adsorbent Yatakların Dinamik Davranışının İncelenmesi Ve Doğal Kaynakların Adsorbent Olarak Değerlendirilmesi." Ege University, 1991.

Parfitt, R. L. "Anion Adsorption by Soils and Soil Materials." In *Advances in Agronomy*, edited by Nyle C. Brady, 30. New Zealand: Academic Press Inc., 1978.

Perry, R. H. and D. W. Green. *Perry's Chemical Engineers' Handbook*: Mcgraw-Hill Companies, 1997.

Qiu, H., L. Lv, B. C. Pan, Q. J. Zhang, W. M. Zhang and Q. X. Zhang. "Critical Review in Adsorption Kinetic Models." *Journal of Zhejiang University-Science A* 10, no. 5 (2009): 716-724.

Reichenberg, D. . "Properties of Ion-Exchange Resins in Relation to Their Structure. Iii. Kinetics of Exchange." *J. Am. Chem. Soc.* 75, (1953): 589–597.

Ritchie, A. G. "Alternative to the Elovich Equation for the Kinetics of Adsorption of Gases on Solids." *J. Chem. Soc., Faraday Trans. 1* 73, (1977): 1650±1653.

Rouquerol, F., J. Rouquerol and K. Sing. *Adsorption by Powders and Porous Solids*: Academic Press, 1999.

Ruthven, D. M. "The Rectangular Isotherm Model for Adsorption Kinetics." *Adsorption-Journal of the International Adsorption Society* 6, no. 4 (2000): 287-291.

Ruthven, D. M. "Diffusion in Zeolites-a Continuing Saga." *Adsorption-Journal of the International Adsorption Society* 16, no. 6 (2010): 511-514.

Ruthven, D. M. "Diffusion in Type a Zeolites: New Insights from Old Data." *Microporous and Mesoporous Materials* 162, (2012): 69-79.

Ruthven, D. M. . *Principles of Adsorption and Adsorption Processes*: John Wiley & Sons, 1984.

Ruthven, D. M., L. Heinke and J. Karger. "Sorption Kinetics for Surface Resistance Controlled Systems." *Microporous and Mesoporous Materials* 132, no. 1-2 (2010): 94-102.

Ryu, Y. K., S. J. Lee, J. W. Kim and C. H. Lee. "Adsorption Equilibrium and Kinetics of H2o on Zeolite 13x." *Korean Journal of Chemical Engineering* 18, no. 4 (2001): 525-530.

Saha, B. B., I. I. EI-Sharkawy, A. Chakraborty and S. Koyama. "Study on an Activated Carbon Fiber-Ethanol Adsorption Chiller: Part I - System Description and Modelling." *International Journal of Refrigeration-Revue Internationale Du Froid* 30, no. 1 (2007): 86-95.

Saha, B. B., I. I. EI-Sharkawy, A. Chakraborty and S. Koyama. "Study on an Activated Carbon Fiber-Ethanol Adsorption Chiller: Part Ii - Performance Evaluation." *International Journal of Refrigeration-Revue Internationale Du Froid* 30, no. 1 (2007): 96-102.

Sakoda, A. and M. Suzuki. "Fundamental-Study on Solar Powered Adsorption Cooling System." *Journal of Chemical Engineering of Japan* 17, no. 1 (1984): 52-57.

Sakoda, A. and M. Suzuki. "Simultaneous Transport of Heat and Adsorbate in Closed Type Adsorption Cooling System Utilizing Solar Heat." *Journal of Solar Energy Engineering-Transactions of the Asme* 108, no. 3 (1986): 239-245.

San, J. Y. "Analysis of the Performance of a Multi-Bed Adsorption Heat Pump Using a Solid-Side Resistance Model." *Applied Thermal Engineering* 26, no. 17-18 (2006): 2219-2227.

San, J. Y. and W. M. Lin. "Comparison among Three Adsorption Pairs for Using as the Working Substances in a Multi-Bed Adsorption Heat Pump." *Applied Thermal Engineering* 28, no. 8-9 (2008): 988-997.

Serbezov, A. and S. V. Sotirchos. "On the Formulation of Linear Driving Force Approximations for Adsorption and Desorption of Multicomponent Gaseous Mixtures in Sorbent Particles." *Separation and Purification Technology* 24, no. 1-2 (2001): 343-367.

Shigeishi, R. A., C. H. Langford and B. R. Hollebone. "Solar Energy Storage Using Chemical Potential Changes Associated with Drying of Zeolites." *Solar Energy* 23, (1979): 489-495

Sircar, S. and A. L. Myers. "Gas Separation by Zeolites." In *Handbook of Zeolite Science and Technology*, edited by S. M. Auerbach, K. A. Carrado and P. K. Dutta. Newyork: Marcel Dekker, Inc, 2003.

Spiewak, B. E. and J. A. Dumesic. "Microcalorimetric Measurements of Differential Heats of Adsorption on Reactive Catalyst Surfaces." *Thermochimica Acta* 290, no. 1 (1997): 43-53.

Srivastava, N. C. and I. W. Eames. "A Review of Adsorbents and Adsorbates in Solid-Vapour Adsorption Heat Pump Systems." *Applied Thermal Engineering* 18, no. 9-10 (1998): 707-714.

Steiner, T. "The Hydrogen Bond in the Solid State." *Angewandte Chemie-International Edition* 41, no. 1 (2002): 48-76.

Sumathy, K. , K.H. Yeung and L. Yong. "Technology Development in the Solar Adsorption Refrigeration Systems." *Progress in Energy and Combustion Science* 29, (2003): 301–327.

Sun, Q. Y. and L. Z. Yang. "The Adsorption of Basic Dyes from Aqueous Solution on Modified Peat-Resin Particle." *Water Research* 37, no. 7 (2003): 1535-1544.

Suzuki, M. *Adsorption Engineering*. Vol. 25: Elsevier Science 1990.

Tahat, M. A. "Heat-Pump/Energy-Store Using Silica Gel and Water as a Working Pair." *Applied Energy* 69, no. 1 (2001): 19-27.

TamainotTelto, Z. and R. E. Critoph. "Adsorption Refrigerator Using Monolithic Carbon-Ammonia Pair." *International Journal of Refrigeration-Revue Internationale Du Froid* 20, no. 2 (1997): 146-155.

Taylor, H. A. and N. Thon. "Kinetics of Chemisorption." In *Chemisorption of Gases on Solids*. Newyork: Division of Colloid Chemistry, 1951.

Techernev, D. I. "Solar Energy Application of Natural Zeolites." *Natural zeolites: Occurrence, properties, use*, (1978): 479-485.

Teng, Y. , R. Z. Wang and J. Y. Wu. "Study of the Fundamentals of Adsorption Systems." *Applied Thermal Engineering* 17, (1996): 327-338.

Thomas, W. J. *Adsorption Technology and Design*. Oxford Boston :Butterworth-Heinemann, 1998.

Tsistsishvili, G. V., T. G. Andronikashvili, G. N. Kirov and L. D. Filizova. *Natural Zeolites*. Chichester, England: Ellis Horwood Limited, 1992.

Ulku, S., D. Balkose and B. Alp. "Dynamic Heat of Adsorption of Water Vapour on Zeolitic Tuff and Zeolite 4a by Flow Microcalorimetry." *Oxidation Communications* 29, no. 1 (2006): 204-215.

Ulku, S., D. Balkose, T. Caga, F. Ozkan and S. Ulutan. "A Study of Adsorption of Water Vapour on Wool under Static and Dynamic Conditions." *Adsorption-Journal of the International Adsorption Society* 4, no. 1 (1998): 63-73.

Ülkü, S. "Adsorption Heat Pumps." *Heat Recovery Systems* 6, (1986): 277-284.

Ülkü, S. "Natural Zeolites in Energy Storage and Heat Pumps." *Studies in Surface Science and Catalysis* 28, (1986): 1047-1054.

Ülkü, S. "Novel Application of Adsorption: Energy Recovery." *Studies in Surface Science and Catalysis Fundamentals of Adsorption* 80, (1993): 685-693.

Ülkü, S. and M. Mobedi. "Adsorption in Energy Storage." *Energy Storage Systems*, (1989): 487-507.

Ülkü, S., S. Beba, Z. Kıvrak and B. Seyrek. "Enerji Depolama Ve Hava Kurutmada Doğal Zeolitlerden Yararlanma." In *Isı Bilim ve Tekniği, 5. Ulusal Kongresi*, 549-558. İstanbul, 1985.

Ülkü, S. and F. Çakıcıoğlu. "Energy Recovery in Drying Applications." *Renewable Energy* 1, (1991): 695-698.

Ülkü, S., E. Değirmen and S. Nikhnam. "Güneş Enerjisinden Faydalanarak Doğal Zeolitlerin Kullanımı Ile Isıtma Ve Soğutma." *Isı Bilim ve Tekniği* 8, no. 4 (1986): 13-20.

Ülkü, S., A. Ç. Gürses and M. Toksoy. "Enerji Tasarrufu Ve Isı Pompaları." In *Enerji Tasarrufu Semineri Bildiriler Kitabı*, 27-38. İstanbul, 1987.

Valsaraj, K. T. and L. J. Thibodeaux. "On the Linear Driving Force Model for Sorption Kinetics of Organic Compounds on Suspended Sediment Particles." *Environmental Toxicology and Chemistry* 18, no. 8 (1999): 1679-1685.

Wang, D. C., Z. Z. Xia and J. Y. Wu. "Design and Performance Prediction of a Novel Zeolite-Water Adsorption Air Conditioner." *Energy Conversion and Management* 47, no. 5 (2006): 590-610.

Wang, L. W., R. Z. Wang and R. G. Oliveira. "A Review on Adsorption Working Pairs for Refrigeration." *Renewable & Sustainable Energy Reviews* 13, no. 3 (2009): 518-534.

Wang, R. Z., J. Y. Wu, Y. X. Xu, Y. Teng and W. Shi. "Experiment on a Continuous Heat Regenerative Adsorption Refrigerator Using Spiral Plate Heat Exchanger as Adsorbers." *Applied Thermal Engineering* 18, no. 1-2 (1998): 13-23.

Wang, X., W. Zimmermann, K. C. Ng, A. Chakraboty and J. U. Keller. "Investigation on the Isotherm of Silica Gel Plus Water Systems - Tg and Volumetric Methods." *Journal of Thermal Analysis and Calorimetry* 76, no. 2 (2004): 659-669.

Wang, Y. and M. D. Levan. "Adsorption Equilibrium of Carbon Dioxide and Water Vapor on Zeolites 5a and 13x and Silica Gel: Pure Components." *Journal of Chemical and Engineering Data* 54, no. 10 (2009): 2839-2844.

Yang, R. T. . *Adsorbents: Fundamentals and Applicatıons*: John Wiley & Sons, 2003.

Yıldırım, Z. E. . "A Study on Isotherm Characteristics of Adsorbent-Adsorbate Pairs Used in Adsorption Heat Pumps." İzmir Institute of Technology, 2011.

Yoshida, H., T. Kataoka and D. M. Ruthven. "Analytical Solution of the Breakthrough Curve for Rectangular Isotherm Systems." *Chemical Engineering Science* 39, no. 10 (1984): 1489-1497.

Yucel, H. and D. M. Ruthven. "Diffusion of Co2 in 4a and 5a Zeolite Crystals." *Journal of Colloid and Interface Science* 74, no. 1 (1980): 186-195.

Zdravkov, B. D., J. J. Cermak, M. Sefara and J. Janku. "Pore Classification in the Characterization of Porous Materials: A Perspective." *Central European Journal of Chemistry* 5, no. 2 (2007): 385-395.

Zhang, X. J. and L. M. Qu. "Moisture Transport and Adsorption on Silica Gel-Calcium Chloride Composite Adsorbents." *Energy Conversion and Management* 48, no. 1 (2007): 320-326.

APPENDIX A

PHYSICAL FORCES INVOLVED IN ADSORPTION PROCESSES

As indicated before, adsorption occurs due to the interactions between adsorbate and adsorbent molecules. Van der Waals forces control the non-chemical interactions between atoms and molecules.

Due to either to a formal charge separation or differences in the electronegativities of the atoms forming a covalent bond, an unsymmetrical distribution of electron density within a molecule occurs which causes a dipole. Van der Waals forces can be classified in three types of atomic and molecular interactions which are permanent dipole, induced dipole and London forces. The molecules can be polar in nature with permanent dipole or they can be polarized by the influence of the neighboring electric field producing induced dipole.

When two polar molecules are near to each other, a dipole-dipole interaction occurs between the magnets. On the other hand, there will occur a dipole- induced dipole interaction if there is a polar and a nonpolar molecule (Figure A.1).

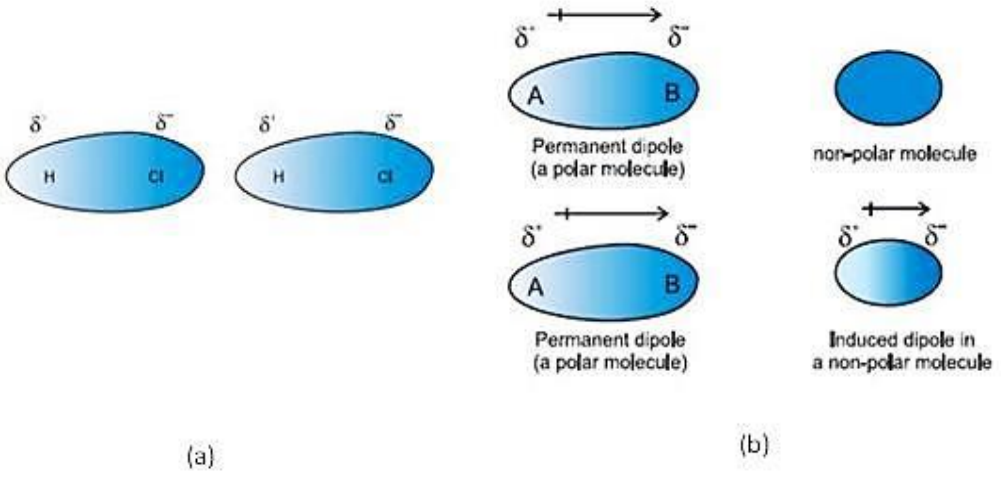

Figure A.1. a) dipole-dipole interaction b)dipole-induced dipole interaction

In the adsorption processes, the most significant force is the London dispersion force that arises from rapid fluctuation in electron density within each atom which causes attraction between two atoms by inducing electrical moment in a near neighbor. The characteristics of dispersion force are (Myers 1999);

- They have long range action that their effect is extending in the range of 0.2-10 nm compared to covalent bonds which is in the range of 0.1-0.2 nm.
- They can be attractive or repulsive.

Due to the fluctuating dipoles, the London dispersion forces are considered as quantum mechanical in nature. Basically, the dispersion force can be described by the following way. Due to the movement of electrons in a molecule or atom, there may have an instantaneous dipole moment. As a result of this instantaneous dipole, a short-lived electrical field will be introduced and then polarized the neighboring atom or molecule by inducing a dipole in neighbor (Figure A.2).

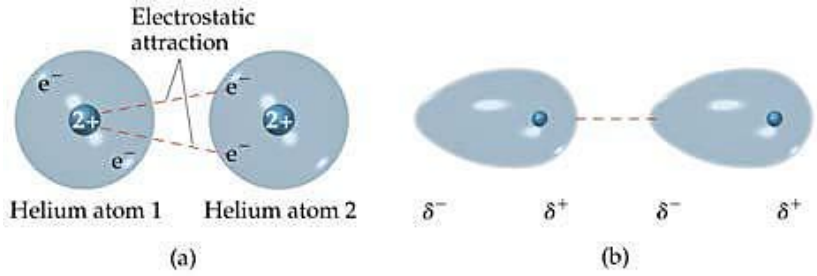

Figure A.2. Schematic illustration of dispersion force

By using the quantum mechanical perturbation theory, potential energy equation of two isolated atoms at distance ‘r’ was derived by London for dispersion and short-range repulsive forces (Gregg and Sing 1982). The sum of the dispersion and repulsive interactions give the total potential value which is also known as Lennard-Jones potential as given in Equation A.1.

$$\Delta G=\Delta G_{rep}+\Delta G_{att}=\frac{B}{r^{12}}-\frac{C}{r^{6}} \qquad (A.1)$$

Where C is dispersion constant associated with the dipole-dipole interaction and B is an empirical constant. The negative sign for C indicates the attraction. Gregg and Sing (1982) denoted that since the number of atoms at a given distance from the gas atom increases when the solid becomes more compacted, the interaction potential becomes larger as the solid particles become larger.

Kiselev (1965) was classified adsorption of molecules on surfaces according to their specific and non-specific interaction capacities to explain the effect of polarity in improvement of interaction energy. While only dispersion and repulsive forces are involved in non-specific interactions, coulombic forces are also involved in specific interactions. Hydrogen bond is an example of the specific interactions.

Hydrogen Bonding

The term of "hydrogen bonding" has been discussed for a long time. While some researchers claim that the hydrogen bond is electrostatic which is caused from the dipole-dipole interactions, others say that it is also a partial covalent in nature. The classical definition of the hydrogen bond is that it is present between molecules where hydrogen atom (H) is connected to fluorine (F), oxygen (O) or nitrogen (N) atoms (Figure A.3). The shared electrons of fluorine, oxygen and nitrogen which have high ionization energies are tightly held to hydrogen. As a result the fluorine, oxygen and nitrogen atoms become negative charged while hydrogen atom has a small positive charge. When the positively charged hydrogen atom interacts with a free electron pair on the negatively charged fluorine, oxygen or nitrogen, the hydrogen bond occurs.

Conversely, some researchers point out the partial covalent nature of the hydrogen bond and they indicate that it is not enough to define the hydrogen bonding in several experiments only with electrostatic forces. Buckingham et al. (2008) defined the hydrogen bond as an attraction between proton donor X-H and a proton acceptor Y. Arunan et al. (2011) stated that X could be any element having electronegativity larger than that of H (F, N, O, C, P, S, Cl, Se, Br and I) and Y could be any of these elements and also π-electrons.

The hydrogen bond has contribution of different interactions. Due to the variations in donor, acceptor and environment, hydrogen bond can transform to pure

van der Waals interaction, covalent bond, purely ionic interaction and cation-π interaction (Steiner 2002).

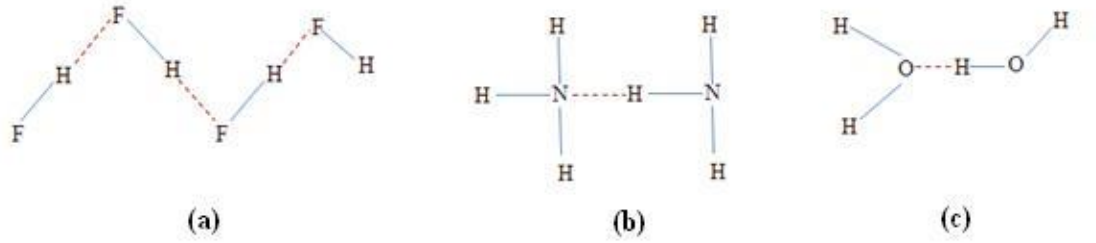

Figure A.3. Hydrogen bonding between a) HF b) NH_3 c) H_2O molecules

Jeffrey (1997) classified the hydrogen bond in three categories as weak, moderate and strong. While the covalent properties are increased in strong hydrogen bonds, electrostatic interactions and dispersion forces are more feasible in weak hydrogen bonds (Steiner 2002).

APPENDIX B

PHYSICAL PROPERTIES OF MATERIALS

Table B.1. Thermophysical properties of silica gel
(Source: Chua et al. 2002)

Property	Type A	Type RD
BET/N_2 Surface Area (m^2/g)	716 (±3.3)	838 (± 3.8)
BET constant	293.8	258.6
BET volume STP (cm^3/g)	164.5	192.5
Pore size (nm)	0.8-5	0.8-7.5
Porous volume (cm^3/g)	0.28	0.37
Micropore volume (%)	57	49
Mesopore volume (%)	53	51
Particle bulk density (kg/m^3)	1306	1158
Surface area (m^2/g)	650	720
Average pore diameter (nm)	2.2	2.2
Apparent density (kg/m^3)	730	700
Mesh size	10-40	10-20
Specific heat capacity (kJ/kg.K)	0.921	0.921
Thermal conductivity (W/m.K)	0.174	0.198

Table B.2 Thermophysical Properties of Water

Molecular Weight (g/mol)	18.015
Critical Temperature (K)	647.1
Critical Pressure (bar)	220.55
Critical Volume (cm^3/mol)	55.9
Normal Boiling Point (K)	373.15
Kinetic Diameter (Å)	2.641
Polarizability $x10^{-25}$ (cm^3)	14.50
Dipole moment $x10^{18}$ (esu cm)	1.87

Table B.3. Physical properties of zeolites
(Source: Perry and Green 1997)

Properties	**13X**	**4A**
Internal porosity	≈ 0.38%	≈ 0.32%
Bulk density (kg/m^3)	580-640	610-670
Average pore diameter (nm)	1	0.4
Surface area (m^2/g)	≈600	≈700
Sorptive capacity (kg/kg)	0.25-0.36	0.22-0.26

APPENDIX C

SAMPLE CALCULATIONS

The procedure for calculation of the adsorbed amount for type RD silica gel-water pair at the temperature of 60°C is given below;

PV=mRT

- For the first pulse;

V_{vapor} = 500ml+4ml = 504 ml = 0.504x10^{-3} m^3 (volume of vapor vessel + pipes)

R = 0.461 m^3Pa/gK

T= 331 K

$P_{initial}$=2479.8 Pa

$$m_{vapor}=\frac{2479.8*0.504*10^{-3}}{0.461*331}=8.17*10^{-3}\ g$$

V_{total}=500 mL+4 mL+50 mL=554 mL = 0.554x10^{-3} m^3(volume of vapor vessel+pipes+adsorbent vessel)

P_{eq}=298.6 Pa

$$m_{total1}=\frac{298.6*0.554*10^{-3}}{0.461*331}=1.08*10^{-3}\ g$$

$$m_{ads}=m_{vapor}-m_{total1}$$

$$m_{ads}=(8.17-1.08)*10^{-3}=7.09*10^{-3}g$$

$$q_1=\frac{m_{ads}}{m_{silica\ gel}}=\frac{7.09*10^{-3}}{0.3}*100=2.36\%\ \text{kg water/kg silica gel}$$

- For the second pulse the procedure is a bit different;

V_{vapor} = 500ml+4ml = 504 ml = 0.504x10^{-3} m^3 (volume of vapor vessel + pipes)

R = 0.461 m^3Pa/gK

T= 331 K

$P_{initial}$=2673.2 Pa

$$m_{vapor}=\frac{2673.2*0.504*10^{-3}}{0.461*331}=8.81*10^{-3}\ g$$

P_{eq}=843.9 Pa

At previous pulse, the equilibrium pressure was 298.6 Pa in the vapor and adsorbent vessels which means that the vapor was not adsorbed. The remaining vapor amount is;

V_{remain} = 50ml+4ml = 54 ml = 0.054x10^{-3} m^3 (volume of adsorbent vessel + pipes) which is nearly one-tenth of the total volume

$$m_{remain}=\frac{m_{total1}}{10}=1.08*10^{-4}g$$

V_{total}=500 mL+4 mL+50 mL=554 mL = 0.554x10^{-3} m^3(volume of vapor vessel+pipes+adsorbent vessel)

P_{eq}=843.9 Pa

$$m_{total2}=\frac{843.9*0.554*10^{-3}}{0.461*331}=3.05*10^{-3}\ g$$

$$m_{ads}=(m_{vapor}+m_{remain})-m_{total}$$

$$m_{ads}=\left[8.81*10^{-3}+1.08*10^{-4}-3.05*10^{-3}\right]=5.86*10^{-3}g$$

$$q_{2pulse}=\frac{m_{ads}}{m_{silica\ gel}}=\frac{5.86*10^{-3}}{0.3}=0.0195\ \text{kg water/kg silica gel}$$

$$q_2=q_1+q_{2pulse}=(0.0236+0.0195)*100=4.31\%\ \text{kg water/kg silica gel}$$

This calculation procedure was repeated for all pulses. After calculation of adsorbed amount for each pulse, adsorption isotherm was obtained.

The effective volume of the systems was 631 mL and 676 mL for type RD silica gel-water and zeolite 13X-water pairs, respectively.

APPENDIX D

PLOTS OF LEAKAGE AND CONDENSATION TESTS

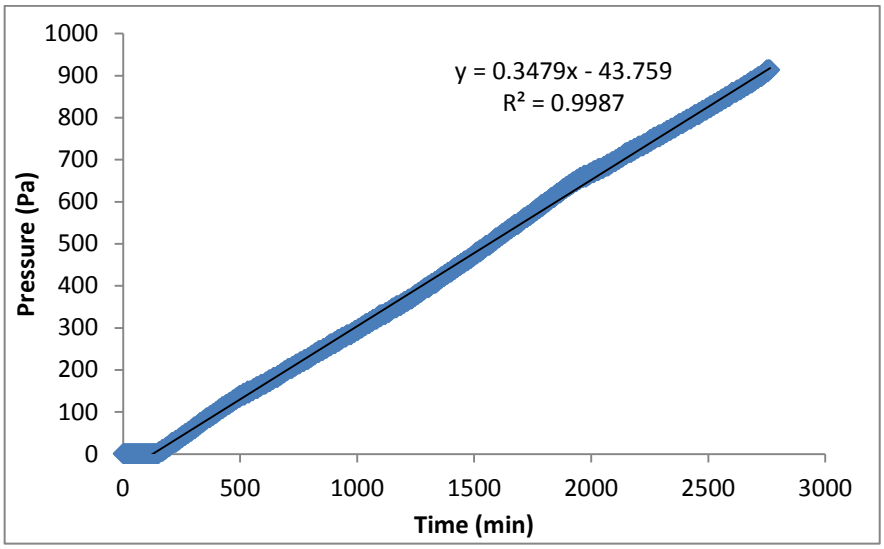

Figure D.1. Leakage test for type RD silica gel-water pair

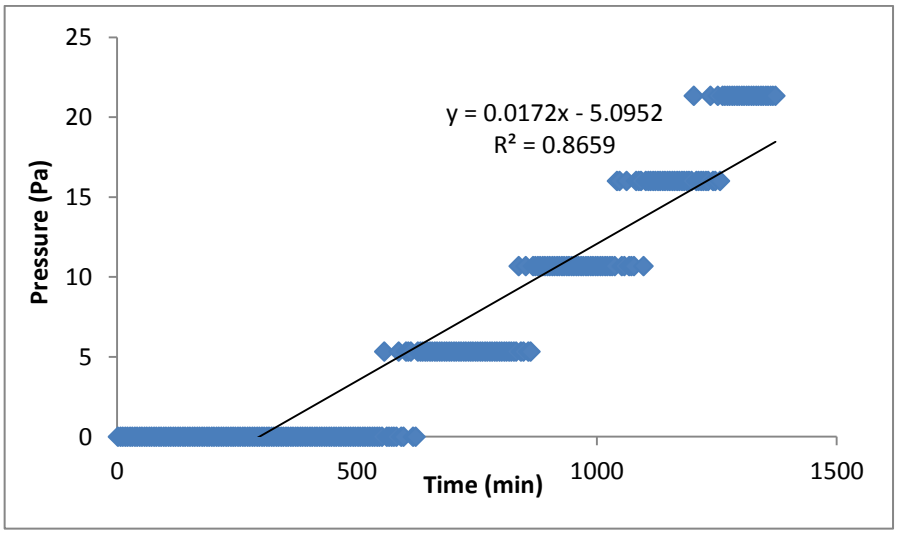

Figure D.2. Leakage test for zeolite 13X-water pair

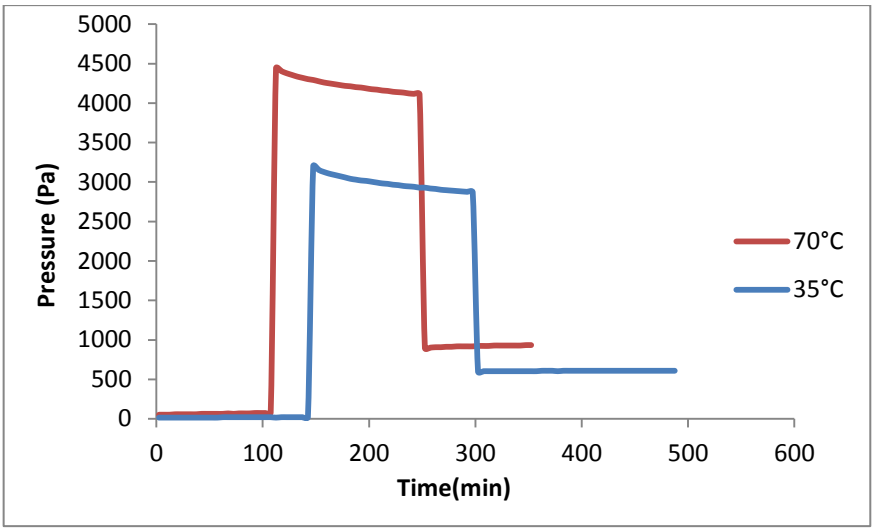

Figure D.3. Condensation test for zeolite 13X-water pair

APPENDIX E

PRESSURE AND TEMPERATURE CHANGES DURING THE EXPERIMENTS

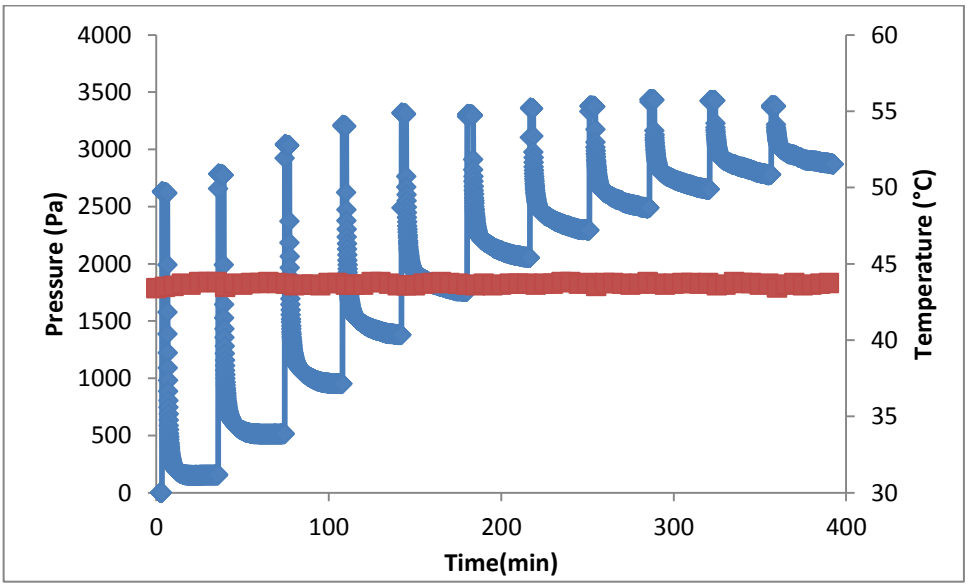

Figure E.1. Pressure and temperature changes during the experiment of type RD silica gel-water at 45°C

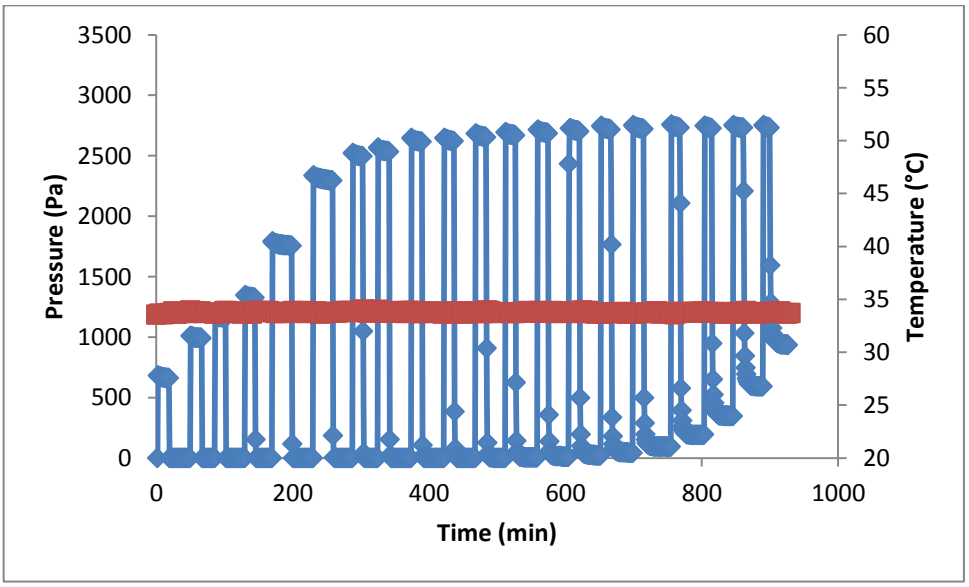

Figure E.2. Pressure and temperature changes during the experiment of zeolite 13X-water regenerated at 60°C

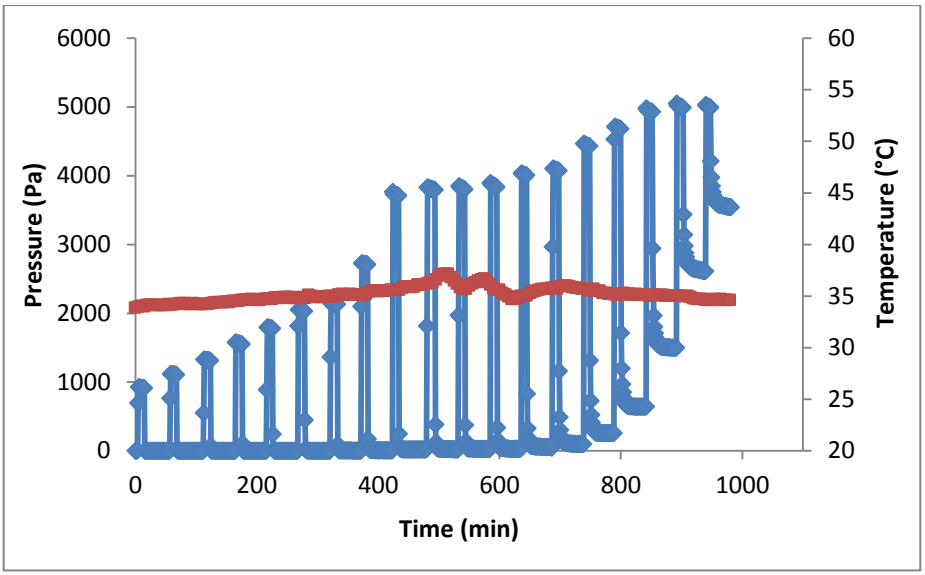

Figure E.3. Pressure and temperature changes during the experiment of zeolite 13X-water regenerated at 90°C

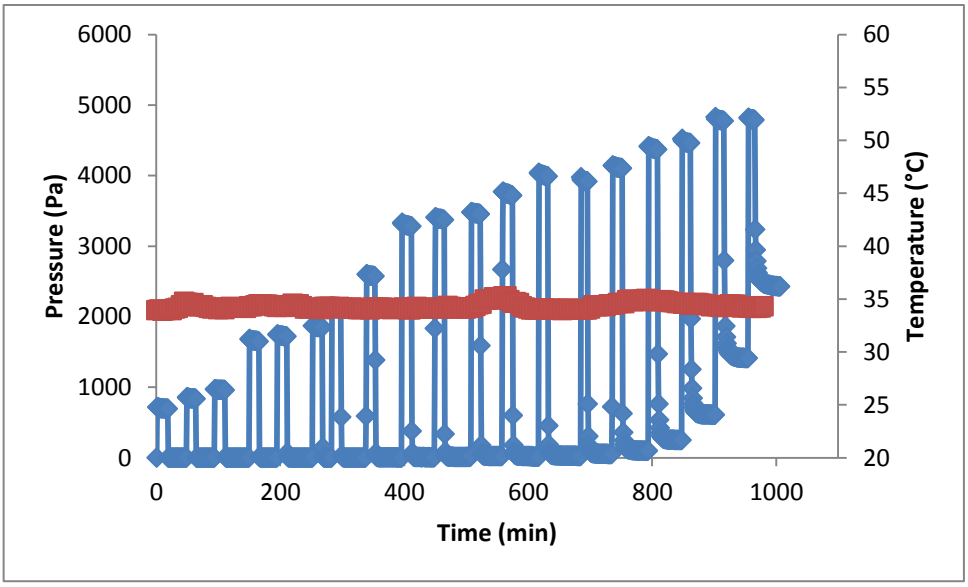

Figure E.4. Pressure and temperature changes during the experiment of zeolite 13X-water regenerated at 120°C

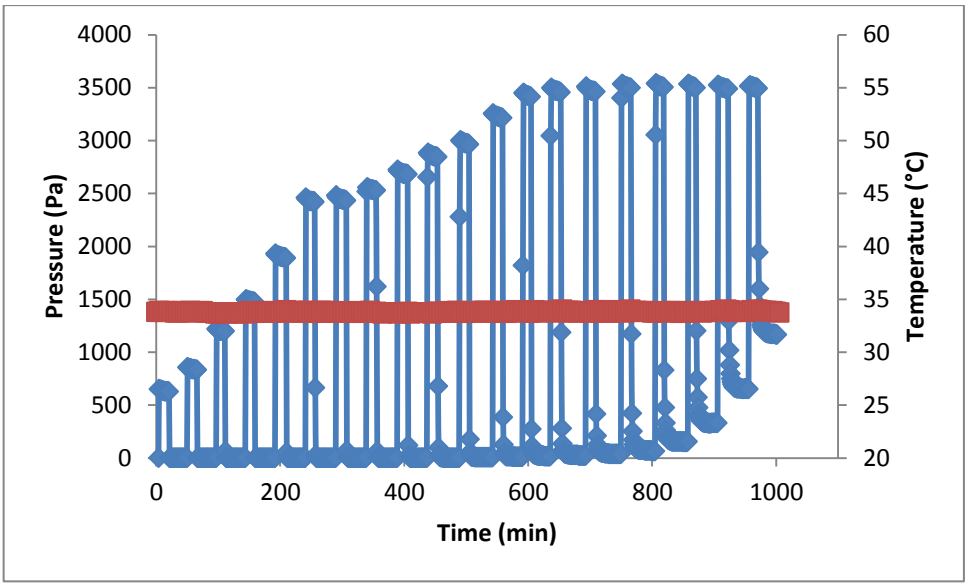

Figure E.5. Pressure and temperature changes during the experiment of zeolite 13X-water regenerated at 150°C

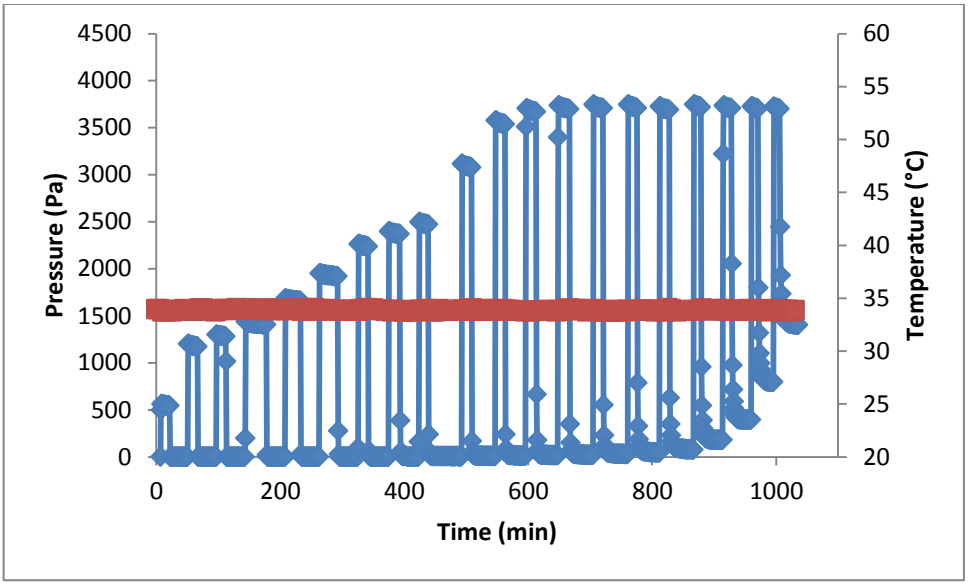

Figure E.6. Pressure and temperature changes during the experiment of zeolite 13X-water regenerated at 200°C

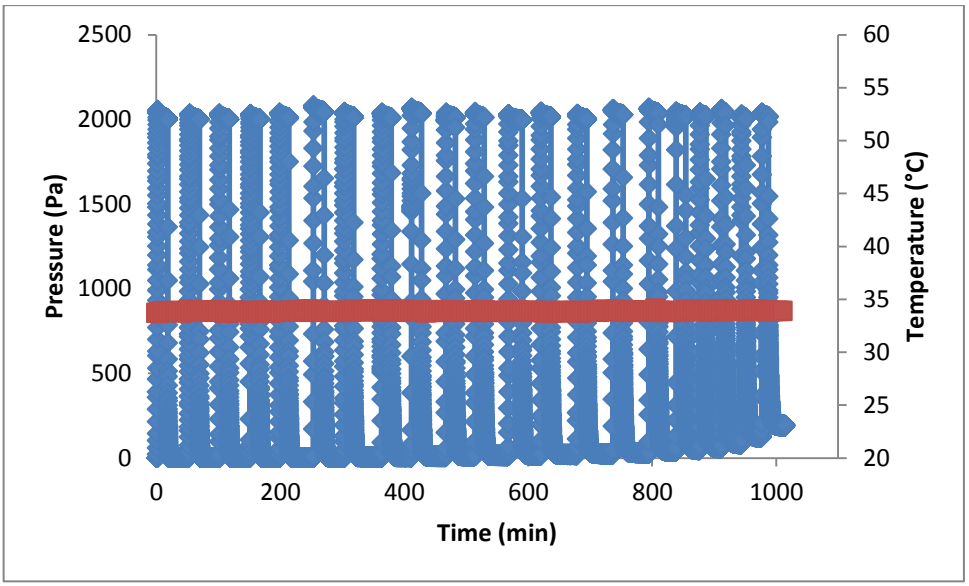

Figure E.7. Pressure and temperature changes during the experiment of zeolite 13X-water regenerated at 120°C for constant initial pressure

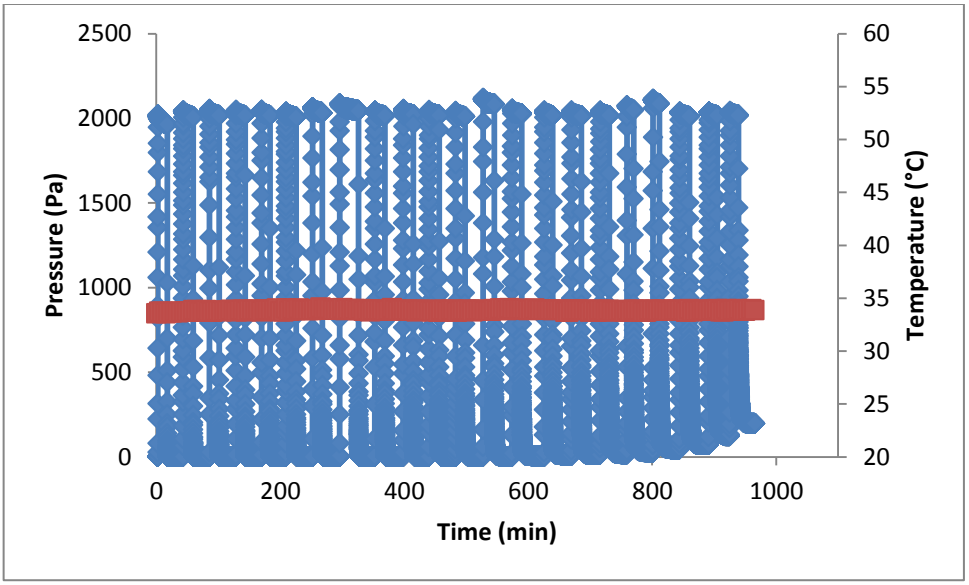

Figure E.8. Pressure and temperature changes during the experiment of zeolite 13X-water regenerated at 150°C for constant initial pressure

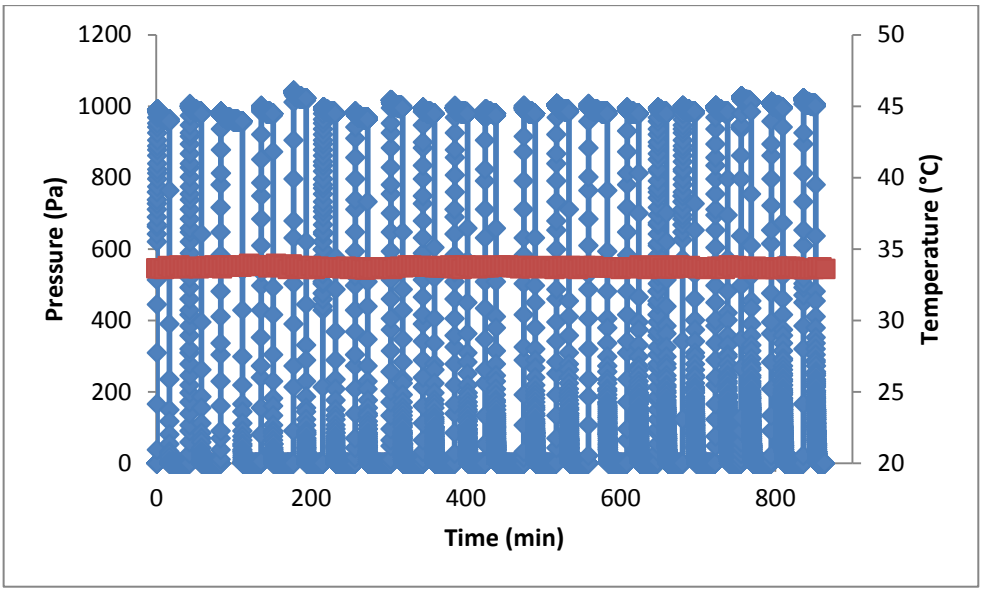

Figure E.9. Pressure and temperature changes during the experiment of zeolite 13X-water regenerated at 90°C for constant initial pressure

The importance of evacuation of liquid vessel was mentioned in chapter 5. The effect of evacuation of liquid vessel is shown in Figure E.10. Both experiments were run at 35°C which was regenerated at 90°C under vacuum. Although zeolite 13X has ability to adsorb water vapor at low pressures, it cannot be observed due to the air inside the system.

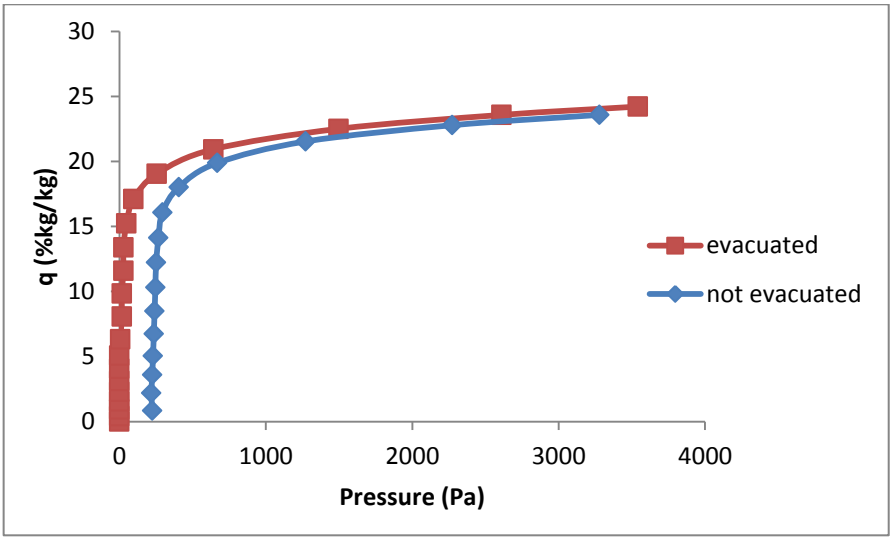

Figure E.10 The effect of evacuation of liquid vessel

APPENDIX F

RAW DATA FOR EXPERIMENTAL STUDY

Table F.1. Raw Data of experimental study of Type RD silica gel-water pair

T_{ads}=35°C				
Pulse number	**P_1 (Pa)**	**P_2 (Pa)**	**q (% kg/kg)**	**D_{eff} (m^2/s) (M_t/M_∞>0.7)**
1	1271.90	10.67	1.49	1.02E-09
2	1351.90	79.99	2.98	5.63E-10
3	1646.50	202.60	4.67	4.74E-10
4	2319.80	410.60	6.91	3.36E-10
5	2955.70	715.90	9.52	3.06E-10
6	3346.30	982.60	12.29	1.97E-10
7	3976.90	1346.50	15.37	1.88E-10
8	4090.30	1651.80	18.23	1.68E-10
9	4351.60	1955.80	21.04	1.58E-10
10	4404.90	2255.80	23.57	1.58E-10
11	4511.50	2495.80	25.95	1.58E-10
12	4516.90	2806.40	27.97	1.97E-10
T_{ads}=45°C				
Pulse number	**P_1 (Pa)**	**P_2 (Pa)**	**q (% kg/kg)**	**D_{eff} (m^2/s) (M_t/M_∞>0.7)**
1	2691.70	154.70	2.82	8.41E-10
2	2774.10	513.30	5.38	4.73E-10
3	3035.70	950.60	7.74	2.9E-10
4	3202.30	1378.90	9.80	2.22E-10
5	3309.00	1758.50	11.56	2.03E-10
6	3298.30	2053.10	12.98	1.93E-10
7	3357.00	2293.10	14.20	1.93E-10
8	3373.00	2490.40	15.22	1.93E-10
9	3431.70	2651.70	16.13	1.64E-10

(cont. on next page)

Table F.1 (cont.)

10	3426.30	2779.70	16.90	1.64E-10
11	3378.50	2870.40	17.51	1.64E-10
T_{ads}=60°C				
Pulse number	**P_1 (Pa)**	**P_2 (Pa)**	**q (% kg/kg)**	**D_{eff} (m^2/s) (M_t/M_∞>0.7)**
1	2501.10	336.00	2.34	9.18E-10
2	2993.00	987.90	4.48	5.03E-10
3	3437.00	1699.80	6.32	2.96E-10
4	3683.60	2319.80	7.77	2.57E-10
5	3838.30	2811.70	8.87	2.27E-10
6	3976.90	3197.00	9.72	1.97E-10
7	4008.90	3463.70	10.33	1.97E-10
8	4030.30	3657.00	10.76	1.97E-10
9	4223.60	3848.90	11.19	2.17E-10

Table F.2. Raw data of experimental study of zeolite 13X-water pair for different adsorption temperatures

T_{ads}=35°C				
Pulse number	**P_1 (Pa)**	**P_2 (Pa)**	**q (% kg/kg)**	**D_{eff} (m^2/s)**
1	1271.90	10.67	1.49	1.02E-09
2	1351.90	79.99	2.98	5.63E-10
3	1646.50	202.60	4.67	4.74E-10
4	2319.80	410.60	6.91	3.36E-10
5	2955.70	715.90	9.52	3.06E-10
6	3346.30	982.60	12.29	1.97E-10
7	3976.90	1346.50	15.37	1.88E-10
8	4090.30	1651.80	18.23	1.68E-10
9	4351.60	1955.80	21.04	1.58E-10
10	4404.90	2255.80	23.57	1.58E-10
11	4511.50	2495.80	25.95	1.58E-10
12	4516.90	2806.40	27.97	1.97E-10
T_{ads}=45°C				
Pulse number	**P_1 (Pa)**	**P_2 (Pa)**	**q (% kg/kg)**	**D_{eff} (m^2/s)**
1	2691.70	154.70	2.82	8.41E-10
2	2774.10	513.30	5.38	4.73E-10

(cont. on next page)

Table F.2 (cont.)

3	3035.70	950.60	7.74	2.9E-10
4	3202.30	1378.90	9.80	2.22E-10
5	3309.00	1758.50	11.56	2.03E-10
6	3298.30	2053.10	12.98	1.93E-10
7	3357.00	2293.10	14.20	1.93E-10
8	3373.00	2490.40	15.22	1.93E-10
9	3431.70	2651.70	16.13	1.64E-10
10	3426.30	2779.70	16.90	1.64E-10
11	3378.50	2870.40	17.51	1.64E-10
T_{ads}=60°C				
Pulse number	**P_1 (Pa)**	**P_2 (Pa)**	**q (% kg/kg)**	**D_{eff} (m^2/s)**
1	2501.10	336.00	2.34	9.18E-10
2	2993.00	987.90	4.48	5.03E-10
3	3437.00	1699.80	6.32	2.96E-10
4	3683.60	2319.80	7.77	2.57E-10
5	3838.30	2811.70	8.87	2.27E-10
6	3976.90	3197.00	9.72	1.97E-10
7	4008.90	3463.70	10.33	1.97E-10
8	4030.30	3657.00	10.76	1.97E-10
9	4223.60	3848.90	11.19	2.17E-10
T_{ads}=25°C				
Pulse number	**P_1 (Pa)**	**P_2 (Pa)**	**q (% kg/kg)**	**D_{eff} (m^2/s)**
1	603.90	0.00	0.29	2.09E-07
2	951.90	0.00	0.75	1.15E-07
3	989.20	0.00	1.23	7.97E-08
4	967.90	0.00	1.70	5.99E-08
5	962.60	0.00	2.17	4.91E-08
6	967.90	0.00	2.64	4.02E-08
7	973.20	0.00	3.11	3.42E-08
8	973.20	0.00	3.58	2.95E-08
9	978.60	0.00	4.06	2.63E-08
10	978.60	0.00	4.53	2.24E-08
11	973.20	0.00	5.00	2.01E-08
12	1031.90	0.00	5.50	1.81E-08
13	967.90	0.00	5.97	1.70E-08
14	983.90	0.00	6.45	1.61E-08
15	983.90	0.00	6.93	1.48E-08

(cont. on next page)

Table F.2 (cont.)

16	999.90	0.00	7.41	1.38E-08
17	973.20	0.00	7.88	1.29E-08
18	978.60	0.00	8.36	1.20E-08
19	973.20	0.00	8.83	1.11E-08
20	989.20	0.00	9.31	1.05E-08
21	983.90	0.00	9.79	9.79E-09

Table F.3. Raw data of experimental study of zeolite 13X-water pair for different desorption temperatures

T_{reg}=60°C; Regeneration time=10300 min; Increasing initial pressure				
Pulse number	**P_1 (Pa)**	**P_2 (Pa)**	**q (% kg/kg)**	**D_{eff} (m^2/s)**
1	662.60	0.00	0.31	
2	989.20	0.00	0.77	
3	1159.90	0.00	1.32	
4	1326.50	0.00	1.94	
5	1754.50	0.00	2.76	
6	2294.40	0.00	3.84	
7	2497.10	0.00	5.01	
8	2534.40	0.00	6.20	
9	2615.70	0.00	7.43	
10	2621.10	0.00	8.66	7.63E-09
11	2653.10	0.00	9.90	4.1E-09
12	2669.10	5.33	11.15	3.97E-09
13	2685.10	10.67	12.41	2.39E-09
14	2701.10	21.33	13.66	1.87E-09
15	2717.10	42.66	14.92	1.84E-09
16	2722.40	90.66	16.15	1.75E-09
17	2733.10	192.00	17.34	2.59E-09
18	2727.70	346.60	18.45	2.36E-09
19	2733.10	593.30	19.44	2.23E-09
20	2733.10	935.90	20.27	1.58E-09
T_{reg}=90°C; Regeneration time=10002 min; Increasing initial pressure				
Pulse number	**P_1 (Pa)**	**P_2 (Pa)**	**q (% kg/kg)**	**D_{eff} (m^2/s)**
1	909.20	0.00	0.43	
2	1106.60	0.00	0.95	
3	1310.50	0.00	1.56	

(cont. on next page)

Table F.3 (cont.)

4	1550.50	0.00	2.29	
5	1775.80	0.00	3.12	1.02E-08
6	2026.50	0.00	4.07	7.72E-09
7	2129.10	0.00	5.07	4.94E-09
8	2706.40	5.33	6.34	4.36E-09
9	3706.30	16.00	8.07	4.98E-09
10	3791.60	16.00	9.84	1.16E-09
11	3802.30	26.66	11.61	4.43E-09
12	3835.60	26.66	13.40	1.68E-09
13	4006.30	48.00	15.25	1.03E-09
14	4070.30	95.99	17.11	1.39E-09
15	4428.90	256.00	19.07	2.39E-09
16	4680.90	641.30	20.94	2.13E-09
17	4926.20	1497.20	22.52	1.26E-09
18	4990.20	2610.40	23.59	6.79E-10
19	4990.20	3541.00	24.23	7.43E-10
T_{reg}=120°C; Regeneration time=9027 min; Increasing initial pressure				
Pulse number	**P_1 (Pa)**	**P_2 (Pa)**	**q (% kg/kg)**	**D_{eff} (m^2/s)**
1	694.60	0.00	0.33	
2	833.30	0.00	0.72	
3	957.20	0.00	1.17	
4	1646.50	0.00	1.94	
5	1722.50	0.00	2.75	7.11E-09
6	1845.10	0.00	3.61	
7	2123.80	0.00	4.61	8.24E-09
8	2573.10	0.00	5.81	3.17E-09
9	3283.70	5.33	7.35	5.59E-09
10	3374.30	10.67	8.93	4.36E-09
11	3455.70	21.33	10.54	3.55E-09
12	3717.00	16.00	12.28	1.45E-09
13	3990.30	21.33	14.14	1.07E-09
14	3915.60	48.00	15.95	1.75E-09
15	4102.30	95.99	17.83	1.07E-09
16	4370.20	250.60	19.76	1.81E-09
17	4460.90	609.30	21.55	1.65E-09
18	4776.90	1411.90	23.09	1.10E-09
19	4787.50	2427.80	24.16	7.43E-10

(cont. on next page)

Table F.3 (cont.)

T_{reg}=150°C; Regeneration time=10100 min; Increasing initial pressure				
Pulse number	**P_1 (Pa)**	**P_2 (Pa)**	**q (% kg/kg)**	**D_{eff} (m^2/s)**
1	625.30	0.00	0.29	
2	833.30	0.00	0.69	
3	1197.20	0.00	1.25	
4	1470.50	0.00	1.94	
5	1887.80	0.00	2.83	
6	2417.10	0.00	3.97	
7	2433.10	0.00	5.11	
8	2529.10	0.00	6.30	
9	2679.70	0.00	7.56	8.34E-09
10	2845.00	0.00	8.90	6.40E-09
11	2962.40	5.33	10.29	4.59E-09
12	3214.30	10.67	11.80	4.49E-09
13	3413.00	16.00	13.40	2.17E-09
14	3455.70	21.33	15.02	1.42E-09
15	3461.00	37.33	16.63	1.55E-09
16	3498.30	63.99	18.24	1.03E-09
17	3503.60	149.30	19.82	2.10E-09
18	3498.30	330.60	21.30	2.49E-09
19	3487.70	651.90	22.62	2.00E-09
20	3493.00	1165.20	23.70	1.29E-09
T_{reg}=200°C; Regeneration time=11400 min; Increasing initial pressure				
Pulse number	**P_1 (Pa)**	**P_2 (Pa)**	**q (% kg/kg)**	**D_{eff} (m^2/s)**
1	545.30	0.00	0.26	
2	1170.50	0.00	0.80	
3	1278.50	0.00	1.40	
4	1406.50	0.00	2.06	
5	1657.20	0.00	2.84	
6	1919.80	0.00	3.74	
7	2235.80	0.00	4.79	6.92E-09
8	2369.10	0.00	5.90	5.53E-09
9	2470.40	5.33	7.06	6.92E-09
10	3075.70	5.33	8.50	3.55E-09
11	3535.60	10.67	10.15	3.30E-09
12	3669.00	16.00	11.87	3.59E-09
13	3695.60	21.33	13.59	2.36E-09

(cont. on next page)

Table F.3 (cont.)

14	3706.30	26.66	15.31	1.29E-09
15	3706.30	42.66	17.03	1.26E-09
16	3690.30	74.66	18.73	1.00E-09
17	3717.00	176.00	20.38	2.04E-09
18	3706.30	394.60	21.93	2.88E-09
19	3701.00	795.40	23.28	2.07E-09
20	3701.00	1401.20	24.33	1.29E-09
T_{reg}=90°C; Regeneration time=9142 min; Constant initial adsorptive pressure				
Pulse number	**P_1 (Pa)**	**P_2 (Pa)**	**q (% kg/kg)**	**D_{eff} (m^2/s)**
1	1994.50	0.00	0.94	
2	1999.80	0.00	1.87	
3	1999.80	0.00	2.81	
4	2031.80	0.00	3.76	
5	2026.50	0.00	4.72	
6	1999.80	0.00	5.65	
7	2010.50	0.00	6.60	
8	2005.10	0.00	7.54	9.86E-09
9	2005.10	0.00	8.48	8.56E-09
10	2010.50	0.00	9.42	7.14E-09
11	1994.50	0.00	10.36	5.24E-09
12	2005.10	0.00	11.30	4.01E-09
13	2031.80	5.33	12.25	4.23E-09
14	2037.10	10.67	13.20	3.68E-09
15	1994.50	16.00	14.13	3.01E-09
16	2005.10	26.66	15.05	2.52E-09
17	1999.80	42.66	15.97	2.62E-09
18	2010.50	69.33	16.88	2.23E-09
19	2090.50	122.70	17.80	2.59E-09
20	2021.10	202.60	18.65	2.78E-09
21	2037.10	304.00	19.46	2.49E-09
22	2021.10	444.00	20.19	2.04E-09
T_{reg}=120°C; Regeneration time=11400 min; Constant initial adsorptive pressure				
Pulse number	**P_1 (Pa)**	**P_2 (Pa)**	**q (% kg/kg)**	**D_{eff} (m^2/s)**
1	1999.80	0.00	0.94	1.23E-08
2	1999.80	0.00	1.88	1.03E-08
3	1999.80	0.00	2.81	9.31E-09
4	1999.80	0.00	3.75	8.31E-09

(cont. on next page)

Table F.3 (cont.)

5	2010.50	0.00	4.70	7.53E-09
6	2042.50	0.00	5.65	6.66E-09
7	2010.50	0.00	6.60	5.88E-09
8	2005.10	5.33	7.54	6.2E-09
9	2037.10	5.33	8.49	5.36E-09
10	2010.50	10.67	9.43	5.53E-09
11	2010.50	10.67	10.37	4.75E-09
12	1994.50	16.00	11.29	4.91E-09
13	2015.80	21.33	12.23	4.72E-09
14	1999.80	21.33	13.16	3.88E-09
15	2026.50	26.66	14.10	3.62E-09
16	2037.10	37.33	15.03	3.94E-09
17	2015.80	48.00	15.96	3.68E-09
18	2015.80	58.66	16.87	3.04E-09
19	2037.10	79.99	17.79	2.81E-09
20	2005.10	122.70	18.67	2.81E-09
21	2015.80	186.60	19.53	2.65E-09
T_{reg}=150°C; Regeneration time=11900 min; Constant initial adsorptive pressure				
Pulse number	**P_1 (Pa)**	**P_2 (Pa)**	**q (% kg/kg)**	**D_{eff} (m^2/s)**
1	1962.50	0.00	0.92	5.69E-08
2	2010.50	0.00	1.87	3.91E-08
3	2015.80	0.00	2.82	2.97E-08
4	2015.80	0.00	3.77	2.39E-08
5	2015.80	0.00	4.72	2.03E-08
6	2005.10	0.00	5.66	1.77E-08
7	2031.80	0.00	6.62	1.52E-08
8	2042.50	0.00	7.58	1.34E-08
9	2015.80	0.00	8.53	1.18E-08
10	2021.10	0.00	9.48	1.05E-08
11	2015.80	0.00	10.43	9.15E-09
12	2010.50	0.00	11.37	7.98E-09
13	2079.80	0.00	12.35	6.66E-09
14	2026.50	0.00	13.30	5.17E-09
15	2015.80	5.33	14.25	4.98E-09
16	2015.80	10.67	15.19	4.62E-09
17	2015.80	16.00	16.13	3.78E-09

(cont. on next page)

Table F.3 (cont.)

18	2047.80	26.66	17.09	3.43E-09
19	2085.10	42.00	18.05	3.04E-09
20	2010.50	69.33	18.96	3.10E-09
21	2015.80	122.70	19.85	3.33E-09
22	2015.80	197.30	20.70	3.07E-09
T_{reg}=90°C; Regeneration time=9180 min; Constant initial adsorptive pressure				
Pulse number	**P_1 (Pa)**	**P_2 (Pa)**	**q (% kg/kg)**	**D_{eff} (m^2/s)**
1	957.20	0.00	0.45	1.39E-07
2	978.60	0.00	0.91	8.71E-08
3	957.20	0.00	1.36	6.65E-08
4	978.60	0.00	1.82	5.03E-08
5	1021.20	0.00	2.30	3.80E-08
6	978.60	0.00	2.75	3.24E-08
7	962.60	0.00	3.21	2.74E-08
8	994.60	0.00	3.67	2.37E-08
9	978.60	0.00	4.13	2.08E-08
10	978.60	0.00	4.59	1.87E-08
11	973.20	0.00	5.05	1.66E-08
12	978.60	0.00	5.51	1.52E-08
13	983.90	0.00	5.97	1.39E-08
14	978.60	0.00	6.43	1.26E-08
15	978.60	0.00	6.89	1.17E-08
16	978.60	0.00	7.34	1.08E-08
17	978.60	0.00	7.80	1.01E-08
18	983.90	0.00	8.27	9.31E-09
19	1010.60	0.00	8.74	8.60E-09
20	994.60	0.00	9.21	8.11E-09
21	999.90	0.00	9.68	7.53E-09

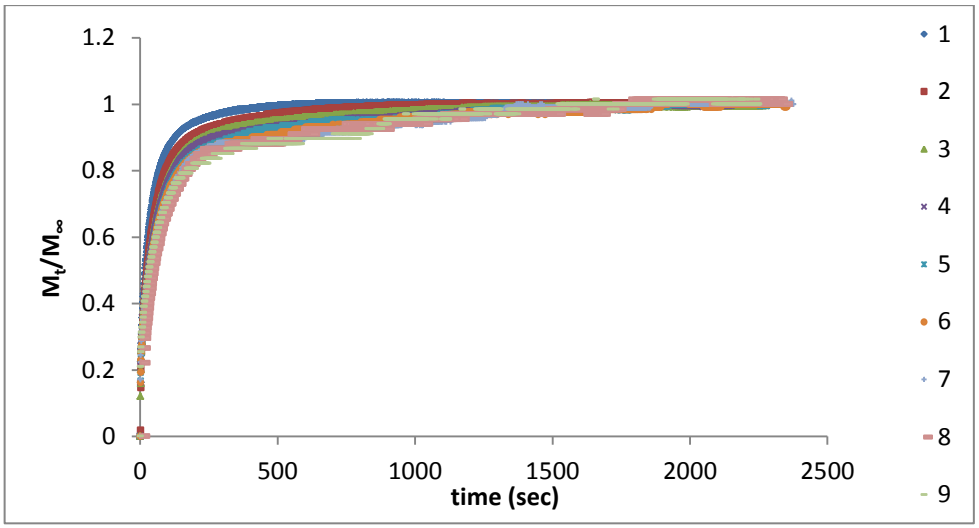

Figure F.1. Uptake curves of type RD silica gel-water pair at 60°C;

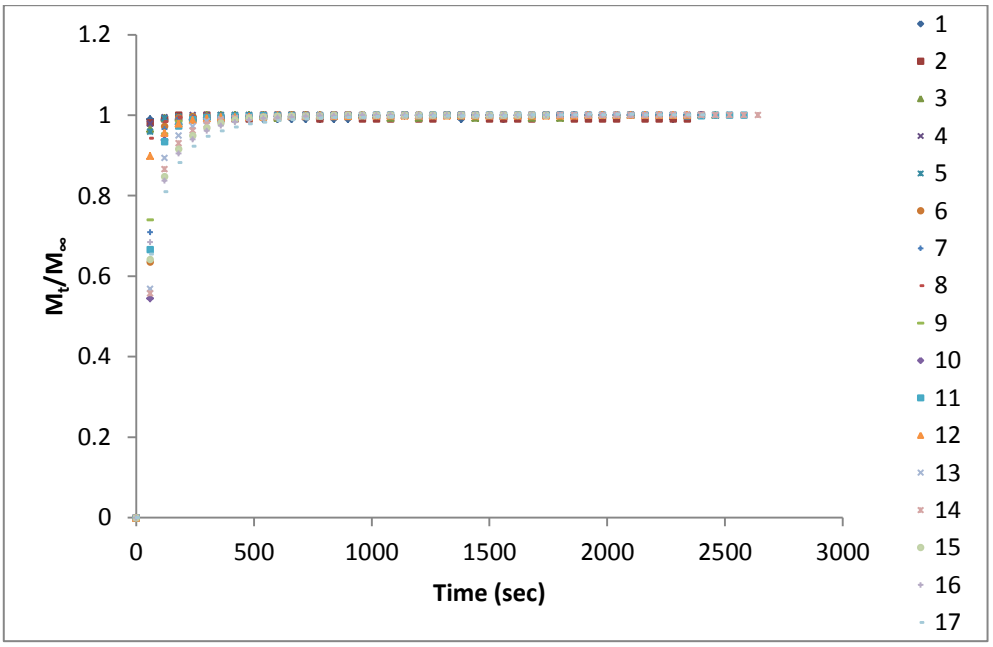

Figure F.2. Uptake curves for zeolite 13X-water pair at 60°C (T_{reg}=90°C)

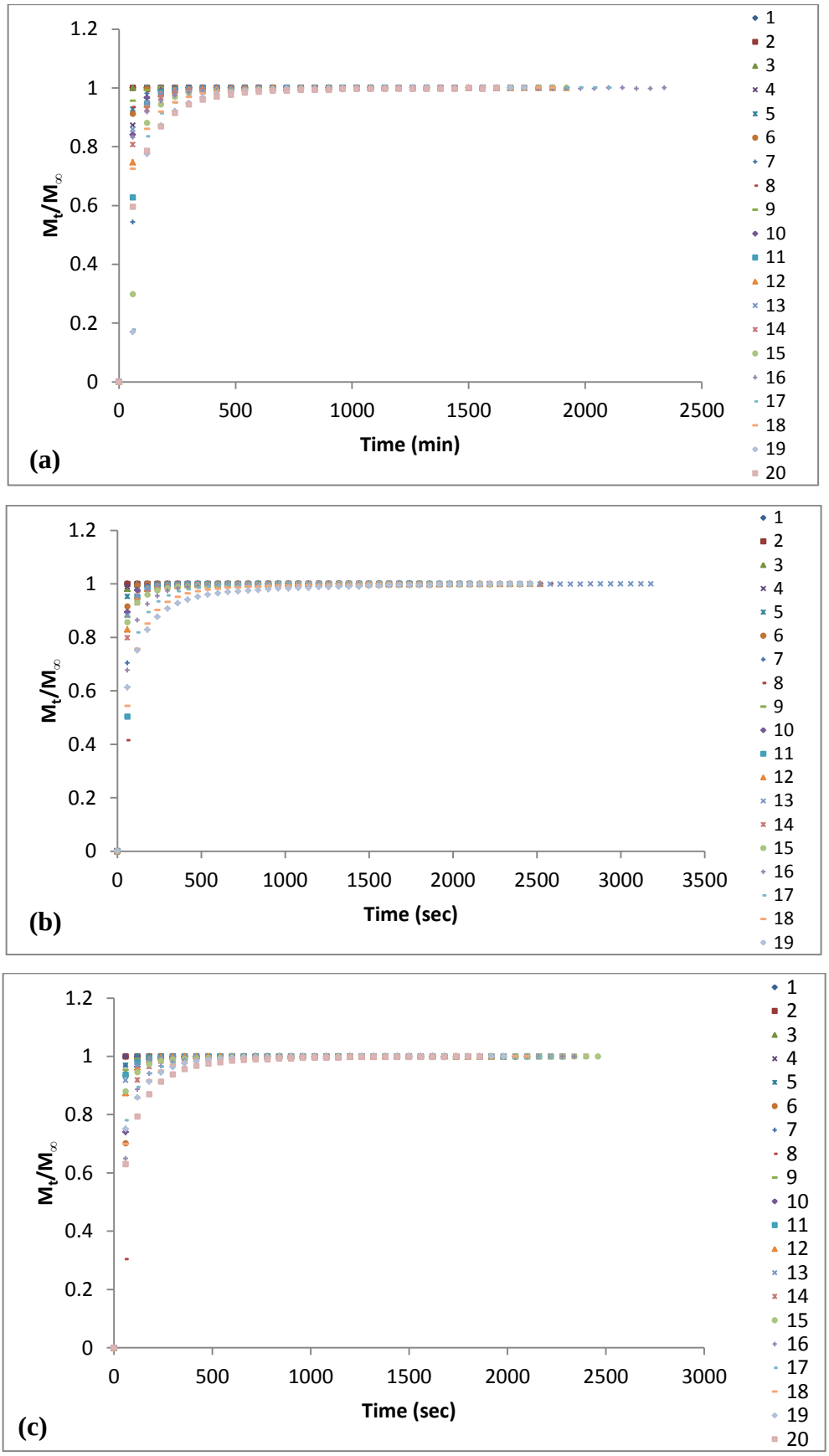

Figure F.3. Uptake curves of zeolite 13X at 35°C a) T_{reg}=60°C; b)T_{reg}=120°C; c)T_{reg}=150°C (increasing initial adsorptive concentration)

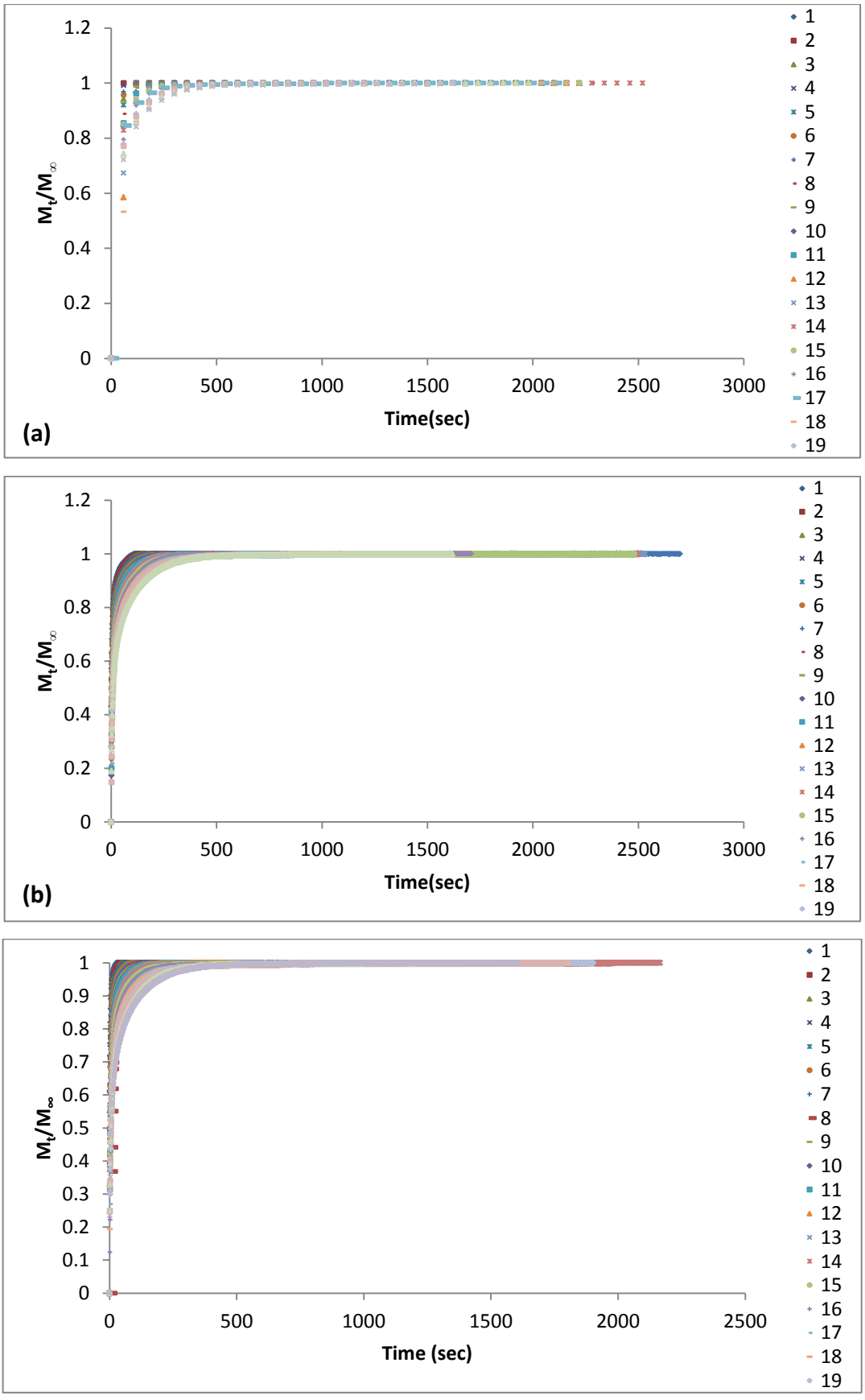

Figure F.4. Uptake curves of zeolite 13X-water pair at 35°C; a) T_{reg}=90°C; b)120°C; c)150°C (Constant initial adsorptive pressure of 2000 Pa)

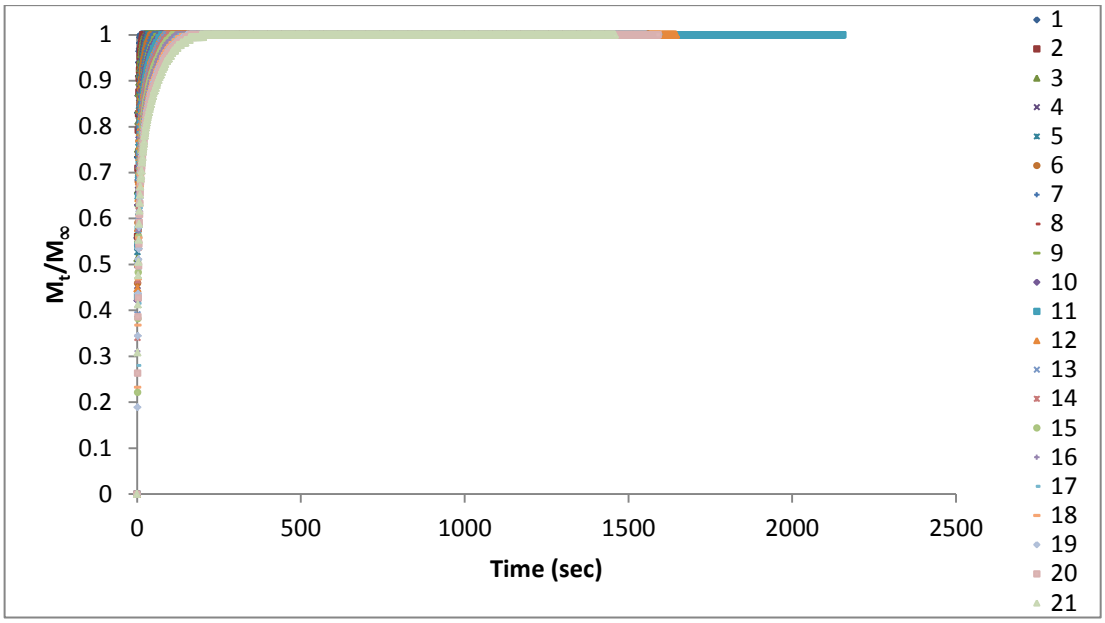

Figure F.5. Uptake curves of zeolite 13X-water pair at 35°C; a) T_{reg}=90°C (constant initial pressure of 980 Pa)

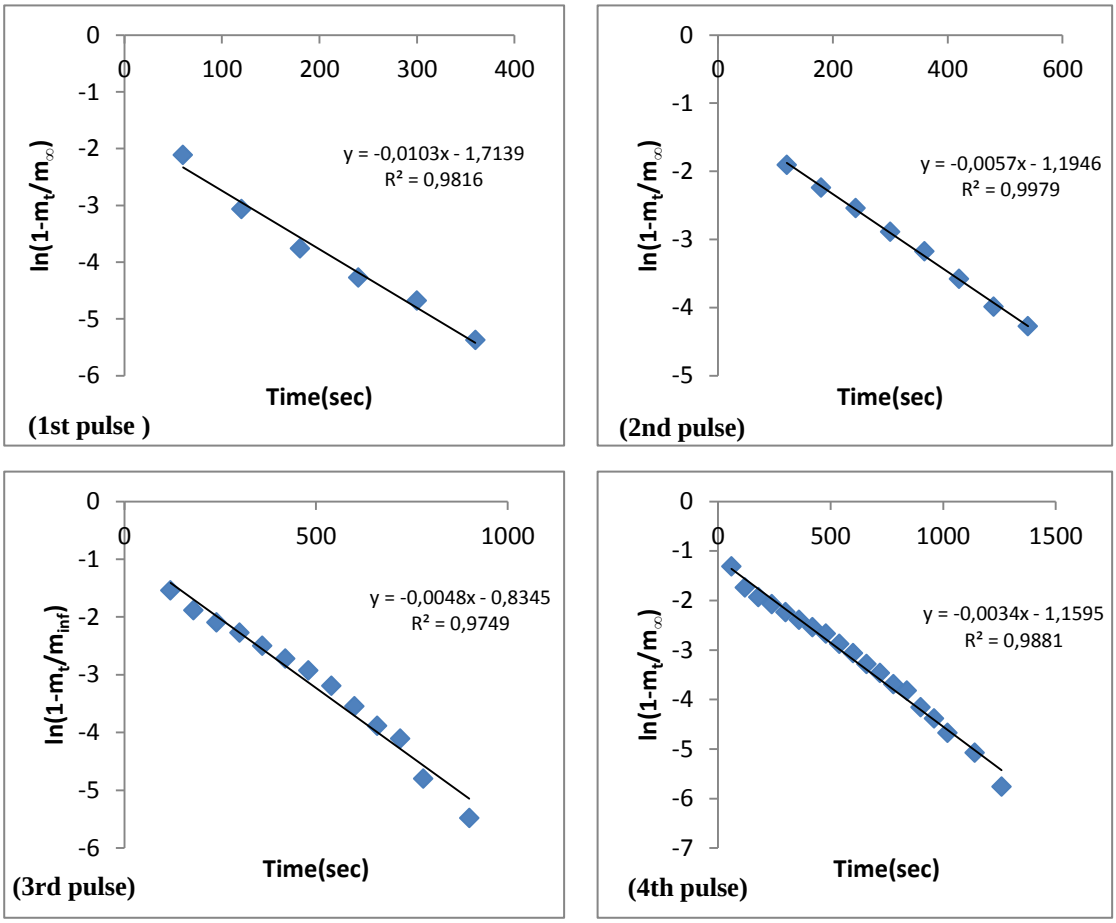

Figure F.6. Linear curves of type RD silica gel at 35°C for long term intraparticle diffusion

(cont. on next page)

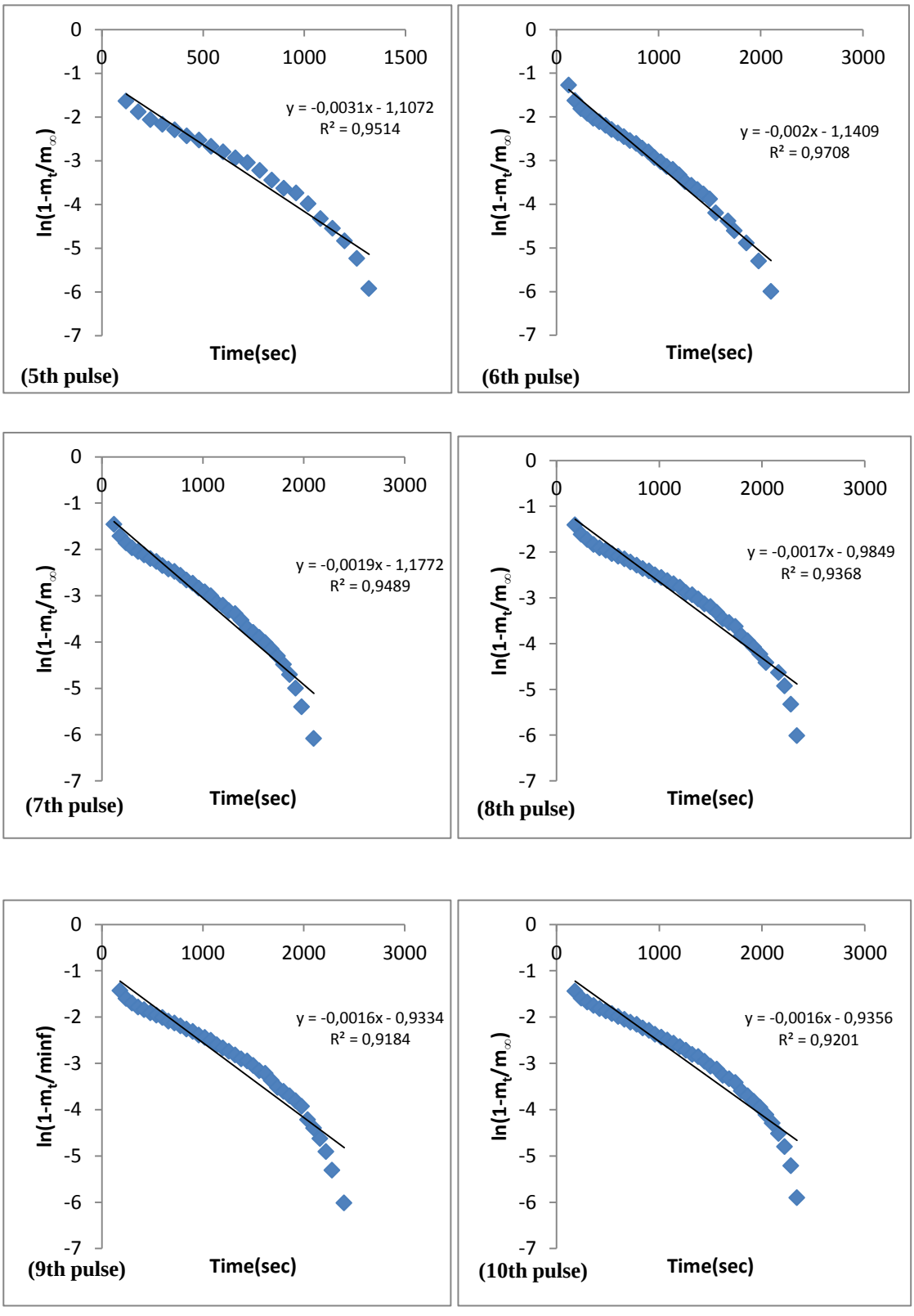

Figure F.6 (cont.)

(cont. on next page)

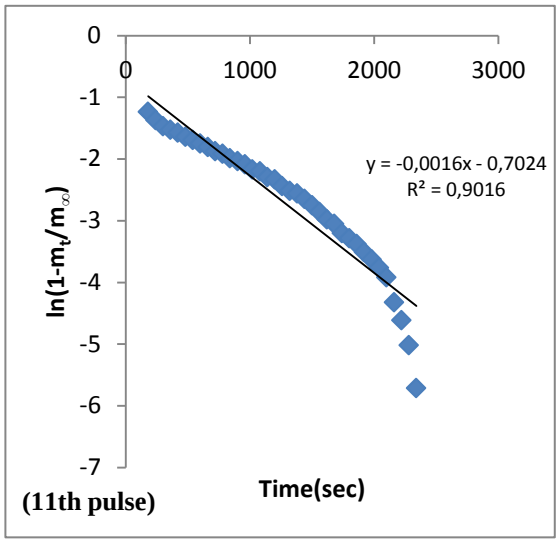

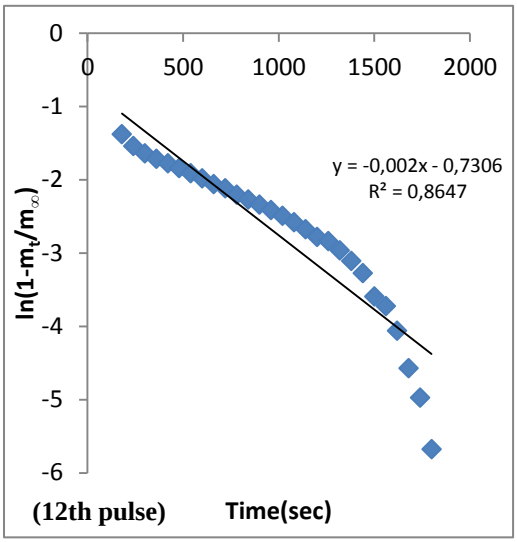

Figure F.6 (cont.)

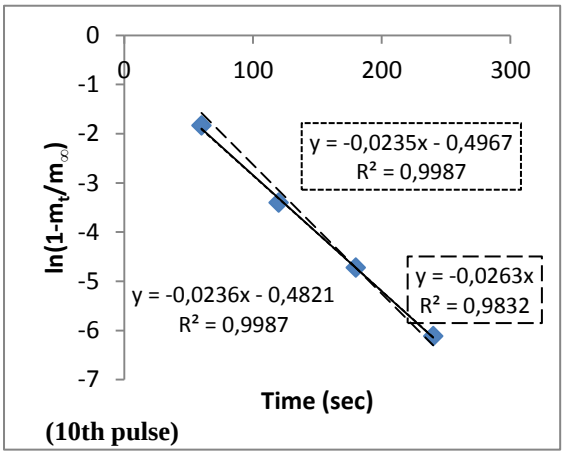

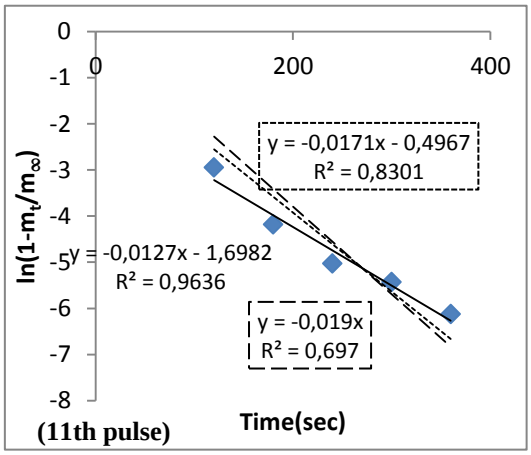

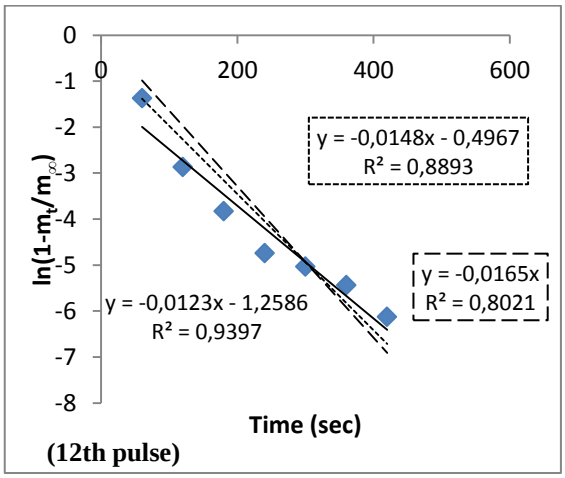

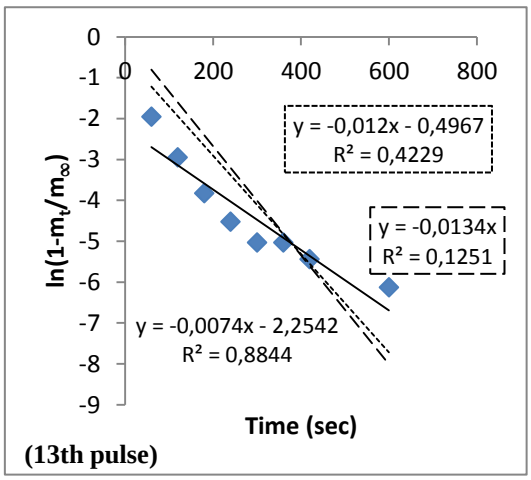

Figure F.7. Linear curves of zeolite 13X-water pair (T_{reg}=60°C); ─ experimental; …. Long term intraparticle diffusion; ---- surface resistance

(cont. on next page)

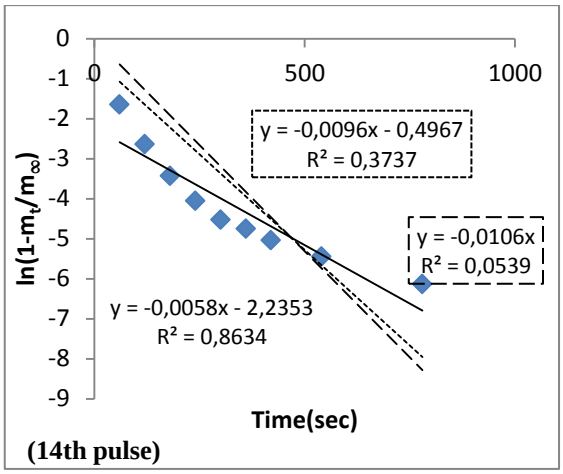

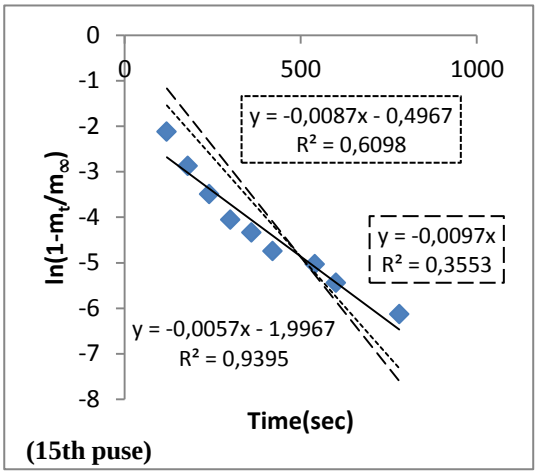

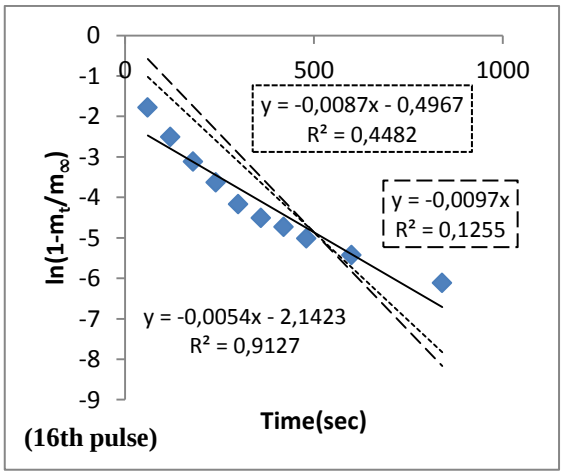

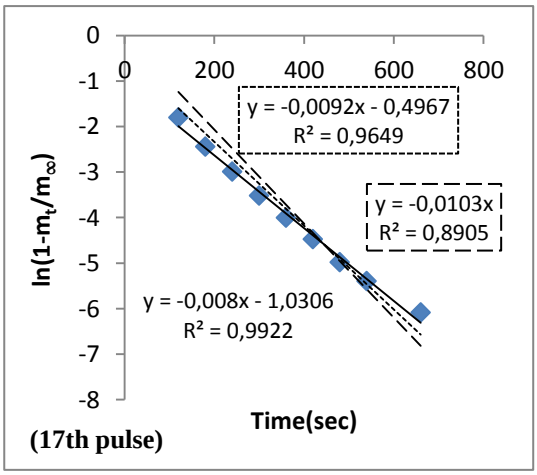

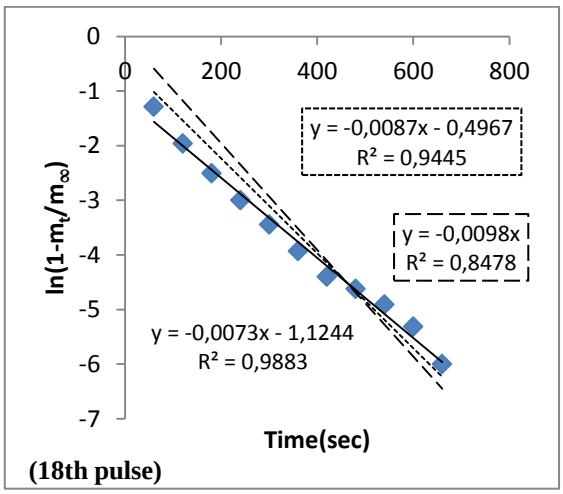

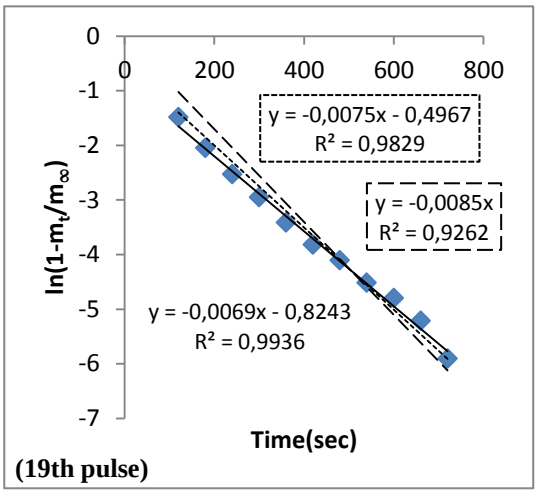

Figure F.7 (cont.)

(cont. on next page)

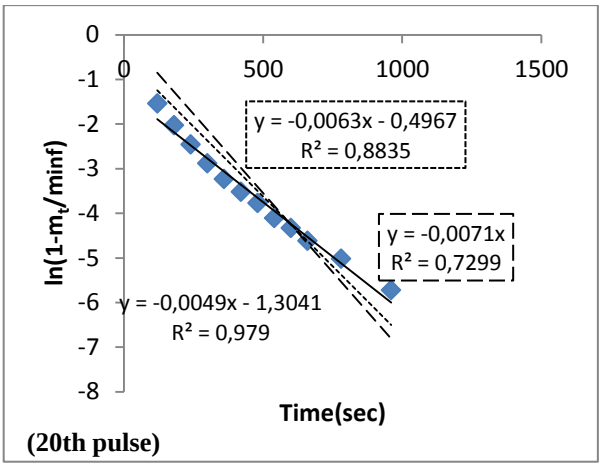

Figure F.7 (cont.)

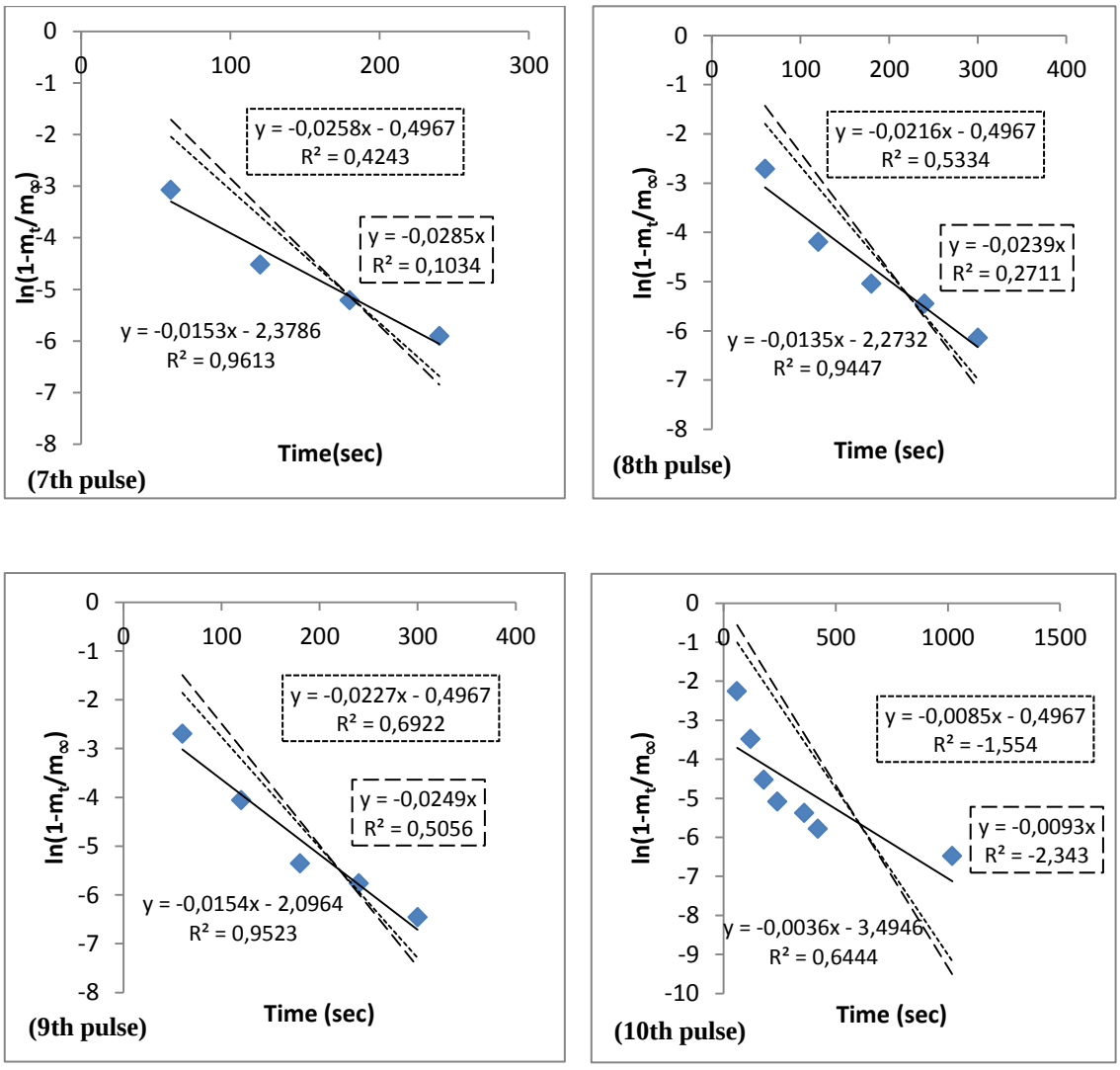

Figure F.8. Linear curves of zeolite 13X-water pair (T_{reg}=90°C) ─ experimental; …. Long term intraparticle diffusion; ---- surface resistance

(cont. on next page)

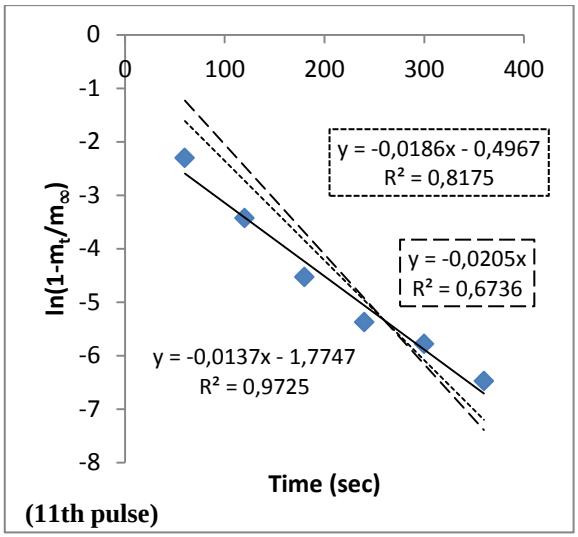

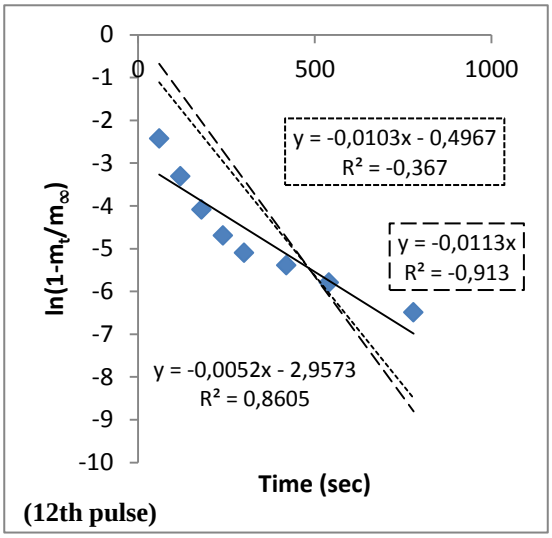

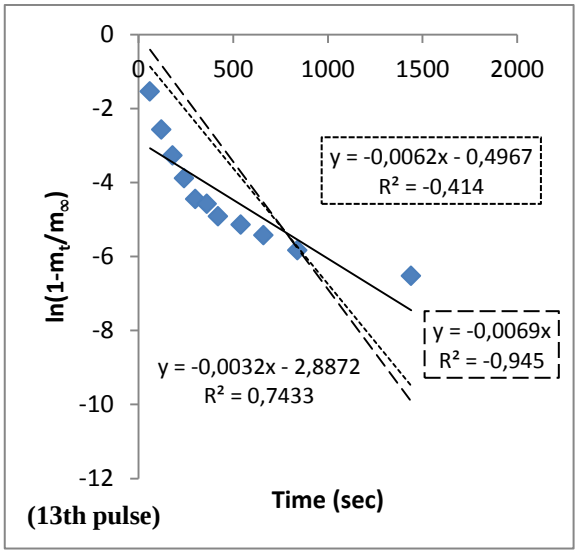

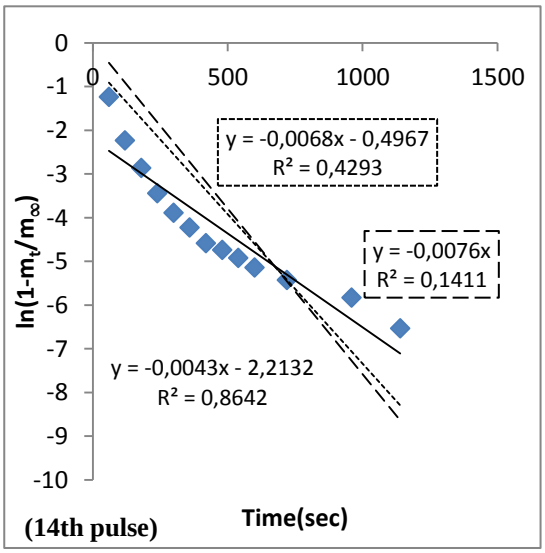

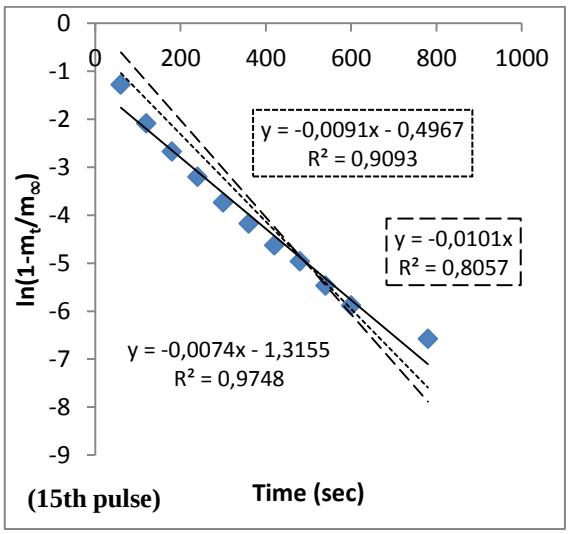

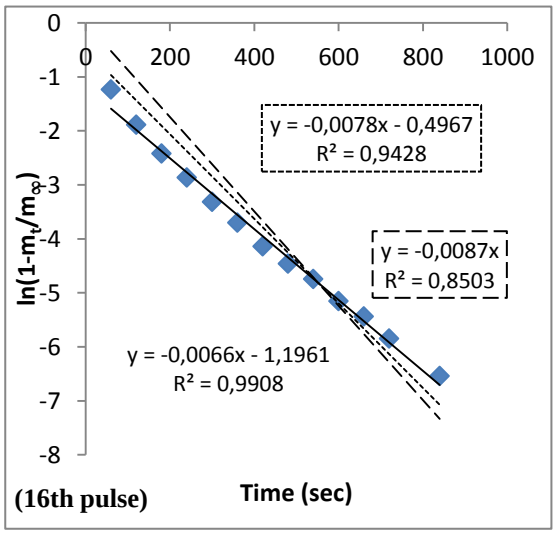

Figure F.8 (cont.)

(cont. on next page)

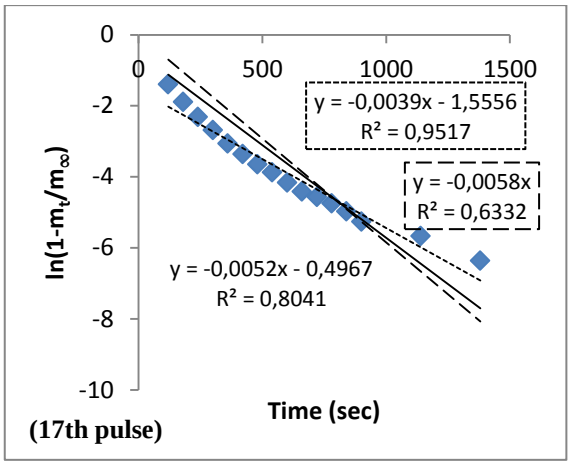

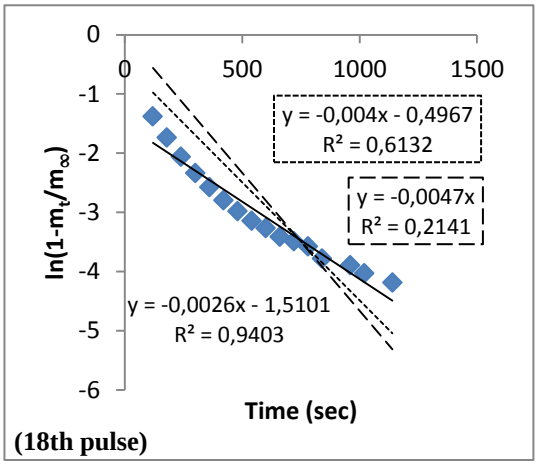

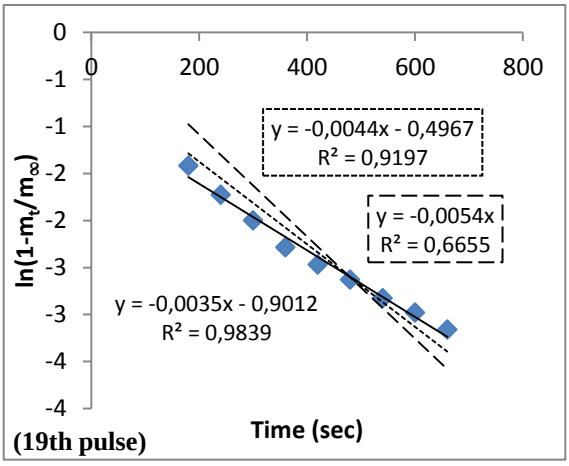

Figure F.8 (cont.)

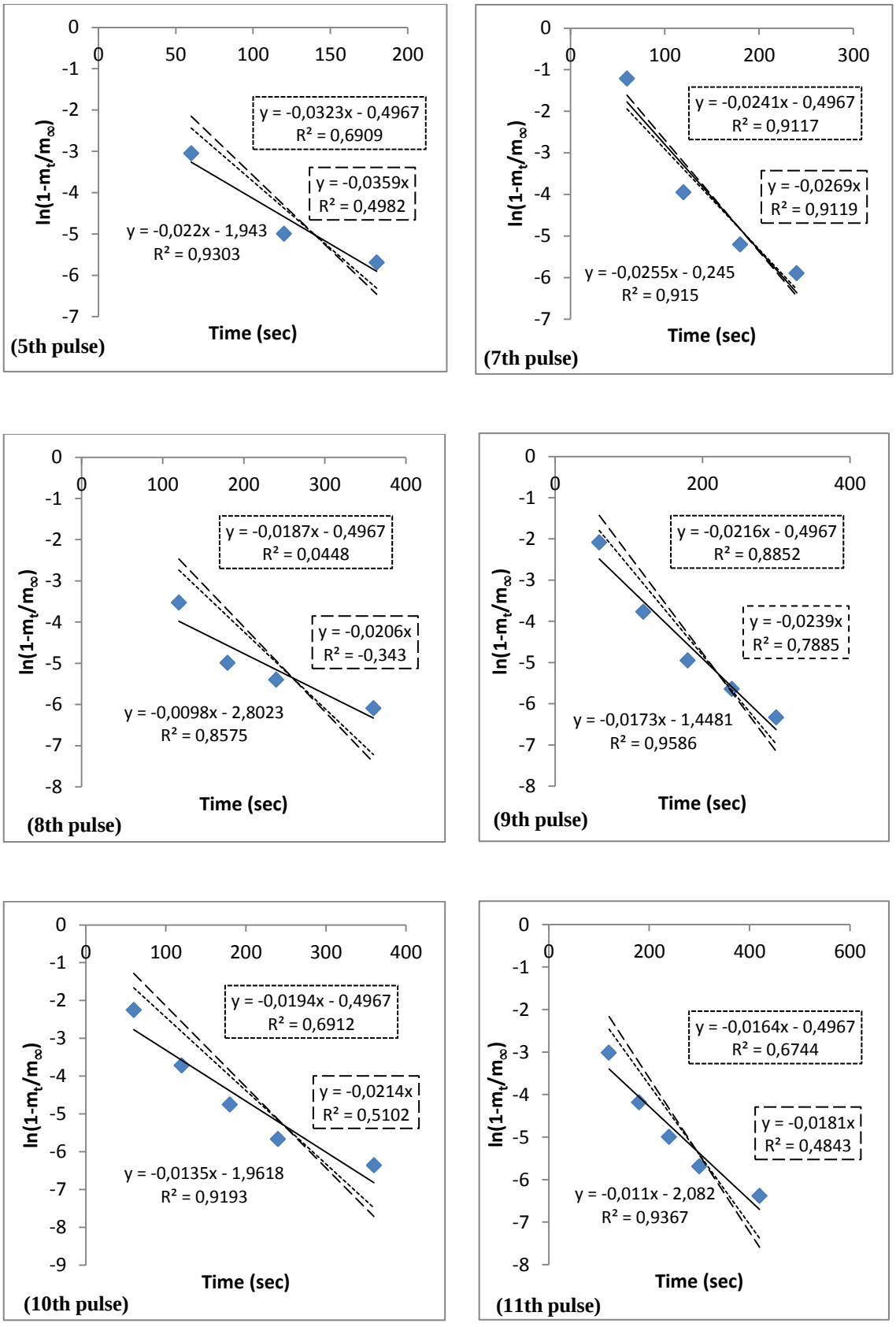

Figure F.9. Linear curves of zeolite 13X-water pair (T_{reg}=120°C) ─ experimental; …. Long term intraparticle diffusion; ---- surface resistance

(cont. on next page)

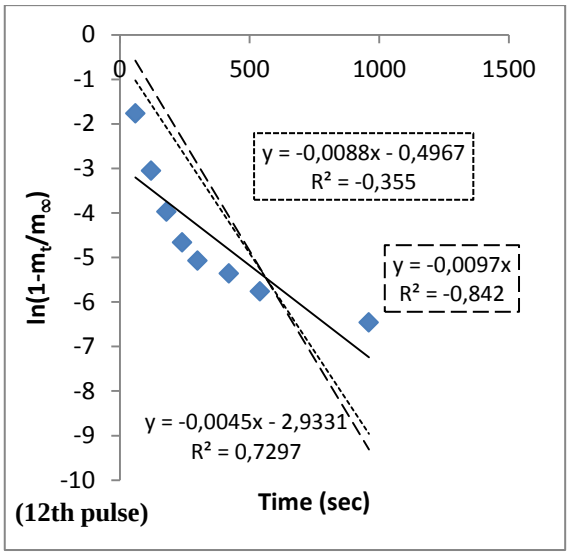

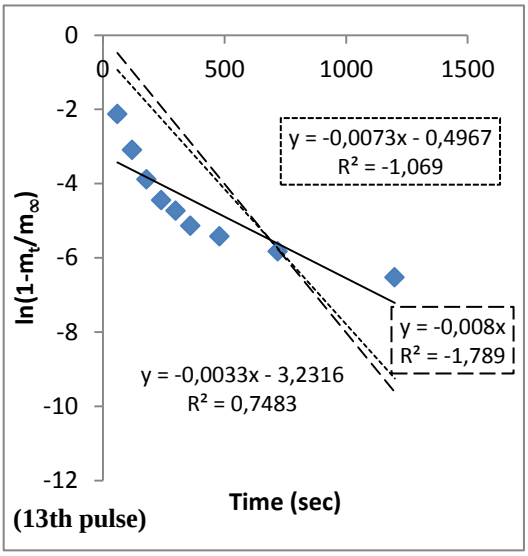

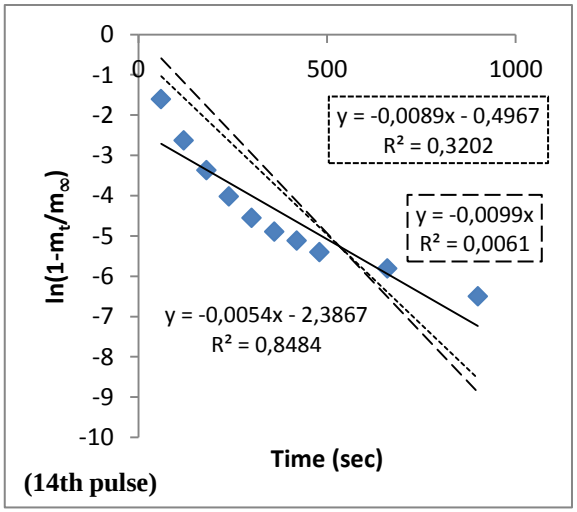

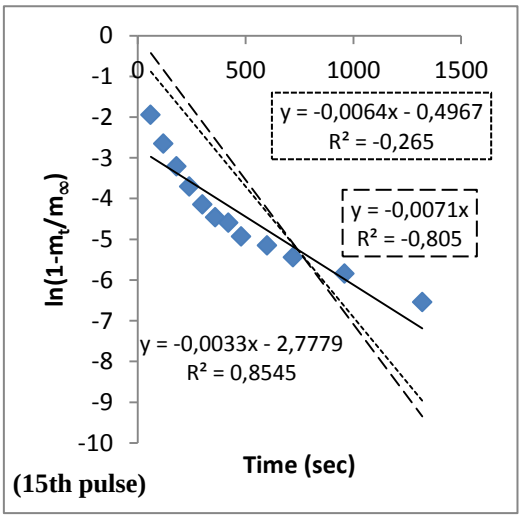

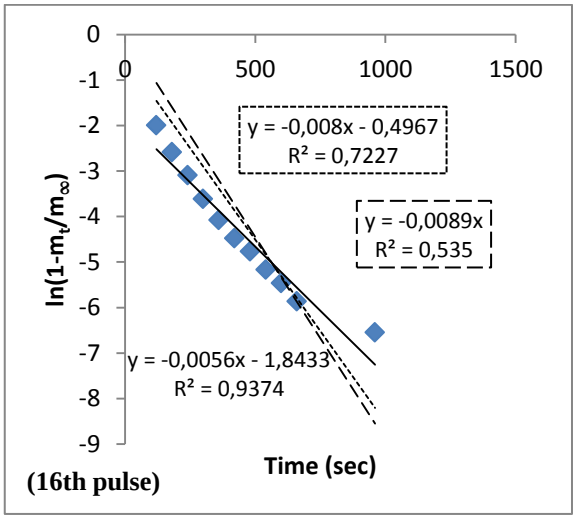

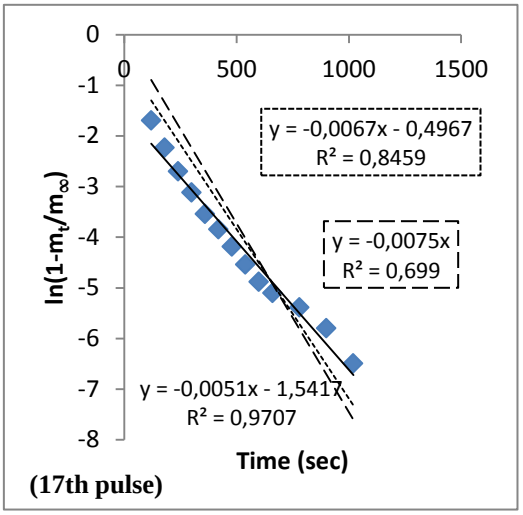

Figure F.9 (cont.)

(cont. on next page)

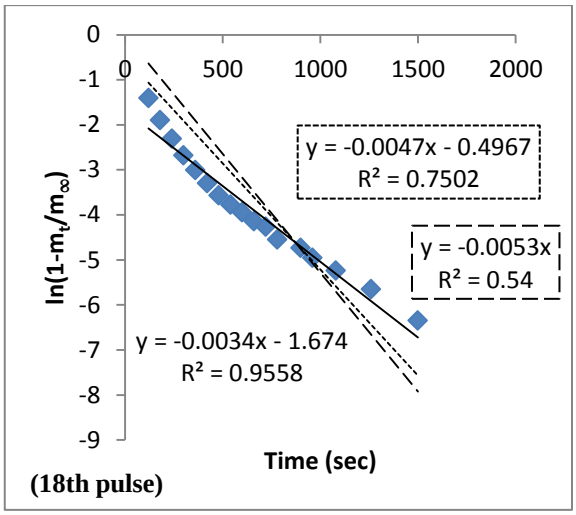

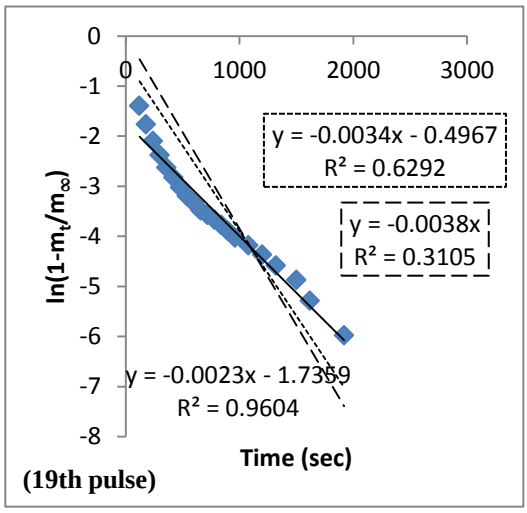

Figure F.9 (cont.)

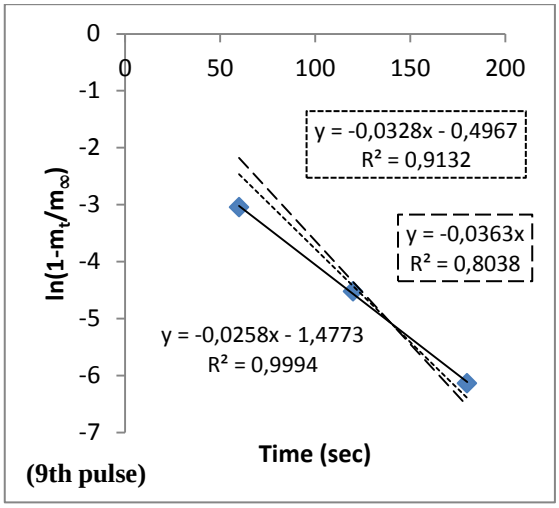

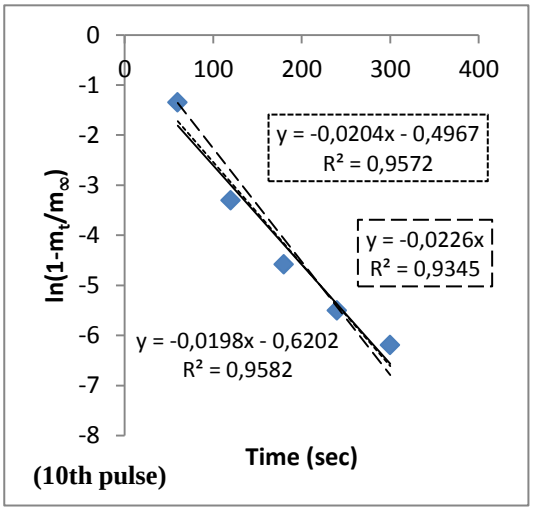

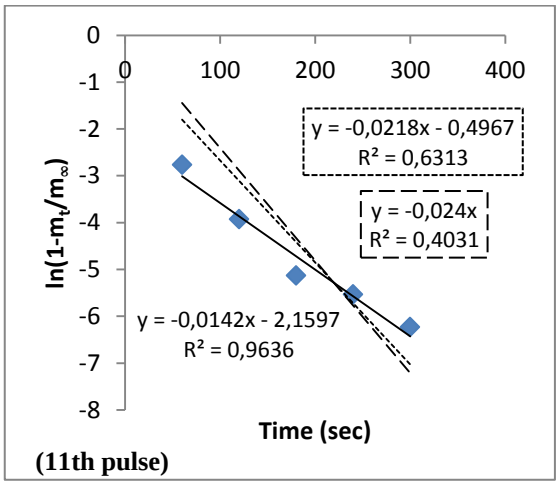

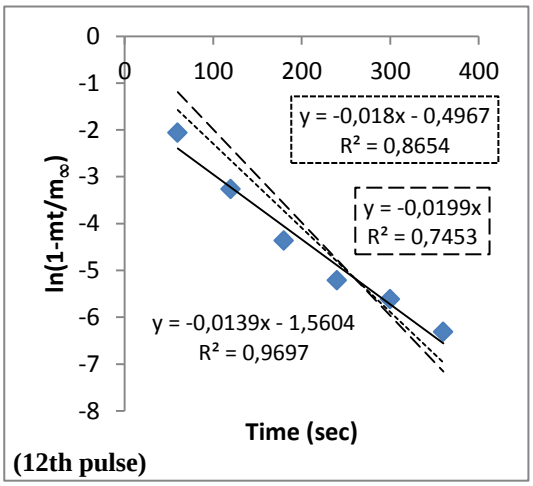

Figure F.10. Linear curves of zeolite 13X-water pair (T_{reg}=150°C) ─ experimental; …. Long term intraparticle diffusion; ---- surface resistance

(cont. on next page)

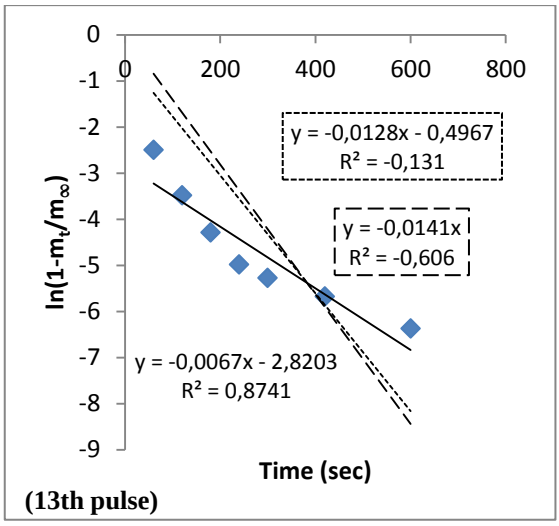

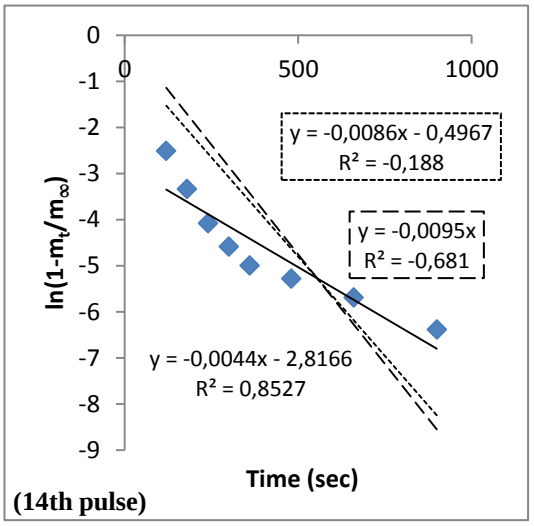

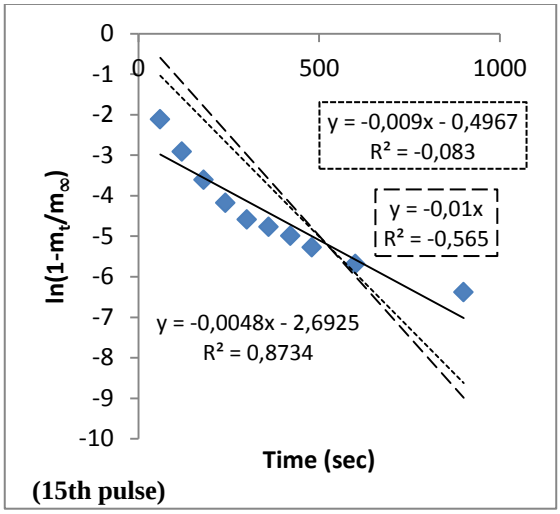

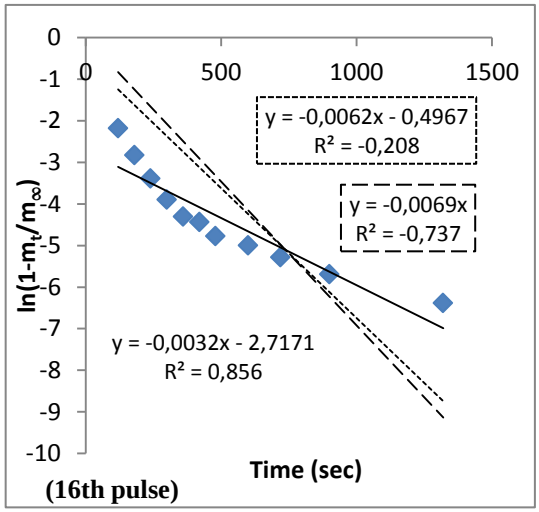

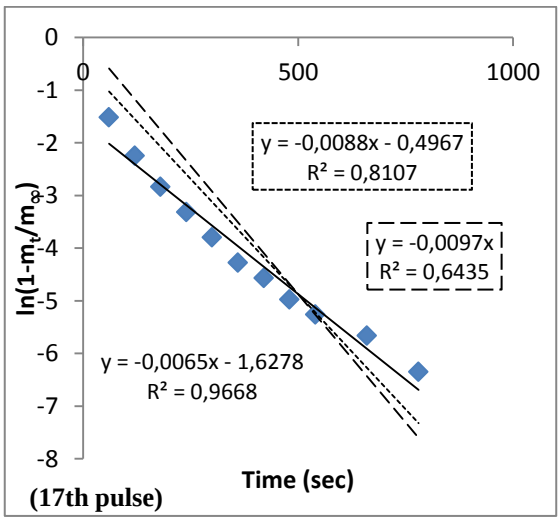

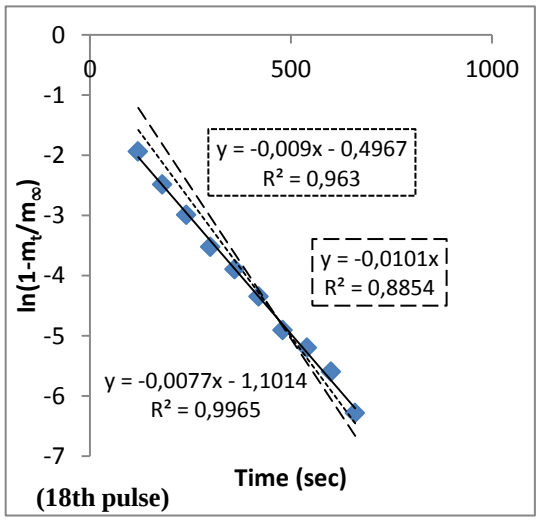

Figure F.10 (cont.)

(cont. on next page)

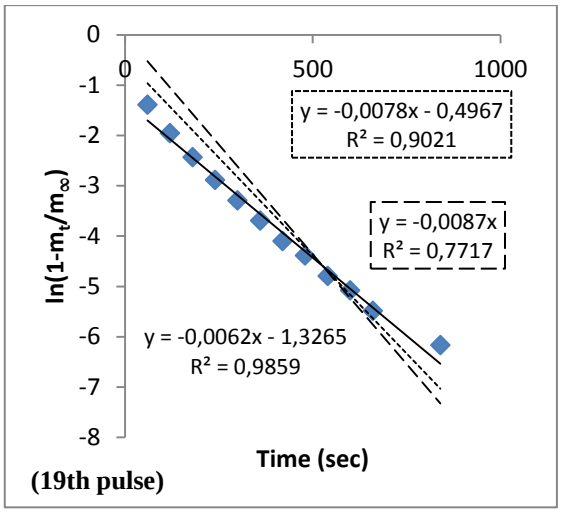

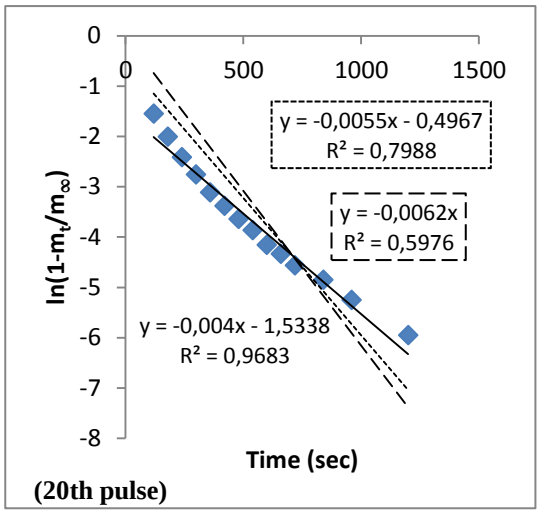

Figure F.10. (cont.)

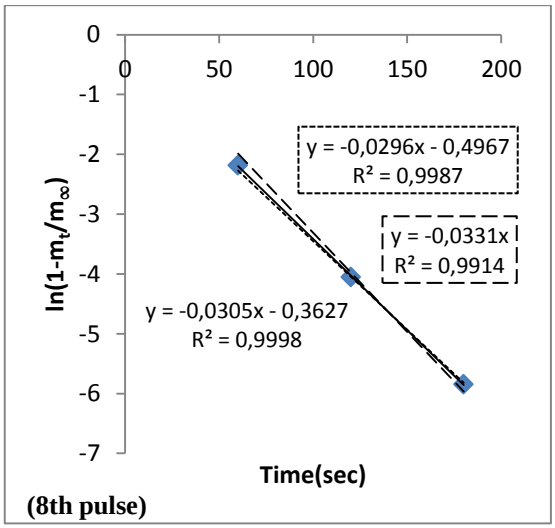

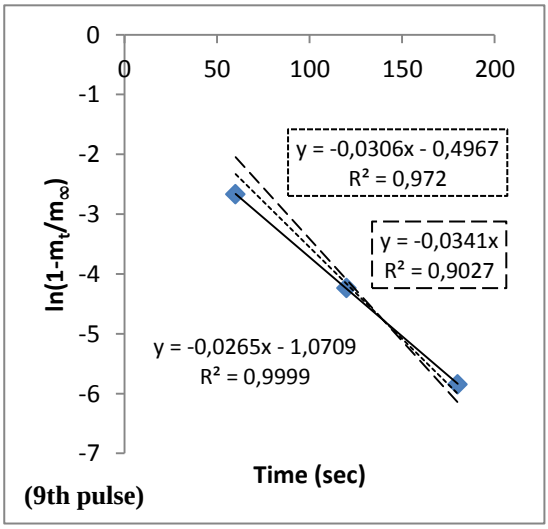

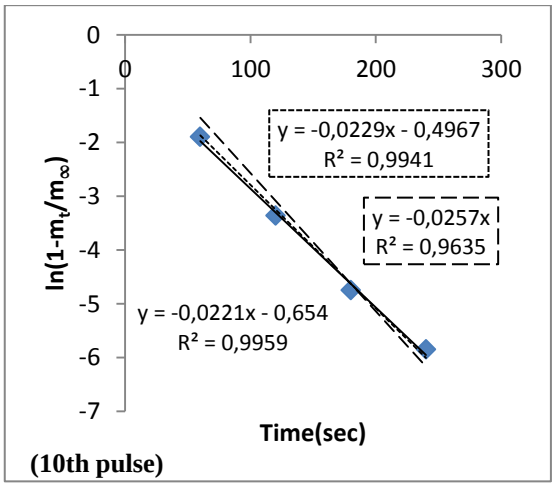

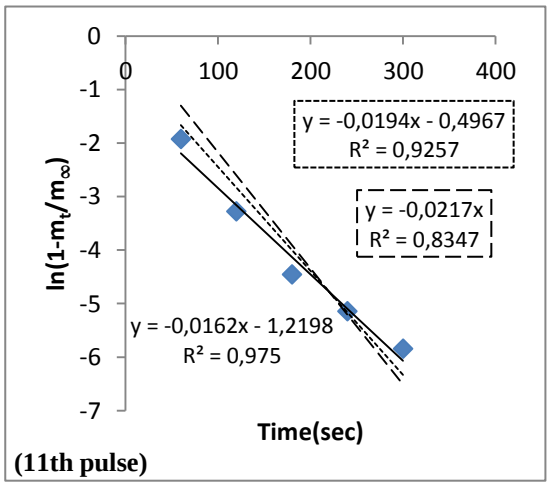

Figure F.11. Linear curves of zeolite 13X-water pair (T_{reg}=90°C, constant initial pressure of 2000) ─ experimental; …. Long term intraparticle diffusion; ---- surface resistance

(cont. on next page)

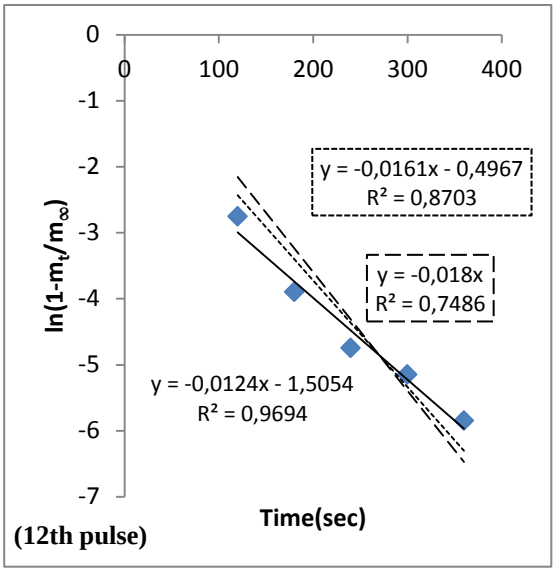

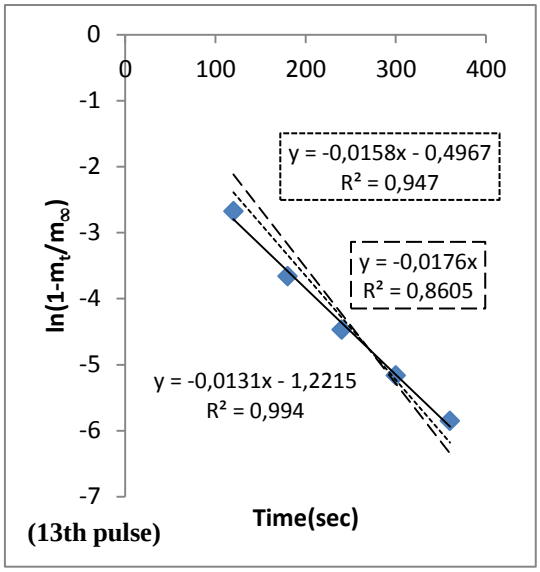

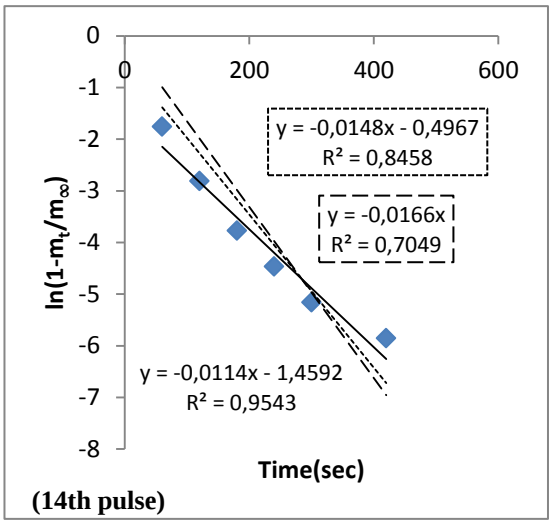

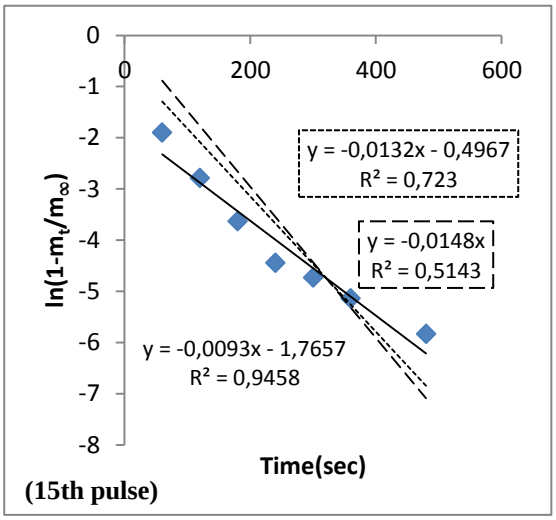

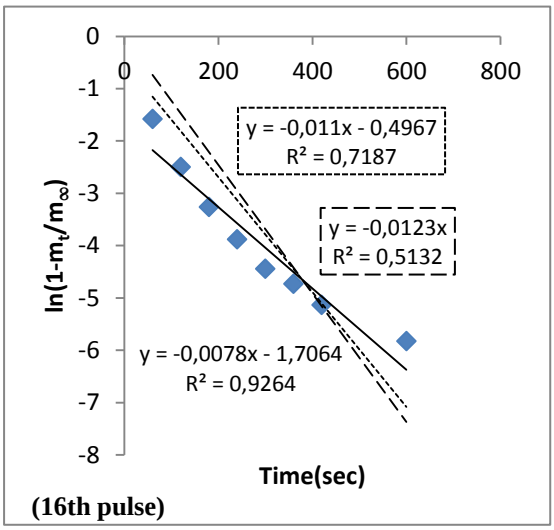

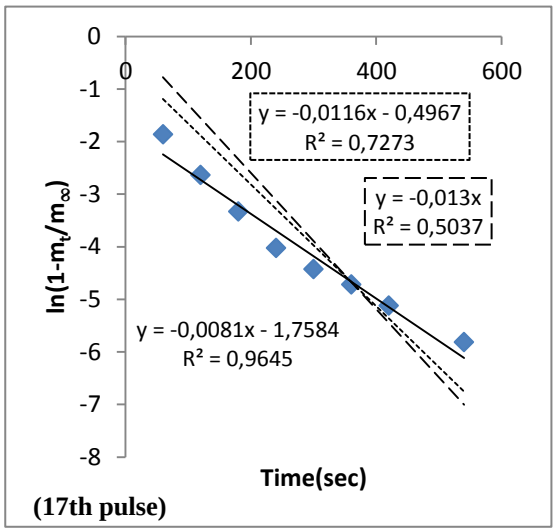

Figure F.11 (cont.)

(cont. on next page)

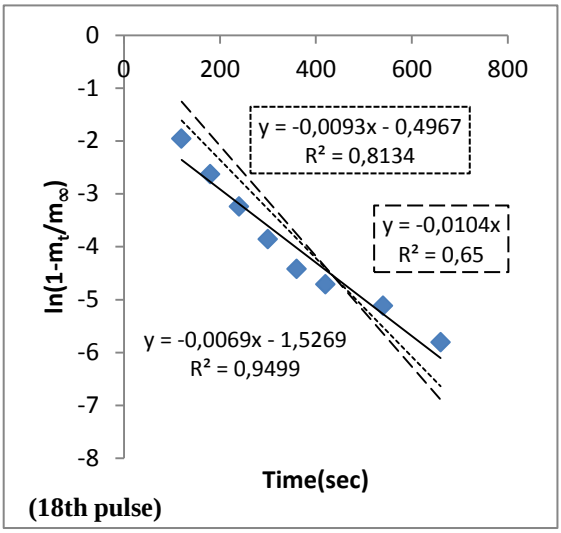

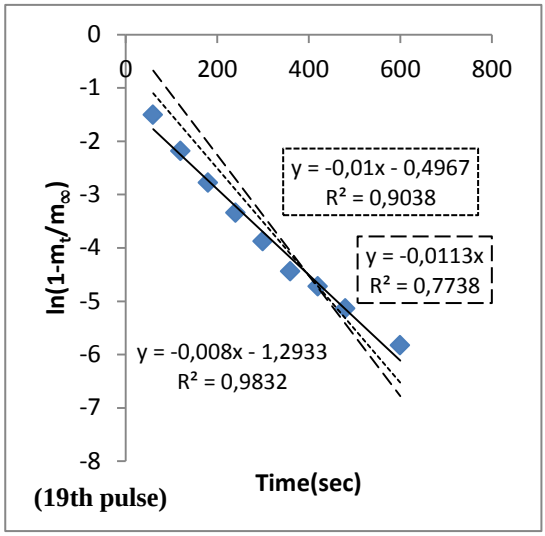

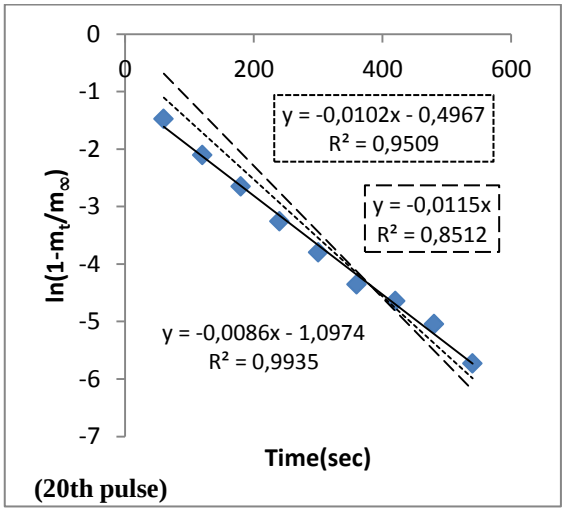

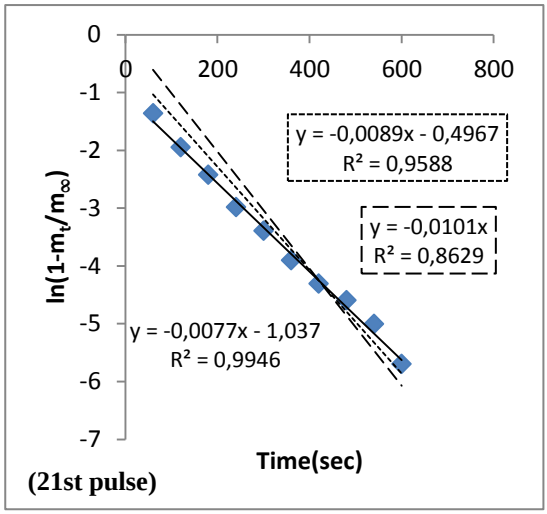

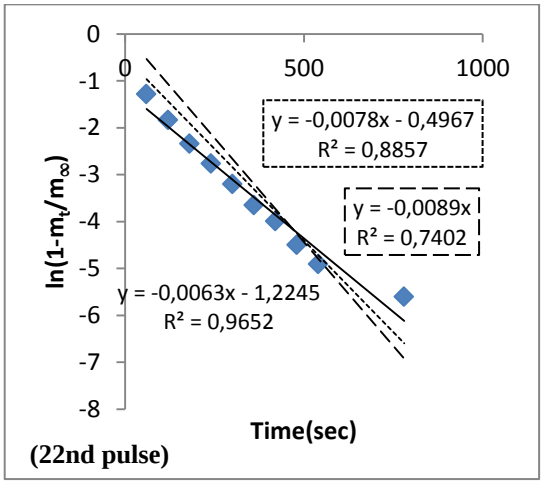

Figure F.11 (cont.)

(cont. on next page)

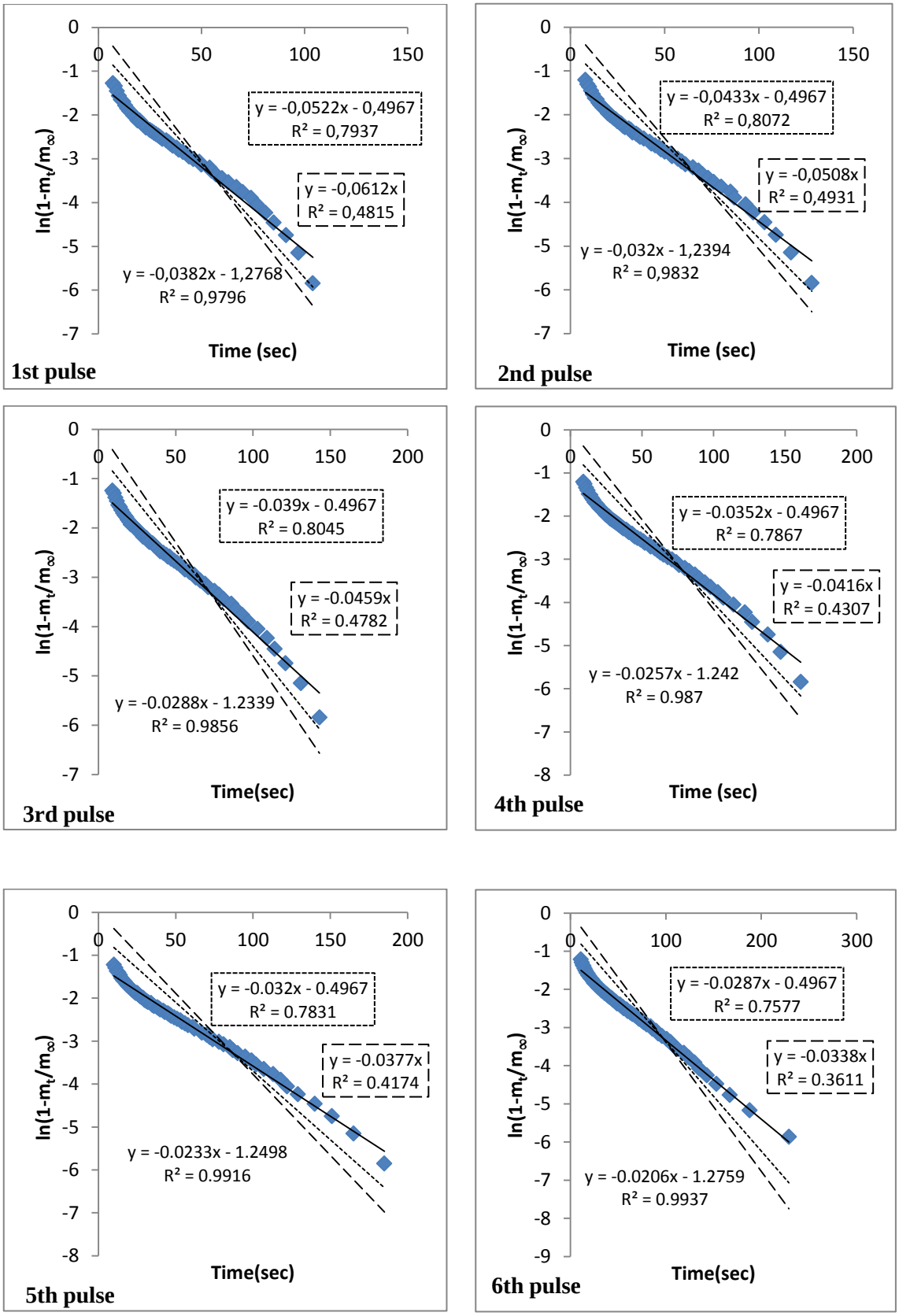

Figure F.12. Long term linear curves of zeolite 13X-water pair (T_{reg}=120°C, constant initial pressure of 2000) ─ experimental; …. Long term intraparticle diffusion; ---- surface resistance

(cont. on next page)

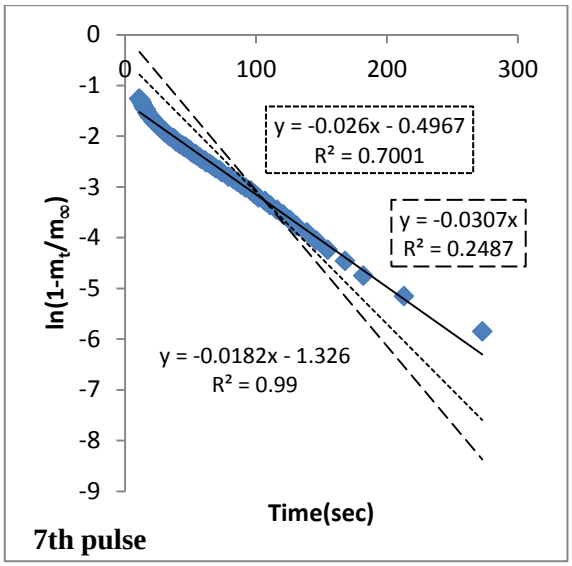

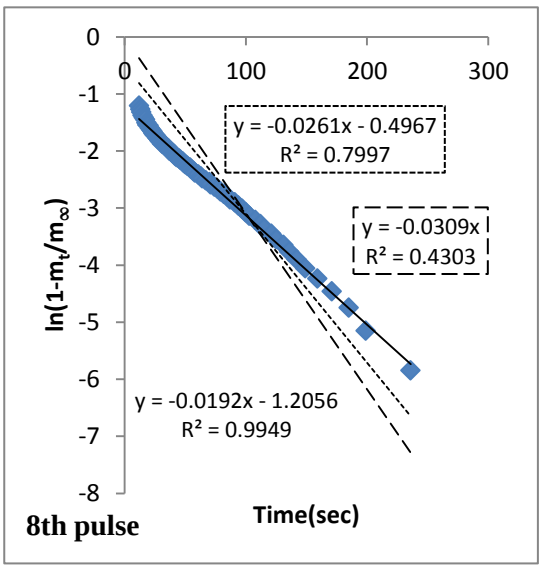

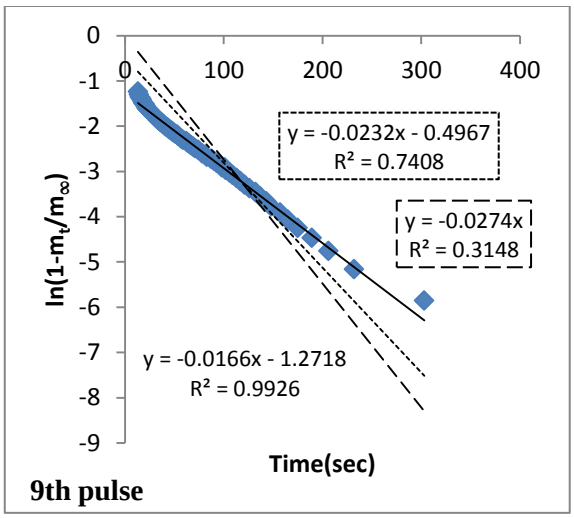

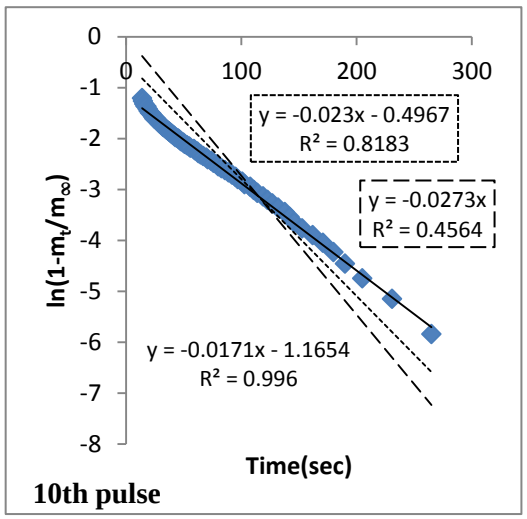

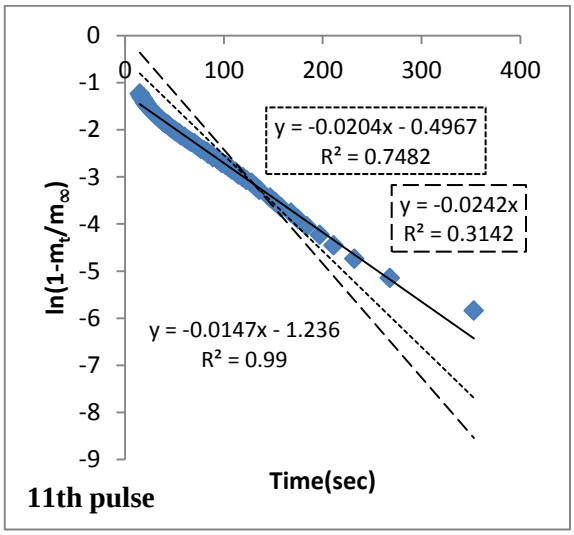

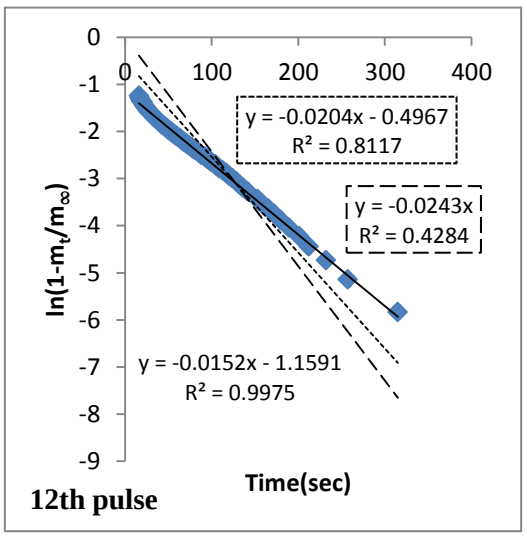

Figure F.12 (cont.)

(cont. on next page)

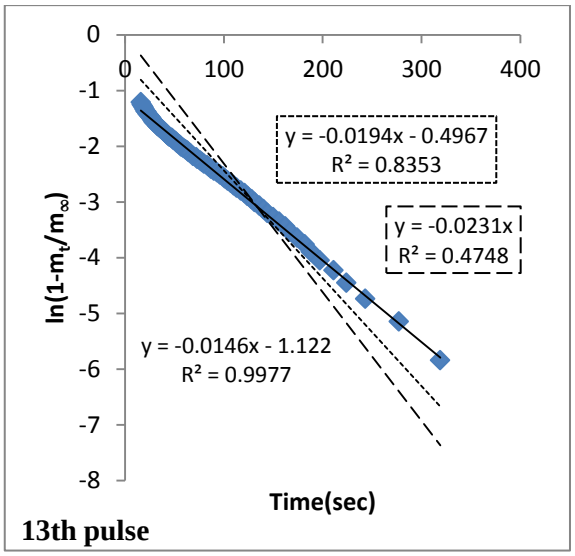

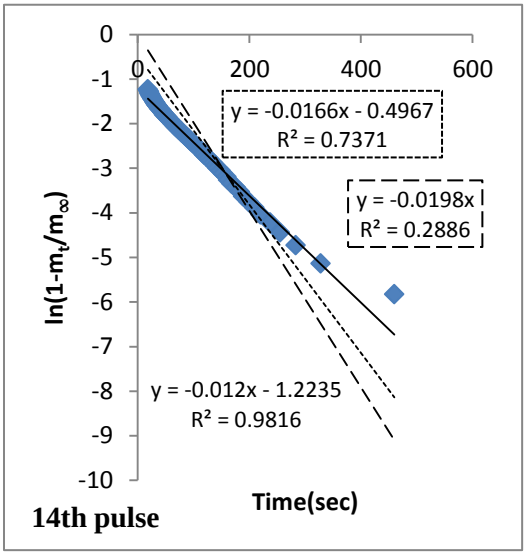

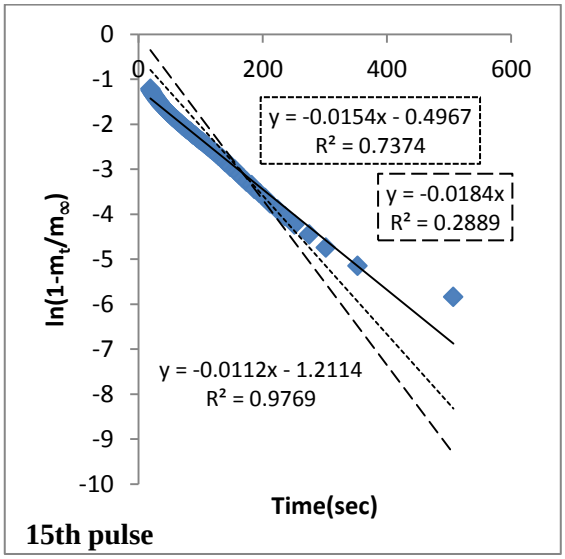

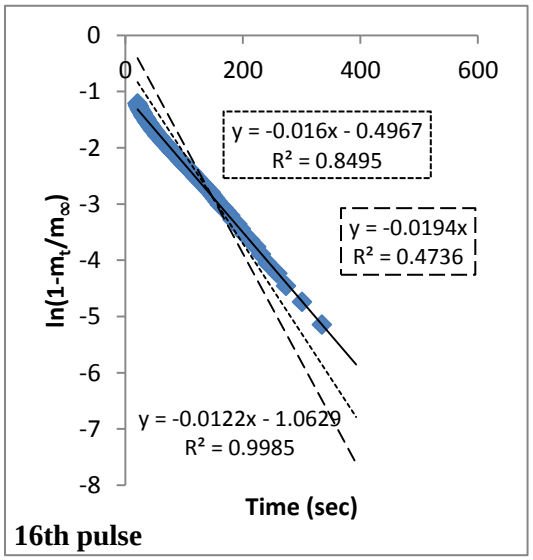

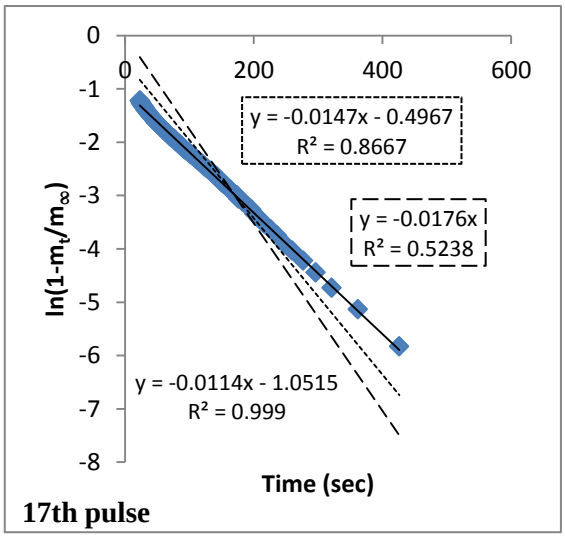

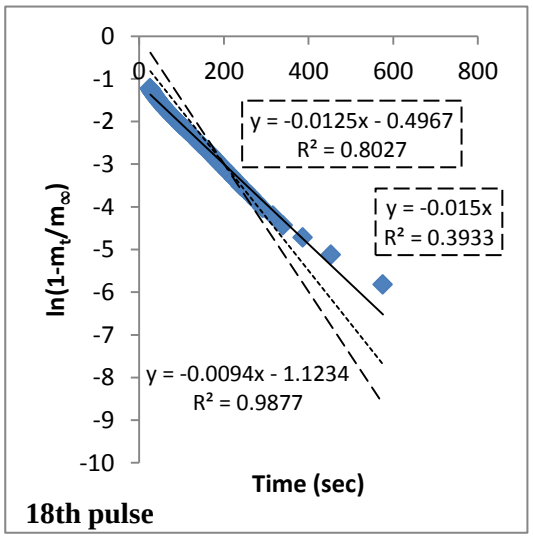

Figure F.12 (cont.)

(cont. on next page)

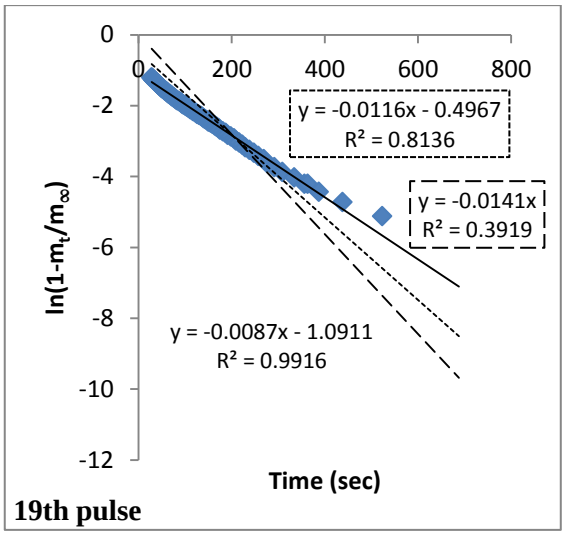

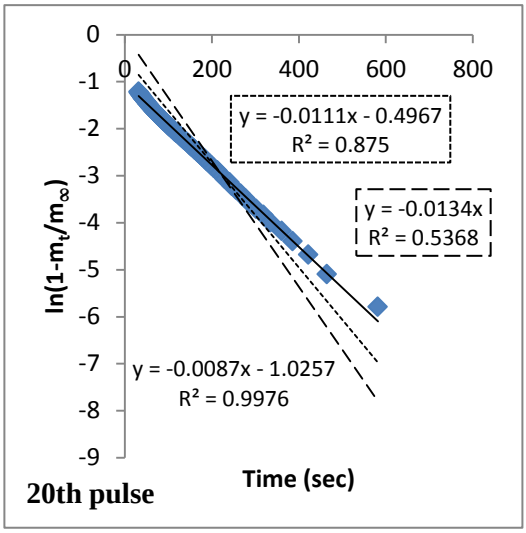

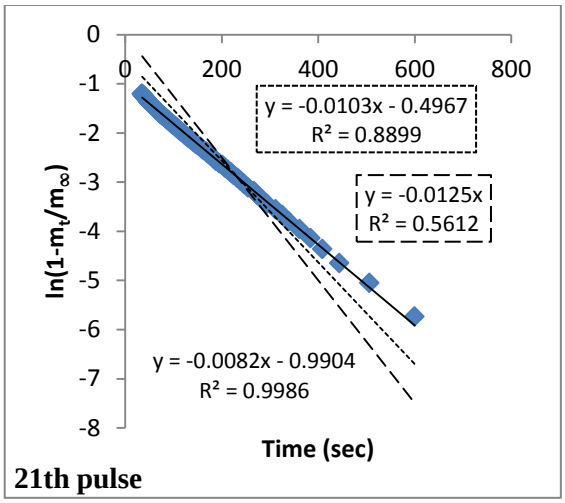

Figure F.12. (cont.)

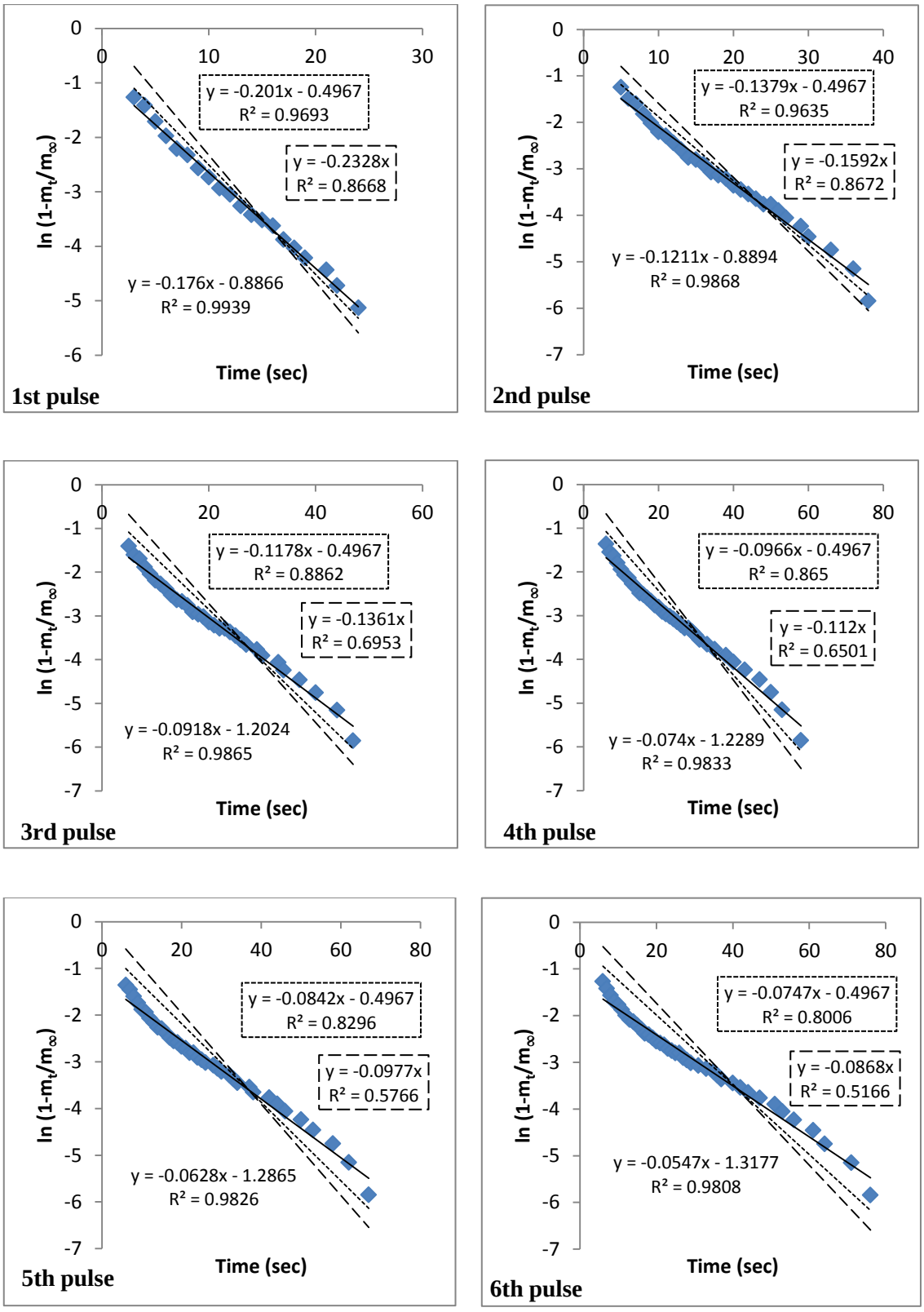

Figure F.13. Long term linear curves of zeolite 13X-water pair (T_{reg}=150°C, constant initial pressure of 2000 Pa) ─ experimental; …. Long term intraparticle diffusion; ---- surface resistance

(cont. on next page)

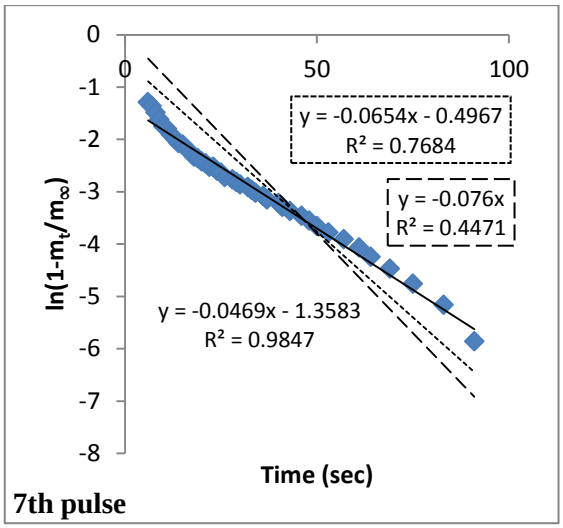

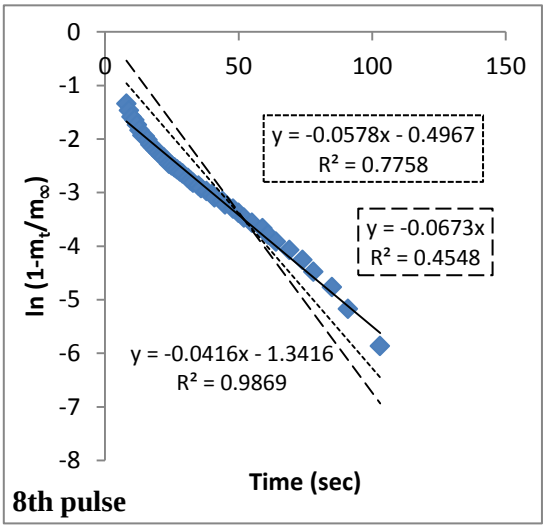

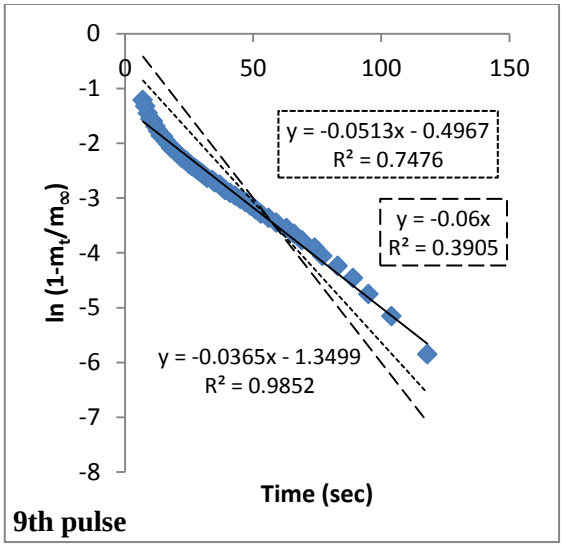

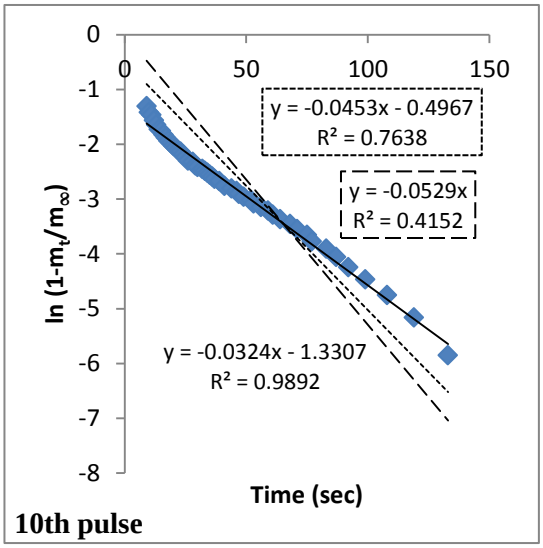

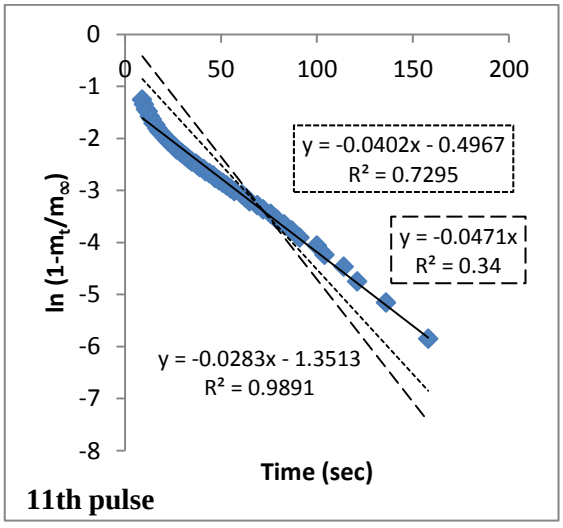

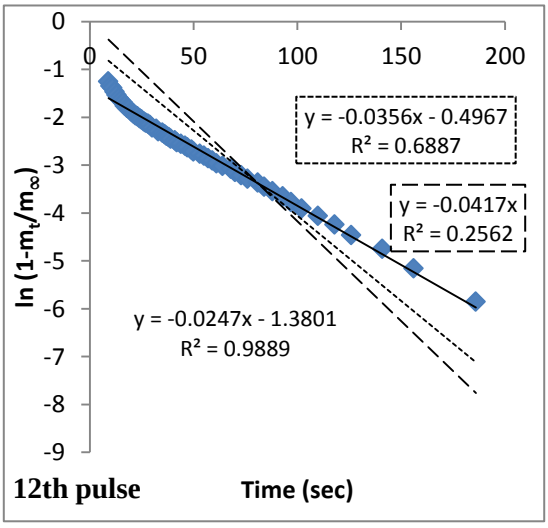

Figure F.13 (cont.)

(cont. on next page)

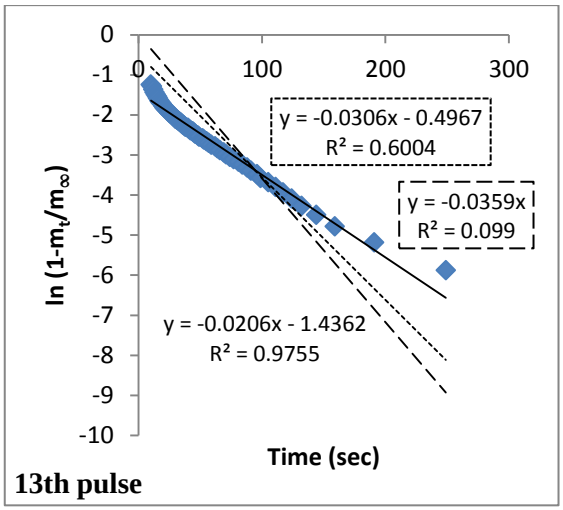

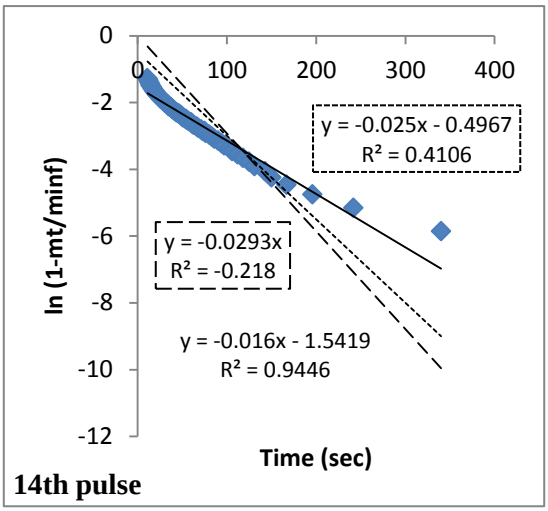

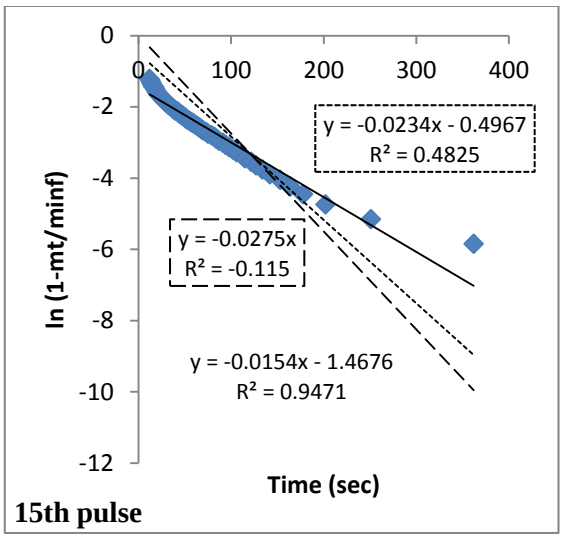

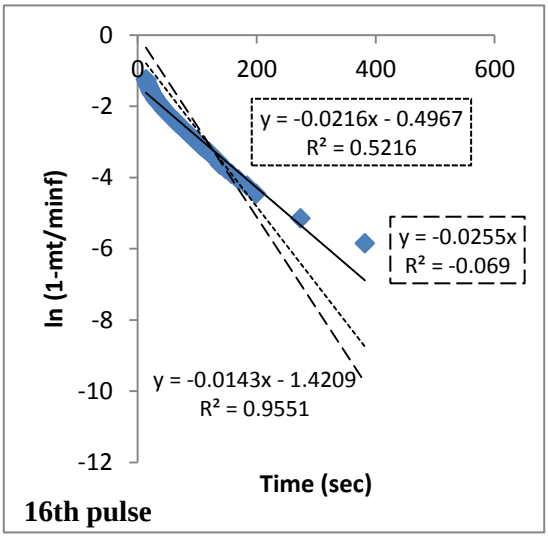

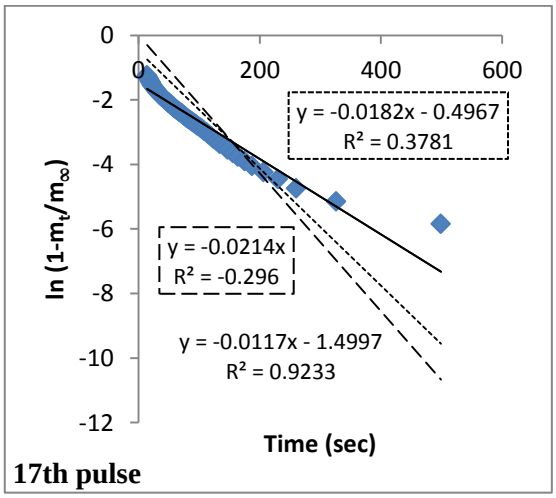

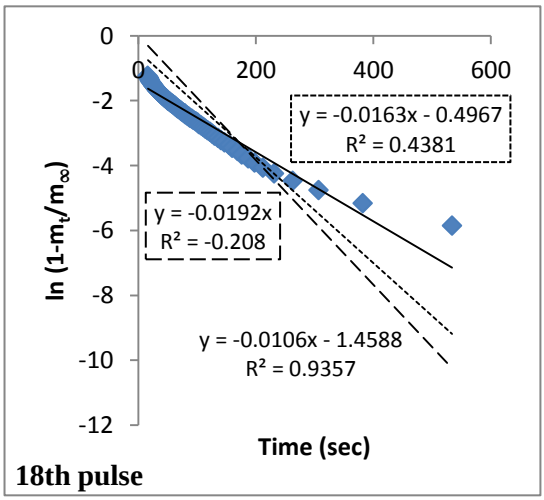

Figure F.13 (cont.)

(cont. on next page)

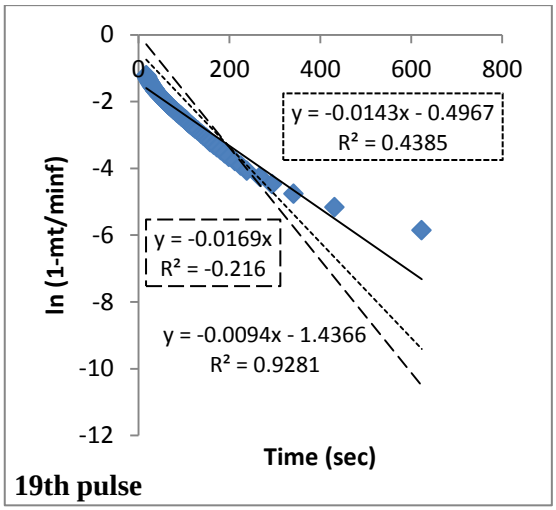

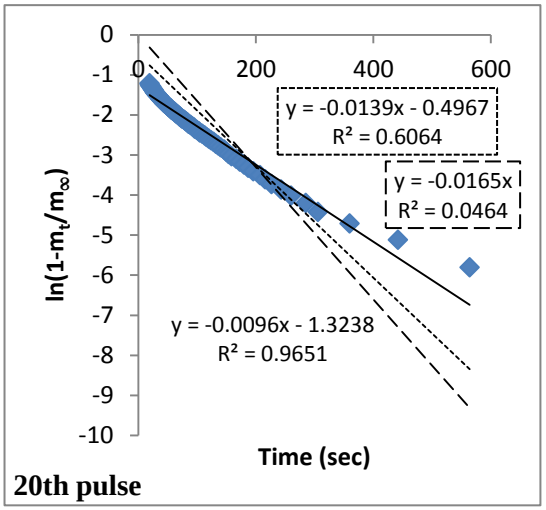

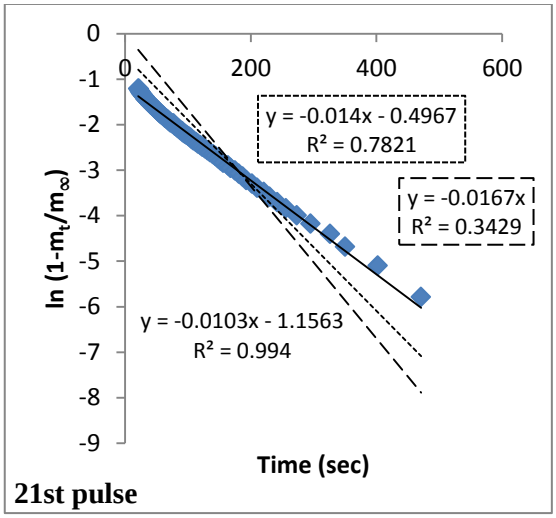

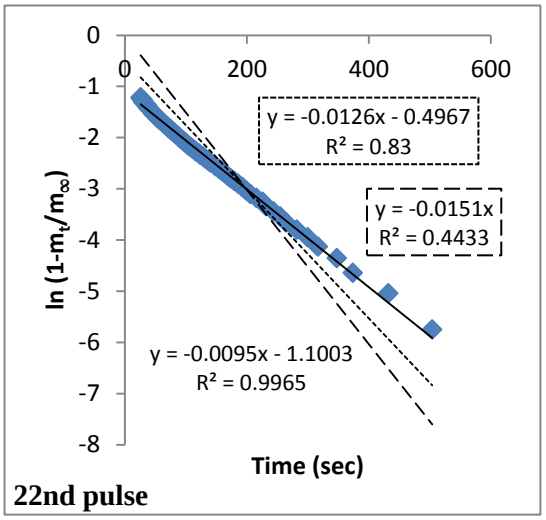

Figure F.13. (cont.)

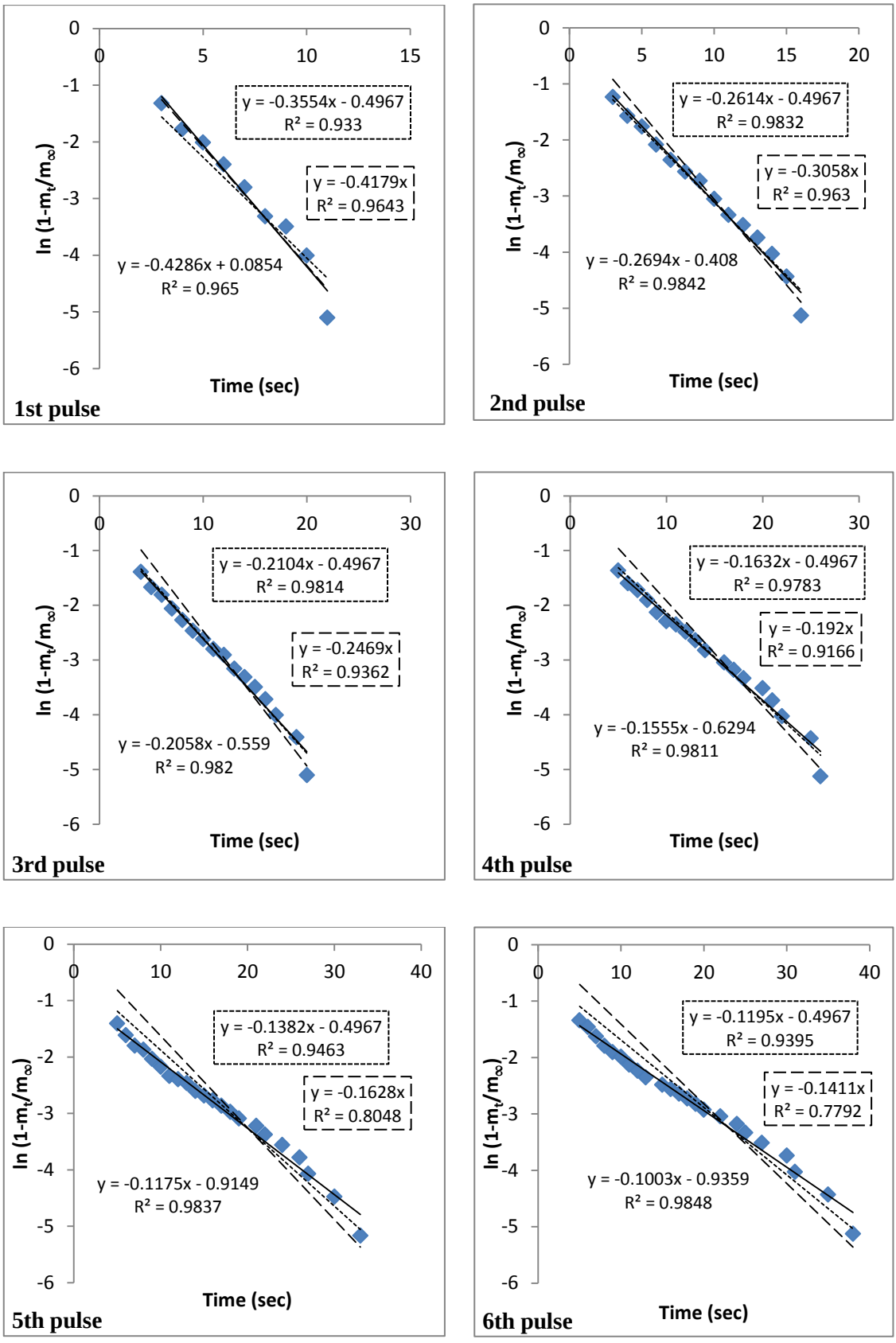

Figure F.14. Long term linear curves of zeolite 13X-water pair (T_{reg}=90°C, constant initial pressure of 980 Pa) ─ experimental; …. Long term intraparticle diffusion; ---- surface resistance

(cont. on next page)

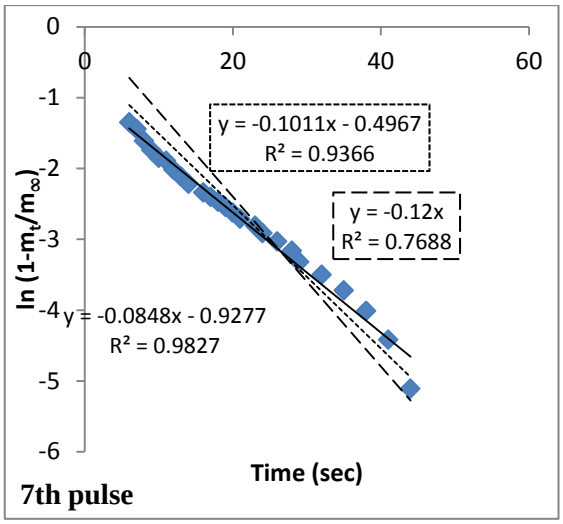

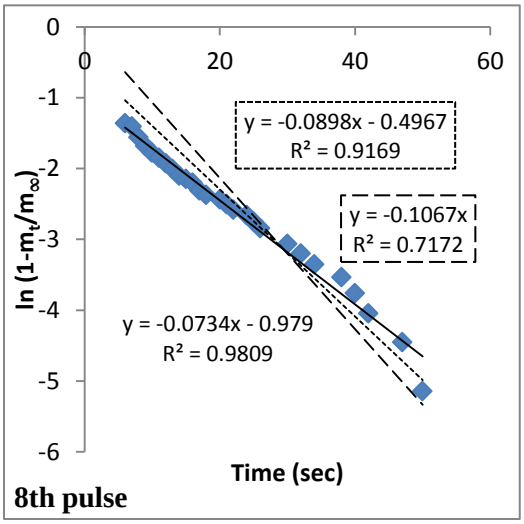

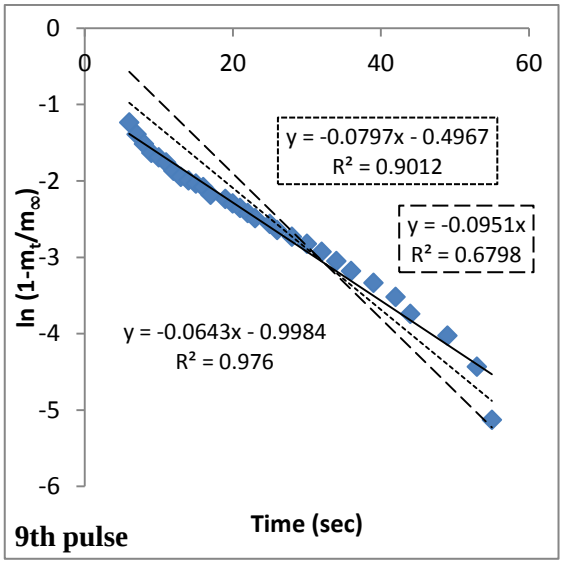

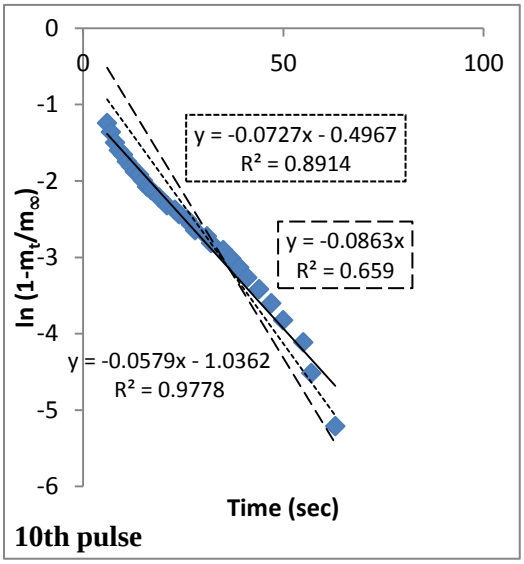

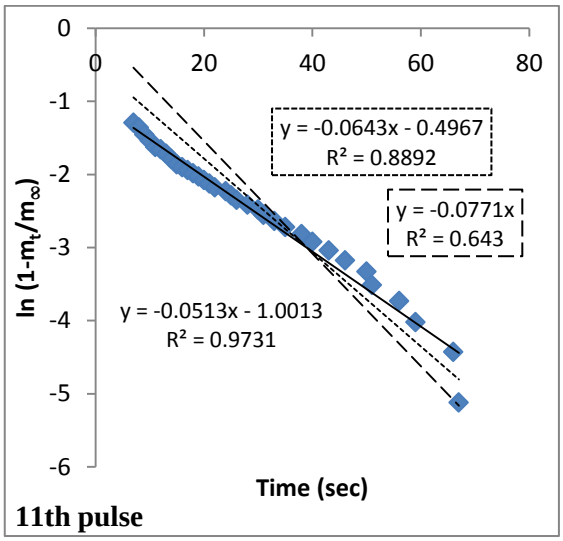

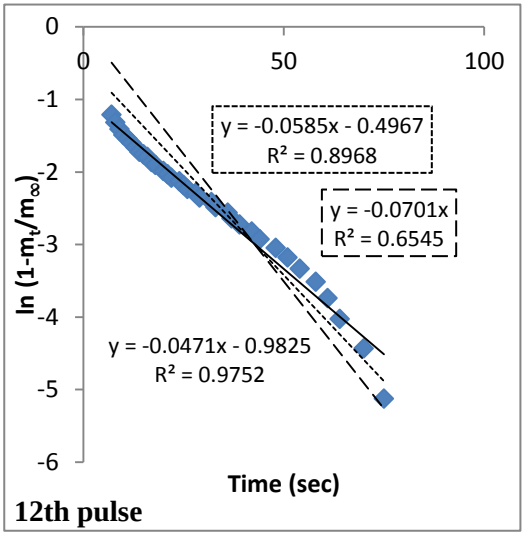

Figure F.14 (cont.)

(cont. on next page)

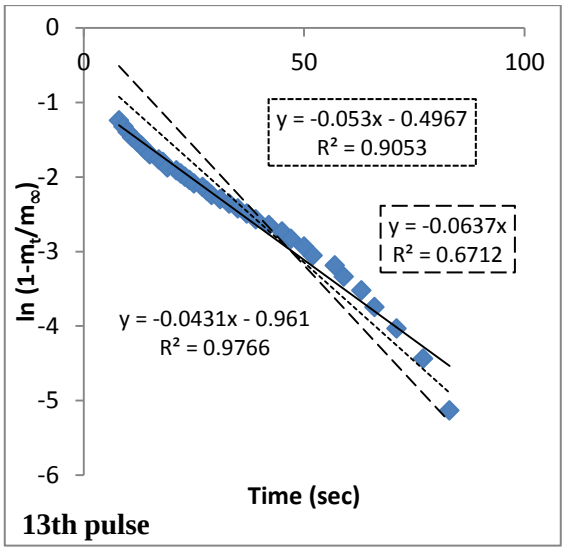

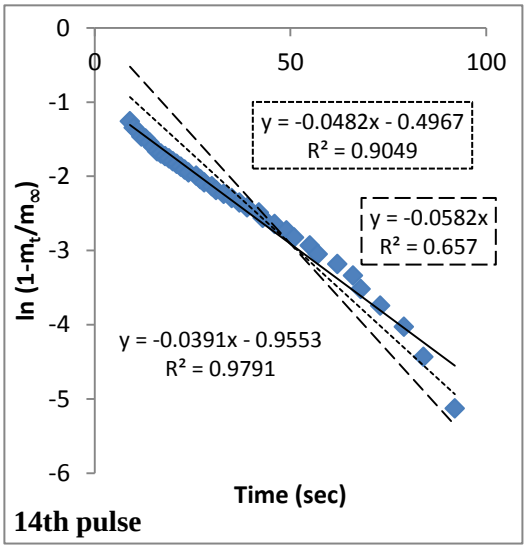

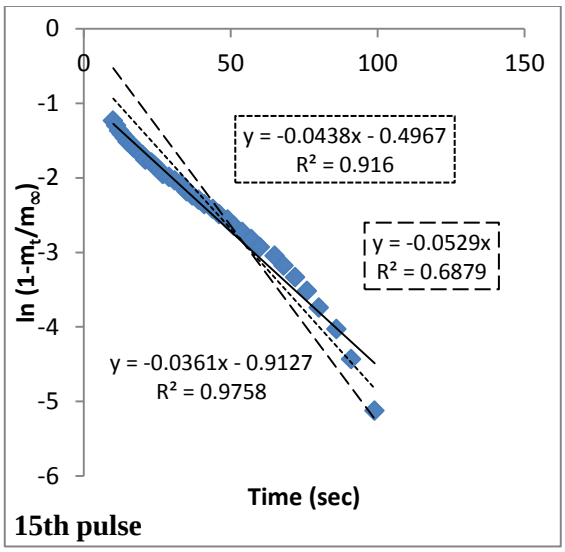

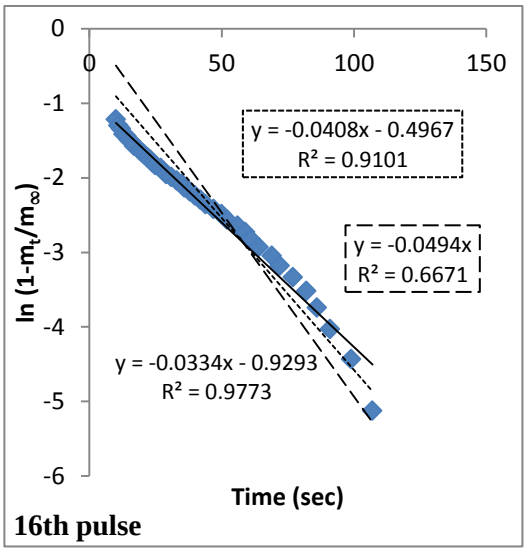

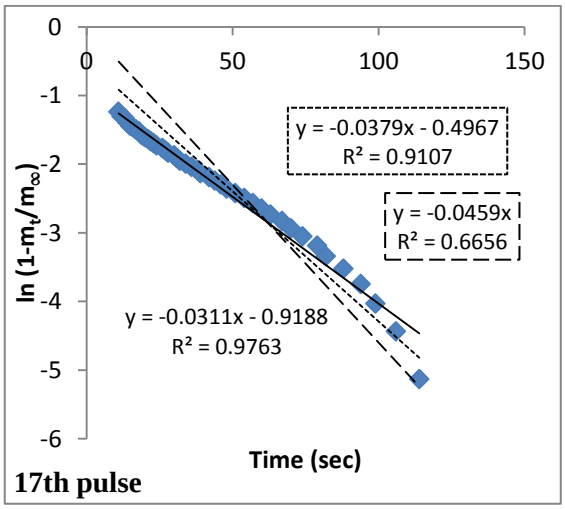

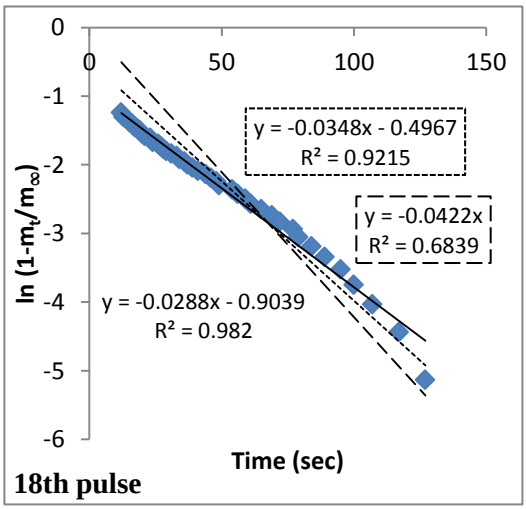

Figure F.14 (cont.)

(cont. on next page)

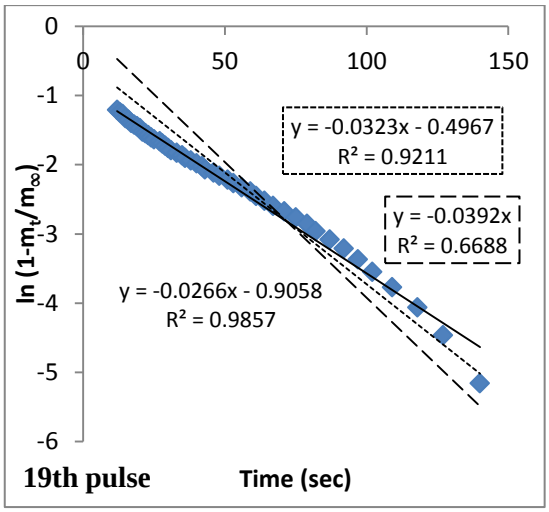

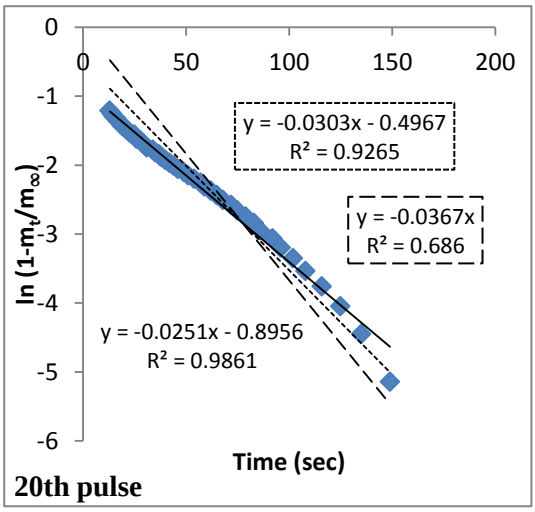

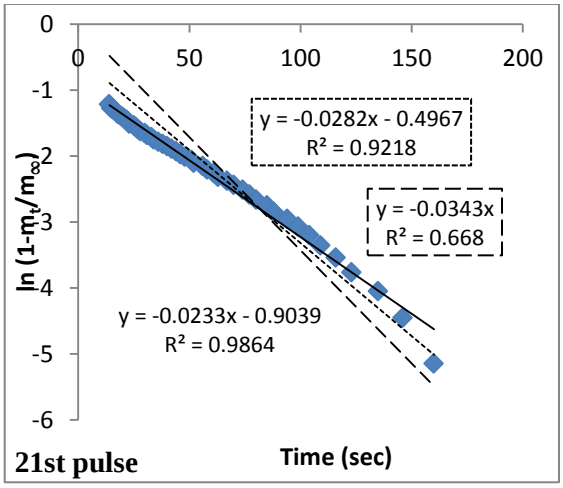

Figure F.14. (cont.)

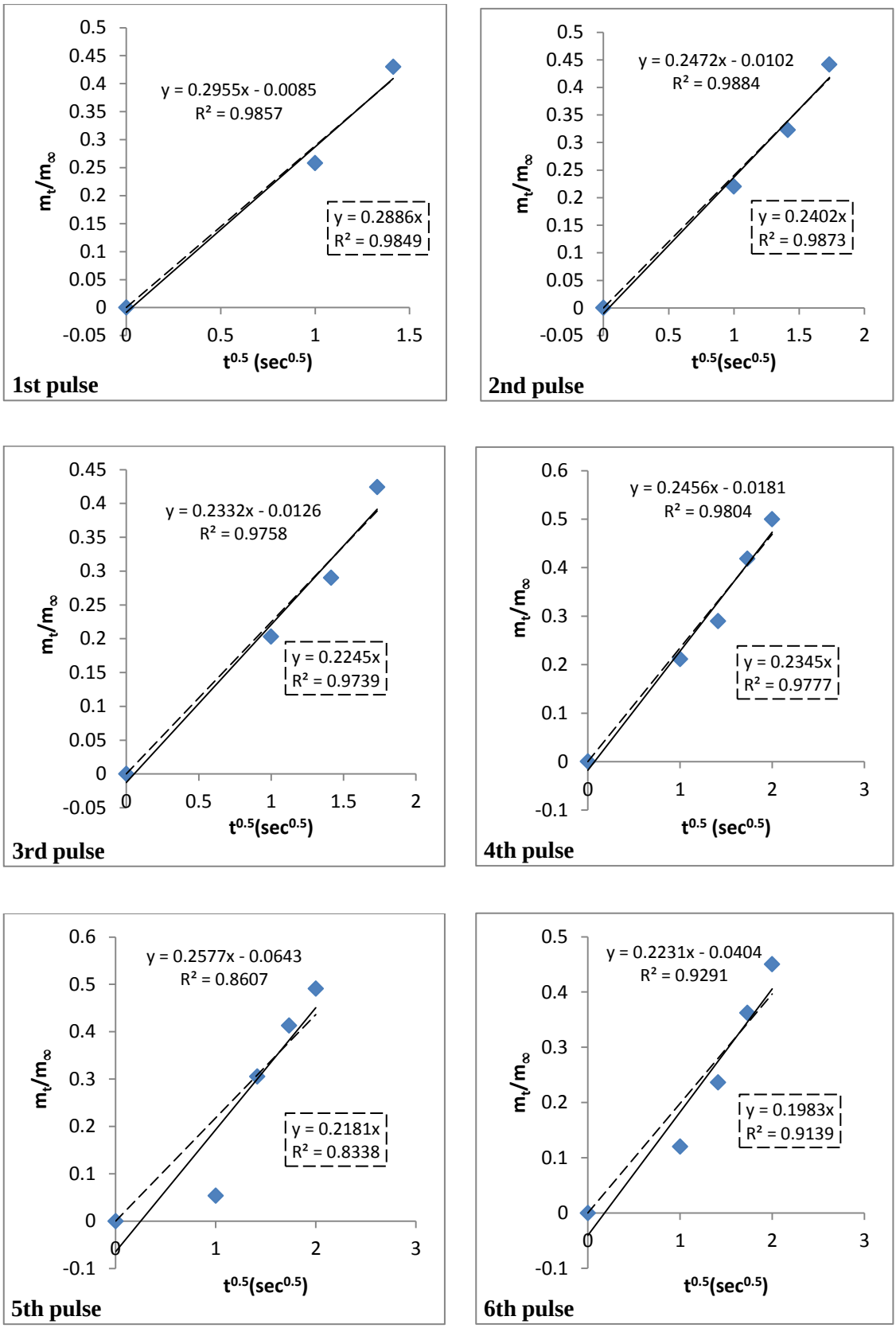

Figure F.15. Short term linear curves of zeolite 13X-water pair (T_{reg}=120°C, constant initial adsorptive concentration) ─ experimental; --- Short term intraparticle diffusion

(cont. on next page)

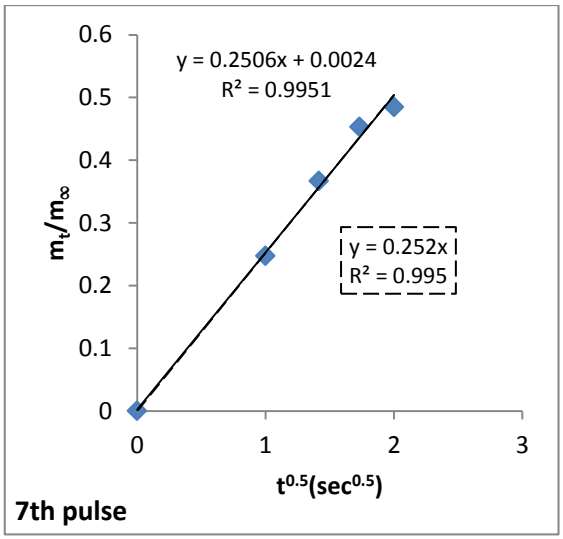

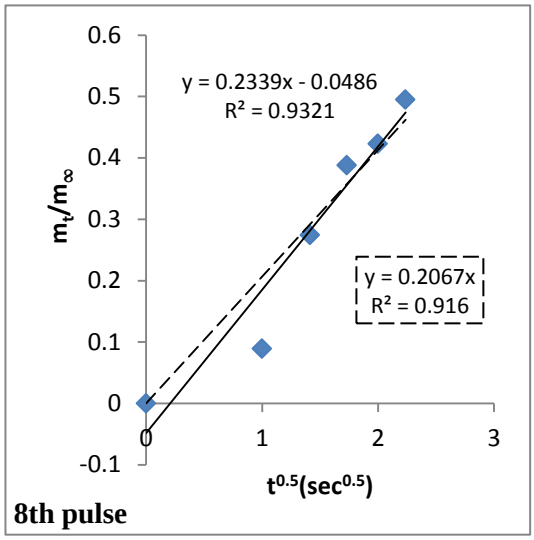

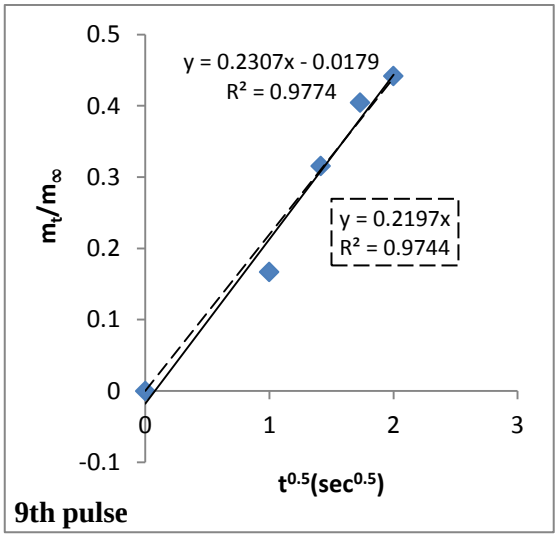

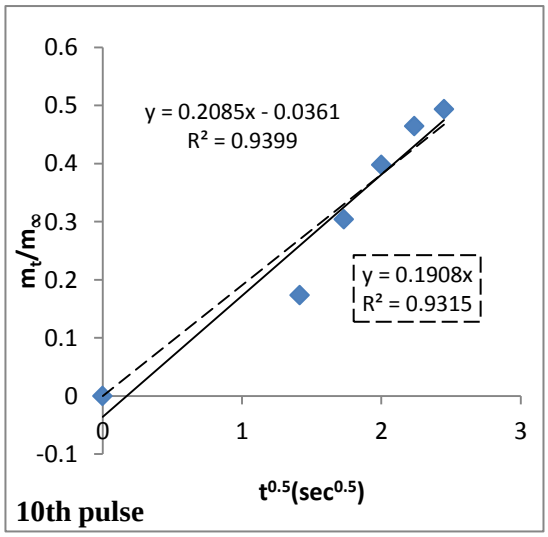

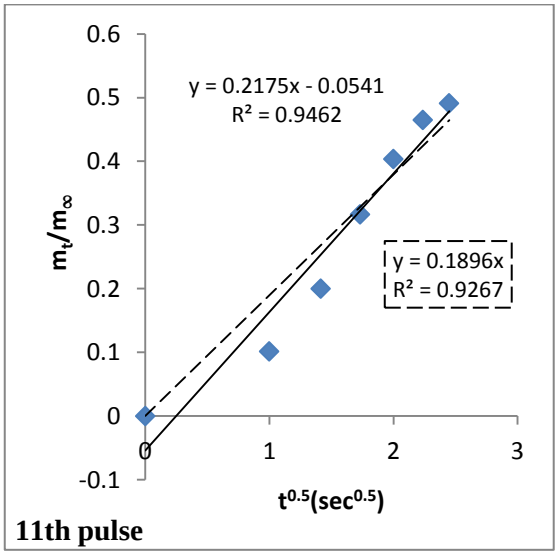

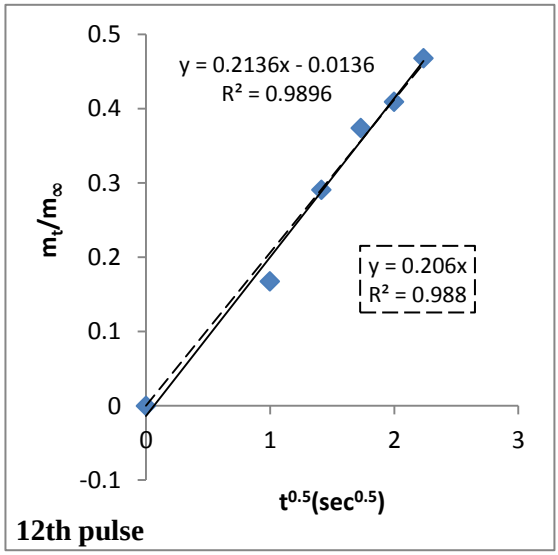

Figure F.15 (cont.)

(cont. on next page)

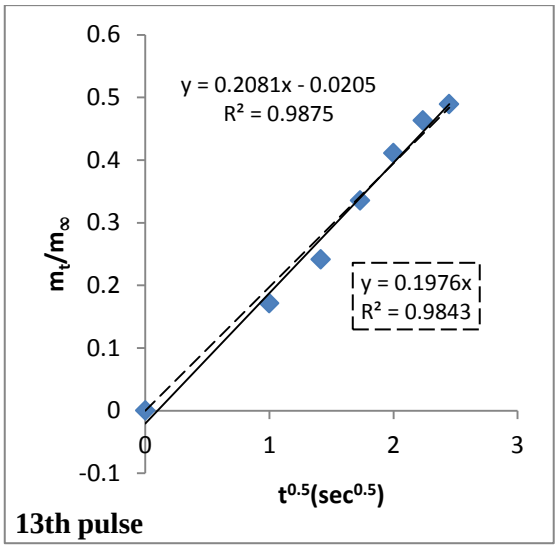

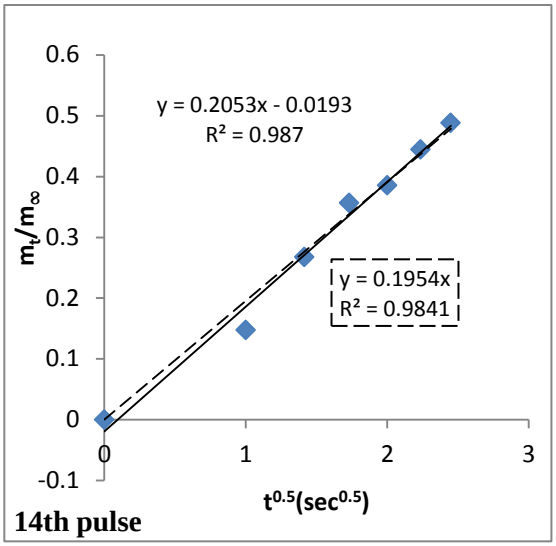

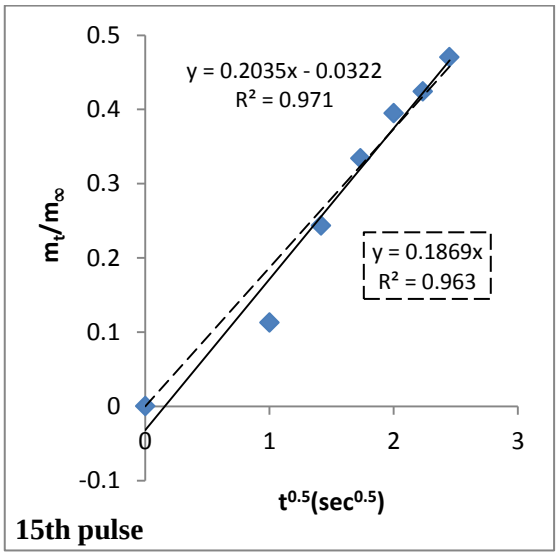

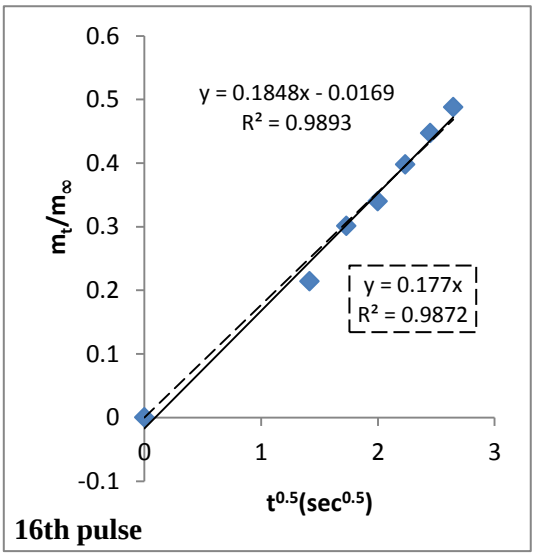

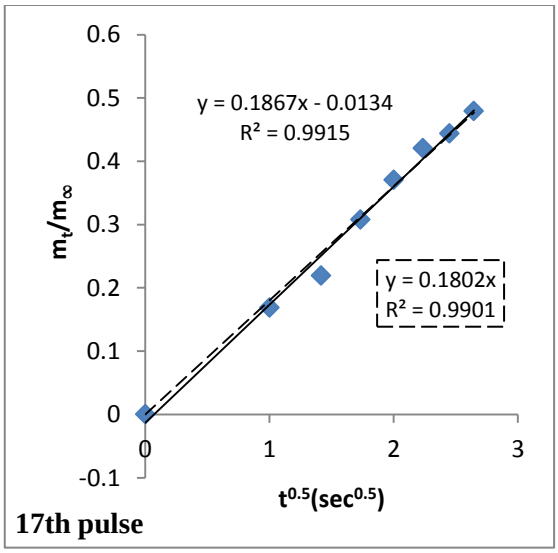

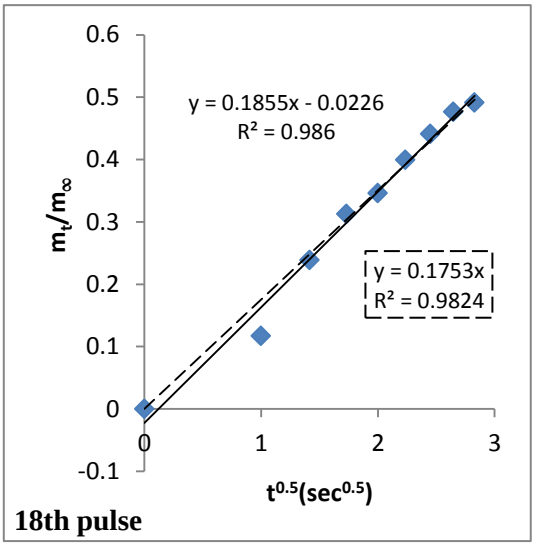

Figure F.15 (cont.)

(cont. on next page)

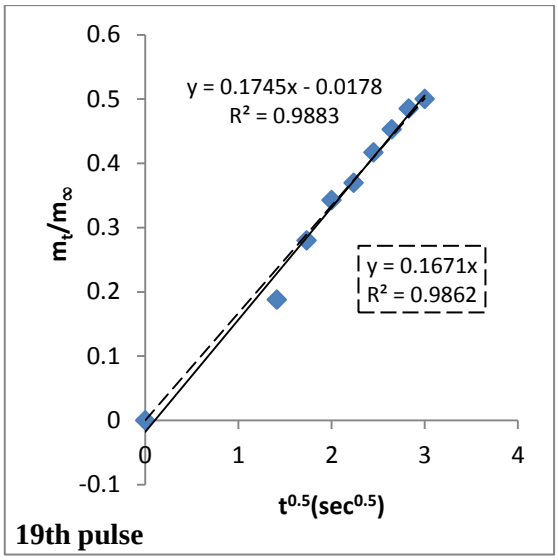

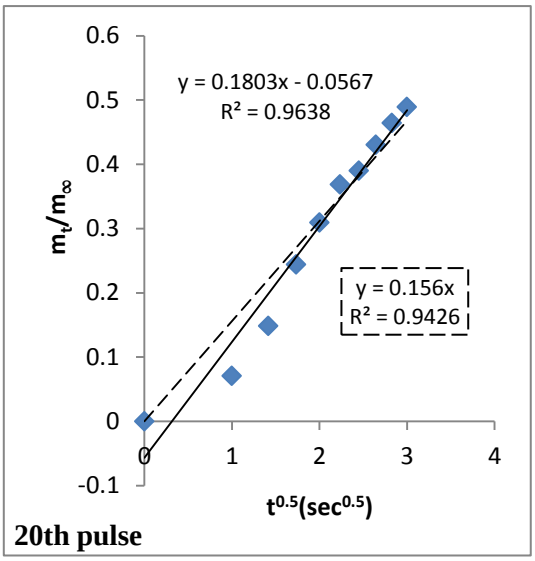

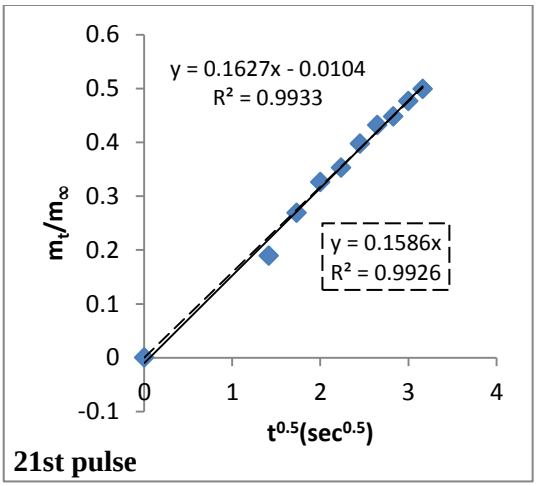

Figure F.15. (cont.)

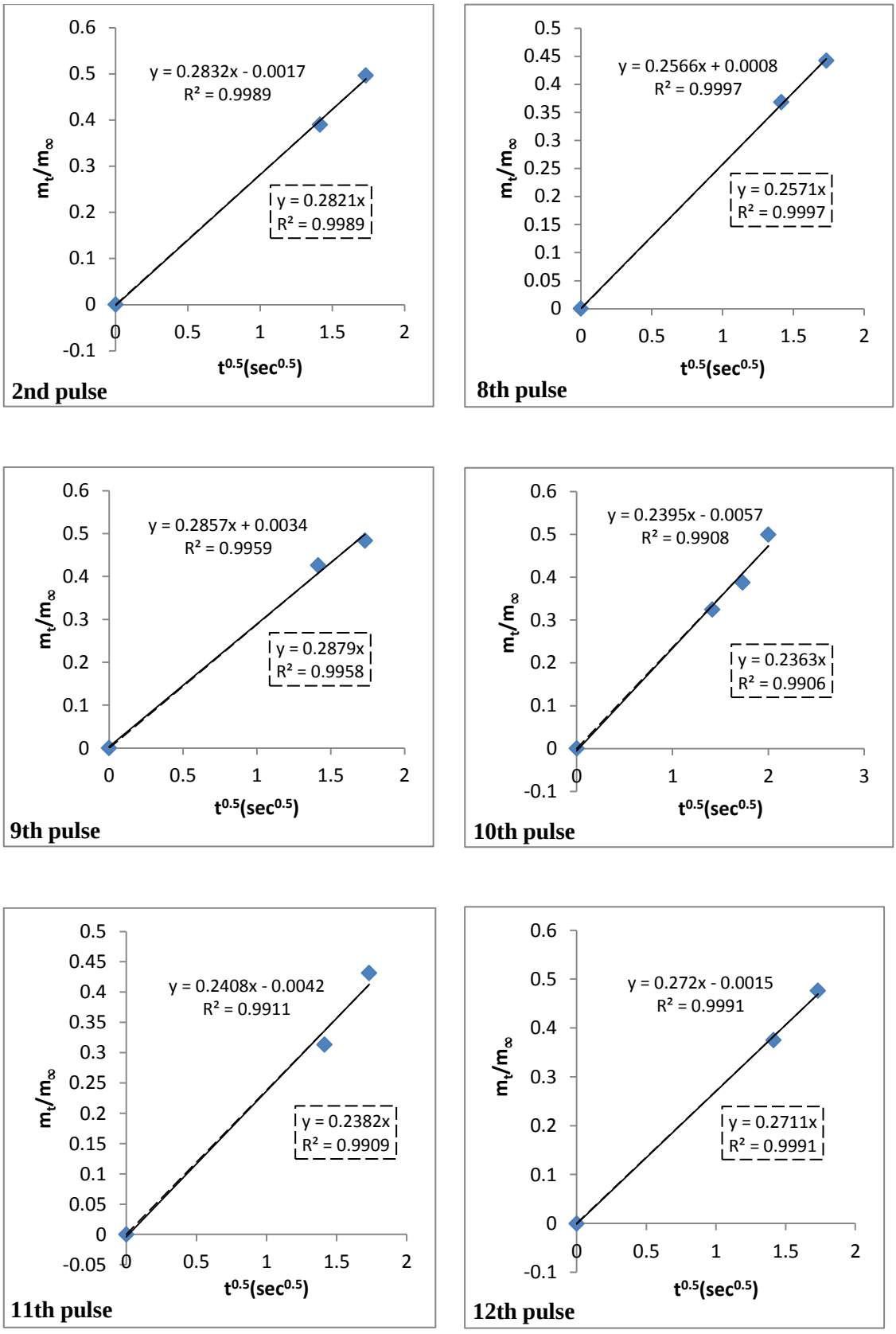

Figure F.16. Short term linear curves of zeolite 13X-water pair (T_{reg}=150°C, constant initial adsorptive concentration) ─ experimental; --- Short term intraparticle diffusion

(cont. on next page)

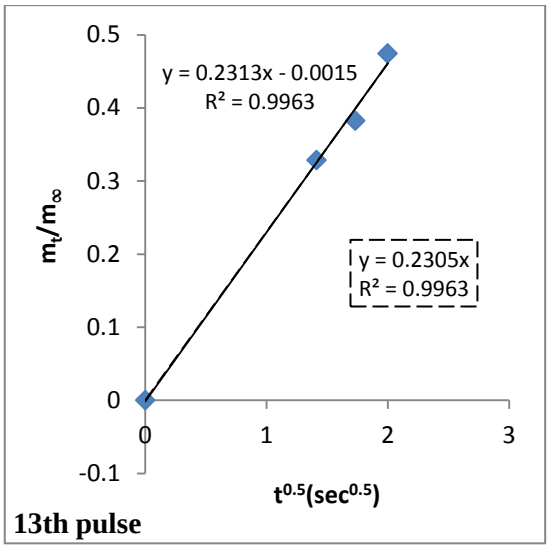

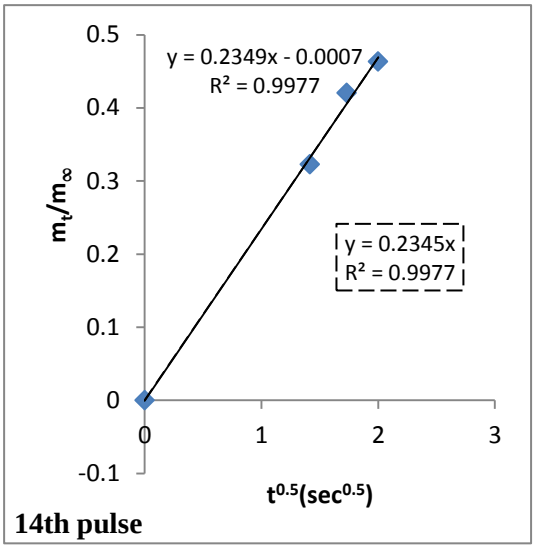

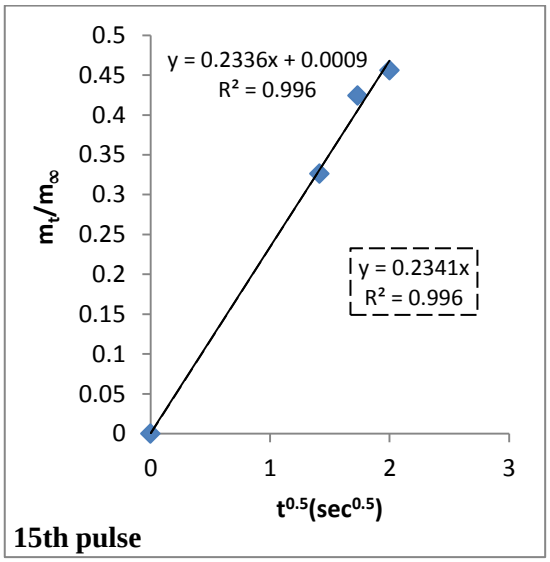

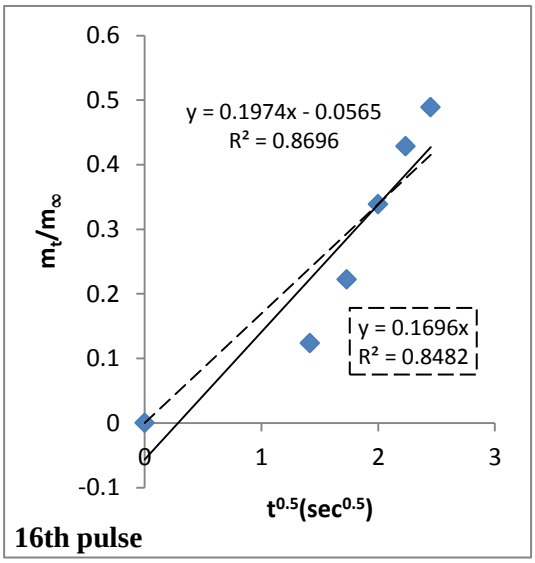

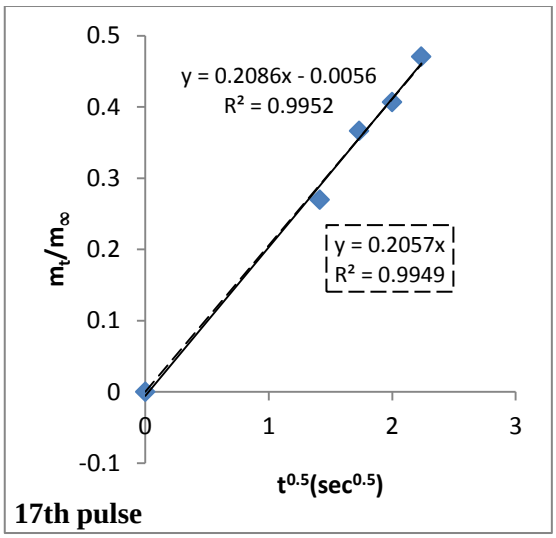

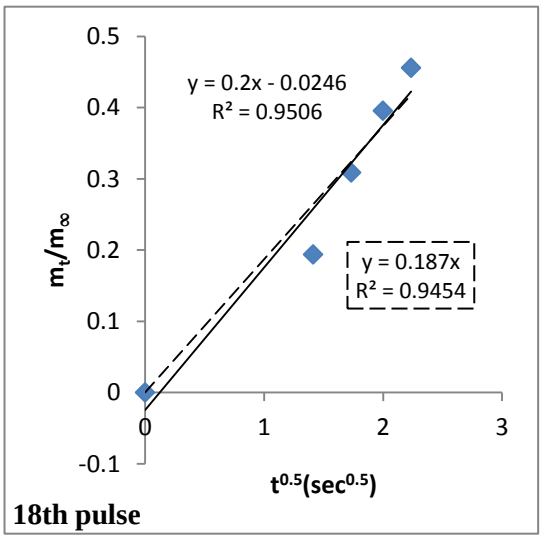

Figure F.16 (cont.)

(cont. on next page)

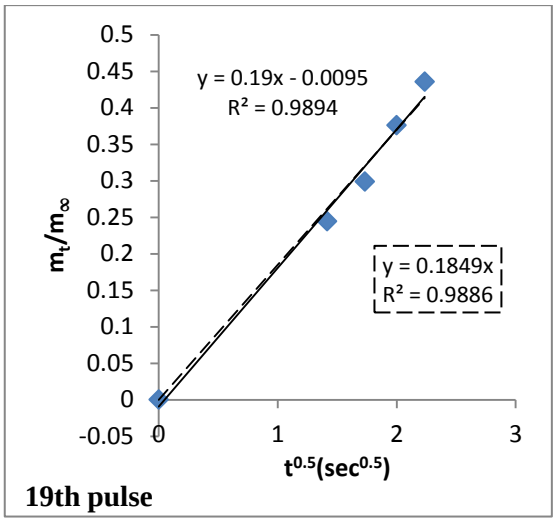

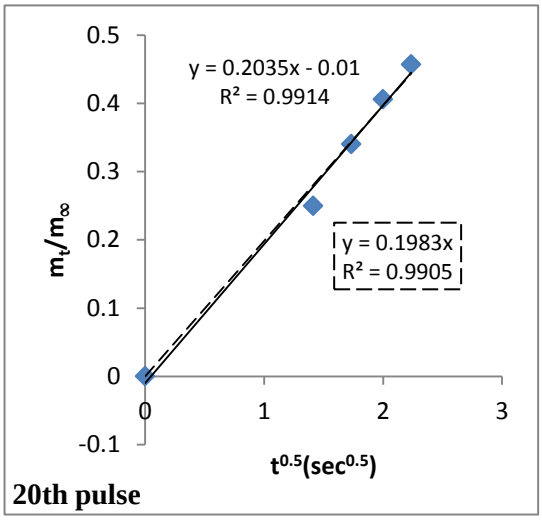

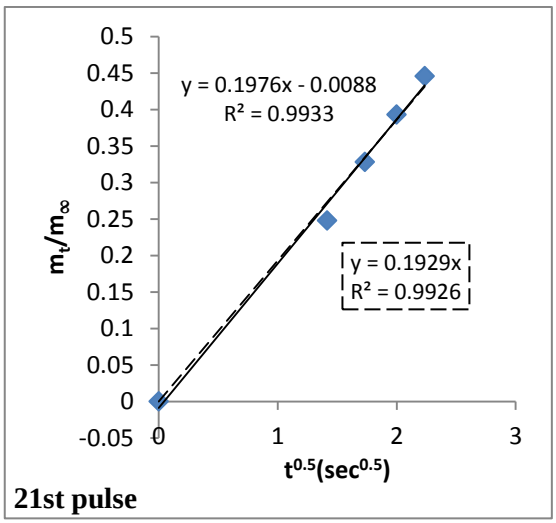

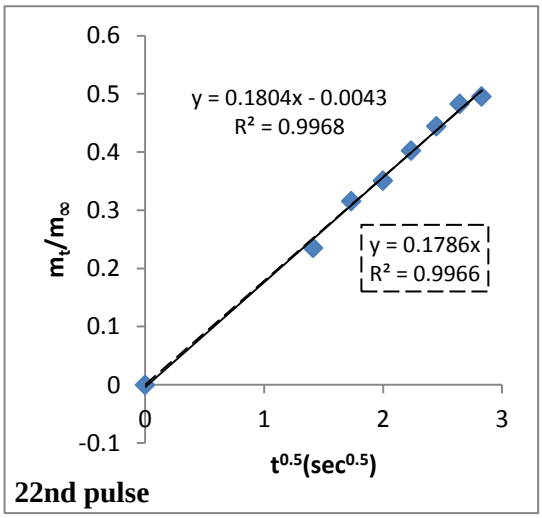

Figure F.16. (cont.)